UNIVERSITY OF LONDON

Imperial College of Science and Technology

Royal College of Science

Department of Physics, Applied Optics Section

SOME ASPECTS OF THE INFLUENCE OF THE MACH EFFECT ON IMAGE FORMATION IN MICROSCOPY

by

STEPHEN HENRY ROWE

Thesis submitted for the Ph.D. degree

1967

Abstract

When an observer views a contoured luminance distribution he may perceive subjective bright and dark bands, an effect first reported by Ernst Mach (1865). The investigations which Mach and other workers have performed to determine some of the factors which influence the visibility of the Mach bands are reviewed in this thesis. Various mathematical models which endeavour to explain Mach effects are discussed.

In microscopy the Mach effect is seen as a complicated band structure (often mistaken for diffraction fringes) which can considerably modify the physical images of particles apertures and edges. Previous work with regard to this phenomenon, as seen in microscopy, is considered. Tests performed on some twenty observers to determine the position, widths and relative luminances of the microscopical Mach bands are shown to expose the wide personal differences that exist between observers in their perception of the Mach bands. Small defocusing errors, less than the Rayleigh quarter-wave limit, are shown to affect the positions of the Mach bands. Scalar diffraction theory calculations are carried out to determine the changes, due to such amounts of defocus, produced in the physical images

of a straight edge in coherent and incoherent illumination. The effect of these small perturbations on the visual interpretation of the edge image is discussed. The influence of retinal location on the perception of the Mach bands is examined. Finally some experiments performed with a binocular eyepiece are described.

Preface

Since some of the work described in this thesis was performed with apparatus constructed by previous workers I should like to enumerate the topics which were originated and carried out by myself:

1) Modification of the visual photometer so that more accurate measurements of the luminances of the Mach bands could be made.
2) Supervision of the survey performed by twenty observers and the statistical analysis of the results thereof.
3) The variation of the visual depth of focus with degree of coherence of the light employed.
4) Effect of small focusing errors on the Mach band measurements.
5) Scalar diffraction calculations which investigate the influence of small amounts of defocusing on edge images and their second derivatives for coherent and incoherent illumination.
6) Measurements of Mach bands extrafoveally.
7) The influence of binocular vision on the Mach bands.

S.H.R.

Contents

	Page
Abstract	(i)
Preface	(iii)
Chapter I. The Mach Effect in Vision	
Introduction	1
Mathematical Models of Mach Effects	17
The investigations of Ludvigh, Green, Ercoles and Fiorentini	31
Applications of the Optical Transfer Function to the problem of Mach bands	34
Chapter II. The Mach Effect in Microscopy	
Early Work	42
Scope of the author's work	51
Chapter III. Apparatus and Techniques	
Introduction	53
The Photo-electric Microscope	55
The Visual Photometer	71
The Test Object	75
Choice of Objective	77
Tube length Setting	78
Scanning procedure to determine physical edges	79

Page

Chapter IV. The variation of the Mach Effect between different Observers

Introduction 82

Calculation of the retinal illumination 83

Experimental procedure to determine the positions of the bands 88

Measurement of the relative luminance of the Mach bands 92

Differences between observers' determinations of the visual edge 104

The relationship between the Mach bands and the physical image 108

The influence of ocular axial length on the Mach bands 117

The effect of physiological differences on the Mach bands 120

Chapter V. The influence of small defocusing errors on the Mach bands

Introduction 122

Strehl Intensity and the Rayleigh limit 122

The Optical Transfer Function 128

Edge Gradient 132

Page

The visual depth of focus 134

Displacements of the Mach bands for small amounts of defocus 139

The influence of different observers' focal settings 141

The relative luminances of the Mach bands 151

Chapter VI. Some diffraction calculations for defocused edges

Introduction 154

General formulae 154

Coherently illuminated extended object 157

Coherently illuminated half-plane (straight edge) 158

Incoherently illuminated half-plane (straight edge) 170

Discussion 183

Chapter VII. The effect of a) retinal location and b) binocular vision on the Mach bands

a) Retinal location - Introduction 185

Apparatus and techniques used to investigate the perception of the Mach bands outside the fovea 188

		Page
b)	Binocular vision - Introduction	195
	Apparatus and techniques	196
Chapter VIII.	Summary of conclusions and discussion	207
Appendix A.	Wave aberrations	211
	Longitudinal displacement of focus	213
	Transverse displacement of focus	215
Appendix B.	Calculation of the image of a luminous point (Point Spread Function)	218
Appendix C.	Some relations concerning Struve functions	227
References		230
Acknowledgements		236

Chapter I

The Mach Effect in Vision

Introduction

When an observer views a contoured luminance distribution, consisting of continuous dark and bright fields separated by a graded luminance distribution, he will generally perceive a subjective increase in the gradient of the graded distribution (often termed "sharpening") and where this graded zone merges into the bright field a subjective band, brighter than the continuous bright field, will be seen while where this zone merges into the continuous dark field a band darker than the dark field will be perceived (see fig. 1.01). This subjective phenomenon is known as the Mach effect and was first reported by the Austrian physicist and philosopher, Ernst Mach, in 1865.

Mach first studied the visual effects of juxtaposing fields of various intensities by using rotating discs on which were painted black and white sectors; the sectors were visually combined by rapidly rotating the discs. Typical discs employed by Mach are shown in figs. 1.02a,b and 1.03a,b. When the discs shown in fig. 1.02a,b were rapidly rotated they appeared grey, increasing in darkness

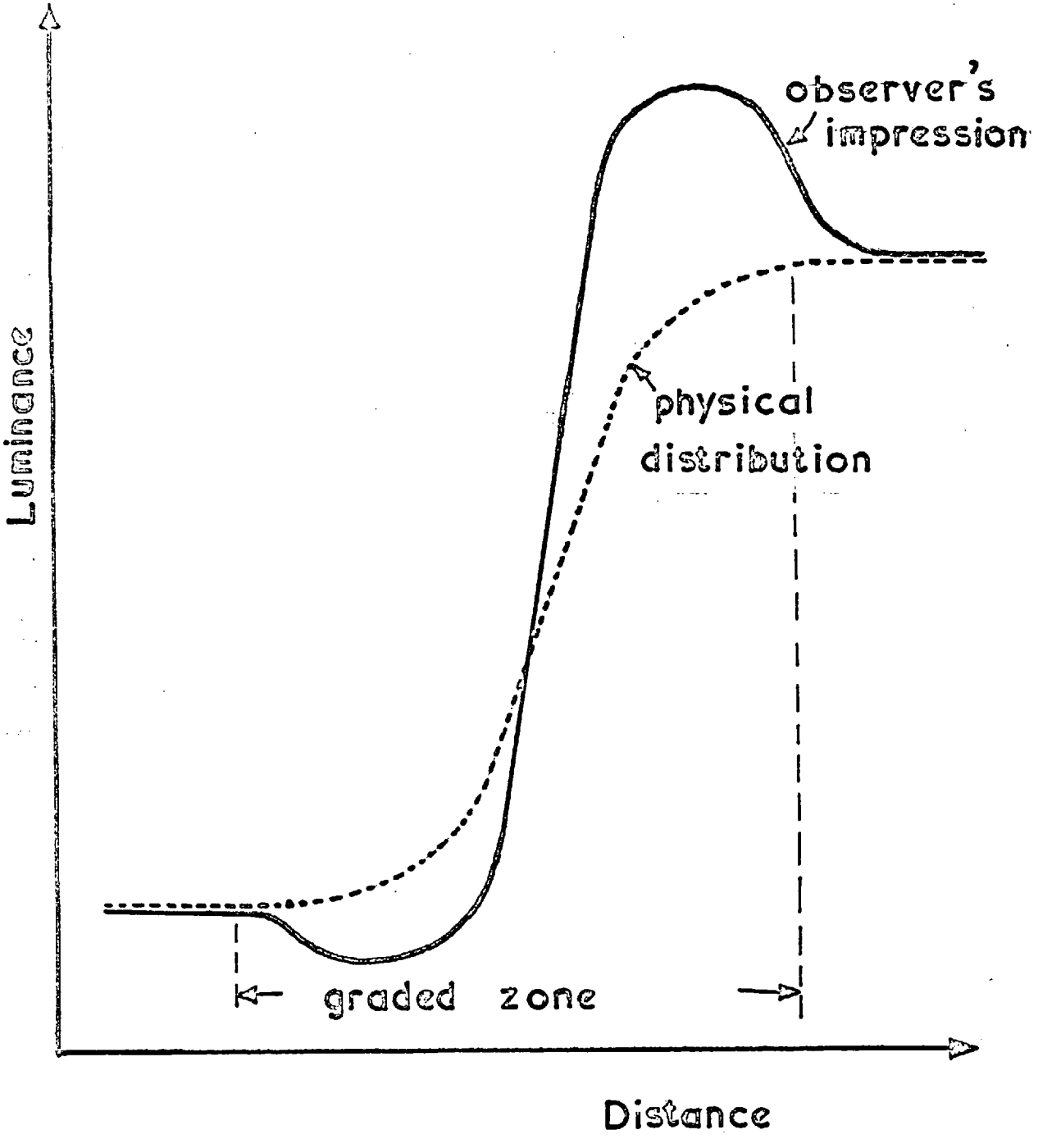
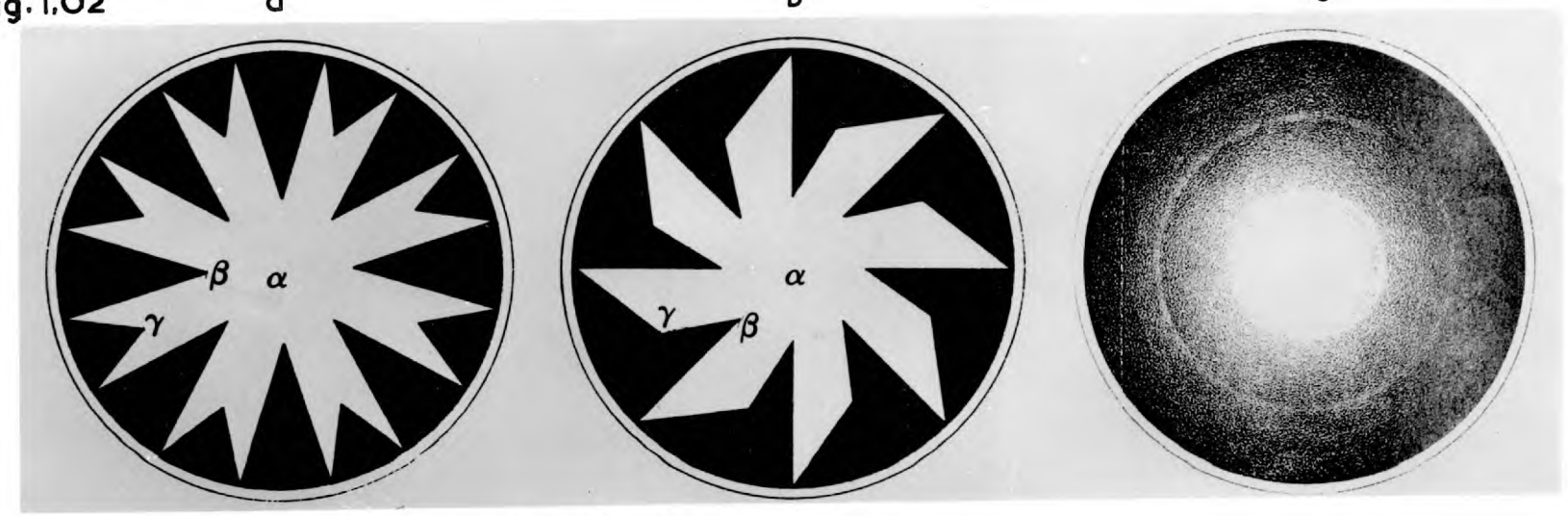


Fig.1.01 The Mach Effect

Fig. 1.02



Mach's discs

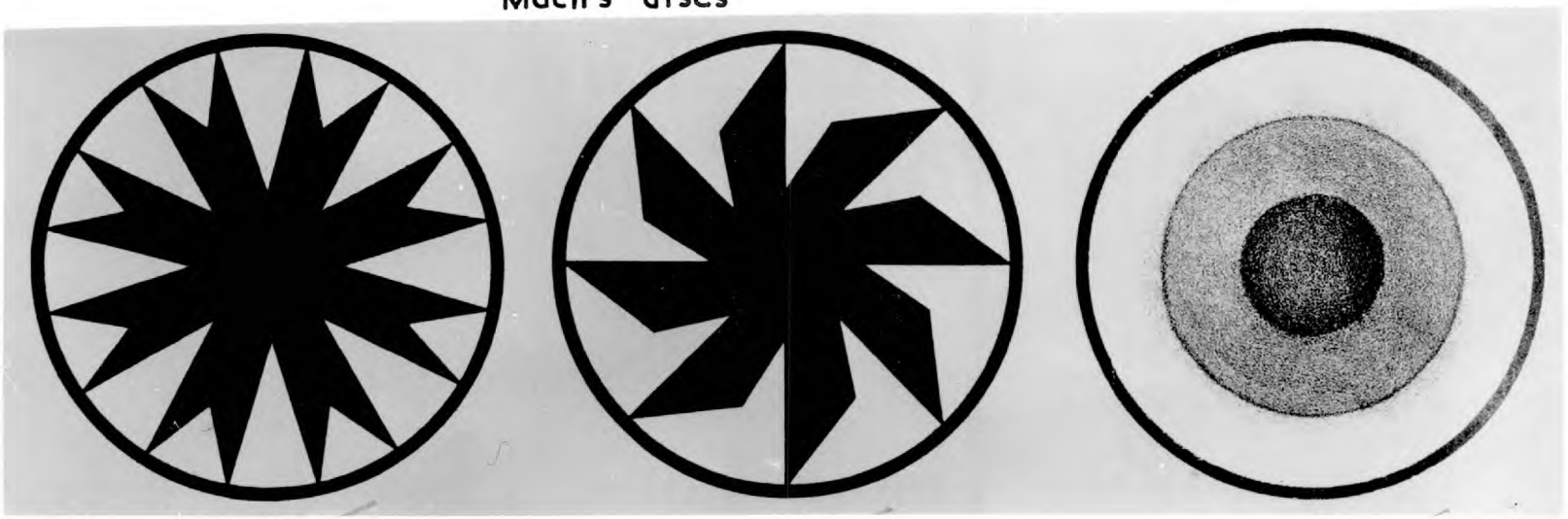


Fig. 1.03.

ω

towards the rim; however this appearance was interrupted by narrow, brighter, somewhat blurred rings in regions where the black sectors end in points (fig. 1.02c). The discs shown in figs. 1.03a,b are the negative images of those shown in figs. 1.02a,b and their appearance, when rapidly rotated, is shown in fig. 1.03c; in this case the discs appeared grey, decreasing in brightness towards the centre and narrow dark bands were seen where the black sectors ended in points. The appearance of the bright and dark bands initially surprised Mach as such a luminance distribution was not predicted by the well tested Talbot-Plateau law. Let there be a regular succession of similar lights of brief duration with frequency of N per second. If N is greater than the critical fusion frequency the observer cannot detect that the real luminance L is varying with time; the impression he receives is that of a perfectly constant luminance L_m which is the mean value of the real luminance taken over one period or over any time t comprising an integral number of periods

$$L_m = \frac{1}{t} \int_0^t L.dt \qquad \text{(Le Grand 1957)}$$

According to the Talbot-Plateau law the perceived luminance of the discs shown in figs. 1.02a,b should have been as

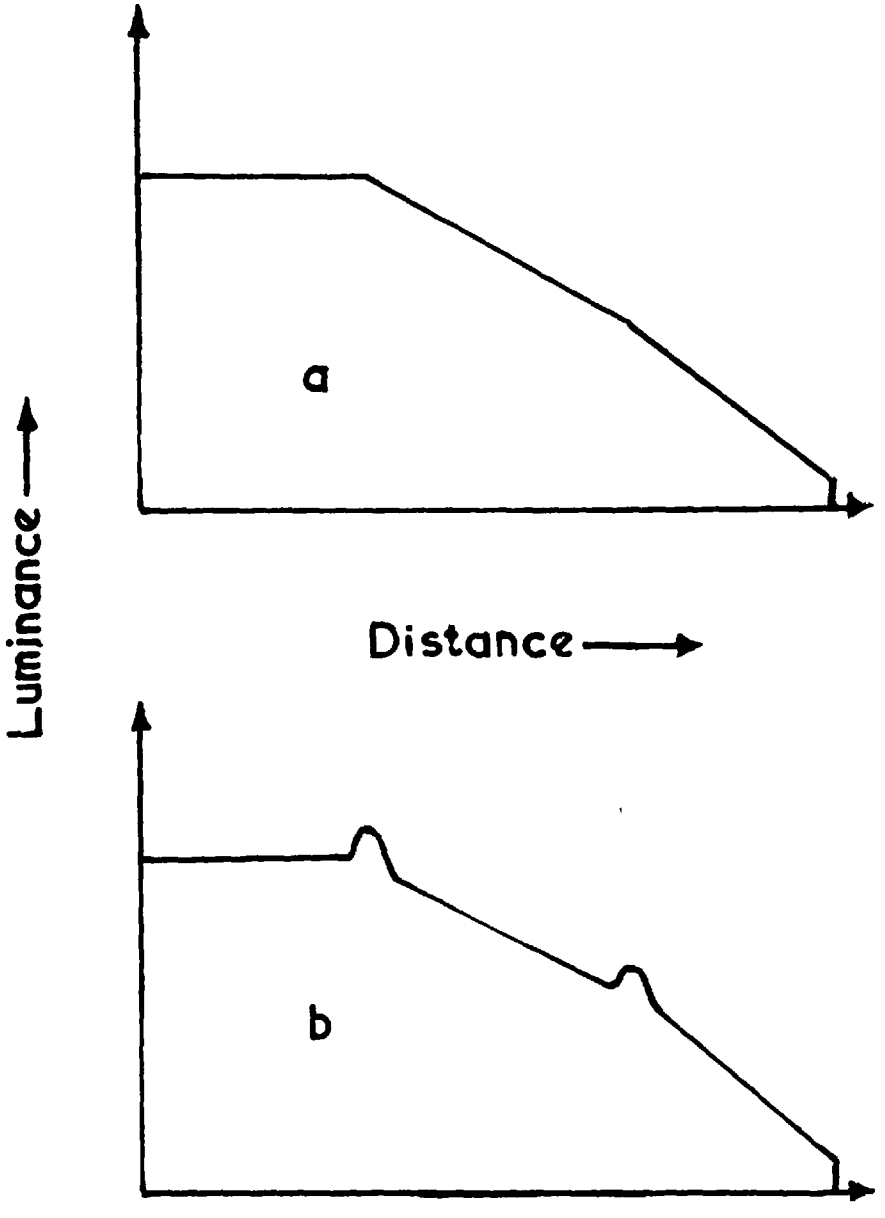


Fig. 1.04 (after Mach)

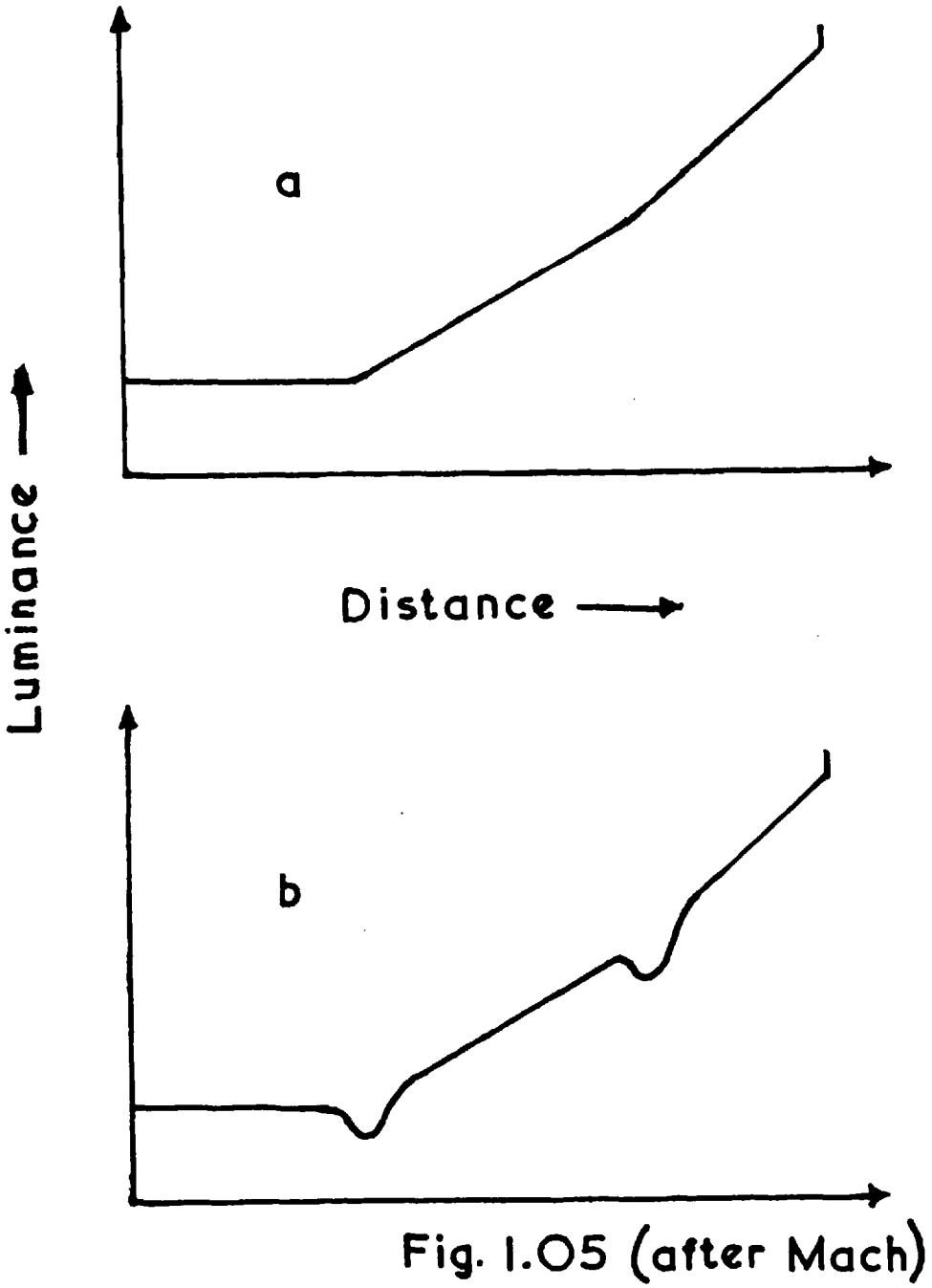


Fig. 1.05 (after Mach)

depicted in fig. 1.04a but, in fact, the appearance was that shown in fig. 1.04b. Fig. 1.05a shows the luminance distribution according to the Talbot-Plateau law for the discs shown in figs. 1.03a,b while fig. 1.05b depicts the observer's impression. By means of various forms of light and dark sectors fixed to rotating discs and cylinders Mach was able to vary the light intensity from place to place according to any chosen rule. As a result of these studies Mach enunciated the following law: Every point where the light intensity curve has a flection will appear brighter or darker than its surroundings. The point where the flection is concave towards the abscissa (distance axis) is brighter and where the flection is convex towards the abscissa it is darker.

It was found that these phenomena were not peculiar to rotating discs and cylinders, nor were they dependent upon fusion of intermittent light signals. Mach demonstrated these facts by photographing the rotating discs and then observing the still pictures. Positive photographs of the rotating discs appeared almost exactly like the rotating discs themselves. The Talbot-Plateau law was shown by Mach to hold for photographic processes (provided there was a linear relationship between the opacity of the film and exposure). Consequently the photographs presented

essentially the same distribution of luminance as the rotating discs. Thus the controlling factor in these experiments was the spatial distribution of luminance rather than the particular method of obtaining that distribution. Mach's papers concerning these phenomena are well translated in the book, "Mach Bands" by Ratliff (1965).

The dependence of the light and dark bands on the spatial distribution of luminance led Mach to conclude that these phenomena had their origin in a functional interdependence of neighbouring elements of the retina. He believed that this interdependence was a reciprocal inhibitory influence and that it was mediated with gradually diminishing effect over the lateral network of neural interconnections in the retina. Mach believed that the purpose of these retinal inhibitory interactions was to enhance the appearance of contours and borders in the spatial distribution of luminance. The German psychophysicist and philosopher Hering held a similar view and remarked, "We must add that the outlines of the individual parts of the retinal image are always more or less washed out; at least they are never so sharp as one is accustomed to assume on the basis of the theoretical dioptrics of the eye". Hering concludes "Thus we come to the conclusion that the retinal image of every such boundary line is in

itself a washed out one even for best accommodation, but that our visual system possesses the capacity to produce from such an imperfect line image, when it is sufficiently intense, a sharp boundary between related colours in the psychological visual field, and thus to create sharply outlined visual objects from parts of the retinal image whose outlines are washed out. Our visual system owes this capacity to reciprocal interactions in the visual field" (Hurvich and Jameson, 1964).

The influence of certain factors on the appearance of the Mach bands.

Given a contoured luminance distribution, a number of workers have investigated the influence of the slope of the gradient between the uniform fields, the luminance of the uniform fields, the colours of the fields, movement of the luminance distribution, short viewing times and the effect of stabilised retinal images.

To investigate the influence of the gradient McCollough (1955) used a pattern consisting of a uniform bright field of constant luminance and an adjacent graded field only. She found that the width of the bright band decreased markedly as the slope of the graded zone increased. Some observers reported that as the slope increased the position

of the bright band shifted slightly away from the bright field. This change in position varied greatly amongst different observers. Of course no measurements were possible on corresponding properties of the dark band as no uniform dark field was present.

Fiorentini and Radici (1958), who used a luminance distribution which produced both a dark and a bright band, also found that the bright band generally became narrower and more distinct as the slope was increased until finally it disappeared when an abrupt step existed between the continuous bright and dark fields. With very gradual slopes the bright band disappeared. Similarly the dark band became more distinct with increasing slope but disappeared when an abrupt step was present. When the slope was made very gradual the dark band also became indistinct but its width appeared constant over a considerable range of change in slope. The bright band generally appeared narrower than the dark band and was nearly centered on the flection; for some observers it shifted slightly off centre into the uniform bright field when the slope was decreased. Fiorentini and Radici report, however, that the greater part of the dark band always appeared in the uniform dark field. The results obtained from different observers commonly revealed consistent individual differences.

Fiorentini and Radici (1957, 58) also turned their attention to the influence of slope variations, on the brightnesses of the Mach bands. Using a method of binocular comparison they measured the apparent brightnesses of the bands. In general they found that the brightnesses of the uniform fields at some distance from the intervening gradient remained constant for all slopes. The intensity of the bright band increased slightly with increasing slope of the gradient, although some observers reported no change but the dark band became darker. Individual differences were great; in fact brightness measurements made by different observers under similar conditions sometimes varied by factors of as much as three to one.

Contrary to the results of Fiorentini and Radici measurements by Lowry and de Palma (1961) showed little change in the intensities of the bands with variations in the slope of the graded zone over an intermediate range. Their results did agree with those of Fiorentini and Radici in so far as they showed that the bright band was more pronounced than the dark band and that it became significantly narrower with increasing slopes. Lowry and de Palma used a monocular bipartite field in the upper half of which the Mach pattern was presented and in the lower half an

illuminated slit was imaged, its length being parallel and adjacent to the Mach bands. The brightness of this slit was adjusted to match the adjacent Mach band pattern. By moving the slit several points on the sensation curve (apparent luminance curve) were determined.

Hartwig (1958) measured the magnitude of the bright band by introducing an adjustable step increment in the bright field and matching it with the maximum of the bright band. This method seems questionable as the addition of an abrupt step to the field must change the gradient and field luminance (the latter two factors are known to influence the appearance of the Mach bands considerably).

Despite some differences in detail reported by the above workers there is agreement on the basic characteristics of the phenomena. The effects usually become more pronounced as the slope of the graded zone is increased. Relative luminances (intensities) of the bright and dark bands increase while they disappear when the slope is very small or very large. The width of the bright band becomes narrower with increasing slope but the dark band remains the same.

It should be stressed that these investigations were performed with constant field luminances. Consequently the width of the graded zone and the slope of the gradient

are not independent variables and thus one cannot say if the effects observed here depend on width or slope or even both.

Mach was only able to perform qualitative experiments to determine the effect of varying the luminances of the uniform fields. He observed his rotating discs in bright sunshine, in twilight and in candlelight; the bands always seemed to contrast equally well with any surrounding background of the same objective luminance as the bands themselves (although Mach does not give us any experimental details). Mach concluded that the bands remained unaltered when the objective luminance curve, $i = f(x)$ was changed to $i = qf(x)$ where q was a constant.

McCollough (1955) found that the width of the bright band increased with increasing bright field luminance when the slope of the gradient remained constant and Hartwig (1958) found that with increasing field luminance (which unfortunately also increased the slope of the graded zone with his particular experimental procedure) the intensity of the bright band increased. No such measurements on the dark band seem to have been made.

Ercoles and Fiorentini (1959) investigated the visibility threshold of the bright and dark bands as a function of the luminance of the neighbouring bright and dark fields.

Their measure of the threshold was the minimum slope m of the gradient between the bright and dark fields (with field luminances held constant) that was just sufficient to produce visible bands. Fig. 1.06 shows results for several luminance levels of the fields with constant ratios of bright field luminance to dark field luminance. At very low levels of L (for the bright band L refers to the bright field luminance and for the dark band L refers to the dark field luminance) the bands are not visible. As L is increased the bands become visible and the ratio $(\frac{m}{L})$ required for visibility decreases rapidly; that is, as the field luminance increases the necessary slope decreases. Over a short range of low intermediate luminances approximately the same slope is required to produce bands that are just visible. At still higher luminances the ratio $(\frac{m}{L})$ decreases very slowly with increasing L.

Mach reasoned that these phenomena occurred equally well for all colours since in his experiments with rotating discs white light was used and no subjective colouring was observed. Later Mach replaced the black sectors of his rotating discs with red and the white ones with yellow; he saw in place of the black bands only red bands and instead of the white bands green. One must proceed with caution here as other well known colour contrast effects, first

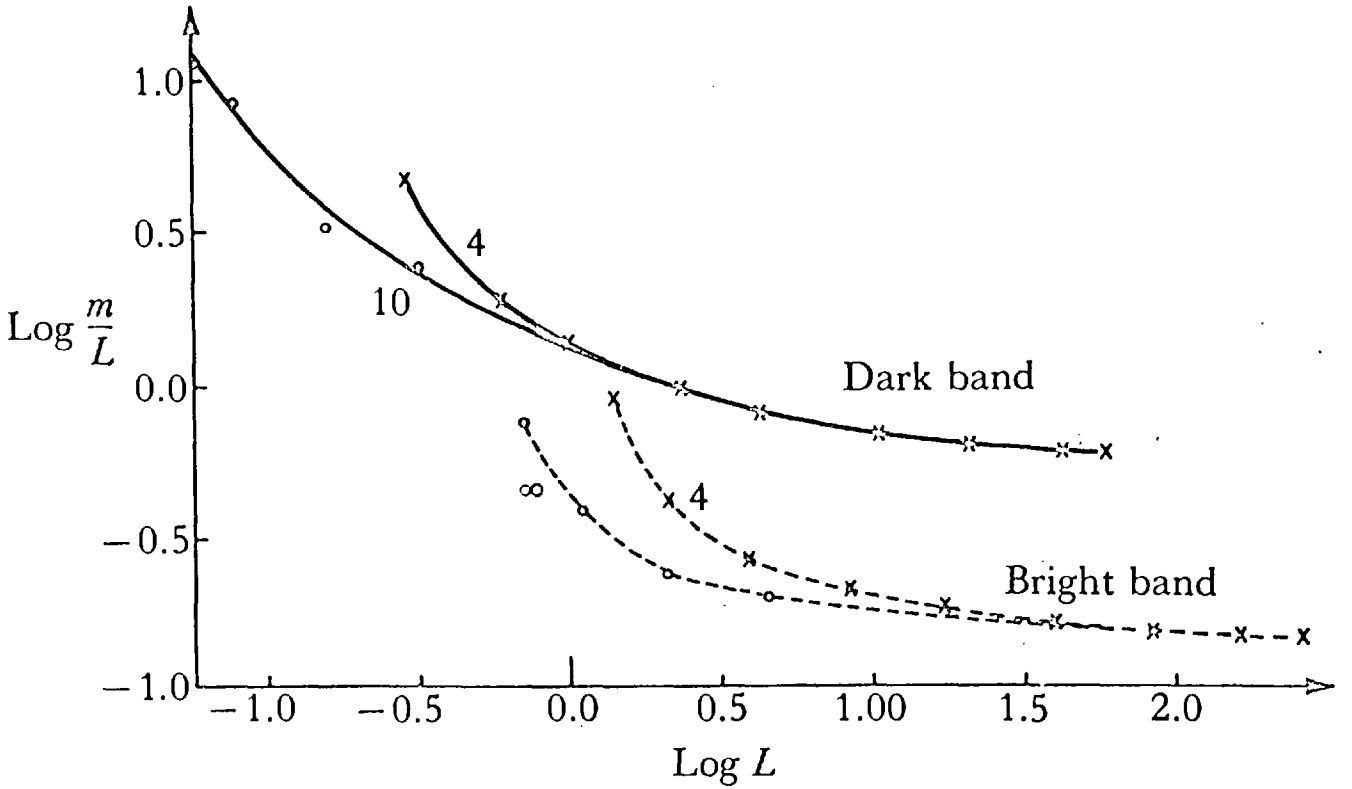


Fig. 1.06. *Log m/L plotted against L for the dark band (solid lines) and for the bright band (dashed lines). From Ercoles and Fiorentini (1959).*

noticed by Chevreul (1890) become prominent when two fields of different colours are juxtaposed.

Bittini, Ercoles, Fiorentini, Ronchi and Toraldo di Francia (1960) investigated the visibility of the moving Mach bands by oscillating a Mach pattern perpendicularly to the line of sight; the amplitude of the oscillations subtended between 0.25 degrees and 2 degrees at the observer's eye. These experiments show that the visibility of the Mach bands is improved by slow oscillatory movements (about two to four cycles per second). The visibility becomes very poor if the patterns are vibrated at frequencies greater than ten cycles per second.

Some workers have investigated the effect of short viewing times on the Mach bands. Cheatham (1952) has shown that sharp contours, of the type which produce Mach patterns, take a finite time (30 to 100 milliseconds) to be perceived and that the latency increases when the luminance is decreased. Mach bands are not visible during short presentations of the field (Fiorentini, 1956). From these results one may assume that the retinal inbibitory processes responsible for Mach effects take a finite time to act.

It appears, on reading Mach's first paper on the subject, that he was well aware of the small involuntary

eye movements that a human eye performs when an observer views a target. In order to rule out eye movements Mach illuminated photographs of his rotating discs with electric sparks produced by a Leyden jar. He found either that he could not see the bands at all or else that he could only see them very weakly and indistinctly. Mach reasoned that the illumination was so brief that significant eye movements were unlikely to occur. This conclusion would appear to be without much substance in the light of the results of the previous paragraph which concern short exposure times.

Ditchburn and Ginsborg (1952) have shown that contours and discontinuities in stabilised retinal images gradually fade from view and the visual field assumes a uniform appearance. Fiorentini and Ercoles (1957) used Ditchburn's apparatus to obtain a stabilised Mach pattern on the retina. They found that the Mach bands disappeared after about five seconds. We may conclude that eye movements are not necessary for the temporary observation of Mach effects but certain transient influences may enhance the visibility to a large extent.

Mathematical Models of Mach Effects.

Mach's first attempt to relate the objective

distribution of luminance I(x,y) with the observer's impression (or response) R(x,y) was given by the equation,

$$R = I - k\left(\frac{d^2I}{dx^2} + \frac{d^2I}{dy^2}\right)$$

where k is a constant. It had been noticed that where there was a flection in the curve of the objective luminance distribution the observer saw a region of marked brighter or darker luminance. Consequently Mach had guessed that the second derivative of the objective luminance distribution must play an important role in determining the response R. This equation was, of course, a gross simplification and did not agree very well with observed phenomena.

Mach believed that the phenomena could be explained on the basis of a reciprocal interaction between neighbouring elements on the retina. Modern electrophysiological evidence supports Mach's belief and we therefore turn to a discussion of his most refined mathematical model which includes modern ideas concerning inhibitory influences between neighbouring retinal areas. It was assumed that the retina was composed of elemental networks, in each of which there was a central excitatory component surrounded by an inhibitory component that diminished with distance. The magnitude of the influence of the excitatory centre and the inhibitory surroundings was proportional to the intensity

on the central element. The individual inhibitory influences exerted on any particular element were additive. The discharge of impulses into the optic nerve, the frequency of which is a measure of the subjective response (Hartline and Graham 1932), was the product of the intensity on that element and the ratio of the excitatory influence to the total of the inhibitory influences acting on it.

Suppose that any two retinal receptors j, p, with surface area Δa stand in a reciprocal relation which is determined by a function ϕ of the distance x_{jp} between them (fig. 1.07). The neural activity r_p discharged from a particular point P illuminated with intensity I_p is given by,

$$r_p = I_p \cdot \frac{I_p \sum_j \phi(x_{jp}) \Delta a_j}{\sum_j I_j \phi(x_{jp}) \Delta a_j} .$$

I_j is the intensity on each of the several separate neighbouring small areas Δa_j. $I_p \sum \phi(x_{jp}) . \Delta a_j$ is an excitatory term. If ϕ is the same function everywhere in the network and Δa is the same for all receptors $\sum_j \phi(x_{jp}) . \Delta a_j$ can be expressed as a single excitatory coefficient R. $\sum_j I_j \phi(x_{jp}) . \Delta a_j$ is an inhibitory term. We may write $\phi(x_{jp}) . \Delta a_j$ as a coefficient R_{pj} which

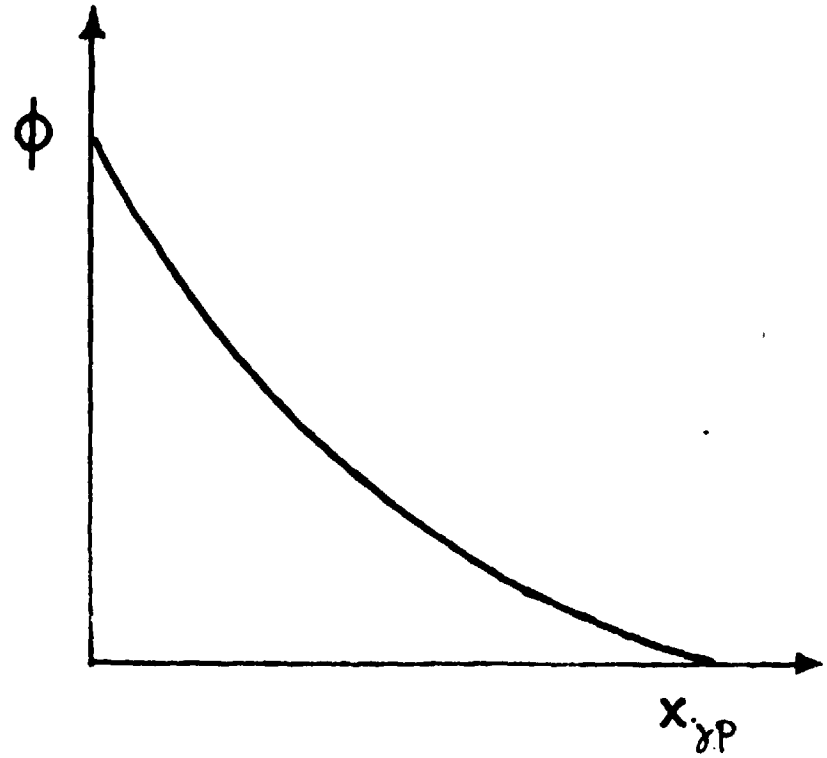


Fig. 1.07 The reciprocal relation between receptors. (after Mach)

represents the inhibitory action of each receptor j on p. Thus the inhibitory term may be represented as $\sum_j I_j . R_{pj}$.

Finally we may say, $$r_p = \frac{I_p . R}{\sum_j I_j R_{pj}}$$

Ratliff (1965) has used this equation to calculate the responses due to two contoured luminance distributions (fig. 1.08).

Fry (1948) assumes that optical stimulation of any receptor mosaic sets up a graded potential difference between the front and back of the retina (this assumption is based on electrophysiological studies performed by Granit (1933, 1946)). This potential difference is greatest at the point of stimulation and gradually diminishes with increasing distance from it. The magnitude of the potential difference at any point in the field is proportional to the magnitude of the stimulus generating it. Suppose that a retinal element of area da is stimulated with retinal illumination I. The stimulation sets up a graded potential difference at any neighbouring point of value dV and we assume that dV decreases about the point of stimulation according to a Gaussian law,

$$\frac{dV}{da} \propto I \exp\left(-\frac{s^2}{\sigma^2}\right)$$

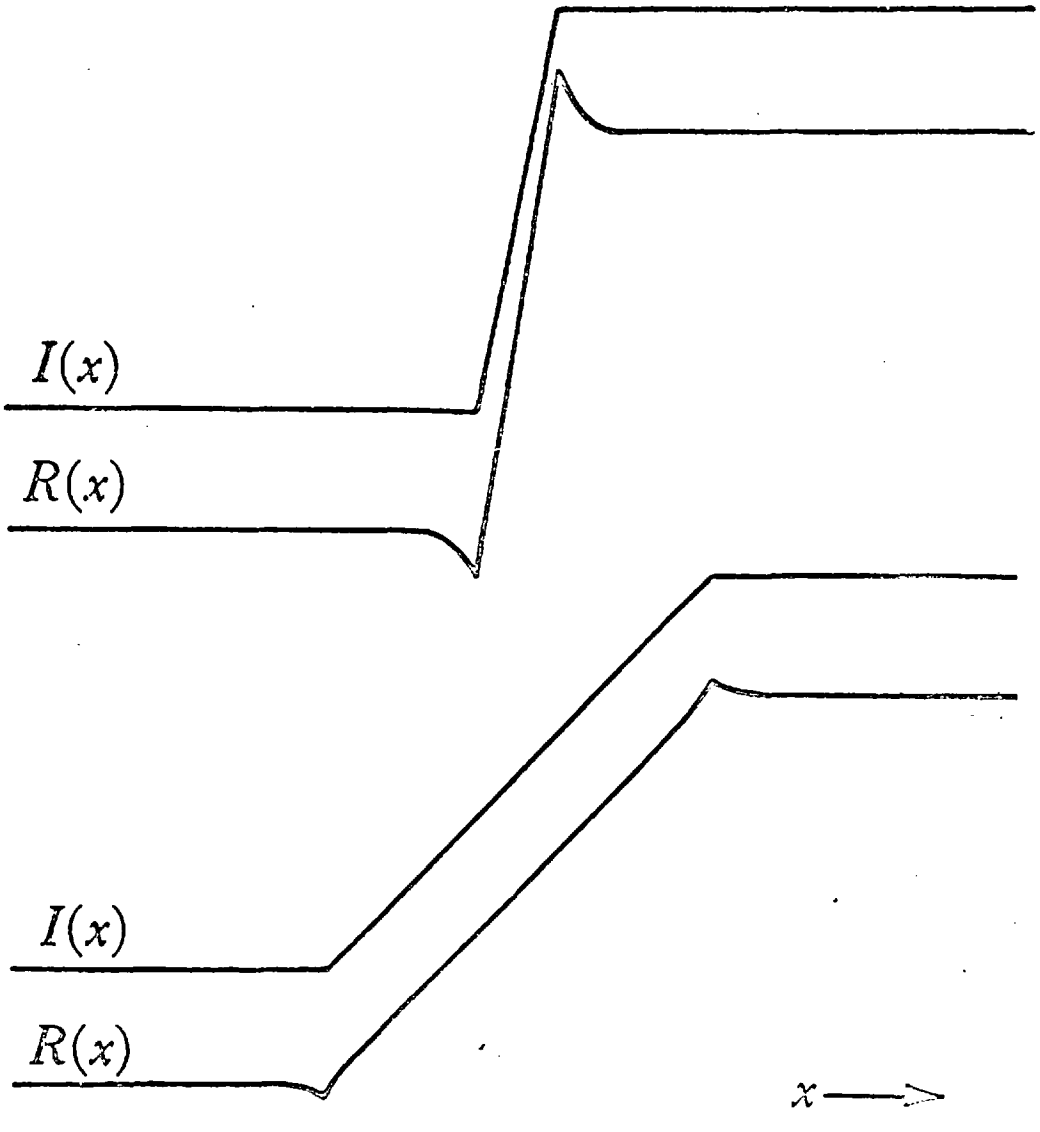


Fig. 1.08. Responses calculated with Mach's equation (Ratliff 1965)

where s is the distance between this point and the point of stimulation, and σ is a constant which is a measure of the extent of the inhibitory field around the point of stimulation. We may integrate all the inhibitory potentials produced by overlapping fields to obtain the potential difference V due to all the stimulated areas. Consider a general point (x,y) and a point P at (0,0) then,

$$V_p \propto \int_{-\infty}^{\infty}\int I(x,y)\ \exp\left(\frac{-(x^2+y^2)}{\sigma^2}\right)dxdy$$

(Since $s^2 = x^2 + y^2$ and $da' = dx.dy$).

The frequency r_p of the impulses discharged in the bipolar neurons at a particular point is assumed to be proportional to the logarithm of the excitatory influence which is directly related to the intensity I_p at that point and inversely related to the total inhibitory potential V_p. Finally Fry arrives at the relation,

$$r_p \propto \log\left(\frac{I_p}{1+V_p}\right)$$

and he has calculated this response for a blurred stimulus distribution (fig. 1.09).

Hartline and Ratliff (1954) suggested a model which is based on experiments performed with the eye of the Limulus crab. The eye consists of approximately 1000

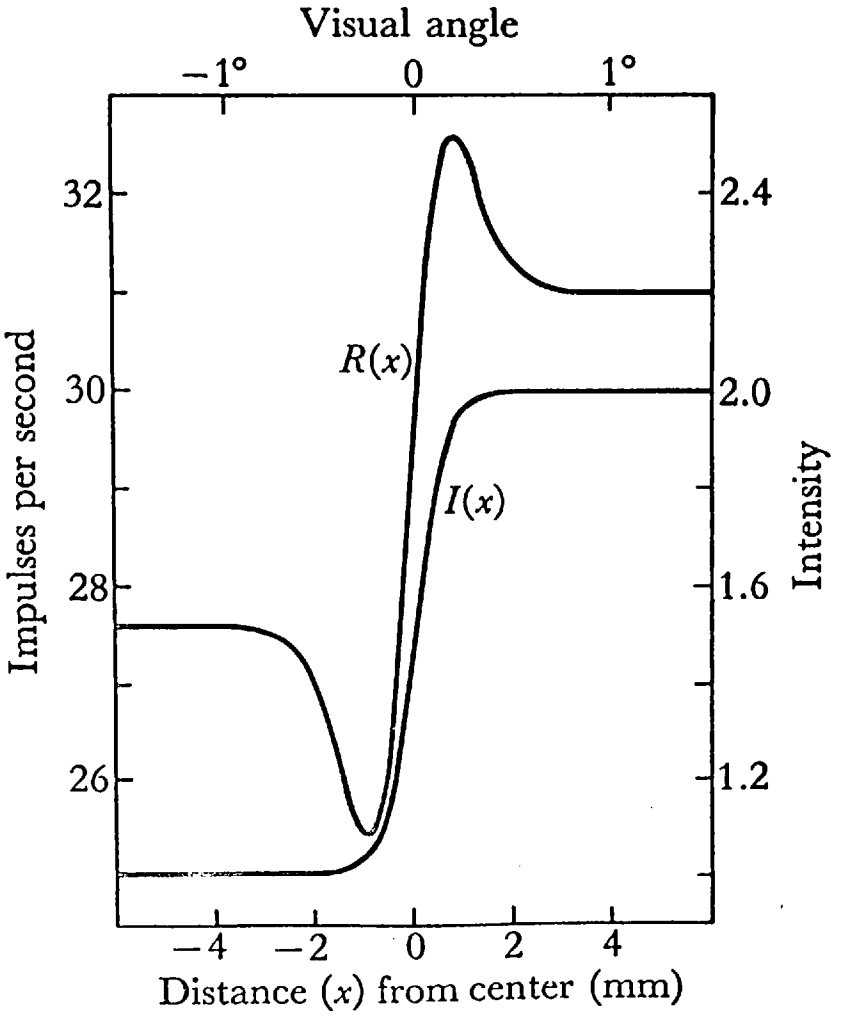


Fig. 1.09. *The response to a blurred stimulus distribution calculated with Fry's equation. From Fry (1948).*

ommatidia, each of which appears as a receptor unit. Using a microelectrode technique Ratliff and Hartline measured the frequency output from individual ommatidia; they found that inhibitory influences were exerted mutually among the ommatidia so that each was inhibited by its near neighbours. The magnitude of the inhibition exerted on a particular element depended upon the response of neighbouring elements rather than upon the stimulus to them.

Consider two neighbouring ommatidia 1, 2; their activity may be described by the following simultaneous equations:

$$r_1 = e_1 - k_{12}(r_2 - r_{12}^{\circ})$$

$$r_2 = e_2 - k_{21}(r_1 - r_{21}^{\circ})$$

r denotes the frequency output of a receptor unit, e is the excitation (illumination) supplied to the receptor, r° is the threshold frequency that must be exceeded before a receptor can exert any inhibition and k is an inhibitory coefficient. r_{12}° is the frequency of receptor 2 at which it begins to inhibit receptor 1 and r_{21}° is the reverse. k_{12} is the coefficient of the inhibitory action of receptor 2 on receptor 1 and k_{21} is the reverse. For an ensemble of receptors the response of receptor p is

determined by n simultaneous equations and we may write,

$$r_p = e_p - \sum_{\substack{j=1 \\ j \neq p}}^{n} k_{pj}(r_j - r_{pj}^{\circ})$$

With increasing distance the threshold r_{pj}° increases and the coefficient of inhibitory action k_{pj} decreases. All solutions of the above equation must be positive as negative frequency outputs have no meaning and therefore we must impose the following restrictions:

$$\text{if} \quad e_p < \sum_{j=1}^{n} k_{pj}(r_j - r_{pj}^{\circ}) \qquad \text{then } r_p = 0;$$

$$\text{if} \quad r_{pj}^{\circ} > r_j , \qquad r_p = e_p.$$

Ratliff and Hartline demonstrated that the response of the Lumulus' eye agreed with that predicted by their model and the response to a step-like area of illumination displayed bands reminiscent of the Mach effect as seen in human vision (fig. 1.10).

Taylor (1956) assumed a receptive field (that is the area of the receptor mosaic that must be illuminated to cause a discharge of nervous impulses) that had a sensitive central excitatory region surrounded by a less sensitive

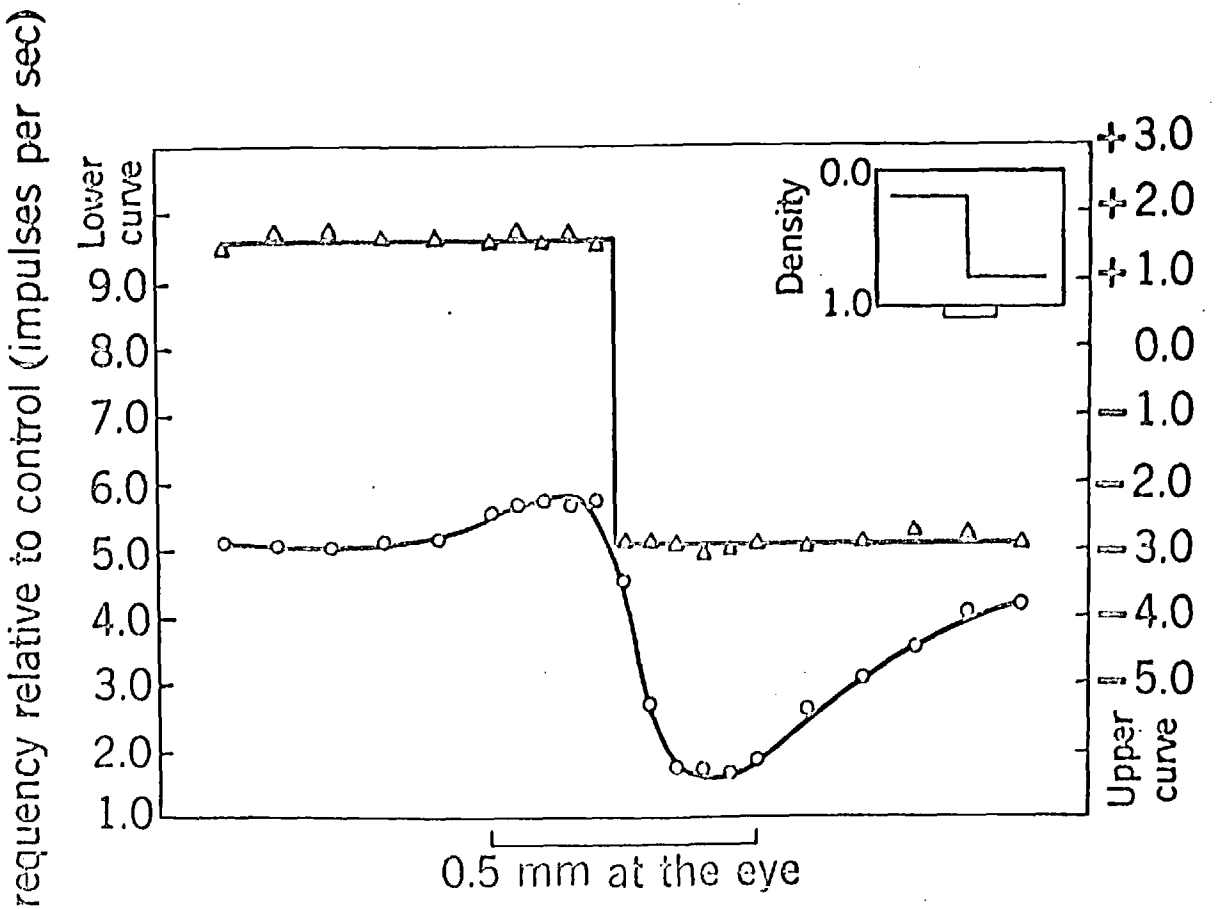


Fig 1.10. Response of the Limulus eye (Hartline and Ratliff 1954)

inhibitory region. It was further assumed that the relationship between the logarithm of the retinal illumination and the frequency of nervous discharge (in the absence of interaction) is linear. Consider a single row of units infinitely long so that end effects can be neglected: the response r_p to a given input e_p of a particular unit is then given by the equation,

$$r_p = e_p + k \sum_{p-s}^{p+s} r_j$$

where k and s denote the average magnitude and spread of the interaction respectively. The gain of each unit is normalised to unity so that if $k = 0$, the response r_p is equal to the excitation e_p resulting from the illumination on the receptor. To simplify it is assumed that the coefficient of the action of each element j on a particular element p is uniform over the distance $\pm$ s from p or, in the two dimensional case, within the circle of radius s centered on P. Taylor suggests that at low levels of illumination the sign of k might be positive (to account for summative excitatory effects noticed by Beitel in 1936) while at a higher level of illumination k would become zero and at a still higher level it would become negative so that inhibition would result. Fig. 1.11 shows responses

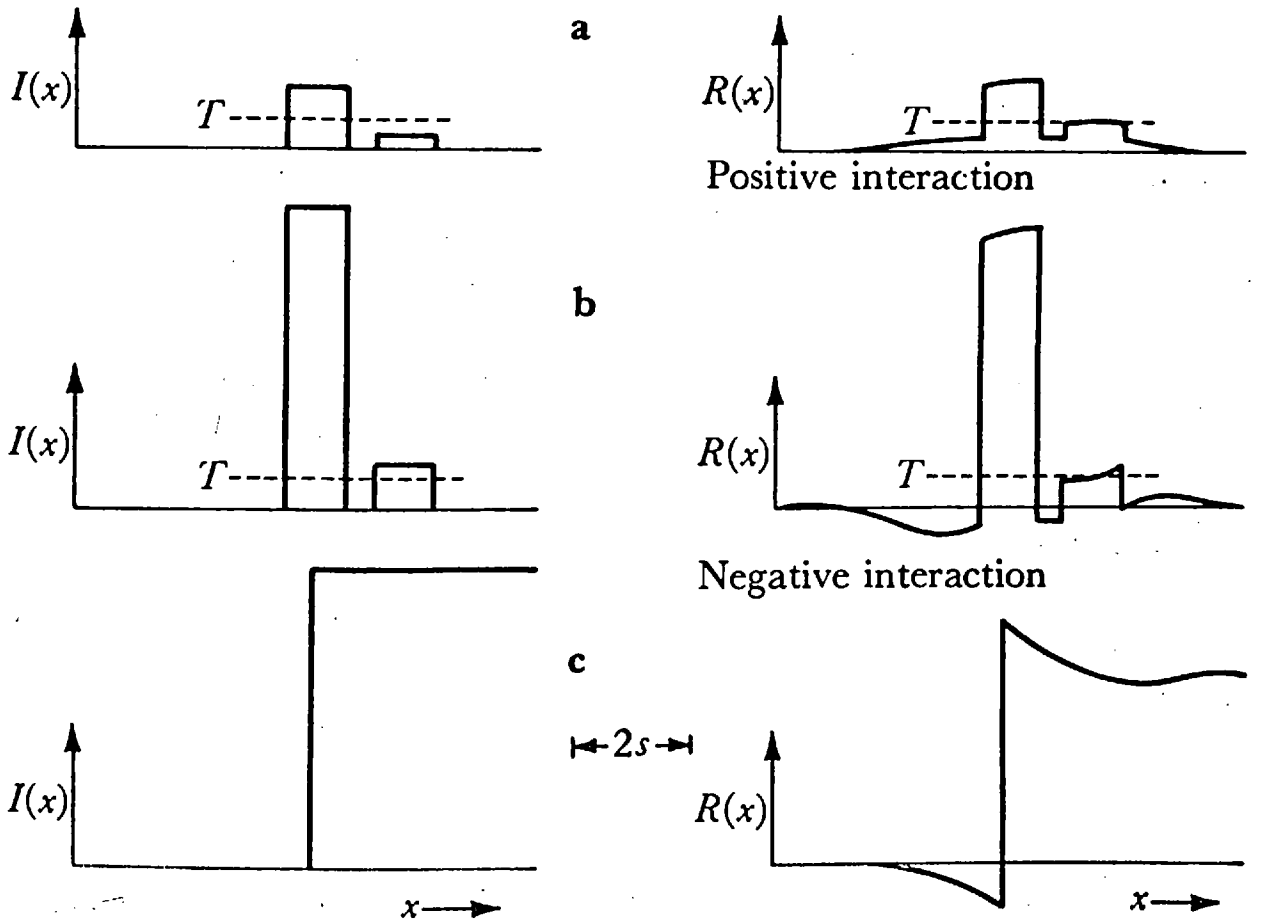
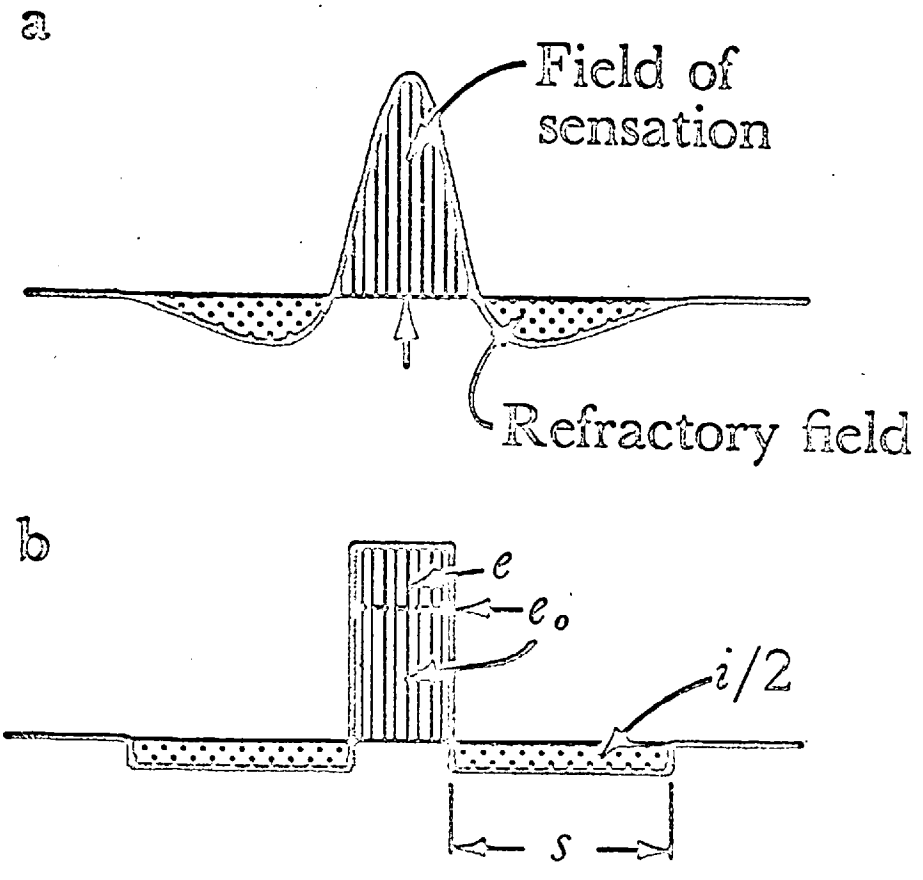


Fig. 1.11. *Responses to various patterns of illumination calculated with Taylor's equations.*

Fig. 1.12. Bekesy's neural unit



to patterns of illumination calculated with Taylor's equations.

Like Mach, Bekesy (1960) concluded that every stimulus on the receptor mosaic produces a local field of sensation (or excitation) surrounded by a more extended refractory (or inhibitory) field. Bekesy called the combination of these opposed influences acting as a whole a "neural unit". For purposes of calculation use was made of a simplified rectangular neural unit (fig. 1.12). Such a neural unit, when employed to evaluate the subjective sensation, produces two Mach bands near the discontinuities of a step-like stimulus.

The investigations of Ludvigh, Green, Ercoles and Fiorentini.

Ludvigh (1953) investigated the relationship between the retinal luminance distribution and the location of subjective contours. He computed the external luminance distribution necessary to give a desired retinal distribution under known experimental conditions. To achieve this he used an artificial pupil of 1 mm. in diameter and a monochromatic source of illumination; such an arrangement reduced eye aberrations to an insignificant amount.

Ludvigh's experiments may be summarised thus:

a) The lowest derivative with respect to retinal distance

which has significance for the perception of contours is the second derivative.

b) A Mach band will be perceived symmetrically distributed about the point where the second derivative has a stationary value.

c) The width of a band will be smaller the greater the value of the fourth derivative.

d) For the formation of the Mach bands the second derivative, at its stationary value, must have some absolute minimum value.

To explain the subjective contour perception (or appearance of Mach bands) Ludvigh assumed the existence of three kinds of elements in the retina:

a) those responsible for the absolute response to light,

b) those responsible for the discrimination of luminance,

c) those concerned with the perception of contours.

The third set would consist of "on-off" elements (Granit 1955) stimulated via either ocular or head tremor so that the rate of change of stimulation would be maximal at the points of stationary values of second derivatives.

Green (1958) postulated the existence of two kinds of elements in the retina: a first set having a response proportional to the local stimulation E and a second set whose response is proportional to $\bar{E}$ the average of E over

a certain region of the retina. The response of the second kind of elements would inhibit the action of the first set so that the resulting response is proportional to $(E-\bar{E})$. Green assumed that a contour is perceived where the first derivative of $(E-\bar{E})$ with respect to distance has a sharp variation. Green has proved for the one-dimensional case that within a small averaging region the difference $(E-\bar{E})$ can be sufficiently approximated by the sum of two terms proportional to the second and fourth derivatives respectively. Green remarks that the ratio $(\frac{E-\bar{E}}{E})$ instead of $(E-\bar{E})$ is better for the description of contour formation when regions of widely differing E are viewed.

Ercoles and Fiorentini (1959) reached the following conclusions after some extensive experiments:

a) At low luminance levels the mechanism responsible for the perception of subjective contours becomes less sensitive and a higher value of $\frac{E-\bar{E}}{E}$ is required to perceive them.

b) The minimum value of $(\frac{E-\bar{E}}{E})$ required for the dark band to be perceived is about four times higher than for the bright band to be seen.

c) The dark band is perceived at lower levels of illumination than is the bright band.

d) Results at different contrast levels cannot be

explained unless, at low levels, the perception of contours does not depend only on the ratio $(\frac{E-\bar{E}}{E})$.

Applications of the Optical Transfer Function to the problem of Mach bands.

The optical transfer function, $A(\nu)$, tells us how the image contrast of a series of sinusoidal gratings, of spatial frequency ν change as they are imaged through an optical system; the object gratings are always assumed to be illuminated incoherently. Since any two dimensional distribution of intensity may be represented by a series of sine gratings (Fourier's theorem) we can calculate the attenuation and phase shifts of the various component gratings as they pass through the optical system and hence we can arrive at the form of the image by summing all the attenuated components, due regard being made for any phase shifts that have occurred.

If the image of a point were itself a point there would be perfect one to one correspondence between the object and image. All the Fourier components in the object would appear with unreduced contrast in the image and with no phase shift. This is an ideal image. In practice, even in the absence of aberrations, diffraction will cause light from any point in the object to spread

in the image. Consequently more light is lost from the maxima of intensity to the regions of minima, with a consequent loss of contrast. The image formed by a perfect system, having no aberration but being diffraction limited, will show a frequency response decreasing with increasing spatial frequency (i.e. the high frequencies are more attenuated than the low ones). Aberrations cause a further reduction in contrast and may also cause a spatial phase shift (fig. 1.13).

More explicitly the optical transfer function is defined as the Fourier transform of A(x) the line spread function (the image of a line):

$$A^{\#}(\nu) = \left|A^{\#}(\nu)\right| e^{i\theta(\nu)} = \int_{-\infty}^{\infty} A(x)\exp[-2\pi i \nu x]dx$$

(Duffieux 1946)

where x is a spatial coordinate ν is the spatial frequency of the component grating in lines or sine cycles per millimetre, θ is the phase shift in radians of the image from its geometric image position and the symbol $\#$ denotes a Fourier transform operation. The above expression is called the complex transfer function because it includes a phase function $\theta(\nu)$ as well as the amplitude function $\left|A^{\#}(\nu)\right|$. The phase shift occurs when

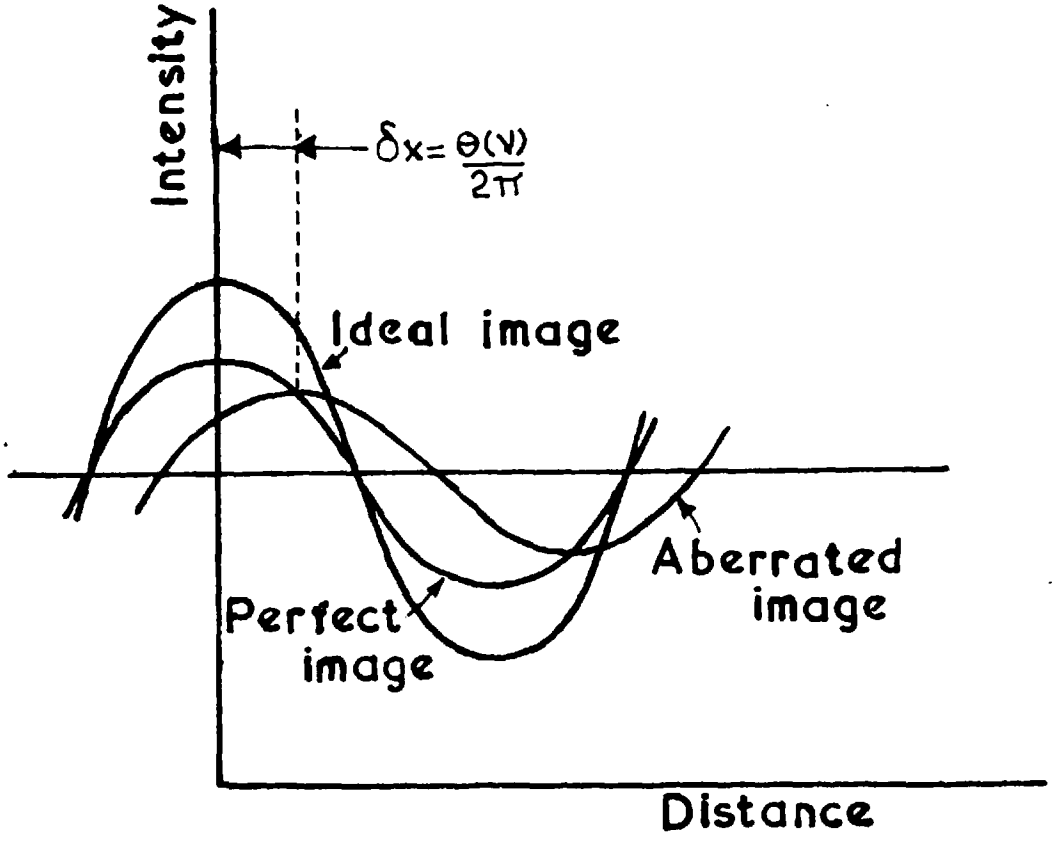


Fig. 1.13 Image of a sine grating

the spread function is asymmetrical. When the spread function is symmetrical, as for example in well corrected systems, $\theta(\nu) = 0$ and we are left with a Fourier cosine transform $A^{\#c}(\nu)$,

$$A^{\#c}(\nu) = \left| A^{\#c}(\nu) \right| = \int_{-\infty}^{\infty} A(x)\cos 2\pi\nu x \, dx \qquad (1.01)$$

Now if a one dimensional object distribution of luminance $O(x)$ is imaged to give an image distribution $I(x')$ we can say,

$$I(x') = \int_{-\infty}^{\infty} A(x'-x)\, O(x)\, dx \qquad (1.02)$$

Furthermore by taking the Fourier transforms of $I(x')$, $A(x)$ and $O(x)$ it can be shown that,

$$I^{\#}(\nu) = A^{\#}(\nu).O^{\#}(\nu)$$

therefore, $$A^{\#}(\nu) = \frac{I^{\#}(\nu)}{O^{\#}(\nu)} \qquad (1.03)$$

where $A^{\#}(\nu)$ is the sine-wave response of the imaging system and is equivalent to the Fourier transform of the line spread function. It should be pointed out that the validity of equations (1.02) and (1.03) for different object and image distributions is dependent on the system

being linear and isoplanatic (Hopkins 1962). The system is said to be linear if, when two separate object distributions $O_1(x)$, $O_2(x)$ give image distributions $I_1(x')$, $I_2(x')$ respectively then an object distribution $O_1(x) + O_2(x)$ yields an image $I_1(x') + I_2(x')$. A system is isoplanatic when the aberrations remain constant over the image field.

Menzel (1959) evaluated the composite transfer function $W(\nu)$ (eye plus visual pathway) by measuring the relative visibility of several sinusoidal distributions of illumination with different spatial frequencies. The composite transfer function not only considers the optical blurring of the eye lens but also the effect of the neural processes which occur in the visual pathway to the visual cortex. Using the composite transfer function $W(\nu)$ to evaluate the line spread function, Menzel used equation (1.02) to calculate the subjective distribution that would result from the objective distribution in a typical Mach pattern. Qualitatively the calculated results agree with the distribution actually seen in the Mach pattern, with the maxima and minima appearing as expected. There were two important discrepancies: the calculated widths of the Mach bands were much larger than those observed and the calculated bands were symmetrical, while the observed bands were not. In a later paper (Menzel et al, 1965) theoretical predictions

of Mach band phenomena and observations were shown to agree quite well when the contrast between the bright and dark fields was small. Fig. 1.13 shows Menzel's results for $W(\nu)$. $W(\nu)$ is normalised so that $W(o) = 1$. ($W(o)$ implies an object of constant luminance with no spatial variations). $W(\nu)$ remains constant for the very low spatial frequencies (for ν less than $\frac{1}{2}$ cycle per degree) and then climbs to a maximum value for $\nu = 5$ cycles per degree after which there is a steady decrease to a cut-off at about 60 cycles per degree which is not shown on the figure.

Lowry and de Palma (1961) measured the objective luminance distributions $O(x)$ in various Mach patterns and the corresponding distributions $I(x)$ seen by the observer. An analysis of the spatial frequencies contained in these distributions yielded their Fourier transforms so that the composite transfer function $W(\nu)$ could be calculated. Using equation 1.03

$$W(\nu) = \frac{I^{\#}(\nu)}{O^{\#}(\nu)} .$$

The general form of the transfer function resembles the one calculated by Menzel but the correspondence between the two functions is far from exact.

Bryngdahl (1964) made similar measurements to determine $W(\nu)$ and suggested that better results were obtained by

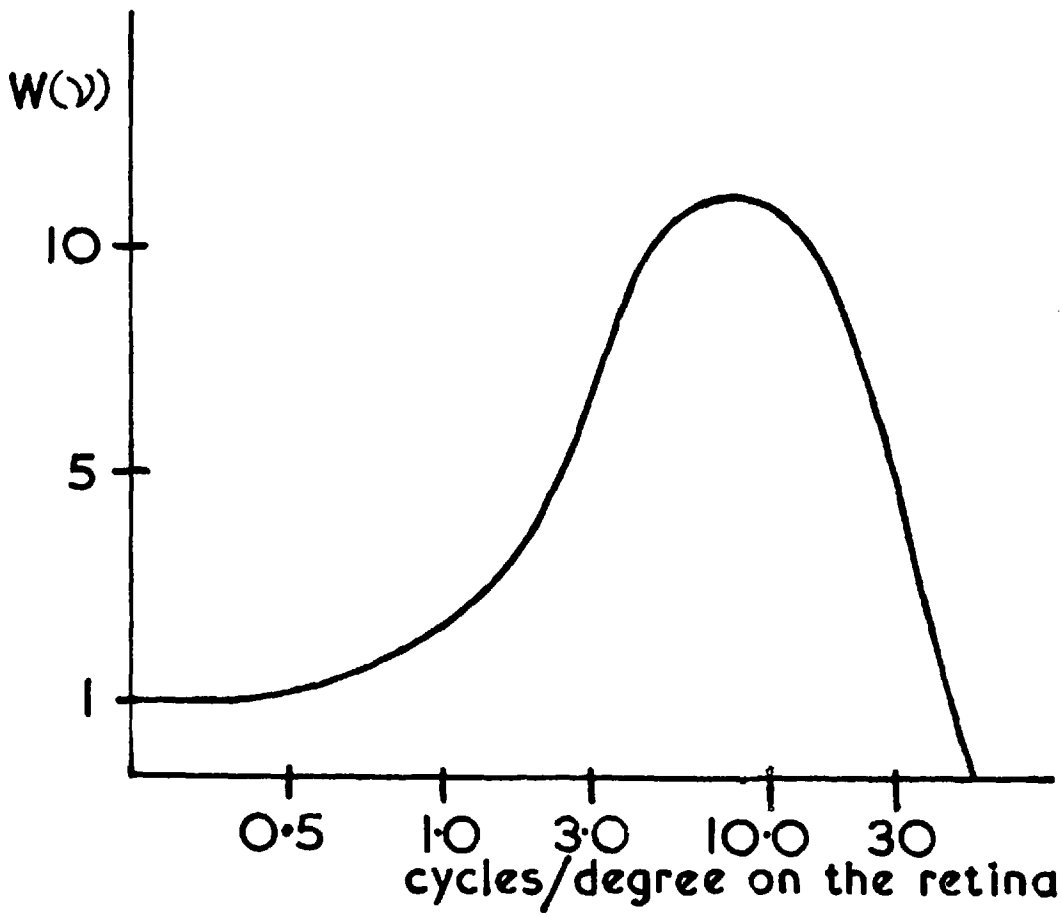


Fig. 1.14 Composite transfer function for the human visual system. (after Menzel)

operating on the logarithm of luminance. Bryngdahl notes, however, that this treatment does not hold for values of ν greater than 1 cycle per degree which is quite a low value for the eye.

It has been shown by Marimont (1963) that the Mach effect is in general a non linear phenomenon so that Fourier theory must be inadequate and this must account for some of the discrepancies found between different workers who used different object and image distributions. (Note that equation 1.03 only yields the same value for $W(\nu)$ when different object and image distributions are used when the imaging system is linear and isoplanatic.

In an interesting paper concerning the optical quality of the eye, Campbell and Gubisch (1966) considered critically the widely held view that the function of the Mach effect is to sharpen blurred borders, thereby compensating neurally for the poor optical quality of the eye. Their results, obtained from measuring the line spread function of the eye indicated that less blur was occurring optically than previously shown. Furthermore they showed that any effect of image sharpening was confined below 10 cycles per degree. For higher spatial frequencies, which help to define sharp edges, the neural mechanisms seem to degrade rather than sharpen the image.

Chapter II

The Mach Effect in Microscopy

Early Work.

In 1960 W. N. Charman, working at Imperial College, noticed gross discrepancies between the visual and physical images, as measured with the aid of a photo-electric microscope and it occurred to W. T. Welford that this might be due to the Mach effect. Subsequent work by Charman and Watrasiewicz (1964) confirmed this and exposed the great differences which may exist between visual and physical images; slight flections, which are extremely difficult to measure photo-electrically, are transformed visually into easily observable bands (sometimes termed "fringes"). The Mach effect observed in microscopy differs radically from what is found in macroscopic studies; in the latter case the diffraction structure in the physical image is not noticed, since it is on too small a scale on the retina, but in microscopy the magnification is so great that this structure is easily resolvable so that a simple object, like a straight edge, acquires a variety of subtle flections, many of which are taken up and accentuated by the Mach effect; in fact a multiple band structure is seen.

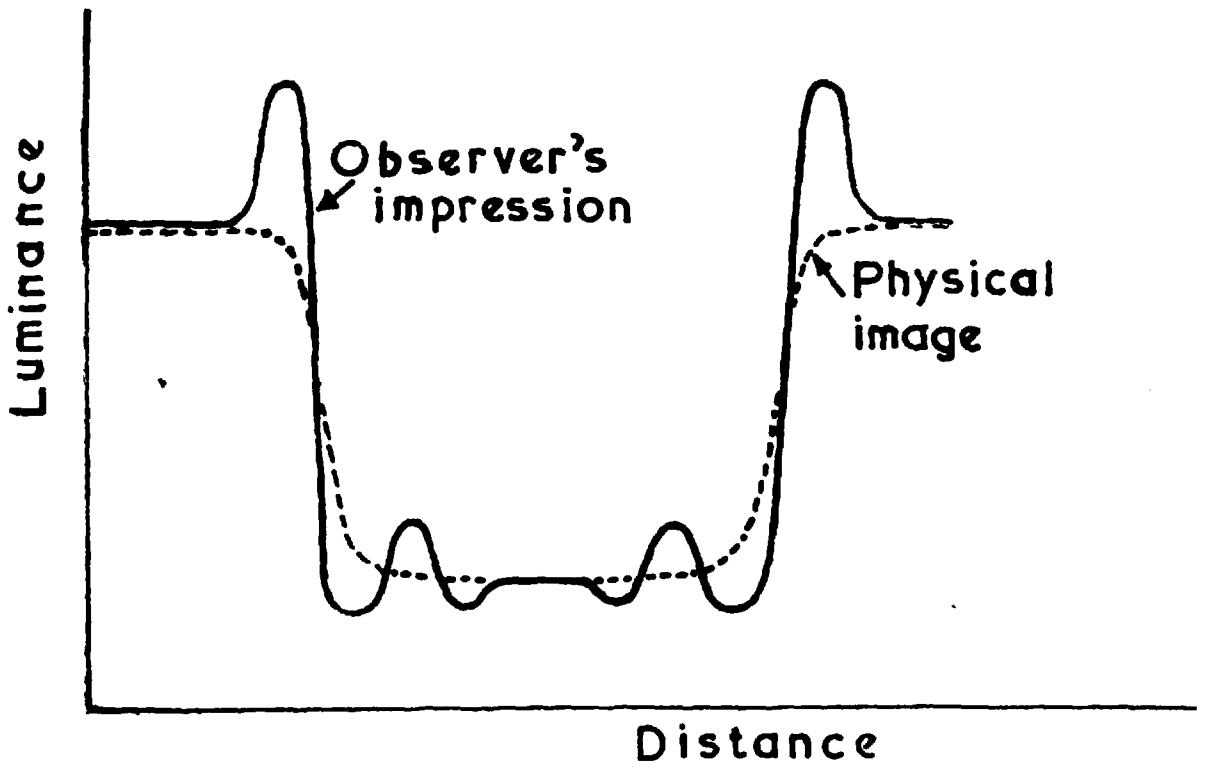


Fig. 2.01 Primary microscope image of an opaque particle

Fig. 2.01 shows the image of an opaque, disc-like, particle as formed in a microscope; the physical image is compared with the observer's impression. The images of discs and apertures always appear to be ringed by these subjective bands and they are often attributed solely to diffraction effects. In general at least three bands are seen at an edge and they subtend a total angle of about half a degree at the observer's eye. The Mach bands become clearly visible when critical measurements are made at the borders of the images of bright or dark regions.

Watrasiewicz (1963) observed the image of a straight edge, illuminated with monochromatic light, with a high power oil immersion objective (fig. 2.02). Qualitatively the Mach effects seen with high and low power objectives are the same. In general an observer sees a bright band, brighter than the clear bright field, then a dark band which is darker than the continuously dark field followed by a series of weaker bright and dark bands which finally merge into the continuous dark field. Watrasiewicz investigated the position and widths of the Mach bands as a function of retinal illumination wavelength of the light, object contrast and polarisation.

For very low values of retinal illumination (15 trolands) the bands disappeared and as the illumination

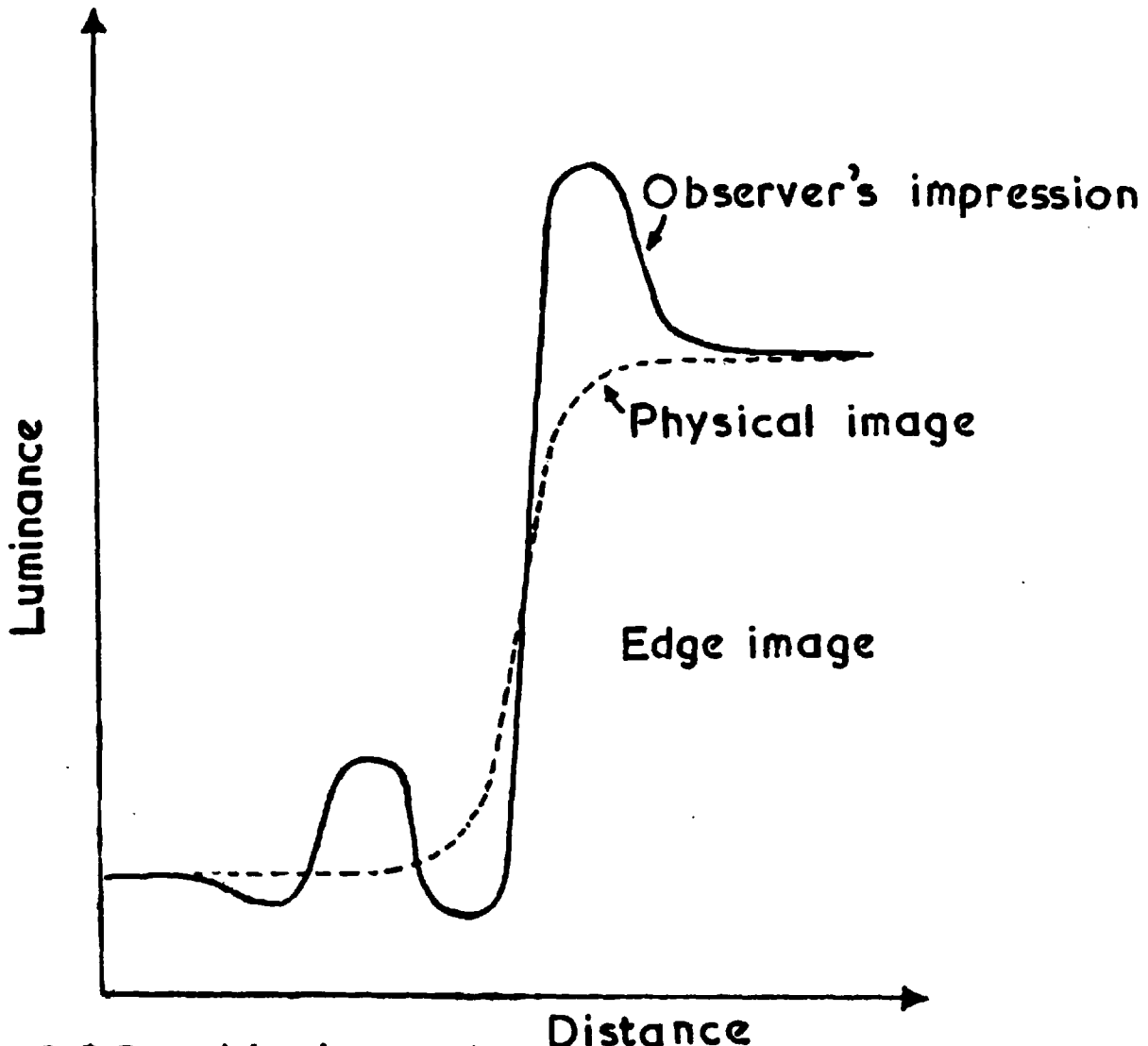


Fig. 2.02 Mach bands seen with a microscope. (after Charman and Watrasiewicz)

was increased the band positions moved towards the continuously bright field. There also seemed to be changes in band widths as well although it is very difficult to pick out any general trend in this respect.

Watrasiewicz showed that if the retinal illumination was kept constant the bands moved towards the bright field as the wavelength of the light was reduced although the range of wavelengths was restricted between 4700Å and 6500Å. It seems a pity that no measurements were made with blue-violet light (4400Å-4500Å) as one would expect the most interesting variations, if any, to occur here. Willmer (1961) has cited a formidable list of peculiarities which occur in vision with the blue wavelengths, among which are that the receptive fields of the cells involved in the blue mechanisms are very much larger than those involved in the red and green mechanisms, rods may participate in colour vision at these wavelengths and the blue mechanism has a considerably lower quantum efficiency than the receptors responsible for the red and green mechanisms.

As the contrast of the edge object decreased the secondary bands became more faint and then disappeared. If the contrast was further decreased the bright band, brighter than the clear field, became narrower and more faint while the band darker than the clear field, became

narrower and more faint while the band darker than the clear field became wider and less dark; eventually with decreasing contrast both bands disappeared.

Watrasiewicz noticed no significant changes in brightness or position of the bands with respect to different modes of polarisation when objectives of low N.A. (< 0.5) were employed. For image formation when a high N.A. (> 0.5) objective is employed slight changes in the physical image distribution occur when the mode of polarisation of the light is varied (Watrasiewicz 1965) and consequent small changes in the Mach band positions can be detected although there is no evidence to suggest that with a given retinal, physical distribution of light the mode of polarisation affects the Mach effect in any way.

Estimates of the brightnesses of the bright bands were made possible by using a photometric arrangement similar to that used by Lowry and de Palma (1961) who carried out measurements on the less complex Mach effect which is seen on a macroscopic scale where only one bright and one dark band are seen. Charman and Watrasiewicz (1964), using a low power dry objective, found that the bands moved towards the bright side of the edge when the condenser aperture was reduced (thereby increasing the spatial coherence of the light illuminating the object) and also the number of bands

increased; the retinal illumination was kept constant by increasing the voltage supplied to the lamp as the condenser aperture was reduced.

The subjective brightnesses of the bright Mach bands were measured when different powered eyepieces were employed. An increase in eyepiece power increased the scale of the retinal image; the same image contours would therefore cover a greater number of receptors. When a greater number of receptors are involved in the retinal interaction the bright bands should appear less bright because of the greater inhibitory factor and this was shown to be the case. Also Watrasiewicz and Charman showed that, with increasing eyepiece power, the bands' positions moved to the brighter side of the edge.

According to Ludvigh (1953) the bright and dark bands should be seen where the second derivative of luminance with respect to distance has minima and maxima respectively. Results for three observers reported by Charman and Watrasiewicz (1964) show reasonable agreement with this theory. However the results obtained by these workers, which showed wide variations of band positions with level of illumination, wavelength and eyepiece power mean that, in general, the amount of agreement with Ludvigh's theory would be rather less than what they originally reported.

R. Leelawongs (1964) showed that the diameter of the eye pupil plays an important role in seeing the multiple Mach bands. She illuminated a sharp straight edge incoherently and showed that at least three bands were seen when artificial eye-pupils less than 0.85 mm. in diameter were employed. With a pupil larger than 1 mm. in diameter only one bright and one dark band were seen; also the position of the bands moved towards the bright field as the eye pupil was increased (fig. 2.03).

The work which has been described so far in this chapter suggests that the Mach effect in microscopy is a very complex visual phenomenon. These results have shown that the Mach bands change their positions and brightnesses for very slight perturbations in the diffraction image of an edge on the retina.

Not only have microscopists mistaken Mach bands for diffraction fringes but it is quite conceivable that the bands have been mistaken for actual detail in the object, the dark bands closely resemble biological membranes. Mach effects must modify the image profoundly in phase-contrast microscopy where very complicated physical images occur (consider the curious haloes seen around particle images for example). However Charman and Watrasiewicz (1964) note that the Mach effect may aid the detection of

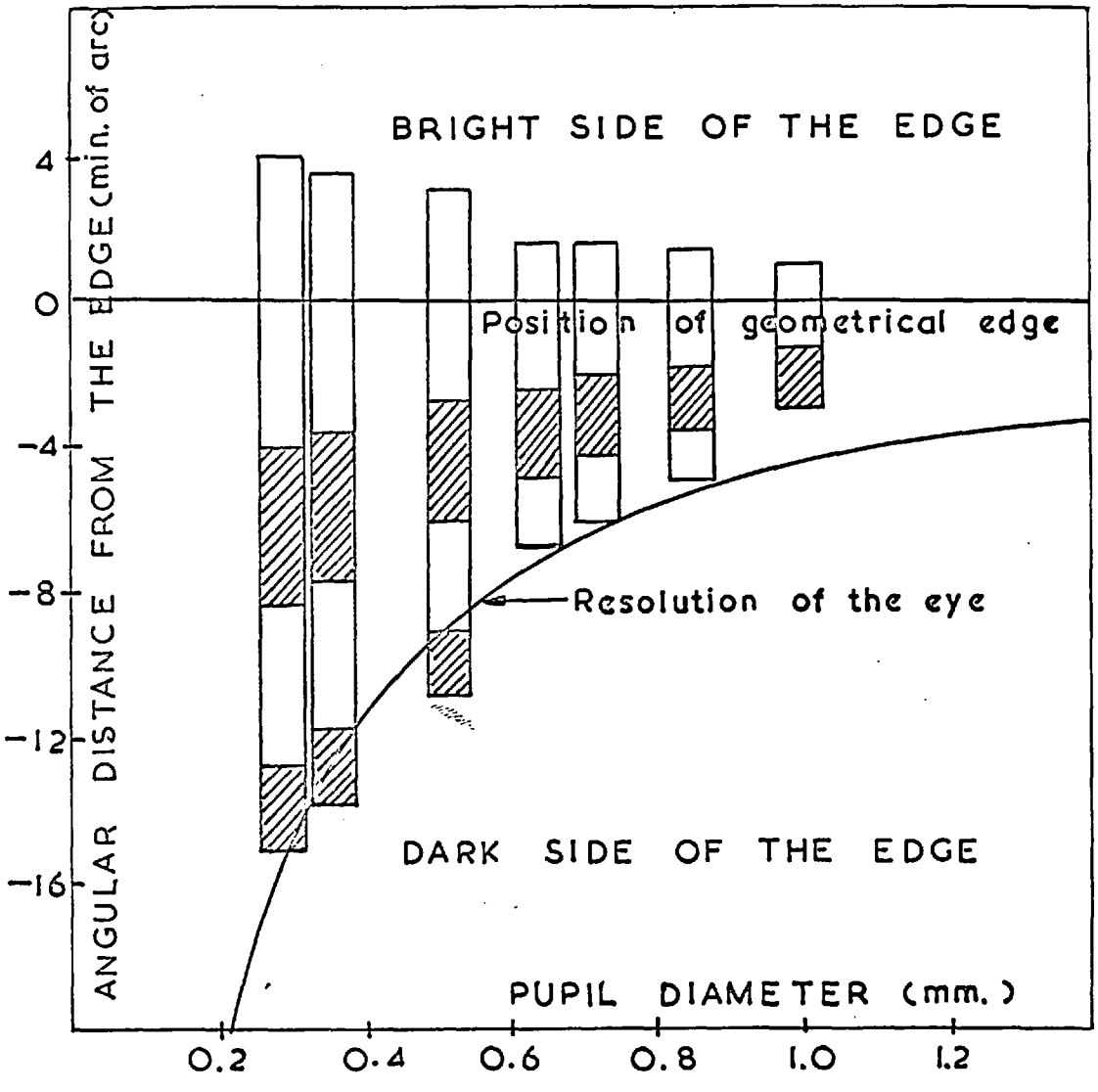


Fig. 2.03. The influence of eye pupil diameter on the width and position of Mach bands; observed in incoherent light, retinal illumination 682 trolands.

(after Leelawongs 1964)

details in the image since edge sharpness is enhanced. This statement implies that the retina, as the first step in the visual pathway, emphasises details which are then presented to the higher centres of detection and recognition located in the brain. The observations of Campbell and Gubisch, which are described in Chapter I, should also be considered in this respect.

Scope of the author's work.

It is well known that certain visual phenomena exhibit significant variations between different observers. In this respect the case of individual colour differences is perhaps the most striking and best known (W. D. Wright 1946). Fiorentini and Radici (1957, 58) have noted individual differences with regard to the Mach effect on a macroscopic scale. Watrasiewicz (1964) thought that individual differences between observers would be unlikely for the case of the Mach effect in microscopy; he performed tests on only three people, besides himself, and this would seem to have been too small a sample from which to draw an inference of this kind. The author carried out tests (described below) to investigate the variation of the Mach effect, as it occurs in microscopy, between some twenty observers.

Of particular interest to the author was Ludvigh's

hypothesis which states that an observer should see a Mach band where the second derivative of luminance with respect to distance was a stationary value. The efficacy of this theory in predicting Mach bands is looked at critically in this thesis.

It is particularly important, from the point of view of the microscopist, to know what kind of errors are introduced by the Mach effect in the determination of the visual edge when particles are sized and these will also be considered.

As a result of the survey performed with twenty people two further interesting fields of study, concerning defocusing and the influence of retinal location, emerged. Also some measurements performed with a binocular eyepiece on five subjects are considered.

Chapter III

Apparatus and Techniques.

Introduction

In order to study Mach effects in microscopy quantitatively apparatus is required firstly to determine the physical distribution of light intensity in the primary image of an object and secondly to measure the subjective appearance (as modified by the Mach effect) of the primary image when viewed through an eyepiece. The first requirement was met by employing a photo-electric microscope similar to that constructed by Charman (1961) and later modified by Watrasiewicz (1964) while the subjective appearances of images were measured by using the techniques employed by Charman and Watrasiewicz (1964) although for more accurate brightness matches of the Mach bands it was found necessary to employ a different method of varying the brightness of the comparison slit in the visual photometer.

A schematic representation of the apparatus is shown in fig. 3.01 where the arrows indicate the direction in which the light travels. The apparatus represented in the figure by the circuit joining the first monochromator

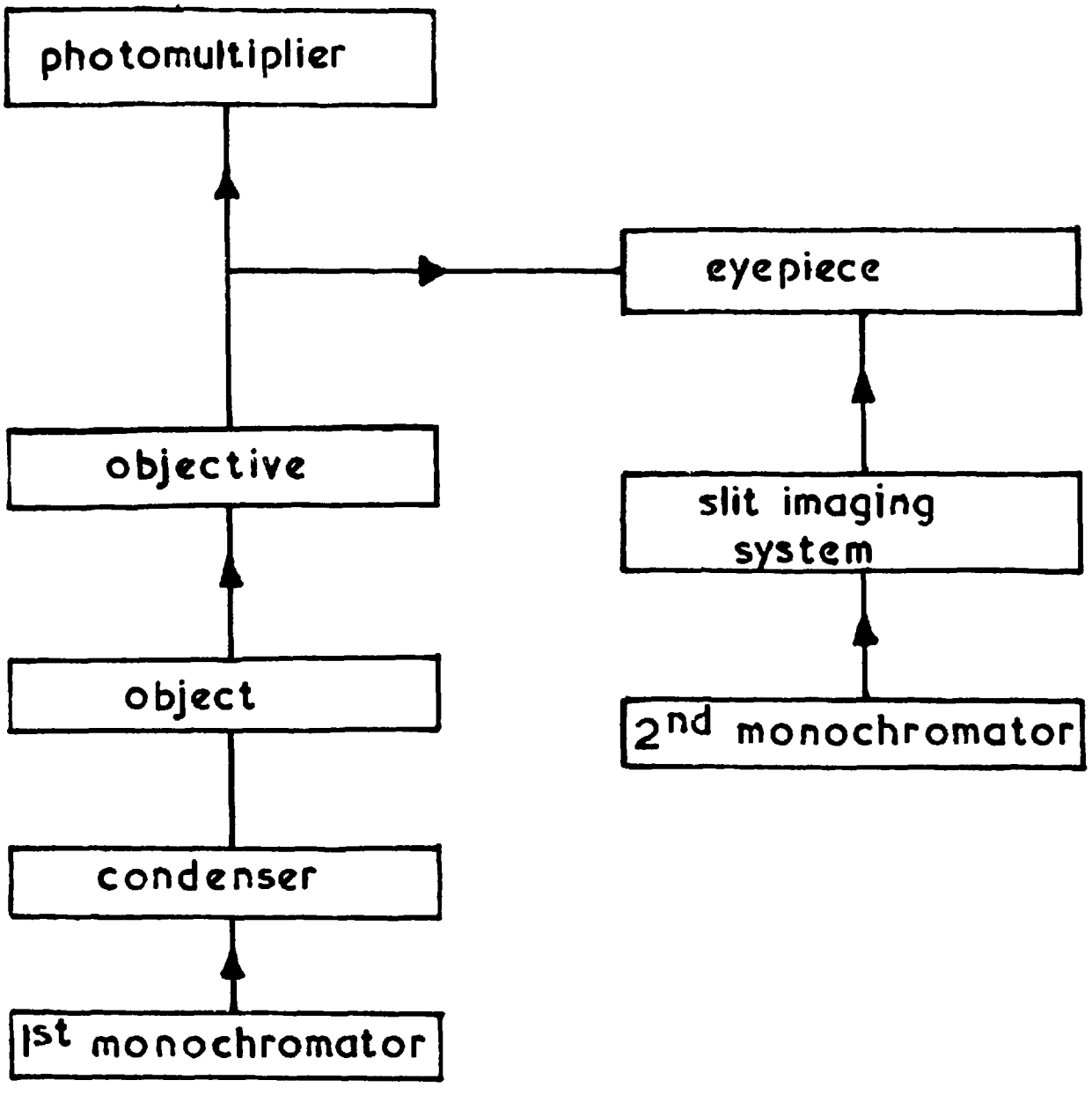

photomultiplier
eyepiece
objective
slit imaging system
object
2nd monochromator
condenser
1st monochromator

Fig. 3.01

to the photomultiplier is essentially a photo-electric microscope while the other branch represents a visual photometer.

The image of an object can be either focused onto a 15μ diameter circular aperture, whose dimensions are much smaller than those of the smallest resolved detail in the image, behind which is a photomultiplier, or the image can be focused at the first focal plane of a suitable eye-piece through which the image is viewed. The light flux passing through the circular aperture is measured by the photomultiplier in conjunction with a galvanometer. Displacements of the image, relative to the photomultiplier aperture, are obtained by using scanning blocks and thus the light distribution in the image can be measured.

To obtain values of the subjective luminances of the Mach bands, seen in the image of a straight edge, the field of view is divided into two equal parts. In the top half the image of an edge is seen while a comparison slit is imaged in the lower half as shown in fig. 3.02.

The Photo-Electric microscope.

The light source used is a tungsten ribbon filament lamp (6V. 18A.) with a colour temperature of about 2850°K at its full working voltage. The lamp is run from the

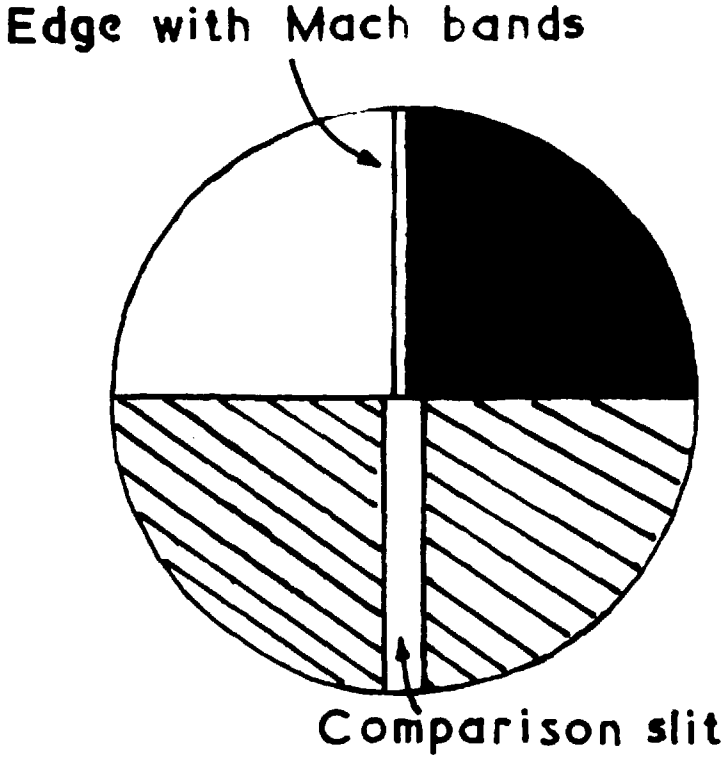


Fig. 3.02 The photometric field.

mains through a voltage stabilising unit and a variac transformer. Since the lamp is run off the A.C. mains without rectification the light intensity has a 100 c.p.s. ripple superimposed on a steady background level. The critical fusion frequency of the eye, for the conditions of the experiments performed below, is much lower (about 15 c.p.s.) than 100 c.p.s. and consequently the ripple does not affect visual measurements while the use of a galvanometer with a time constant of about 2 seconds allows the small ripple in the signal to pass undetected. Light from the lamp is focused onto the adjustable entrance slit of a monochromator based on a type originally devised by Wadsworth (1894).

Figs. 3.03a,b give the optical layout of the monochromator; the essential features are an achromatic collimating lens, a 60° prism and a plane mirror arranged to rotate together about an external axis, a second fixed mirror to bring the light at minimum deviation parallel to the axis of the collimating lens again and a final achromatic doublet to focus the resultant spectrum in the plane of the exit slit. Light from the exit slit diverges to fill the whole of the entrance pupil of the microscope condenser which images the exit slit in the plane of the object. Any wavelength between 4000Å and 6600Å can be selected by

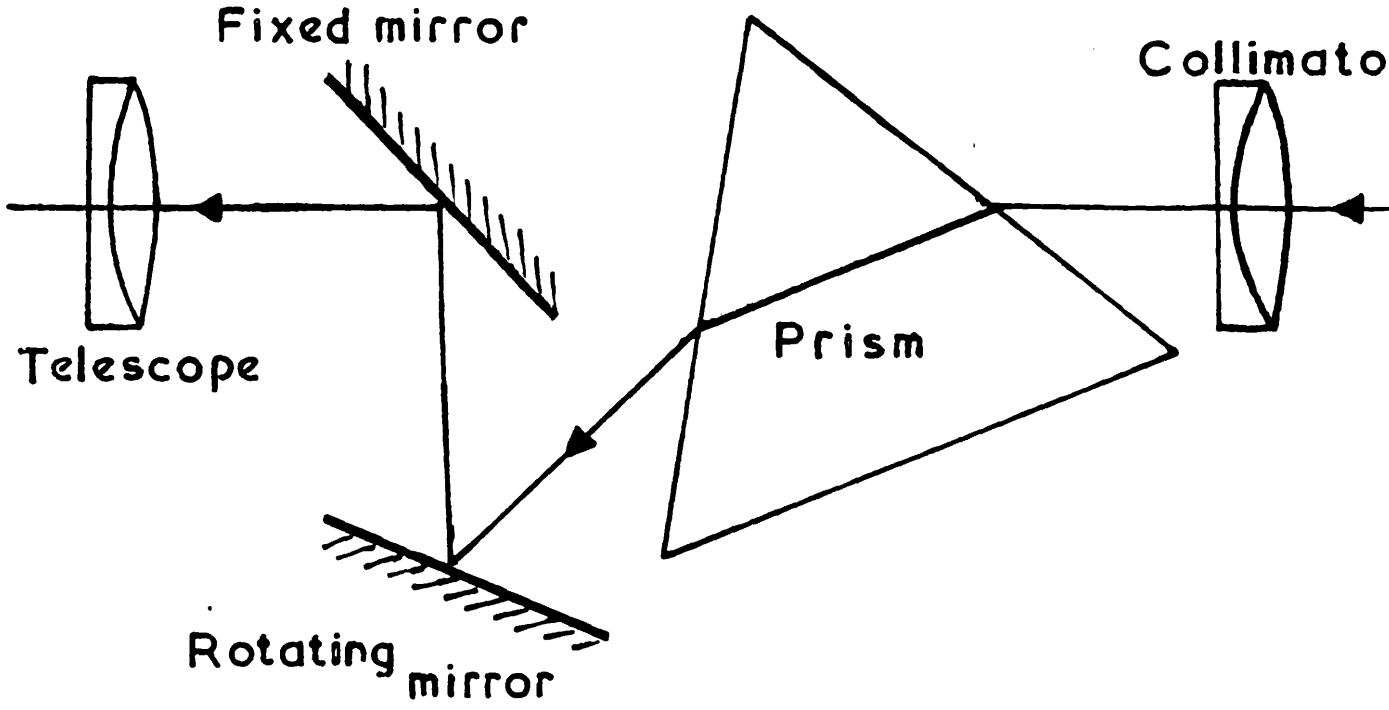


Fig. 3.03a The monochromator

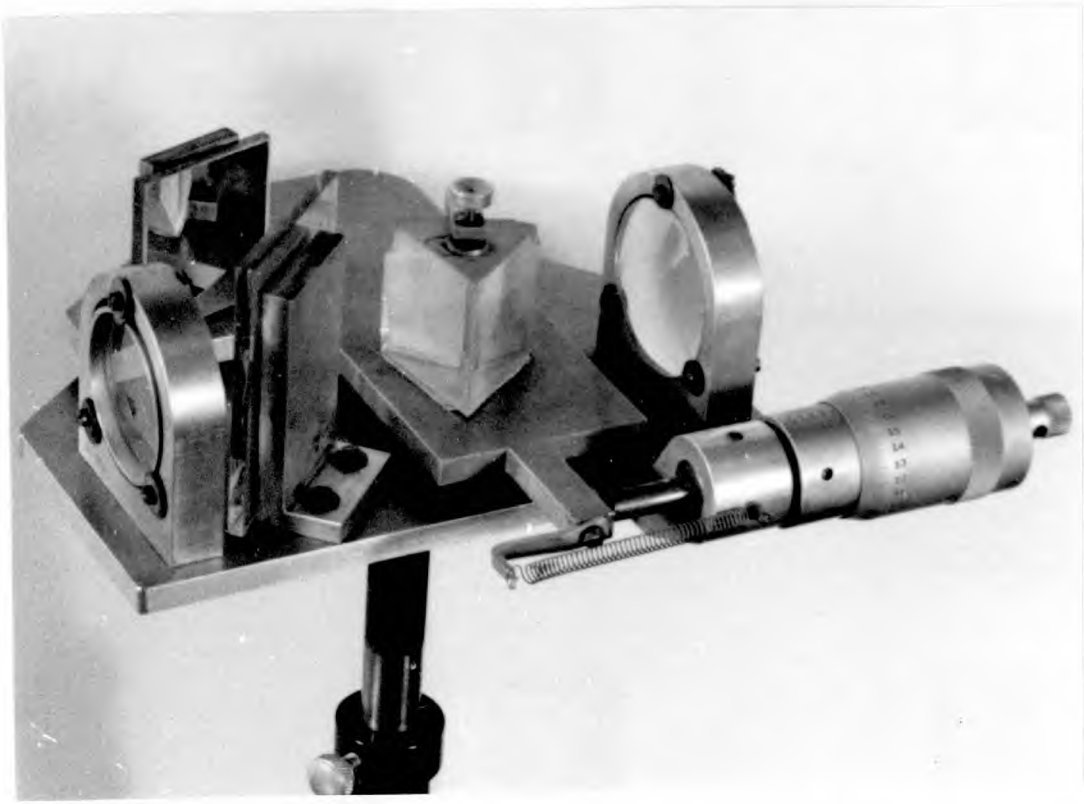


Fig. 3.03. b Monochromator

rotating a micrometer drum, the drum is calibrated by inserting successively mercury, sodium and cadmium lamps in place of the sodium lamp, the drum setting necessary to bring each line of the known wavelength of the various spectra into the centre of the field of view is noted and hence a calibration curve is plotted. The entrance and exit slits of the monochromator were adjusted to give an effective band width of 100Å for green light.

A limb of a Beck microscope (London Model 48 LI) carries the condenser stage and objective and is bolted rigidly to a sturdy five foot optical bench that carries all the components. The angular aperture of the illuminating beam that emerges from the monochromator exit slit is sufficiently large to evenly fill the entrance pupil (back aperture) of the condenser with light, a necessary condition if experimental results concerning physical images are to be compared with diffraction theory. A calibrated iris diaphragm, mounted in approximately the back focal plane of the condenser, permits the numerical aperture of the illuminating cone of rays emerging from the condenser to be varied between 0.03 and 0.26; the calibration of the condenser was performed using an apertometer designed by Spencer and Welford (1961). The condenser is focused by the usual rack and pinion device.



Fig 3.04 a. Photo-electric microscope

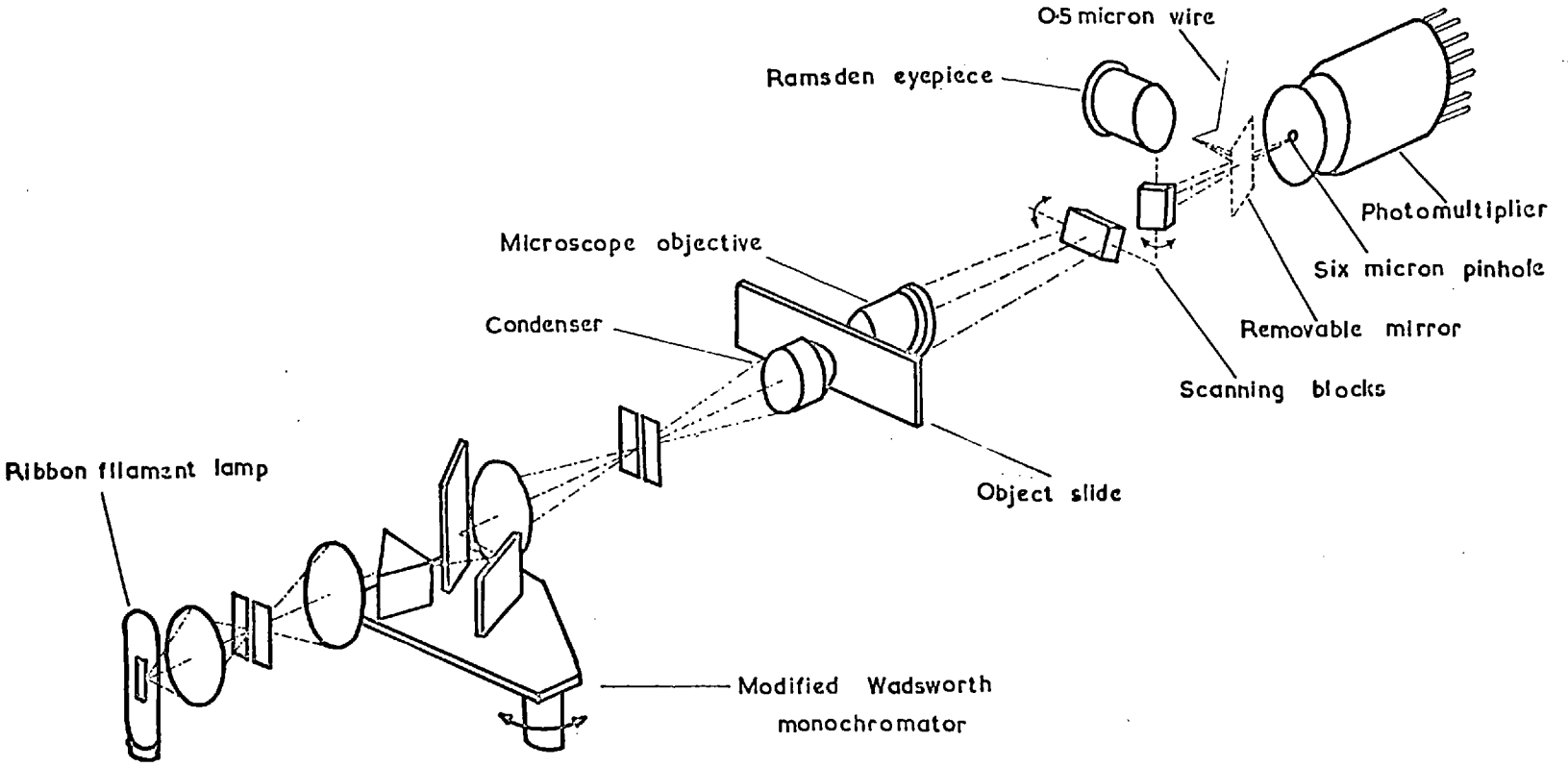


Fig. 3.04 b. The photoelectric microscope.

A rectangular precision mechanical stage, fitted with a rotating slide carrier, carries the object so that any portion of the object can be brought into the field of view and orientated in any desired direction.

A well corrected Beck objective of numerical aperture 0.28, which has been stopped down to yield a numerical aperture of 0.12, in order to reduce aberrations to a minimum, was used for most of the experiments although for the experiments concerned with binocular vision an objective of numerical aperture 0.65 was employed. The objectives are carried in a screw mounting. Coarse focusing is again by rack and pinion and the absence of backlash and the smoothness inherent in the fine focusing enables a very precise focus to be obtained. Figs. 3.04a,b show the optical layout of the photo-electric microscope.

Fig. 3.05 shows the scanning block unit which enables the image to be displaced in the focal plane of the eyepiece or in the plane of the photo-multiplier aperture. The two glass scanning blocks (A) are arranged to move the image in two mutually perpendicular directions. Each block is mounted on a spindle (B) which turns in two ball races, the axes of rotation being perpendicular to the axis of the microscope. The angle through which each spindle turns is controlled by a lever connected at right angles to

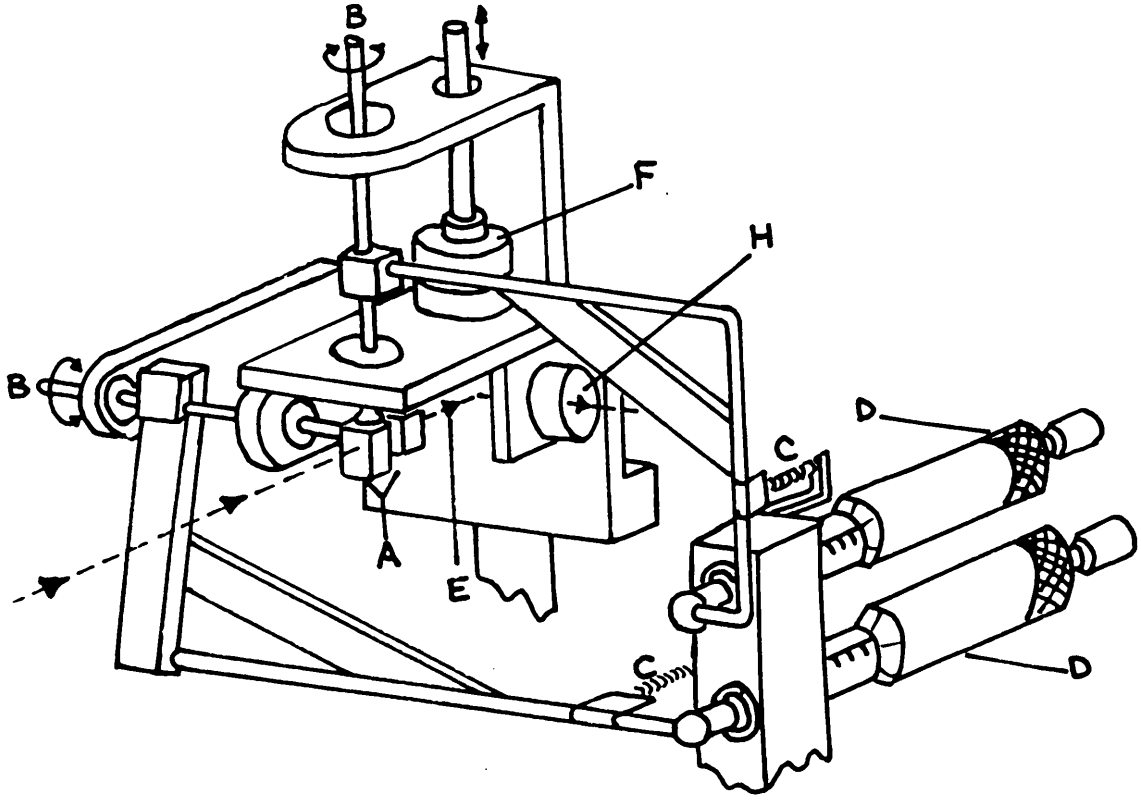


Fig. 3.05 The scanning block unit

the spindle. A phospor bronze ball, brazed onto the free end of each lever is kept in contact by a weak spring (C) with the free end of an inch micrometer head (D); a movement of the micrometer results in a rotation of the block which in turn facilitates a displacement of the image in its own plane. Charman (1961) has shown that, within the limits set by other experimental conditions, there is a linear relationship between the displacements of the image and the movement of the micrometer. Also Charman has shown that the aberrations introduced by the insertion of the blocks into the image forming wavefront are well within the Rayleigh tolerance. Two stage micrometers were used to calibrate the scanning unit and measurements taken with separate micrometers agreed to within $\frac{1}{2}$ %.

A front aluminised mirror (fig. 3.06) (E) can be placed so that it directs light from the objective into the eyepiece; alternatively the light can pass straight up the microscope axis to reach the photomultiplier aperture. The mirror unit (F) can be positioned in a kinematic mount when the light is directed into the eyepiece; three steel balls engage in three V-slots in a steel ring (G) to ensure precise positioning and the mirror mounting is spring loaded to ensure good location in the V-slots. A catch secures the mirror when physical measurements are being made so

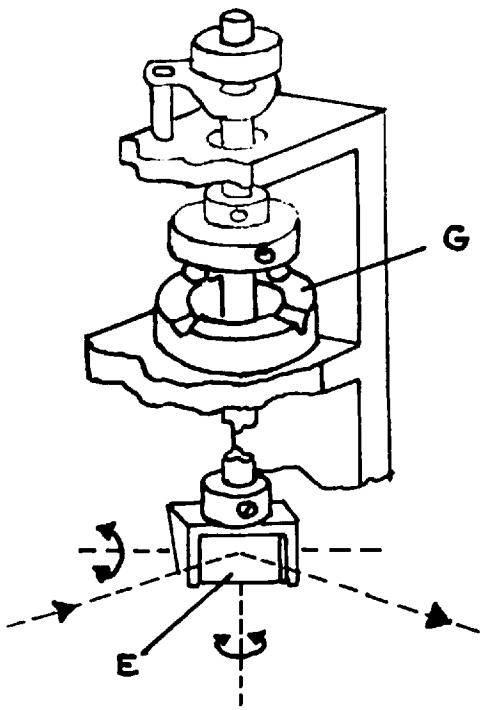


Fig. 3.06 The mirror unit

that the light travels straight from the objective to the photomultiplier. The scanning blocks, eyepiece and photomultiplier aperture can be moved as a complete unit up and down the bench so that the tube length of the microscope can be altered when different objectives are employed. The distance between the mirror (E) and the first focal plane of the eyepiece and the distance between this mirror and the photomultiplier aperture are made as equal as possible to ensure that a tube length setting which is an optimum visually (as found by the star test) is equal to the setting which gives an optimum tube length when determined photo-electrically (see below).

An E.M.I. 13-stage photomultiplier (type 6094B) is used as a detector and the voltage supplied to it is provided by a highly stabilised Panax (type 3000) power pack whose output is variable from 0 to $\pm$ 3 KV., 1.5 KV. is normally used. The collector current is proportional to the incident light flux up to at least 1 mA; the dark current is less than 0.1 μA and by use of suitable screening around the apparatus stray light is kept to a minimum. A glass sphere 6 mm. in diameter (fig. 3.07) is used as a lens to image the aperture onto the photomultiplier cathode. A Pye-spot galvanometer registers the photomultiplier current. The full scale deflection on the least sensitive

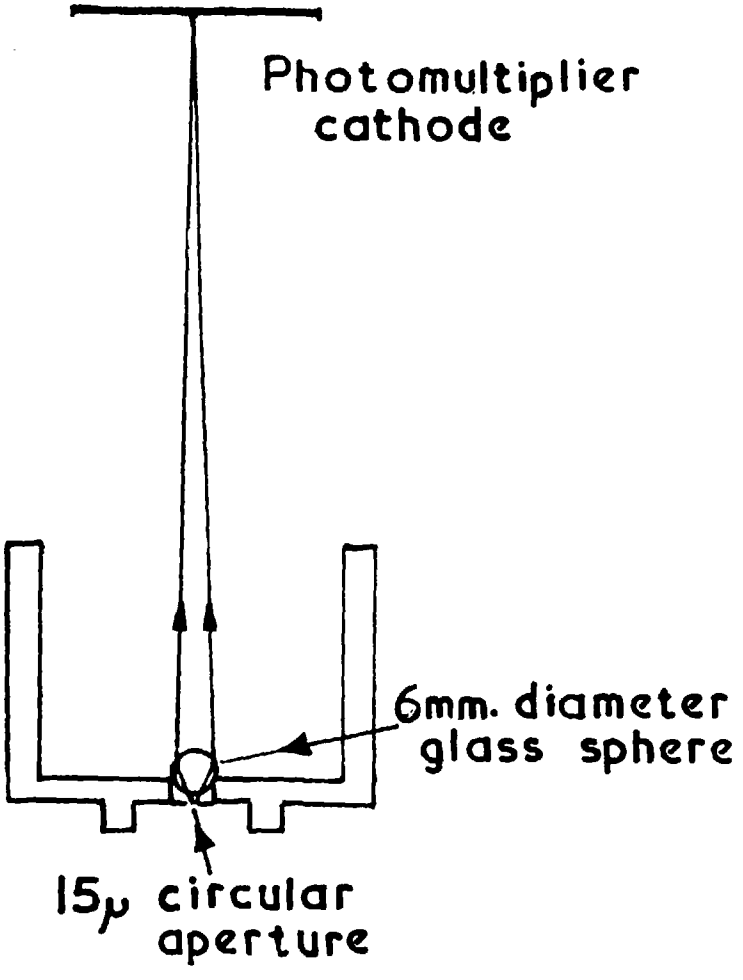
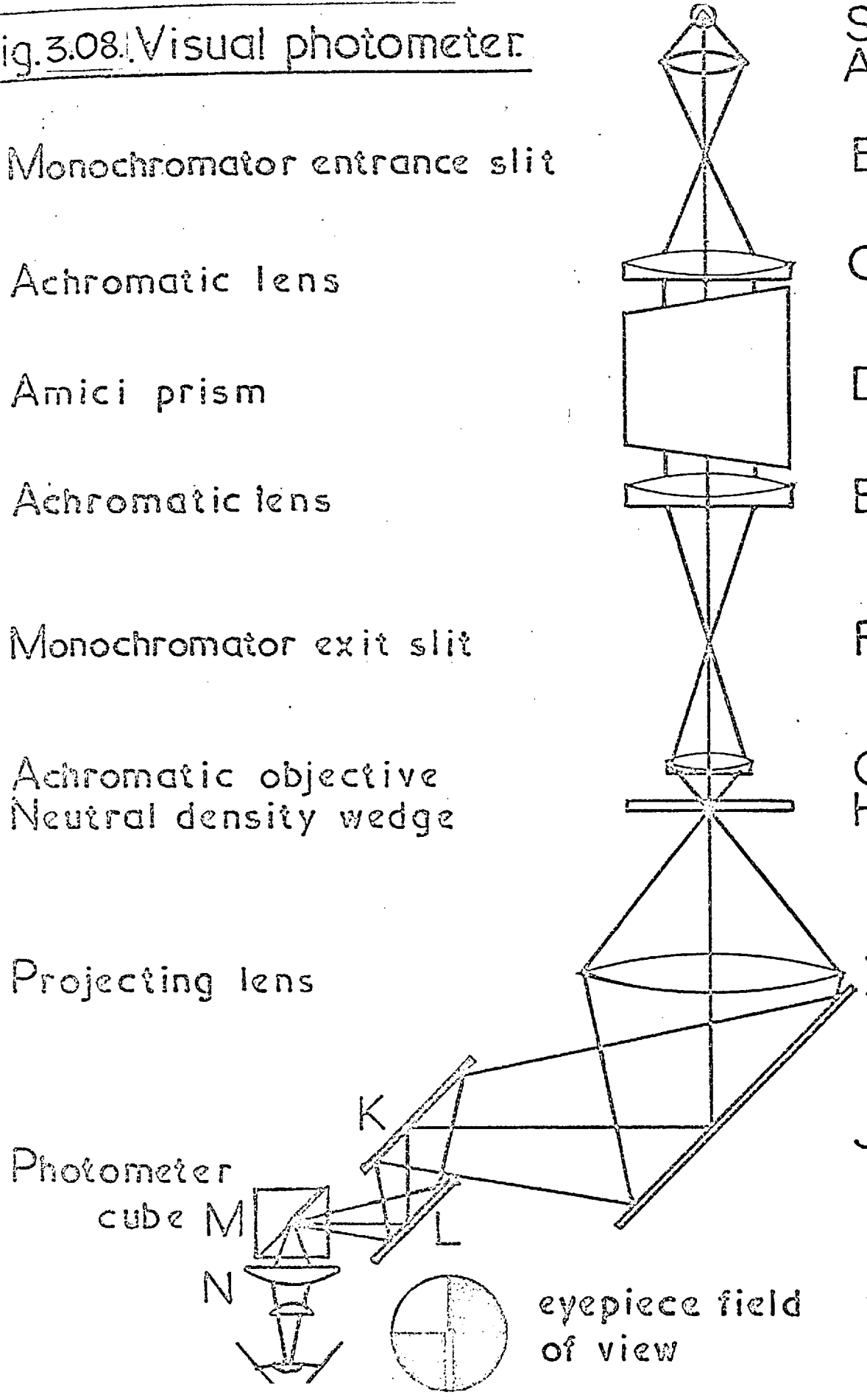

Photomultiplier
cathode
6mm. diameter
glass sphere
15μ circular
aperture

Fig.3.07

range corresponds to about 45 μA but most measurements are taken on the X 0.1 scale.

In determining the image intensity profile under a particular set of optical conditions, the image is first focused and centered visually using the eyepiece. Next the mirror is removed and the scanning blocks are adjusted to centre the image onto the photomultiplier aperture. Using one scanning block only a complete scan is then made across the image, the galvanometer signal being recorded at regular intervals as the controlling micrometer is adjusted. An unobstructed area of the slide is then brought into the centre of the field and the galvanometer reading is recorded as the clear signal. The ratio of the galvanometer reading at any point in the image to the clear field value gives the intensity of that image point normalised in terms of the intensity of the image of a completely transparent uniform object, it being convenient to specify this as a percentage transmission or a relative luminance. Hence if we know by calibration, with a stage micrometer, the lateral movement produced by the scanning blocks, the intensity profile of the image can be expressed as a transmission profile.

Fig. 3.08. Visual photometer



The Visual Photometer.

The optical arrangement is shown in fig. 3.08. Again the light source is a tungsten ribbon filament, lamp (6V. 18A.) run from the mains through a voltage stabiliser and variac transformer. Light from the lamp is focused onto the slit (B) and is then made parallel by the lens (C). The parallel beam of light passes through an Amici dispersing prism (D) and the resultant spectrum is focused by the lens (E) onto the slit (F). Lenses (C) and (E) are both achromatic. A reduced image of the slit (F) is formed on a neutral density wedge (H) by means of a low power microscope objective. Finally the lens (I) focuses the real image of the slit via the mirror systems (J), (K), (L) and the photometer prism (M) onto the first focal plane of the eyepiece.

The diagonal surface of the prism, half of which is aluminised to form a reflecting surface, divides the eyepiece field of view into two parts. In the bottom half the image of the slit (F) appears; the top half contains the image of the edge formed by the microscope objective, the length of the slit image was made parallel to the edge. The width of the slit was made as narrow as possible but not so narrow that the Mach bands at the edges of this slit image could interfere with the main area of the slit which

was used for matching purposes. At the eye the slit image subtended about 2 degrees.

Watrasiewicz (1964) used a neutral density wedge 3 cm. long to vary the luminance of the comparison slit. The overall attenuation of this wedge was about 40 to 1 and a considerable amount of difficulty was encountered in making a quick, accurate photometric match, as small changes in luminance of the comparison slit could not be performed. In order to circumvent this difficulty an improved wedge was employed.

A neutral density wedge was obtained from Kodak Ltd., and is of the photographic type; it provides an overall attenuation of 1000 to 1. The photographic emulsion is in the shape of a ring of external diameter 13 cm. and 1 cm. width. The emulsion was supplied affixed to a glass disc; in order to protect the emulsion another disc, made of Perspex, is fixed to the glass disc with Araldite so that the emulsion is sandwiched between the two discs. The two discs are fixed with Araldite to a brass bearing which is free to revolve around a steel bearing. A circular scale, graduated in degrees, is marked on the outer bearing so that angular displacements can be read relative to a mark on the inner bearing. Fig. 3.09 shows the wedge mounted on the bearings. The wedge is rigidly mounted

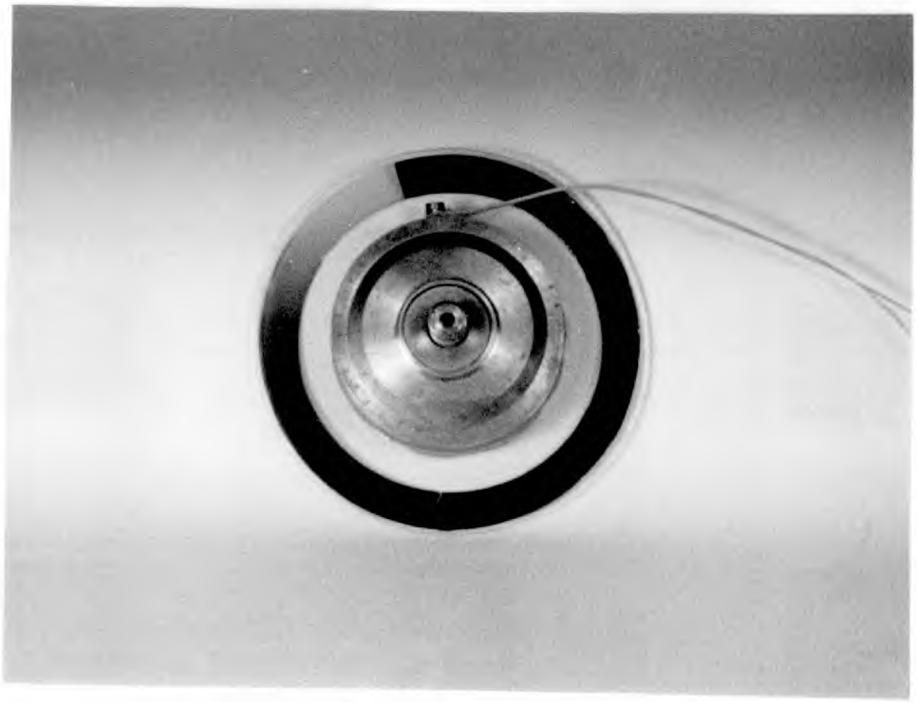


Fig. 3.09. Photometric wedge

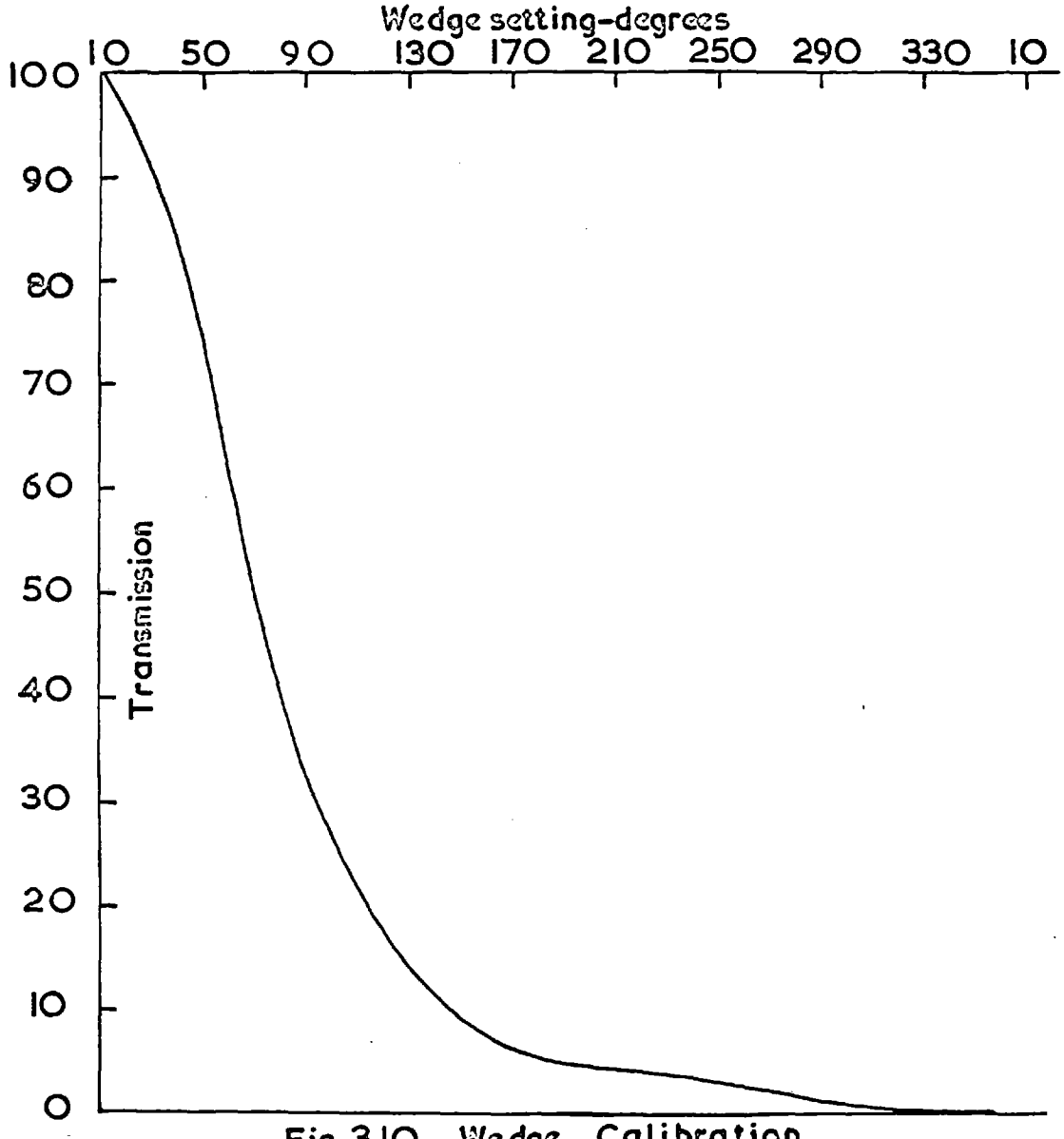


Fig. 3.10 Wedge Calibration

with its plane perpendicular to the optical axis of the photometric system. Rotation of the wedge is effected by two strings which are operated by a hand drive. The wedge was calibrated by focusing the light from the comparison slit onto the photomultiplier. Intervals of 5 degrees were chosen in obtaining the calibration curve shown in fig. 3.10.

The wavelength of the photometer beam can be changed by shifting bodily the source (S) condenser (A) and the slit perpendicularly with respect to the optical axis of the system. The size of the slit (B) was chosen to give a band width of 100Å. A visual colour matching procedure was adopted to equate the colours of the clear field image produced by the microscope objective and the image of the comparison slit. A perfect match between two unequal clear fields does not seem possible however, as the larger field always seems to be more saturated than the small field (comparison slit).

The Test Object.

The investigations described below were performed using a thin, high contrast, straight edge as an object because it presents a relatively simple visual field to the observer and also the physical image profiles of edges

have been previously determined theoretically and practically. The method of production was essentially the same as that described by Watrasiewicz (1964).

A microscope slide was first cleaned with a dilute solution of Teepol and then alcohol. When the slide was quite dry filaments of Formvar (type 1595E), dissolved in Chloroform, were laid on the slide. Also some polystyrene spheres, 1.2μ in diameter (supplied by the Dow Chemical Co. of Michigan) were placed on the slide. The polystyrene spheres were taken from a test-tube containing a solution (pure water) of the spheres. When the water had dried the spheres were found to adhere to the slide. Spectroscopically pure aluminium was then evaporated onto the slide at nearly normal incidence at a pressure of about 10^{-5} cm. of mercury. The evaporating plant used was an Edwards type 12E/221 and in order to reduce penumbra effects to a minimum the distance between the evaporation source and the slide was made as large as possible (35 cm) and the source was made as small as possible. On viewing the white hot source through the slide the source was eventually seen to disappear and the evaporation was then complete. After the evaporation the filaments of Formvar were gently pulled off to leave clear areas bounded by the required straight edges. Next the spheres were removed from the

slide by a jet of distilled water directed at grazing incidence, thus leaving circular apertures with diameters close to the diameters of the spheres (Slater 1960) together with the clear areas bounded by the straight edges. The apertures were to serve as reference apertures next to the edges. Finally a cover slip was cemented onto the slide with Canada balsam. The procedure described here is a difficult one and several attempts were necessary before a suitable straight edge with a neighbouring aperture were obtained. When viewed under a 1.32 N.A. oil immersion objective the edge had to appear straight for about 200μ before it was considered suitable. In addition to this an aperture had to exist about 15μ from the edge. Also when the edge was viewed with the low aperture test objective the opaque field had to have no bright inclusions other than the reference aperture.

Choice of Objective.

The multiple Mach band structure is normally seen when many different types of microscope objectives are employed. It is useful, however, to be able to compare the visually observed structure at an edge with the physical luminance distribution and with this in mind a well corrected low numerical aperture (0.12) objective was chosen; the use

of a low numerical aperture allows a direct comparison with scalar diffraction theory to be made. Charman (1963) and Watrasiewicz (1965) have demonstrated that scalar diffraction theory breaks down for numerical apertures greater than 0.8. Measurements made with this low N.A. objective by Charman (1963) and the author have shown good agreement with scalar diffraction theory. Another advantage of the objective was that its low magnification of 13X was such as to afford great mechanical stability, as compared with objectives giving higher magnifications. Focal settings remained steady for periods of up to one hour and were not subject to the annoying drifts due to temperature changes of $1^{o}C$ or so which are encountered when using objectives with higher magnifications.

Tube Length Setting.

With light of wavelength $0.53\mu \pm 0.05\mu$, the image of a 1.2μ diameter aperture was centered onto the photomultiplier aperture with the aid of the scanning blocks. Fine focusing and the centration were adjusted until the maximum signal on the galvanometer was obtained. The precision mechanical stage was then adjusted until the image of the clear field was obtained at the photomultiplier aperture and the consequent clear field signal on the

galvanometer was noted. The ratio of these two signals gave the maximum transmission T through the object aperture. Different tube lengths (defined here as the distance between the photomultiplier aperture and the back aperture of the objective) between 210 mm. and 140 mm. were used to find a set of values for T. Over the range 160 mm. to 200 mm. there was no significant difference in T and throughout this range T had a maximum value so that the optimum tube length which was finally chosen was 180 mm. An application of the star test (Welford 1959) yielded the same value for the optimum tube length.

Scanning procedure to determine physical images.

After an initial warming up period of 30 minutes the image of the 1.2μ reference aperture is brought to a sharp focus at the photomultiplier aperture. Readings of the galvanometer are noted as the edge image is scanned past the photomultiplier aperture until the readings become uniform indicating that the clear field has been reached. It is important that scans should be made perpendicular to the edge and therefore the precision mechanical stage is adjusted so as to give the steepest gradient in the physically recorded image.

The position of the edge, according to geometrical

optics, can be found in the following way. Incoherent illumination is obtained by making the numerical aperture of the condenser about five times that of the objective. The point where the transmission is 50% that of the clear field is then the geometrical edge as pointed out by Welford (Weinstein 1954). Scans yield the position of the geometrical edge relative to the reference aperture. In practice, due to scattering at the various optical surfaces of the objective and scanning blocks, there is a background level of about 3% transmission which is duly subtracted from all readings when the geometrical edge is located by the above method. See fig. 3.11.

It is convenient to introduce a term S defining the coherence of the light employed:

$$S = \frac{\text{Numerical aperture of the condenser}}{\text{Numerical aperture of the objective}}$$

When S exceeds 5.0 we have conditions approaching incoherent illumination of the object and when S tends to zero the object becomes illuminated with spatially coherent light. The intermediate range of S defines the realm of partial coherence which is normally encountered in microscopy.

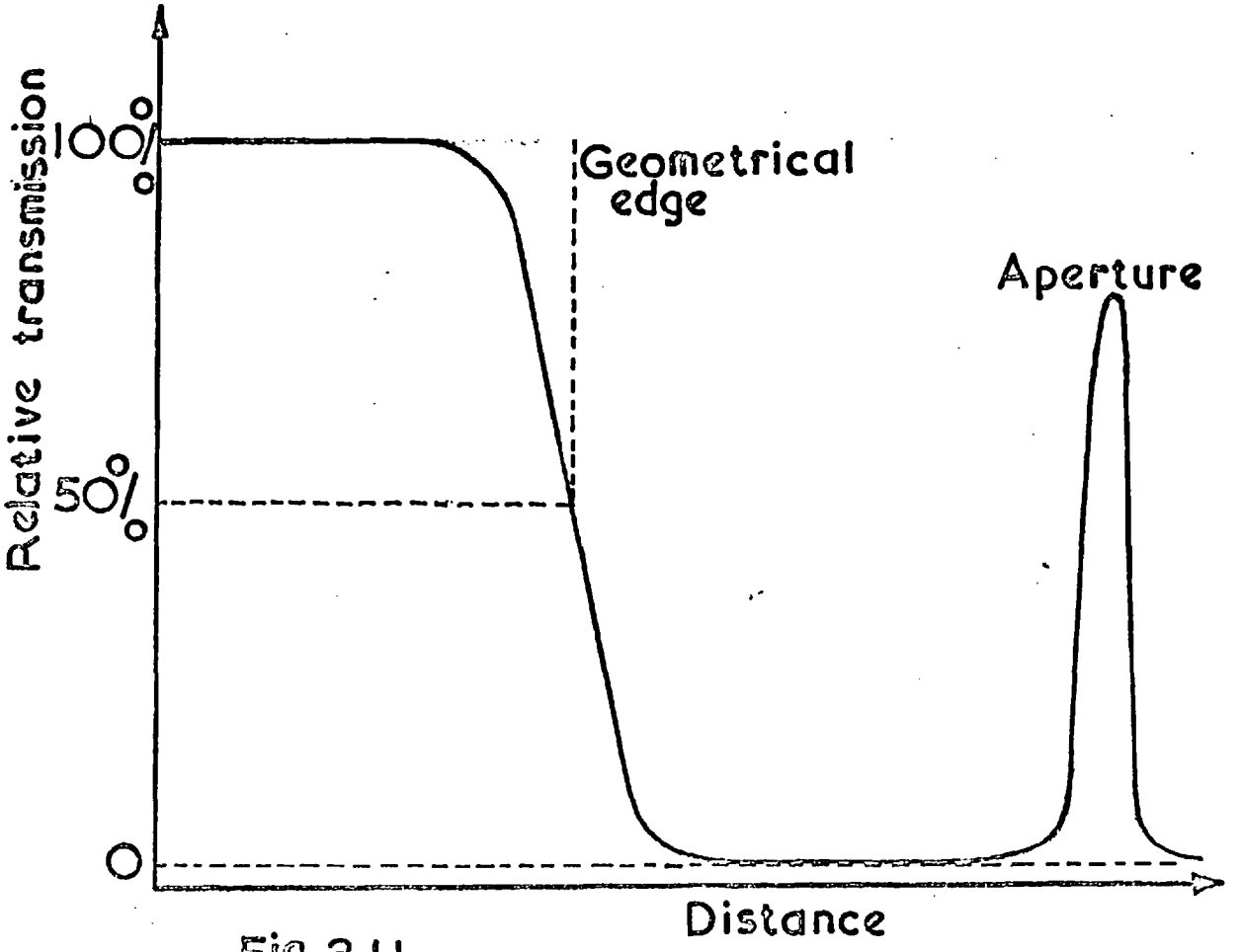


Fig 3.11 A scan with incoherent illumination

Chapter IV

The Variation of the Mach Effect between different Observers

Introduction

The variation of certain visual functions with age is well known. In this respect Ruddock (1964) has demonstrated the variation of colour response. Said and Weale (1959) have demonstrated that the transmission of the eye lens decreases steadily with age. Mazow (1960) reports that as age increases the retina becomes thinner and optically denser. In order to reduce variations due to age effects some twenty observers were chosen between the ages 20-24 years; they had no serious defects of vision apart from the observers M.J.M. and A.E.S. who were slightly myopic (minus one dioptre).

During the survey the diameter of the exit pupil of the microscope (0.23 mm.) was very much smaller than that of the natural pupil of the eye (about 3 mm.) and since the observations were made on axis with monochromatic light optical aberrations present in the eye were reduced to a minimum. Consequently the distribution of retinal illumination might be expected to correspond (apart from the effect of scatter in the ocular media) with the distribution of luminance in the primary microscope image.

Each observer performed the measurements with two values of S. Firstly the condenser aperture was opened to its full extent and this gave S = 2.2 which resulted in a physical distribution of luminance across the edge which was almost entirely free from diffraction bands (fig. 4.01). For the second set of observations the condenser aperture was stopped down to give an S value of 0.60 and here the physical distribution had diffraction fringes present, also shown in fig. 4.01.

The clear field luminance was made equal for both values of S and its value was monitored to within $\pm$ 5% throughout the experiments. The luminance of the clear field was such that it provided a retinal illumination of 1500 trolands. (The retinal illumination is equal to one troland when an area of luminance 1 cd./m^2 is seen through a pupil of 1 mm^2 in area.) Under these conditions we may assume that vision is photopic (i.e. both cones and rods are functioning).

Calculation of the retinal illumination.

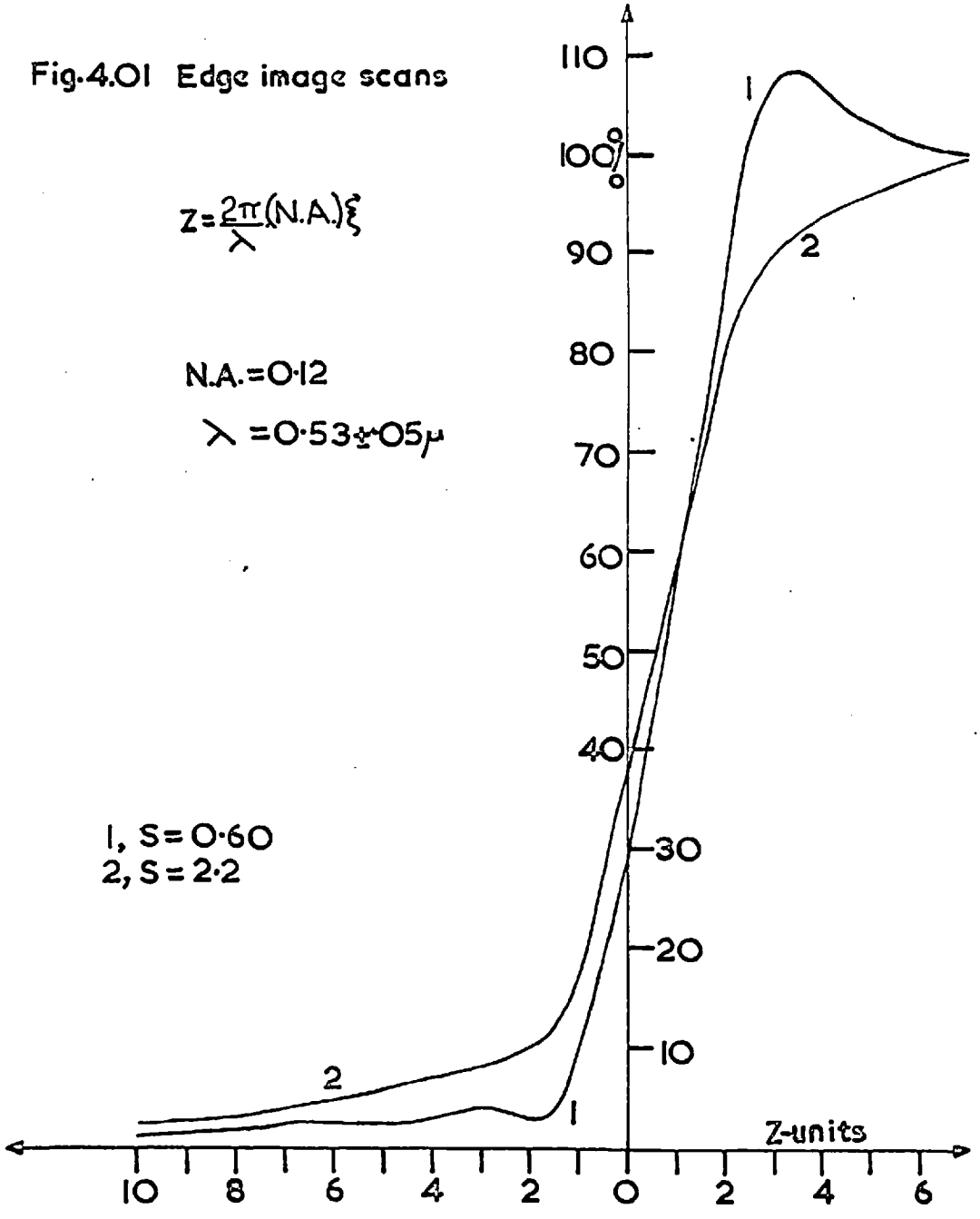
We assume that the eye pupil is coincident with the exit pupil of the microscope and that these pupils are co-axial. Furthermore, since the exit pupil of the eye-piece is very much smaller than the entrance pupil of the

Fig.4.01 Edge image scans

$$Z=\frac{2\pi}{\lambda}(N.A.)\xi$$

N.A.=0·12

λ =0·53±·05μ



eye all the luminous flux emerging from the microscope must enter the eye.

In order to determine the retinal illumination the luminance L_2 of a perfectly diffusing magnesium oxide screen placed 10 cm from the exit pupil was measured with an S.E.I. photometer (fig. 4.02). The screen is viewed through the telescope of the photometer and a small spot in the middle of the field of view is made to coincide with that portion of the screen which is illuminated with light emerging from the exit pupil of the microscope. The photometric setting is then made by causing the brightness of the spot to match that of the screen. Let the distance of the screen from the exit pupil (area A) be R and suppose that the image, which is observed through the eyepiece, is of area S_1 and has luminance L_1. Also let the distance of this image from the exit pupil be r. We assume that paraxial optics holds and consequently an evenly illuminated area S_2 of luminance L_2 is obtained at the magnesium oxide screen.

Since we have a perfectly diffusing screen at S_2 the flux F incident on it is reflected equally in all directions through a solid angle of 2π steradians and hence,

$$L_2 = \frac{F}{2\pi . S_2} .$$

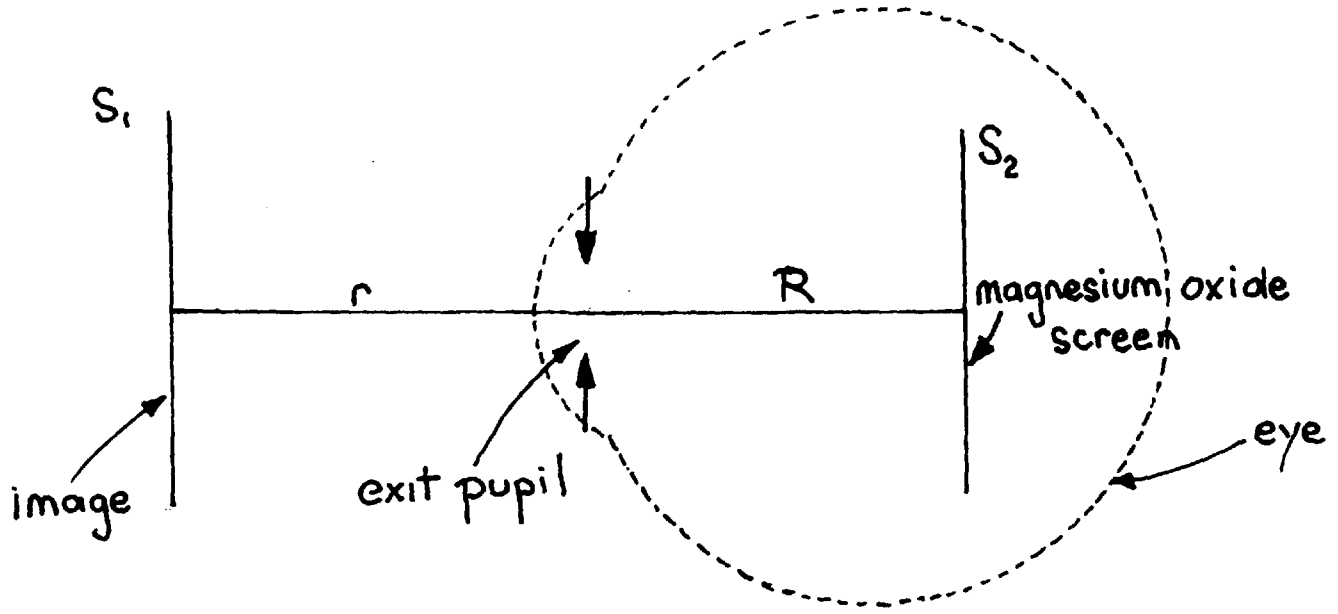


Fig.4.02

All the flux has come from the image S_1 through the exit pupil. Now the element of flux dF which passes through an element of the exit pupil dA due to an element of area dS_1 in the image is given by,

$$dF = dS_1 \, L \cdot \frac{dA}{r^2} .$$

Hence the total flux F emerging from the exit pupil is given by,

$$F = S_1 L_1 \frac{A}{r^2} .$$

Thus $$\frac{S_1}{S_2} \cdot \frac{L_1 \, A}{2\pi r^2} = L_2 ,$$

hence $$L_1 A = 2\pi L_2 \frac{S_2}{S_1} \cdot r^2$$

But $$\frac{S_2}{S_1} = \frac{R^2}{r^2} .$$

Therefore $L_1 A = 2\pi L_2 R^2$ which is the retinal illumination expressed in trolands since one troland is equivalent to 1 candela/sq.m. viewed through a pupil of 1 sq. mm.

The output of the lamp was adjusted until the luminance L_2 of the magnesium oxide surface as measured with the S.E.I. photometer was such that the value of $2\pi L_2 R^2$ equalled 1500 trolands and at the same time the

photomultiplier output was noted. The luminance of the magnesium oxide surface could only be measured to an accuracy of ± 20% which resulted in a similar uncertainty in the measurement of the retinal illumination although its magnitude (as measured by the photomultiplier output) was held constant to ± 5% for each observer.

The area of the exit pupil was measured with a travelling microscope.

Experimental procedure to determine the positions of the bands.

Experiments were performed in a darkened room as this greatly aided concentration when monocular measurements were being made. Observers were asked to look at the field of view for ten minutes with the right eye; during this period they described their impressions of the Mach bands seen at the edge. This initial period allowed the observer to be accustomed to the conditions and also facilitated adaptation of the observer's eye. With the eye relaxed the observer focused the eyepiece on the tip of a 0.5μ tungsten wire which was fixed to the microscope barrel so that the tip was centrally disposed with respect to the visual field. With the aid of the objective fine focus screw, the observer focused to obtain the sharpest visual edge which,

in this connection, inferred the border between the band brighter than the clear field and the dark band adjacent to it. The scanning blocks were adjusted until the image of the 1.2μ reference aperture and the tip of the 0.5μ wire were coincident and this setting was noted. The settings were made successively across the edge image at the borders of the various bright and dark bands by scanning the eye along the length of the bands whilst the observer slowly moved the image until the border between two adjacent bands appeared to be in line with the tip of the wire, after which the micrometer reading was noted. Care was taken to move the image in one direction only, so as to avoid errors due to backlash. The first scan served merely to acquaint the observer with the required technique and these results were rejected. Ten subsequent scans were then made to determine mean positions of the bands. These experiments were very tiring and after five scans a rest of about a quarter of an hour was allowed.

The results for S = 2.2 and S = 0.60 are shown in figs. 4.03 and 4.04 respectively. Hatched areas represent dark bands while clear areas depict bright bands. Distances are measured in dimensionless z units relative to the geometrical edge which was determined to within an accuracy of $\pm$ 0.1μ by scanning with incoherent illumination, as described in Chapter III,

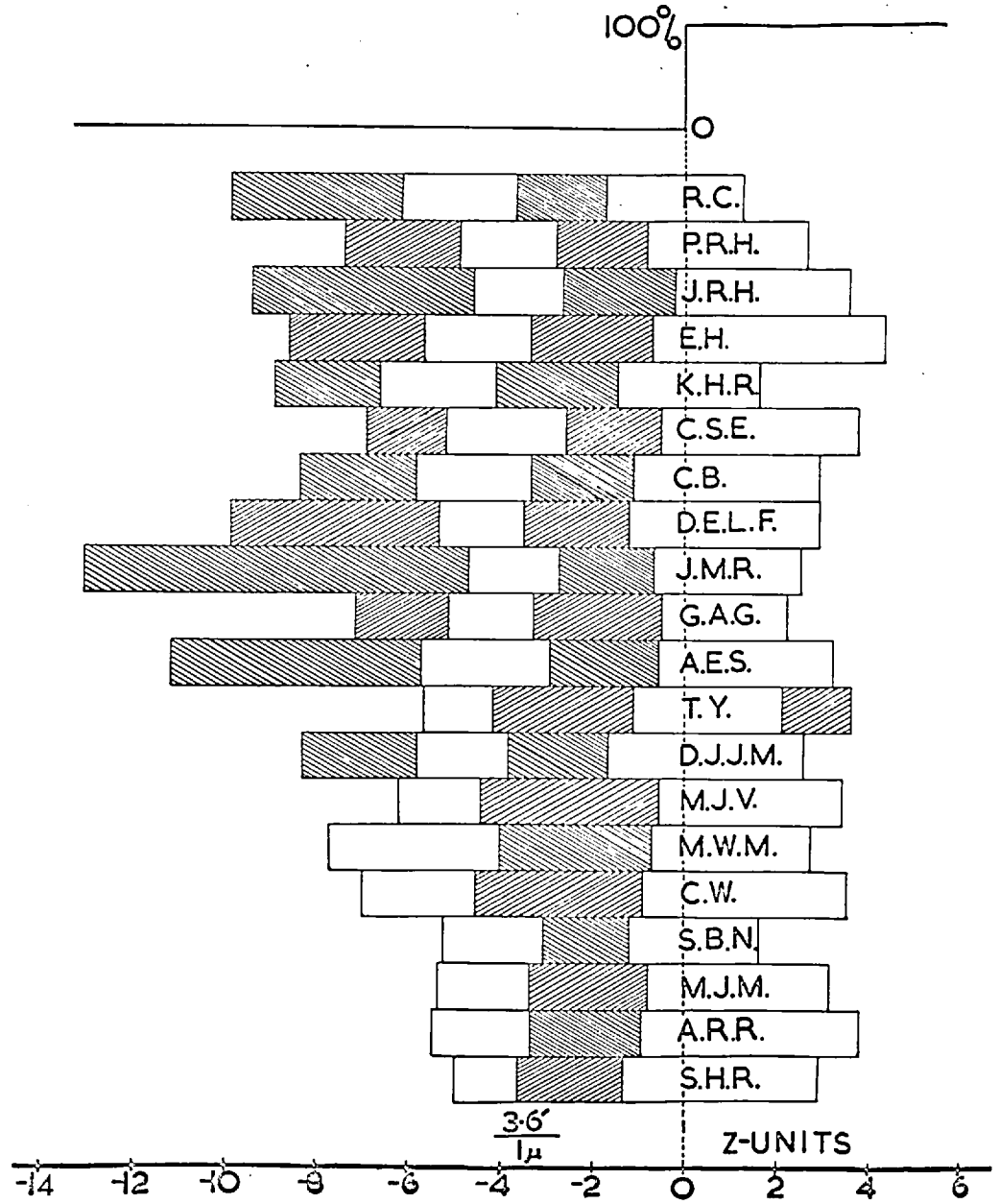


Fig.4.03. Mach bands seen at an opaque edge. S=2.2.

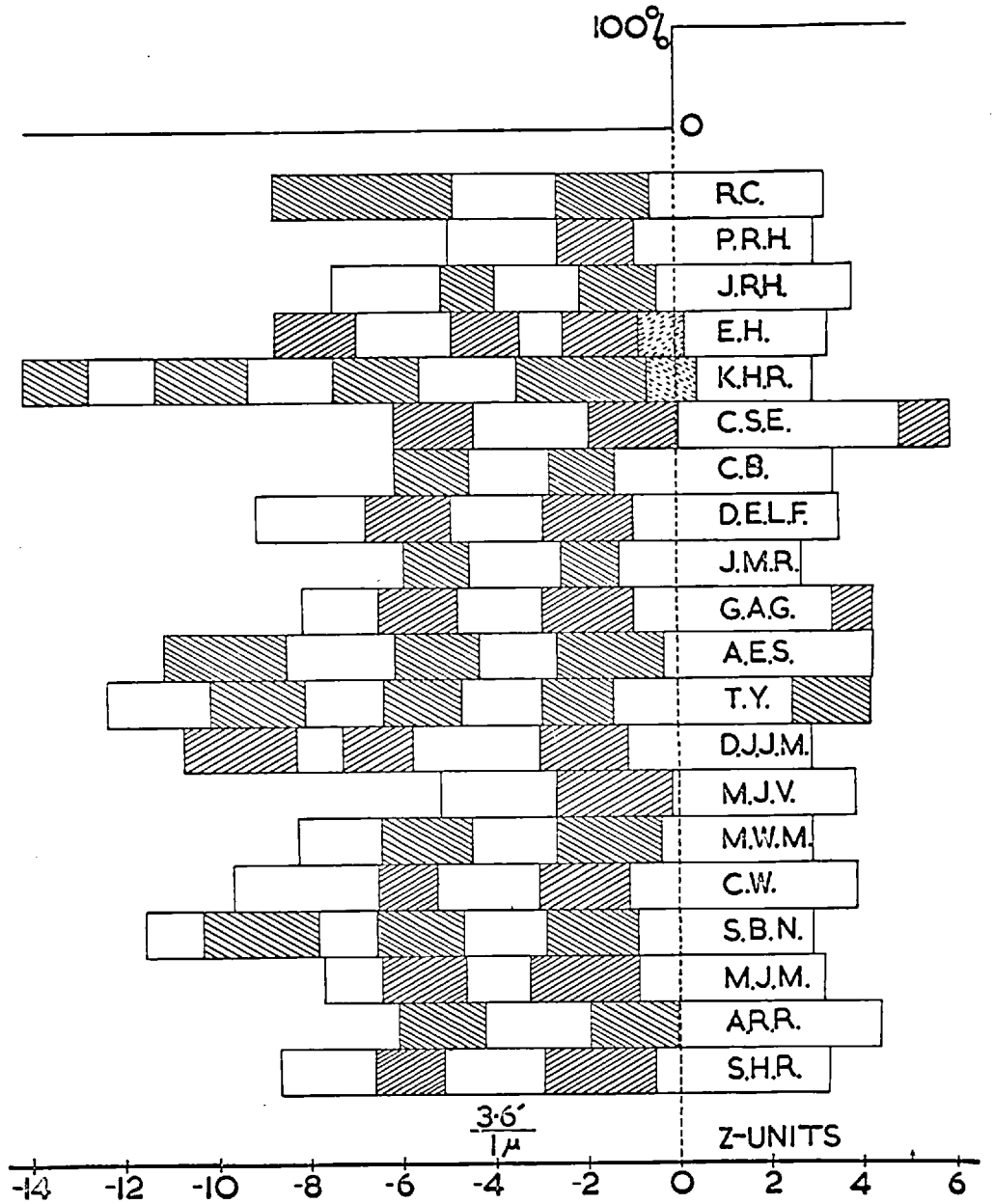


Fig.4.04. Mach bands seen at opaque edge. S=0.60".

$$z = \frac{2\pi}{\lambda} \times (\text{N.A.}) \times \xi$$

where λ equals the wavelength of the light employed ($0.53 \pm 0.05\mu$), ξ equals the distance in the object space and (N.A.) is the numerical aperture of the objective. Calculations based on scalar diffraction theory are usually expressed in z units and distances expressed thus are invariant with respect to the conjugate plane considered.

Measurement of the relative luminance of the Mach bands.

The photometer prism was added to the eyepiece so that the edge with the Mach bands appeared in the upper half of the field of view while the comparison slit appeared in the lower half, as described on page .

After an initial adaptation period of five minutes an observer made brightness matches with the continuous bright and dark fields. Since the angular subtenses of the Mach bands were so small (on average bands subtended 7 minutes of arc at the observer's eye) it was only possible to make a brightness match with the centre portion of each band; six matches were made for each band in order to obtain a mean value of its relative luminance. A precision better than $\pm$ 10% of the mean relative luminance could not be obtained for most observers when they made measurements

on the bright bands while the relative luminance of the dark bands could only be measured to an accuracy of ± 30%

Luminance profiles are plotted on a logarithmic scale in figs. 4.05, 6, 7 and 8; they are normalised so that the clear field luminance was 100%. The measured physical distribution of luminance is shown as a dotted curve on each diagram. In some cases an observer could measure the position of a particular faint band but when the photometer prism was added to the eyepiece the band could no longer be discerned owing to the presence of scattered light. Such bands are indicated by dotted lines in the luminance profiles. On each diagram a line is drawn to represent 1μ in the object space; it is also equivalent to 3.6 minutes of arc subtended at the observer's eye.

The general appearance of the edge reported by the observers was as follows:

1) The continuously bright field (clear field).

2) A bright band of greater luminance than the clear field (referred to below as "the first bright band").

3) A dark band, darker than the continuous dark field (referred to below as "the edge band").

4) A bright band (referred to below as "the second bright band").

5) A series of less distinct bright and dark bands.

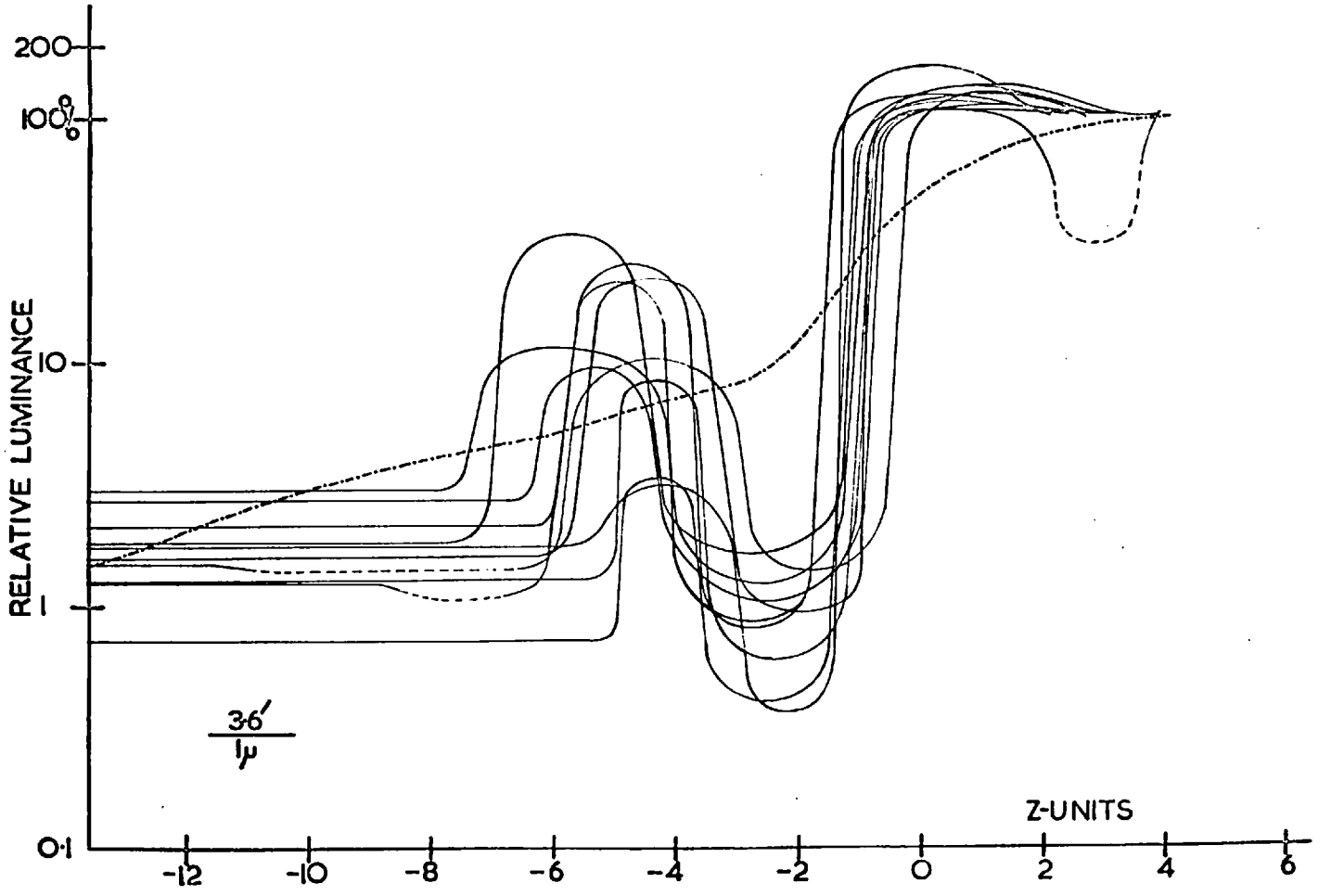


Fig. 4.05. Luminance profiles as seen by the observers A.E.S., T.Y., D.J.J.M., M.J.V., M.W.M., C.W., S.B.N., M.J.M., A.R.R. and S.H.R. S=2.2

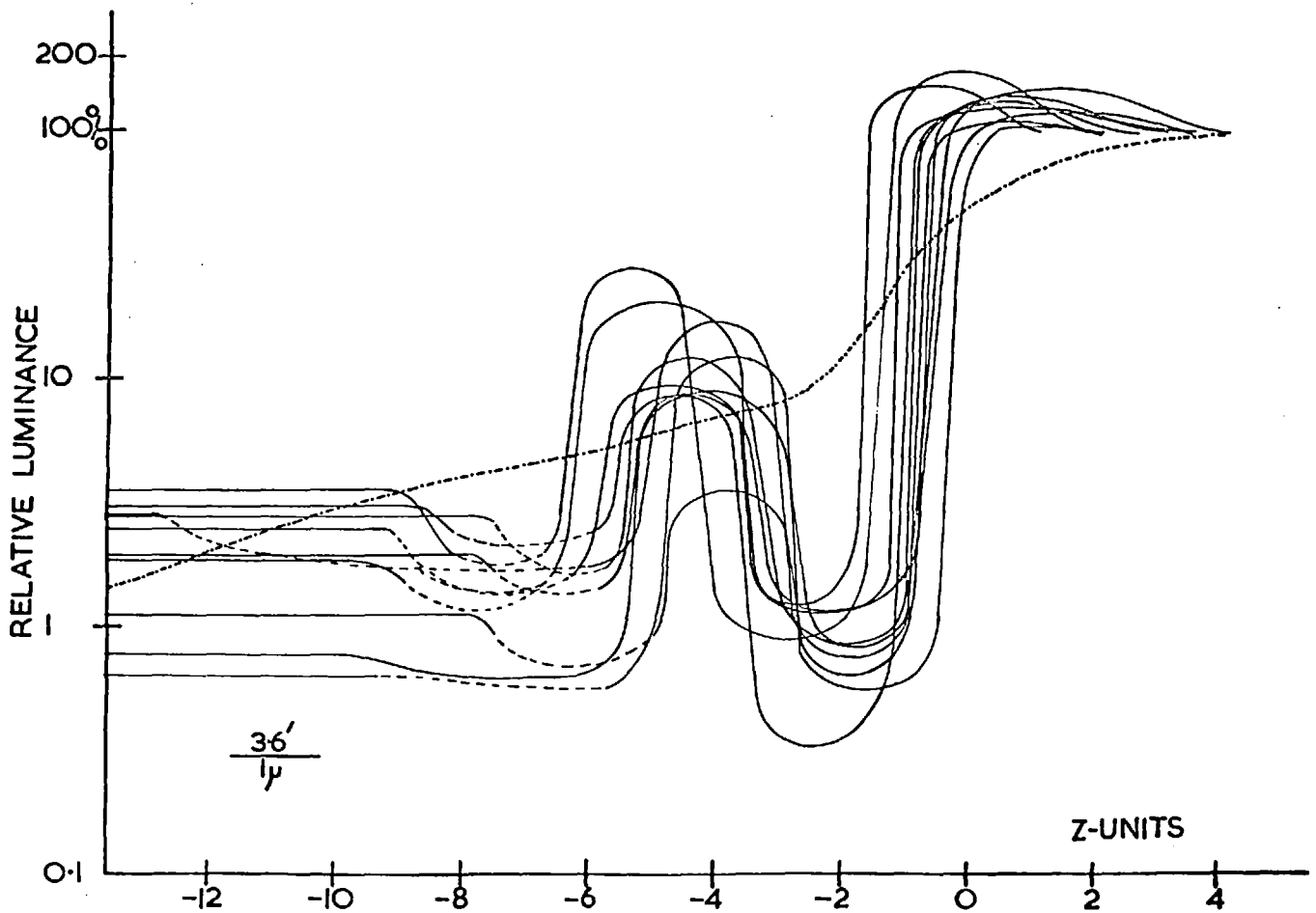


Fig. 4.06. Luminance profiles as seen by the observers R.C., P.R.H., J.R.H., E.H., K.H.R., C.S.E., C.B., D.E.L.F J.M.R., and G.A.G. S=2.2.

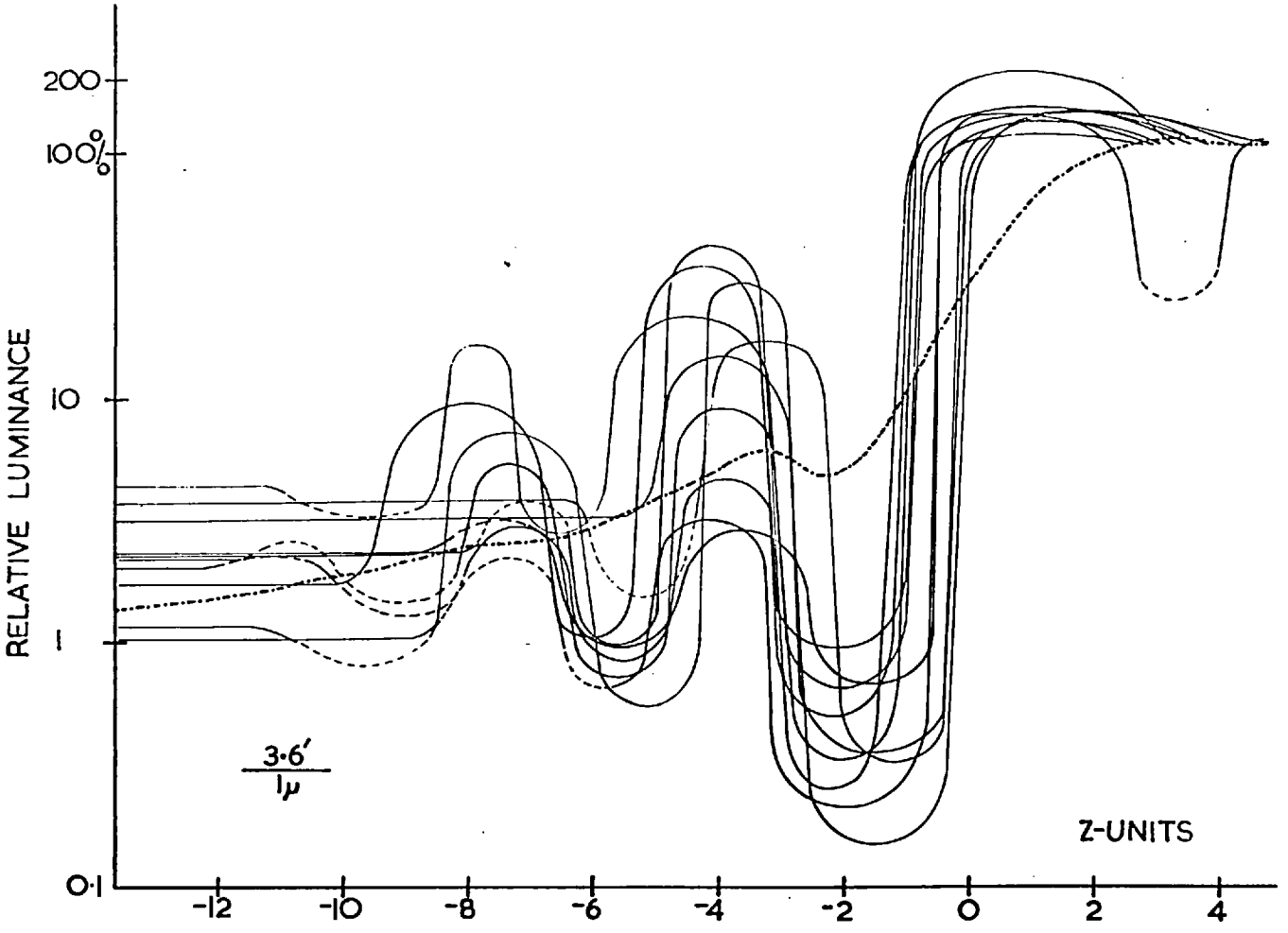


Fig. 4.07. Luminance profiles as seen by the observers A.E.S., T.Y., D.J.J.M., M.J.V., M.W.M., C.W., S.B.N., M.J.M. A.R.R., and S.H.R. S=0.60.

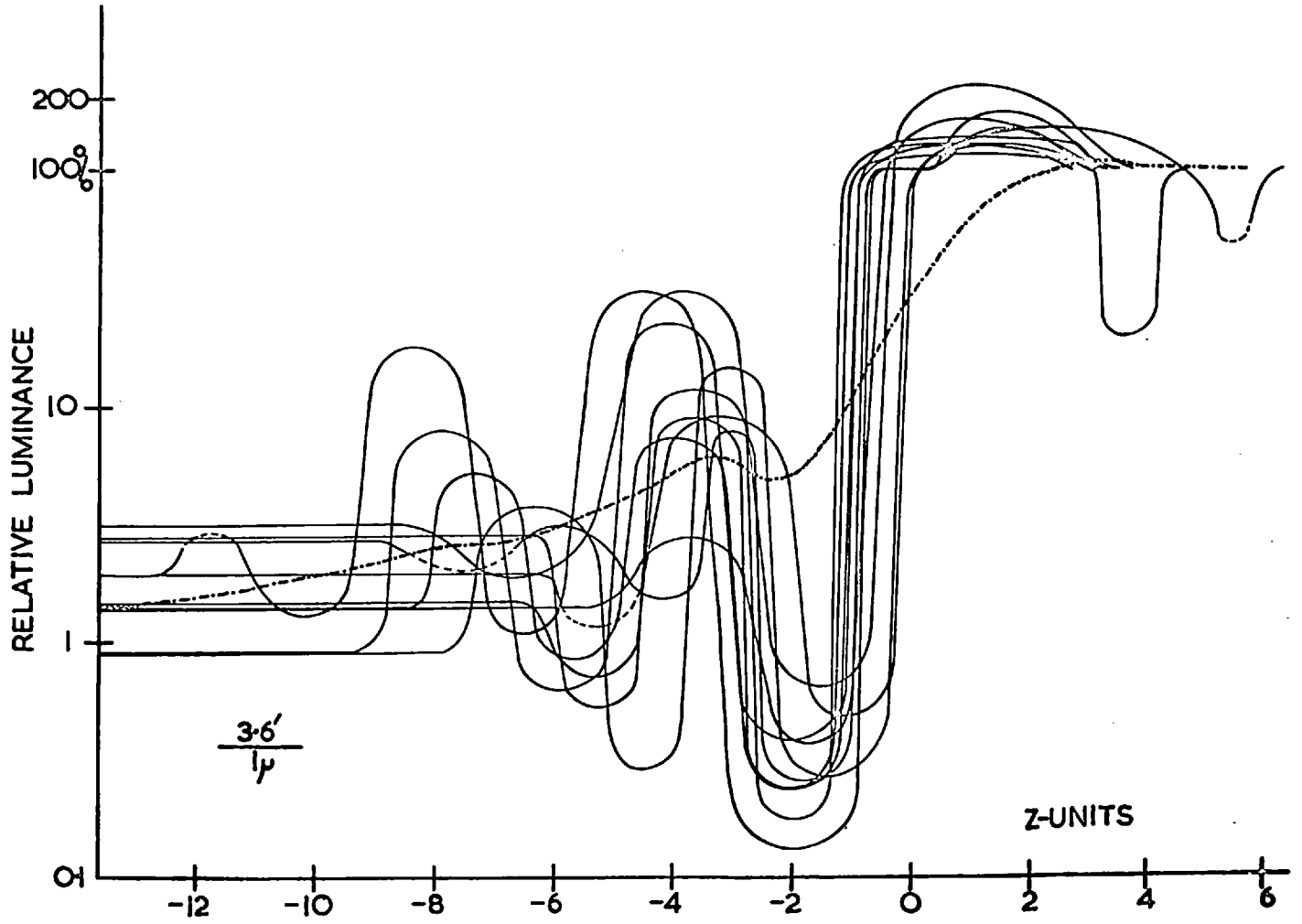


Fig. 4.08. Luminance profiles as seen by the observers R.C., P.R.H., J.R.H., E.H., K.H.R., C.S.E., C.B., D.E.L.F., J.M.R., and G.A.G. S=0.60.

6) The continuously dark field.

If we adopt the conventional formula for the resolving power $\Delta\xi$,

$$\Delta\xi = \frac{0.61\ \lambda}{(N.A.)}$$

we find a value of $\Delta\xi = 2.7\mu$ in the object space. In many cases the observed bands have widths as small as 1μ so it is extremely unlikely that they represent actual detail in the object. (In fact an examination with a high power oil-immersion obective showed that no such detail of these dimensions existed). Alternatively it might be argued that the bands seen are actually present in the diffraction image. That this is not the case can be seen from looking at the physical scans. Not only are the observed bands much more accentuated than the physical bands but they do not correspond in position with any possible physical counterpart. Therefore we may safely assume that these phenomena are subjective in their origin.

While the general appearance of the Mach patterns is substantially the same figs. 4.03 and 4.04 show that there are some striking differences between observers with regard to the number of bands seen. For S = 2.2 observers S.H.R., A.R.R., M.J.M., S.B.N., C.W., M.W.M., and M.J.V., saw three bands while the other observers clearly saw four bands.

One of the latter group of observers T.Y., saw a dark band on the bright side of the edge while for S = 0.60 observers C.S.E. and G.A.G. saw this band also.

In the case of S = 0.60 K.H.R. and E.H. saw hitherto unreported inflection points in the image; between the first bright band and the edge band a region of luminance equal in magnitude to the clear field was seen (these are indicated by dotted hatching in figs. 4.03, 4). The variation in the number of bands observed for S = 0.60 was greater than when S = 2.2. For example K.H.R. and T.Y. saw nine and eight bands respectively while P.R.H. and M.J.V. could only see three bands.

When observers scanned their eye rapidly across the edge one or two extra bands in the dark field were seen although these were not evident for most of the observation time. Direct fixation on a band decreased its visibility and observers found that the best procedure was to scan constantly along the edge while making position and luminance measurements. Most observers noted that a bright band appeared most distinct when they fixated about 20 minutes of arc from that band although it is not possible to make any measurements under such conditions.

Figs. 4.05, 6, 7 and 8 show that variations between observers were very pronounced. It is difficult to pick

out any general trends from these figures and attempts to correlate position or widths of bands with their relative luminances have not been successful. However fig. 4.09 shows a scatter diagram in which the relative luminances for the first bright band for S = 0.60 is plotted against its relative luminance for S = 2.2 for each of the twenty observers. Fig. 4.10 shows a similar diagram for the second bright band. It is apparent from these diagrams that certain observers see a given Mach band more brightly than others. However, an observer who sees a particular band (e.g. the first bright band) more brightly than average does not necessarily see another band (e.g. the second bright band) more brightly than average.

On each scatter diagram two regression lines (Davies, 1947) (1) and (2) are drawn. Let us denote readings taken for S = 0.60 by y and those for S = 2.2 by x. The equation of (1) is

$$Y = \bar{y} + b(x-\bar{x}),$$

where $\bar{y}$ is the mean value of y and $\bar{x}$ that of x and,

$$b = \frac{\sum(x-\bar{x}) \times (y-\bar{y})}{\sum(x-\bar{x})^2};$$

this gives us the best estimate of y when x is known by minimising the sum of the squares of the vertical

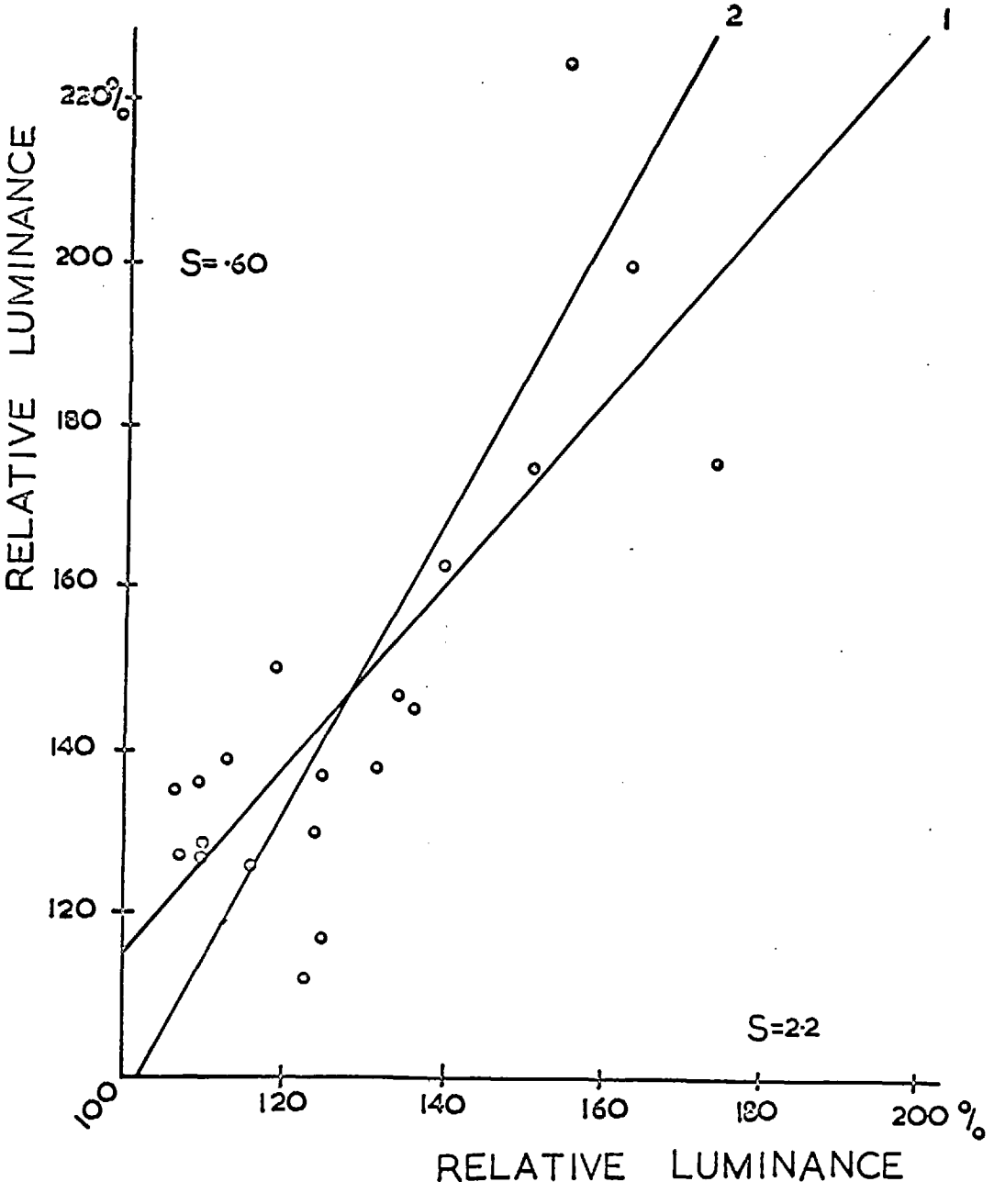


Fig. 4.09. Scatter diagram. The relative luminance for the first bright band for S=0.60 is plotted iagainst its relative luminance for S=2.2.

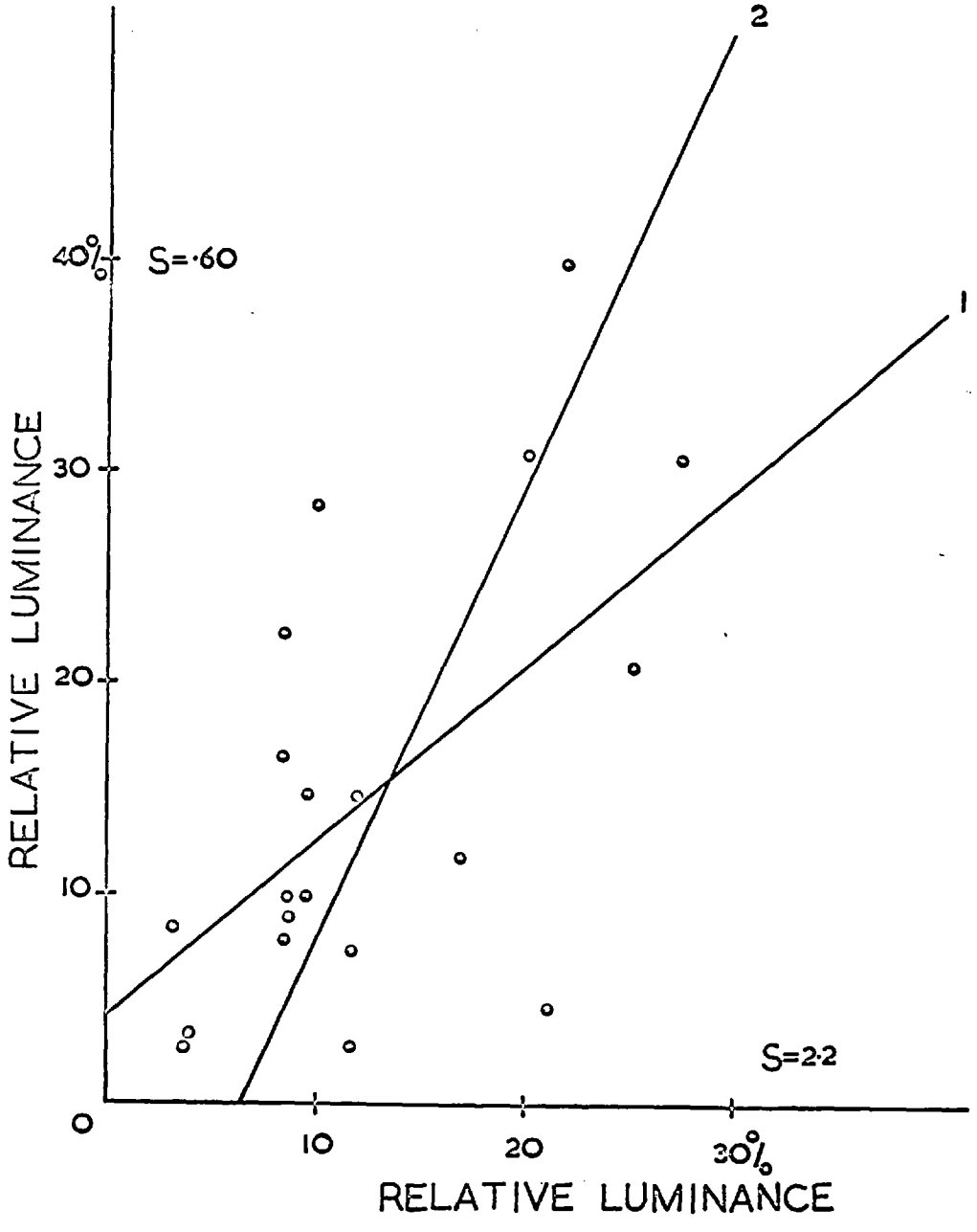


Fig. 4.10. Scatter diagram. The relative luminance for the second bright band for S=0.6o is plotted against its relative luminance for S=2.2

deviations from the line (1). The best estimate of x when y is known is obtained from the equation of (2),

$$X = \bar{x} + b'(y-\bar{y})$$

where $$b' = \frac{\sum(x-\bar{x}) \times (y-\bar{y})}{\sum(y-\bar{y})^2} ;$$

this minimises the sum of the squares of the horizontal deviations from the line (2). If the variables x and y were perfectly linearly correlated (1) and (2) would be the same. A measure of the degree of correlation is the correlation coefficient r (Davies, 1947) given by,

$$r = \frac{\sum(x-\bar{x}) \times (y-\bar{y})}{\sqrt{\sum(x-\bar{x})^2 \sum(y-\bar{y})^2}}$$

which would be unity for a perfectly linearly correlated sample.

The correlation coefficients for the first and second bright bands and also for the dark edge band were calculated. To assess the significance of the correlation coefficient recourse is made to statistical tables (Davies 1947) which give the probability P that a given correlation coefficient could be obtained from the same number of samples drawn at random from an uncorrelated population.

For the first bright band r = 0.79 and P = 0.001. For the second bright band r = 0.62 and P = 0.001. For the edge band r = 0.28 and P was greater than 0.1 This showed that a definite correlation existed in the case of the first and second bright bands but no such correlation could be inferred for the edge band.

The results obtained for brightness matching show that if an observer sees a particular Mach band more brightly than the average value obtained for all observers when viewing a given physical distribution of luminance (i.e. for S = 2.2) it will be highly probable that he sees the same band more brightly than average when the physical distribution is changed (i.e. for S = 0.60). Similarly there are observers who see a particular Mach band less brightly than average in both cases. From these results it would seem worthwhile to perform experiments using more S values to confirm the trend suggested by the results for the two S values quoted above.

Differences between observers' determinations of the visual edge.

From the point of view of the microscopist, who is engaged in the visual sizing of particles, it is of great importance to be aware of any personal differences which

may exist between different observers in their measurement of the visual edge which we shall assume to be the border between the first bright band and the edge band. From figs. 4.03, 4 in which the band positions are plotted we can see that there are differences in the positions of the boundaries as determined by different observers. Now each plotted position was the mean of ten readings and clearly we require some statistical evidence to determine if the differences between observers could have been solely due to random measuring errors or if fundamental personal differences existed between observers. The method which can deal adequately with these problems is the Analysis of Variance (Davies, 1947).

Consider the measurements made on one boundary. Let r = the number of observers, m = the number of observations made by each observer, then n = rm the total number of observations. Let x_{it} denote the t^{th} observation made by the i^{th} observer. Then,

$$x_i = \frac{1}{m} \sum_{t=1}^{m} x_{it} =$$

the mean value for the i^{th} observer. Let

$$\bar{x} = \frac{1}{r} \sum_{i=1}^{r} x_i = \frac{1}{n} \sum_{it} x_{it} = \text{the grand mean.}$$

The sum of the squared deviations of all n observations from the grand mean $\bar{x}$ can be written as m times the sum of the squared deviations of the r observer means from the grand mean plus the sum of the squared deviations from their respective observer means:

$$\sum_{i=1}^{r}\sum_{t=1}^{m}(x_{it}-\bar{x})^2 = m\sum_{i=1}^{r}(x_i-\bar{x})^2 + \sum_{i=1}^{r}\sum_{t=1}^{m}(x_{it}-x_i)^2$$

We now make the null hypothesis that the means of the populations of observations x_{it} for the r observers are all equal (i.e. there are no personal differences between observers' measurements apart from random sampling errors). If the null hypothesis is true we have three unbiased estimates of the common variances of the r populations obtained by dividing the sums of squares in the equation by their respective degrees of freedom. These estimates are:

$$S_1^2 = \frac{1}{n-1}\sum_{i}\sum_{t}(x_{it}-\bar{x})^2$$

$$S_2^2 = \frac{m}{r-1}\sum_{i}(x_i-\bar{x})^2$$

$$S_3^2 = \frac{1}{n-r} \sum_i \sum_t (x_{it}-x_i)^2 \ .$$

If the null hypothesis of equal means is true the last two quantities should be equal (except for a sampling error). We divide S_2^2 by S_3^2 to form the F ratio:

$$F = \frac{S_2{}^2}{S_3{}^2} \ .$$

We reject the null hypothesis of equal means at the significance level of probability P if F exceeds the critical value of F given in statistical tables of the F distribution. With the value of F must be associated the number of degrees of freedom involved which for S_2^2 is (r-1) and for S_3^2 is (n-r). (A probability P = 10% means that the observed value of F would occur about once every ten trials if the null hypothesis were true. A low probability indicates that the null hypothesis is false.)

An analysis of variance was firstly carried out on the results of the twenty observers with regard to the position of the visual edge. The F ratios obtained for S = 0.6 and S = 2.2 were 3.92 and 8.11 respectively. Both these ratios lie below the 1% probability level of significance so that the null hypothesis could be confidently rejected and personal differences were therefore present. Having

established that personal differences were present it was decided to divide the twenty observers into groups whose means (for the visual edge) did not differ significantly. Three such groups of five were isolated:

1) C.S.E., A.E.S., M.J.V., M.W.M., A.R.R.,

2) C.B., D.E.L.F., T.Y., C.W., S.B.N.,

3) P.R.H., E.H., J.M.R., G.A.G., M.J.M.

In each of these groups, for both S = 0.60 and S = 2.2, the F ratio was above the 10% significance level of probability so that there was no evidence to suggest that the null hypothesis was false. The remaining five observers could not be specified into any such group although it is plausible that if the number of observers were increased further special groups would become evident. However when an analysis of variance was performed on any of the above groups with regard to the position of the other Mach band boundaries significant variations between individual observer's means within the groups were shown.

The relationship between the Mach bands and the physical image.

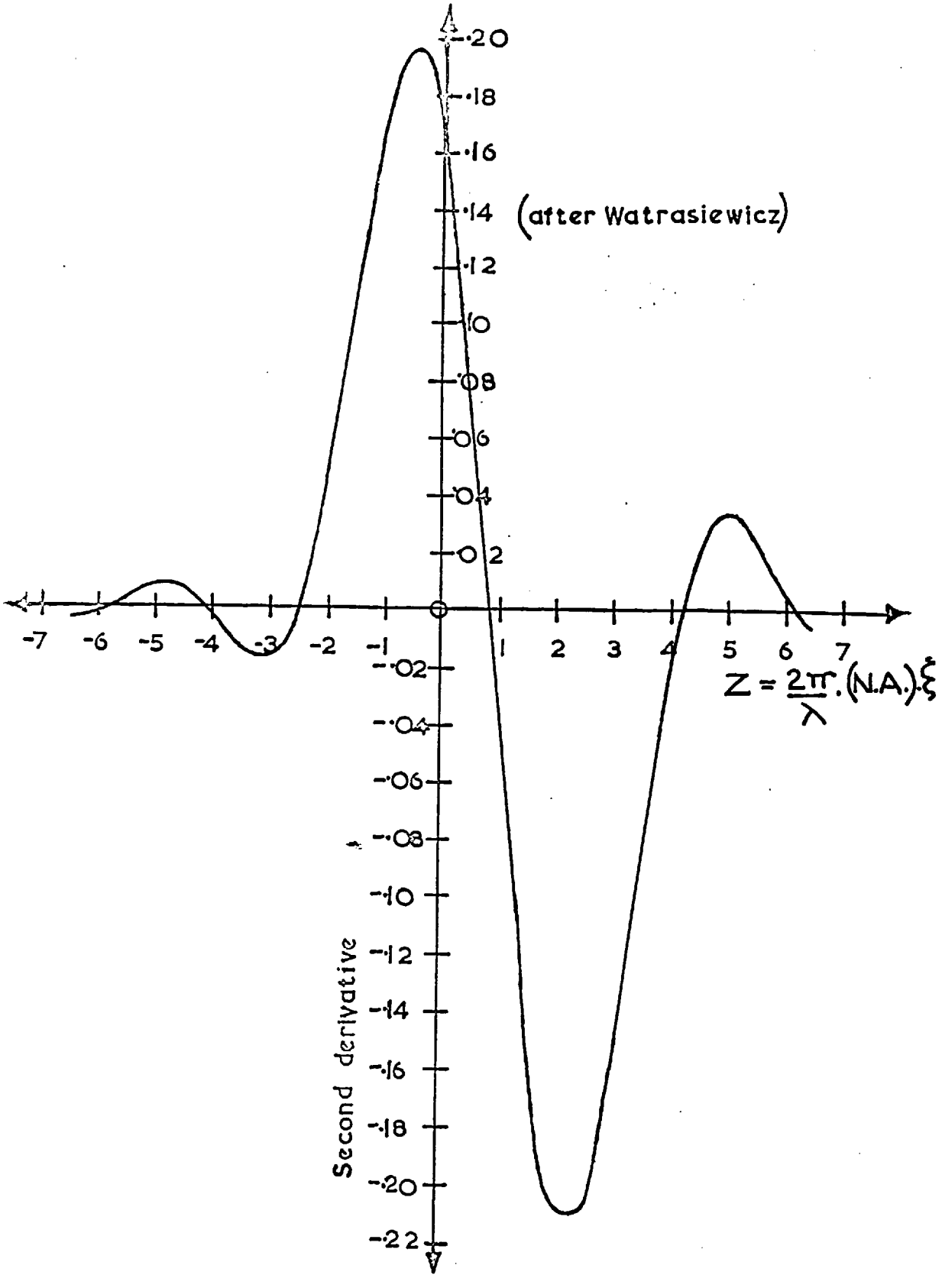
It is apparent that the Mach bands are a source of artifacts in microscopy like diffraction, aberrations and

the curious haloes seen in phase contrast techniques. Of particular interest to microscopists would be a method whereby the Mach bands' positions and relative luminances could be calculated if the physical distribution of luminance were known. Reference to figs. 4.09 and 4.10 shows that any attempt to predict the luminances of the bands would be rather difficult as any theory must incorporate a "personal equation". In the case of S = 0.60 the relative luminance of the first bright band varies between 225% and 112% while the second bright band assumes values from 41% to 5% and when S = 2.2 we have corresponding ranges of 173% to 105% and 27% to 5% respectively.

In connection with the prediction of band positions the second derivative postulate, which was first suggested by Mach (1865) and used subsequently by Ludvigh (1954) and Watrasiewicz (1964) seems worthy of serious consideration.

In order to determine the second derivative of luminance with respect to distance one method of approach would be to numerically differentiate twice the physical distribution curve (determined with the photo-electric microscope). This, unfortunately, is a very inaccurate process. Watrasiewicz (1965) has given the second derivative of luminance for the theoretical image profile of an edge when $S \leq 1$ (assuming scalar diffraction theory).

Fig. 4.11 The second derivative of the edge image. S= 0·60



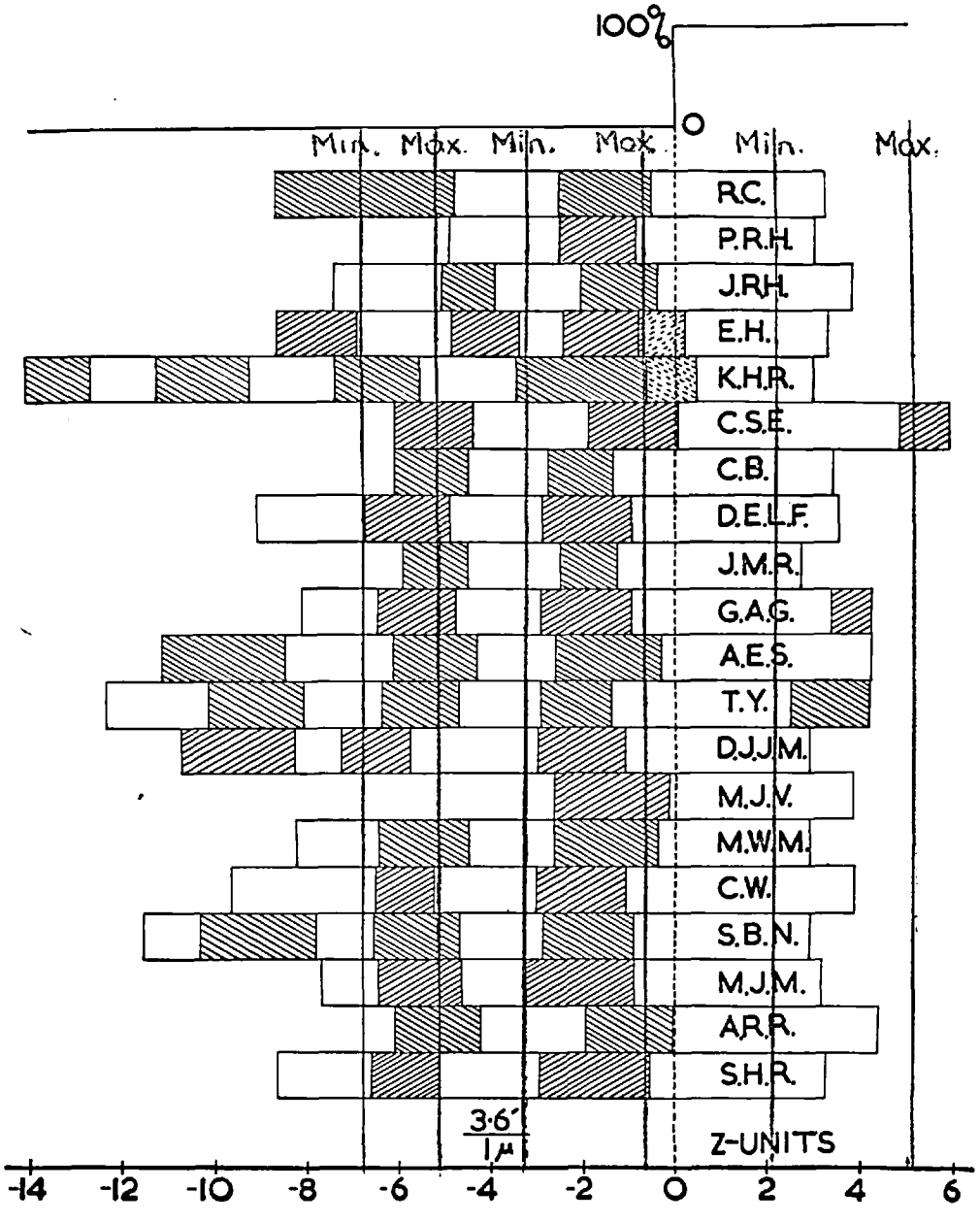


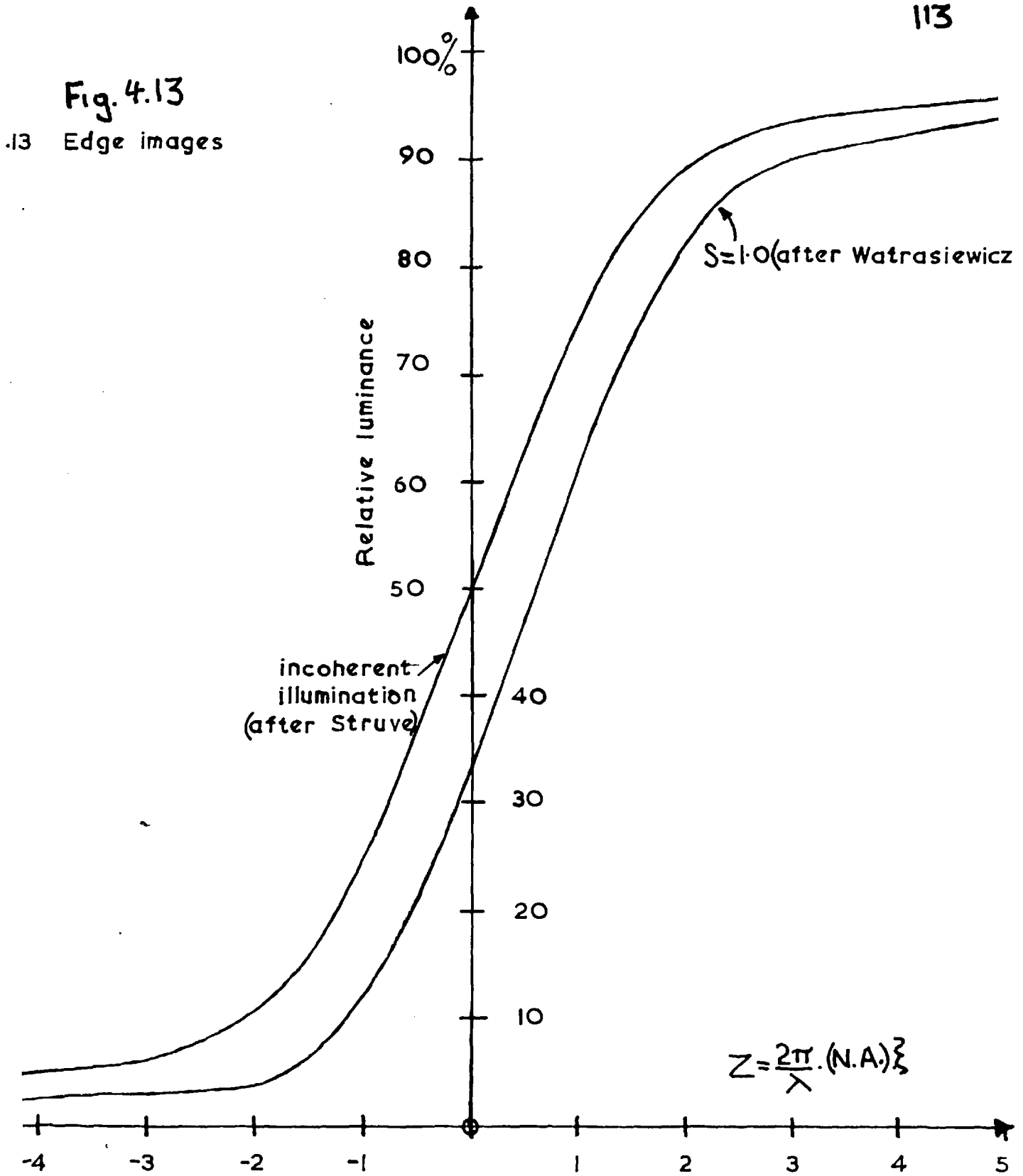
Fig. 4.12. Mach bands and the stationary values of the second derivative of the physical luminance distribution. S=0.60

The only numerical work involved was one stage of integration. Fig. 4.11 shows Watrasiewicz's results for S = 0.60. According to the second derivative postulate bright and dark bands should be seen where this curve has minima and maxima respectively. The maxima and minima are indicated in fig. 4.12 together with the plotted positions of the Mach bands for S = 0.60. The amount of agreement with the postulate for the first and second bright bands is generally reasonable while for the observers C.S.E., A.E.S., M.W.M., and A.R.R., both dark and bright band positions agree well with the theory.

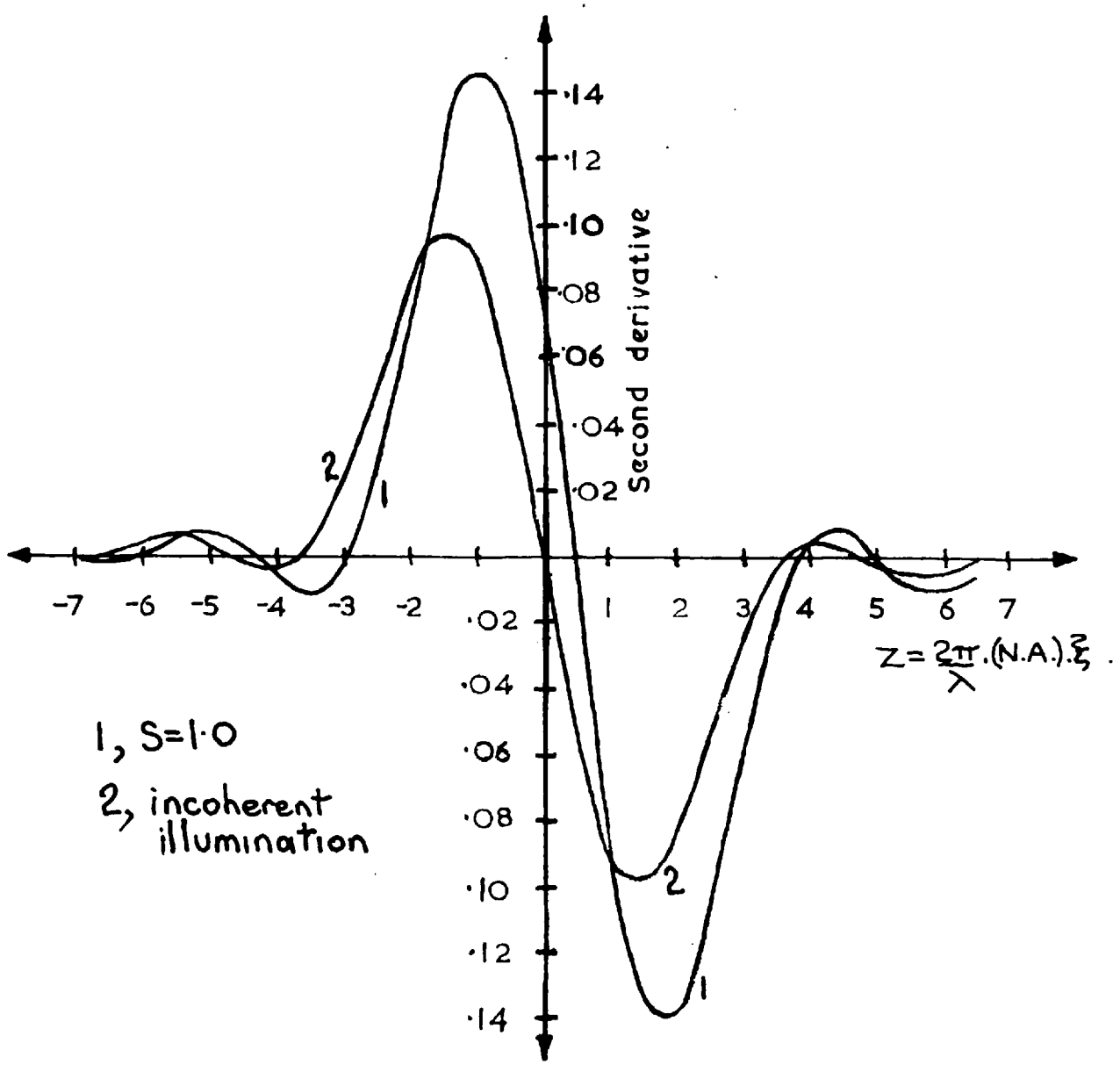
No calculations have been published for the physical luminance profiles of edges when S > 1 except for the extreme case of incoherent illumination when S theoretically assumes an infinite value, but for all practical purposes these conditions are realised when S exceeds 5.0. The calculation for the incoherent case was first performed by Struve (1882). Fig. 4.13 shows the calculated physical luminance profile across an edge for incoherent illumination and for S = 1.0. These curves appear very similar apart from the fact that the curve for S = 1.0 is displaced by roughly half a z unit towards the bright field. The curve for S = 2.2 must lie somewhere between the two curves. Watrasiewicz's results for the second derivative for S = 1.0

Fig. 4.13

.13 Edge images



Fig·4.14 Second derivatives of edge images



are plotted in fig. 4.14 together with the second derivative for S = ∞ (obtained by differentiating Struve's expression analytically; see Chapter VI). Here the stationary values of the curves are separated by about half a z unit and we can arrive at an estimate of where the curve for S = 2.2 has maxima and minima by taking the mean values of the separate maxima and minima shown in fig. 4.14. These mean values are plotted in fig. 4.15 together with the plotted Mach band positions for S = 2.2. Results for P.R.H., J.R.H., C.S.E., J.M.R., and G.A.G., show reasonable agreement with the second derivative postulate and the positions of the first and second bright bands are generally well accounted for by this theory.

For both S values, however, there are a number of observers' measurements where the second derivative postulate seems generally of little use when all the observed Mach bands are considered: the results of R.C., K.H.R., and S.B.N., for S = 2.2 and the results of R.C., E.H., K.H.R., C.W., S.B.N., and S.H.R., for S = 0.60.

In conclusion we may say that, while the second derivative postulate gives us a good idea of the relative separations of the Mach bands its usefulness in predicting actual band positions is rather limited.

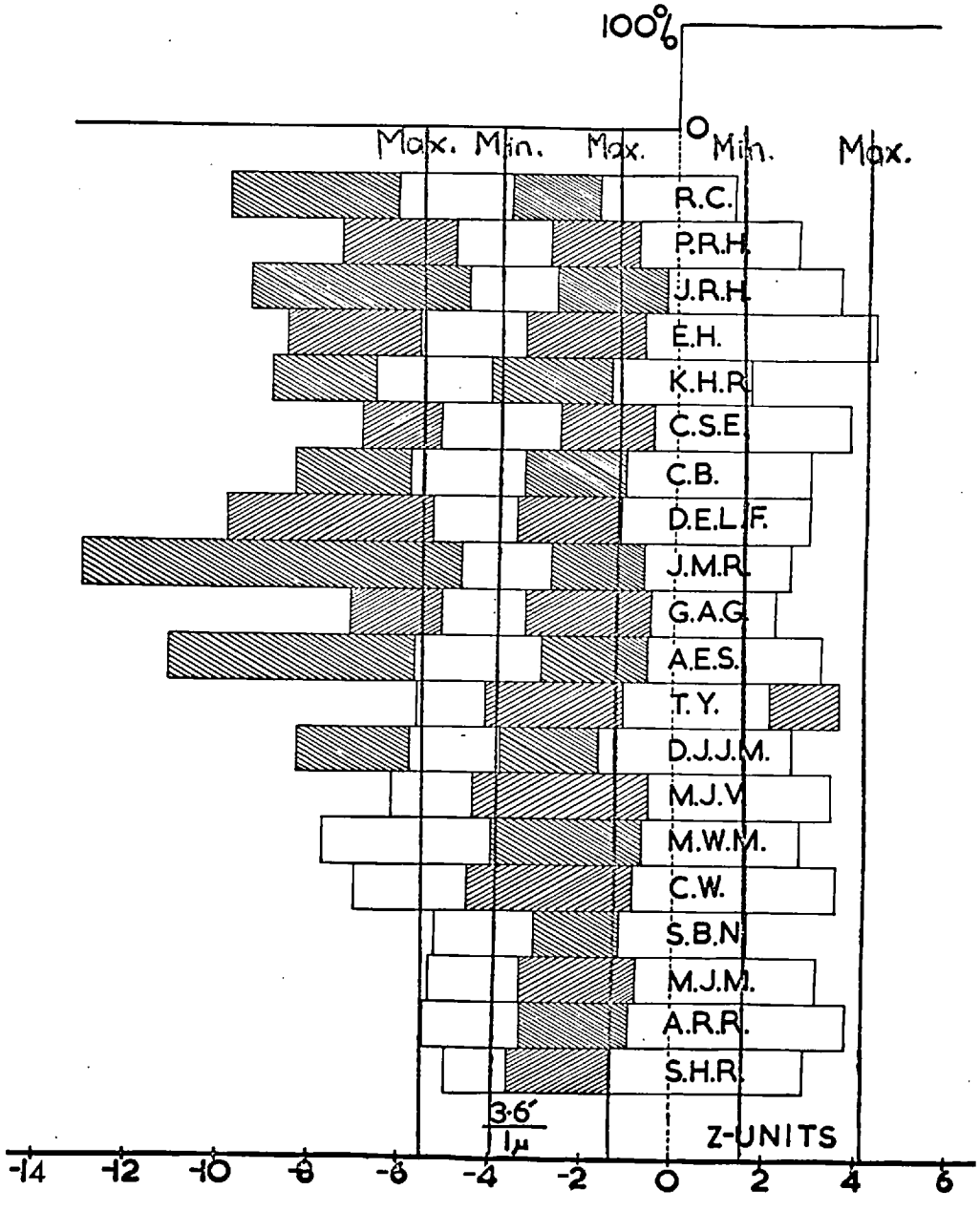


Fig. 4.15. Mach bands and the stationary values of the second derivative of the physical luminance distribution. S=2.2

The influence of ocular axial length on the Mach bands.

Stenström (1946) measured the axial lengths (anterior of the cornea to the retina) of one thousand adult eyes using Rushton's X-ray technique. His results are shown in fig. 4.15. He found a marked departure from a symmetrical statistical distribution. Eyes with an axial length of over 27.5 mm. invariably show conus (displacements of the inner coats of the eye indicating elongation of the eye-ball accompanied by angling of the optic nerve exit) and if such cases are eliminated from the results, together with the results of observers who have serious refractive errors, the distribution curve for axial length becomes symmetrical (the full curve shown in fig. 4.16). The distribution gives a mean value of 23.5 mm. and has extreme values of 21 mm. and 26 mm. This 20% variation between observers for axial lengths of the eye must be accompanied by a similar percentage variation in the focal length of the eye lens if light is to be focused onto the retina.

Fig. 4.17 shows the eye viewing the primary microscope image at P through an eyepiece. It is assumed that the eye is relaxed and that it focuses parallel light onto the retina as P lies in the first focal plane of the eyepiece. A variation of 20% in the focal length of the eye will result in a similar variation in the overall magnification

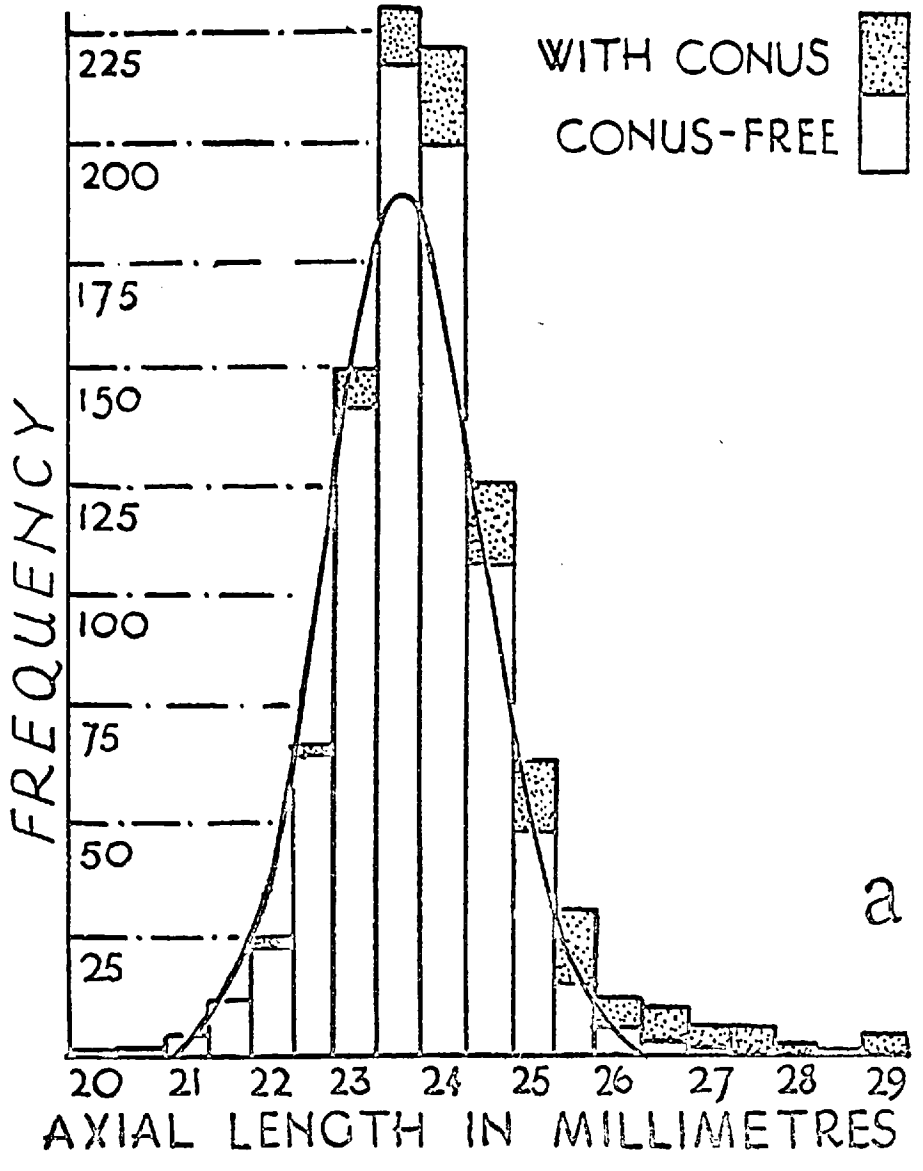


Fig. 4.15. Variation of ocular axial length (Stenstrom 1946)

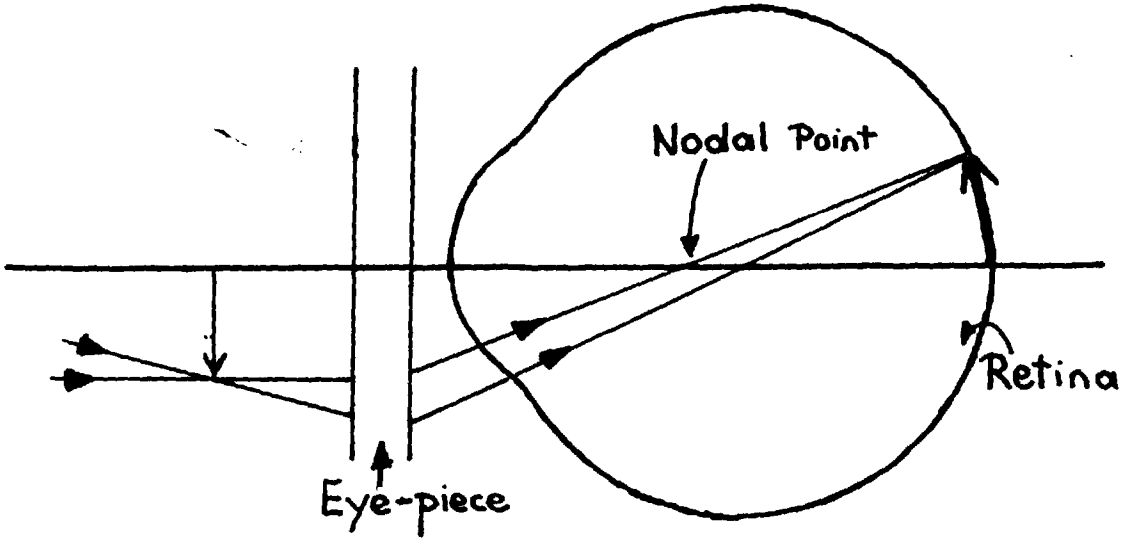


Fig. 4.17

of the system comprising the eyepiece plus the eye. Consequently the scale of the diffraction structure in the edge image might be expected to vary by as much as 20% between different observers. If this structure is more spread out it will cover more receptors and therefore the total inhibitory effect will be greater and thus the Mach bands should appear less accentuated than in the case where the image structure is not so elongated. (A similar argument applies to the question of decrease in the slope of the graded zone which is considered in Chapter I.) It is therefore plausible that observer variations in ocular axial length result in some of the personal differences described earlier in this Chapter.

The effect of physiological differences on the Mach bands.

Pedler (1965) has carried out extensive electron-microscopical studies on the retina of man and other primates. His work has revealed the existence of a very complex interconnecting network between the retinal receptors and it is presumably this network which is responsible for mediating the lateral inhibitions between the receptors which give rise to Mach effects. With such a complicated system it is highly probable that physiological differences occur between individuals with a consequent variation in

the inhibitory coefficient R in the Ratliff Hartline equation

$$r_1 = e_1 - k_{12} (r_2 - r_{12}^{o})$$ (see page 25)

which would yield different responses to a given distribution of illumination on the retina.

Chapter V

The influence of small defocusing errors on the Mach bands.

Introduction

The measurements on the Mach band positions, which have been described in Chapter IV, were performed when the observer had obtained as sharp a focus as possible so that the transition of apparent luminance from the first bright band to the edge band was most rapid i.e. the visual edge appeared sharpest. It is well known that for any optical instrument there is a range of focal positions, known as the depth of focus, through which no noticeable degradation in image quality occurs and we shall now recall some of the image quality criteria used to estimate tolerances on defocusing.

Strehl Intensity and the Rayleigh limit.

For small aberrations a measure of image quality can be made by considering the intensity of the central maximum in the image of a point source (often referred to as the Airy pattern after Sir G. B. Airy, who first gave the correct mathematical formulation for the image of a point source in 1835. It may be argued that if the elementary

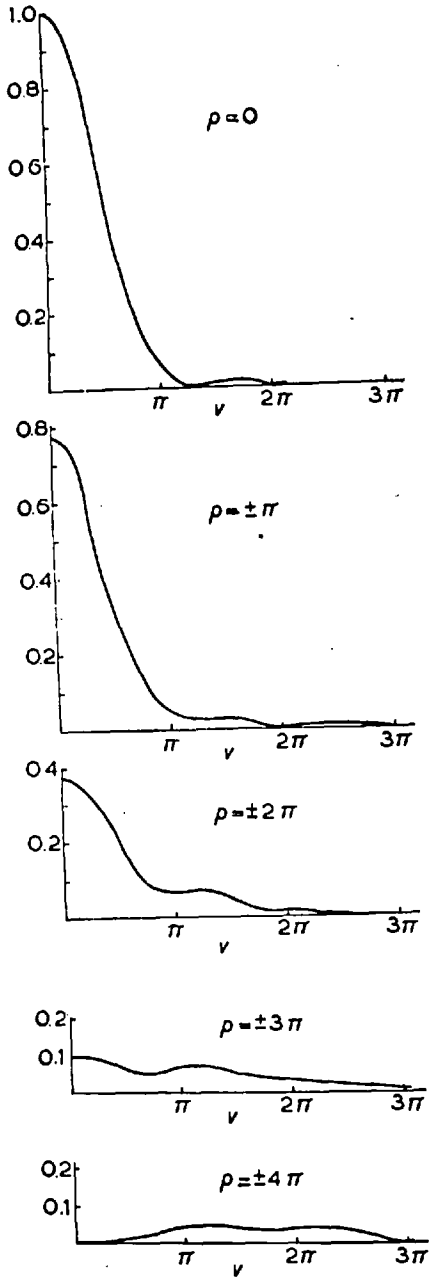


Fig. 5.01. Defocussed images of a point source. The ordinate is the light intensity, normalized to unit intensity at the centre of the in-focus image ($p = 0$) and the abscissa v is the radial distance from the centre of the image. (after Welford, 1962)

point image shows an appreciable change the modification is likely to be transferred to the image as a whole, independently of the particular character of the image. Fig. 5.01 shows some defocused images of a point source; it is assumed that there are no other aberrations present except defocusing. Amounts of defocusing are expressed by the parameter p where

$$p = \frac{2\pi}{\lambda} \cdot u^2 . \delta$$

where δ is the actual distance from the geometrical focal plane, λ is the wavelength of the light and u is the convergence angle which the marginal ray makes with the optical axis of the system (fig. 5.02). (Here p is twice the value considered in chapter VI.) For values of p less than 2π the effect of defocusing is simply a reduction in intensity of the central maximum accompanied by a slight increase in intensity of the fringes outside the maximum. Strehl (1902) used this property of the defocused Airy pattern to formulate a tolerance on defocusing and he introduced the notion of the "Definitionshelligkeit" S (now referred to as the Strehl Intensity)

$$S = \frac{I}{I_G}$$

where I_G is the central intensity in the Airy pattern at

the Gaussian (geometrical) focus with no aberrations and I is the value for the aberrated image. It is customary to take as the tolerance limit, the amount of defocusing (or more generally aberration) for which S is reduced to 0.8. This occurs when $p = \pm \pi$ approximately so that the total tolerance range on defocusing (above and below the Gaussian focus) is given by,

$$\delta = \frac{\lambda}{u^2}$$

Some years earlier than Strehl, Rayleigh (1879) had proposed his celebrated "quarter wave limit" for use as a tolerance on aberrations and we shall consider this applied to simple defocusing. Let there be an axial Gaussian image point O_1 (fig. 5.02) which is at the centre of the reference sphere $\sum_1$ situated in the exit pupil of the optical system. Let O_2 be another axial point distant δ from O_1 and at the centre of the reference sphere $\sum_2$. O_2 is then regarded as within the depth of focus if the radial separation between $\sum_1$ and $\sum_2$ (MP) at the edge of the exit pupil is less than $\frac{\lambda}{4}$ where λ is the wavelength of the light. We require a relation between the depth of focus $\delta(O_2O_1)$ and MP which is set equal to a quarter of a wavelength.

Drop a perpendicular from O_2 onto MPO_1 to meet this line in B. We have,

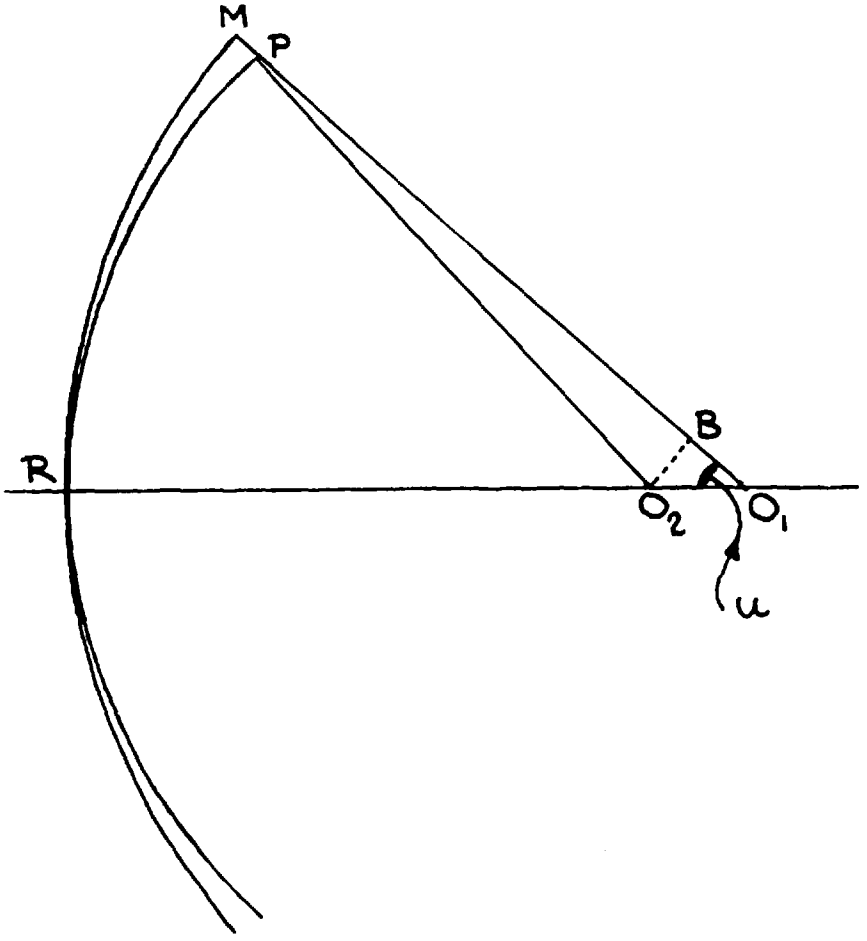


Fig. 5.02 The Rayleigh tolerance.
O_1 is the Gaussian focus. $MP \leq \frac{\lambda}{4}$

$$MP = MO_1 - PO_1$$

$$MP = MO_1 - PB - BO_1$$

But $PB \doteqdot PO_2$

therefore $MP = RO_1 - PO_2 - BO_1$ with an order of inaccuracy which is small compared to MP.

therefore $MP = RO_1 - RO_2 - BO_1$,

therefore $MP = O_2O_1 - BO_1$.

Hence $MP = O_2O_1(1 - \cos u)$

and therefore $MP = O_2O_1 \cdot 2 \sin^2 \frac{1}{2} u$.

With $MP = \frac{\lambda}{4}$ and $O_2O_1 = \delta$ we have, $\frac{\lambda}{4} = 2 \cdot \delta \sin^2 \frac{1}{2} u$.
The total value of δ, above and below the Gaussian focus is therefore given by,

$$\delta = \frac{\lambda}{4 \sin^2 \frac{1}{2} u} .$$

For systems of small numerical aperture (i.e. where N.A. < 0.3), when $\sin^2 \frac{1}{2} u = \frac{u^2}{4}$ the expression reduces to the one obtained by Strehl,

$$\delta = \frac{\lambda}{u^2} .$$

Using this criterion the total depth of focus for the 0.12 numerical aperture objective with $\lambda = 0.53\mu$ would be 37μ.

The Optical Transfer Function.

The optical transfer function D(s) (see page 34) of a defocused system has been examined by Hopkins (1955). Hopkins defines the frequency variable S of a periodic (sinusoidal) incoherently illuminated object by the relation,

$$S = \frac{\lambda}{n \sin \alpha} .R = \frac{\lambda}{n' \sin \alpha'} .R'$$

where R is the number of lines per millimetre, λ the wavelength of the light, α the marginal ray inclination and n is the refractive index in the object space while the dashed symbols apply to the corresponding quantities in the image space.

In Chapter I (page 34) the optical transfer function has been defined from the relation,

$$A(\nu) = |A(\nu)|e^{i\theta(\nu)},$$

but here we shall adopt Hopkins' nomenclature, namely that,

$$D(s) = T(s)e^{i\theta(s)}$$

If the pupil is symmetrical about the axis and the only aberration present is pure defocusing the phase shift $\theta(s)$ is always zero. The transfer functions were calculated for various defects of focus expressed in terms of the

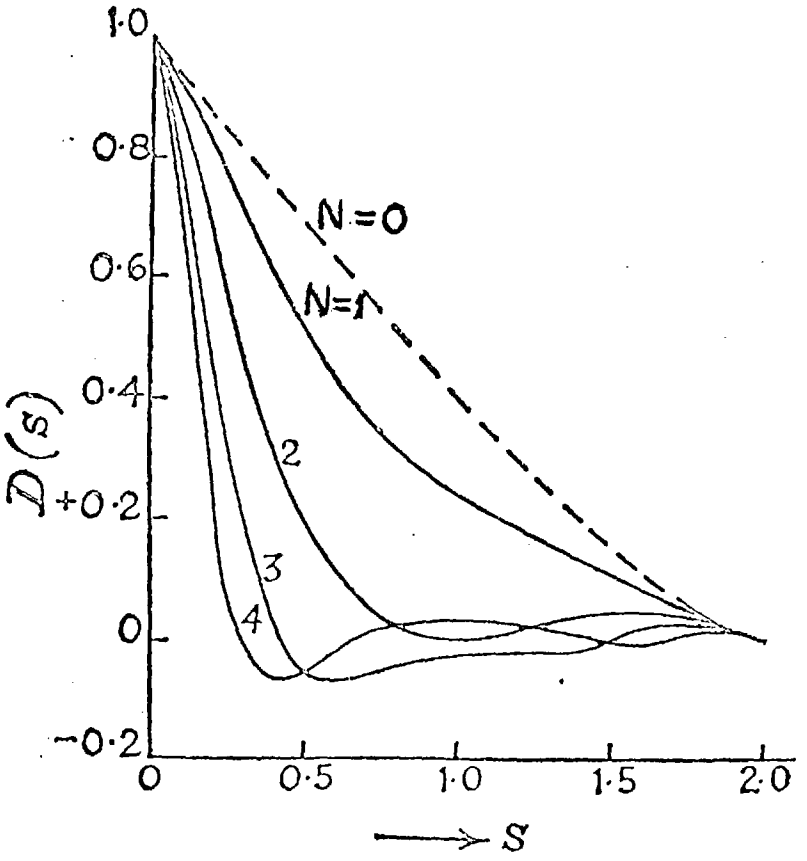


Fig. 5.03. Out-of-focus response as a function of object frequency *s*. The curve numbers relate to a defect of focus given by N. (Hopkins).

maximum optical path discrepancy found amongst the disturbances arriving at the extra focal point from the elements of the aperture. Suppose that the axial shift of focus is $d\ell'$ then the maximum optical path discrepancy is $\pm \frac{1}{2} n' \sin^2\alpha' \, d\ell'$. We let $\pm \frac{1}{2} n'\sin^2\alpha' d\ell' = \frac{N\lambda}{\pi}$ where N is a numerical coefficient. Hence $\frac{2\pi}{\lambda} (n'\sin^2\alpha' d\ell') = 4N$. The Rayleigh limit corresponds to $N = \frac{\pi}{8}$ and if we include defocusing on either side of the geometricalfocus we put $N = \frac{\pi}{4}$. Hopkins studied cases for which N ranged from 0 to 60. Fig. 5.03 shows the transfer function plotted as a function of line frequency S for various defects of focus. As the focus defect increases beyond N = 1 there is a marked deterioration in the response of the system for higher frequencies. An interesting feature of these curves is the occurrence of values of D(s) of alternating sign above the frequency for which resolution has ceased (i.e. D(s) = 0). This is, in fact, an indication of "spurious resolution"; the negative values of D(s) represent a phase shift of π radians in the image and accounts partly for the fact that the appearance of apparent reso-l lution in the case of a periodic object may sometimes be a deceptive test for a true focus. Hopkins suggests a tolerance for defect of focus based on the fact that the contrast in the defocused image should not fall below 80%

of that at the Gaussian focus. The formula is,

$$d\ell' = \frac{\pm\ 0.2}{R' \sin \alpha'}$$

and it is interesting to note that the formula involves only the first power of sin α' rather than its squared value as in the Rayleigh and Strehl tolerances. This approach is useful insofar as it demonstrates that the defocus tolerance for high spatial frequencies is smaller than for the lower frequencies but in microscopy the efficacy of this method is rather limited. Truly incoherent illumination is seldom achieved in microscopy but even if this condition were realised an application of the above formula to determine a tolerance on defocusing would be extremely difficult. Most objects contain components of differing spatial frequencies and we must ask if there is a given spatial frequency in the distribution which, subject to the equation,

$$\delta\ell' = \frac{\pm\ 0.2}{R' \sin \alpha'}$$

governs the tolerance on defocusing for the whole image. One possible answer might be that the highest frequency, since it yields the smallest value of d , is just this frequency. This answer would only be feasible if all the frequency components present in the object had the same

modulation (contrast). In general this certainly is not the case and therefore the optical transfer function approach is of little worth as there exists no method of weighting different modulations of frequencies (particularly where visual assessment of the image is involved).

Edge Gradient.

It is a common experience that the edges present in a defocused image appear blurred and in terms of visual appraisal of the image it is generally edge sharpness that governs, from an aesthetic and informational viewpoint, the ultimate tolerance on defocusing. The edge gradient (taken at the 50% transmission point) would therefore seem to be a useful measure of image quality (fig. 5.04). Welford (Weinstein, 1953) has shown that, with incoherent illumination, the edge gradient steadily decreases as the amount of defocusing is increased. Calculations performed by the author (see fig. 6.03) show that a similar result (for small amounts of defocus at least) obtains in the case of coherent imagery. Using the formulae developed by Welford (Weinstein, 1953) and Steel (1952) it can be shown that for an amount of defocus corresponding to the Rayleigh $\frac{\lambda}{4}$ limit the edge gradient has been reduced to 85% of its value at the geometrical focus and this provides us with a

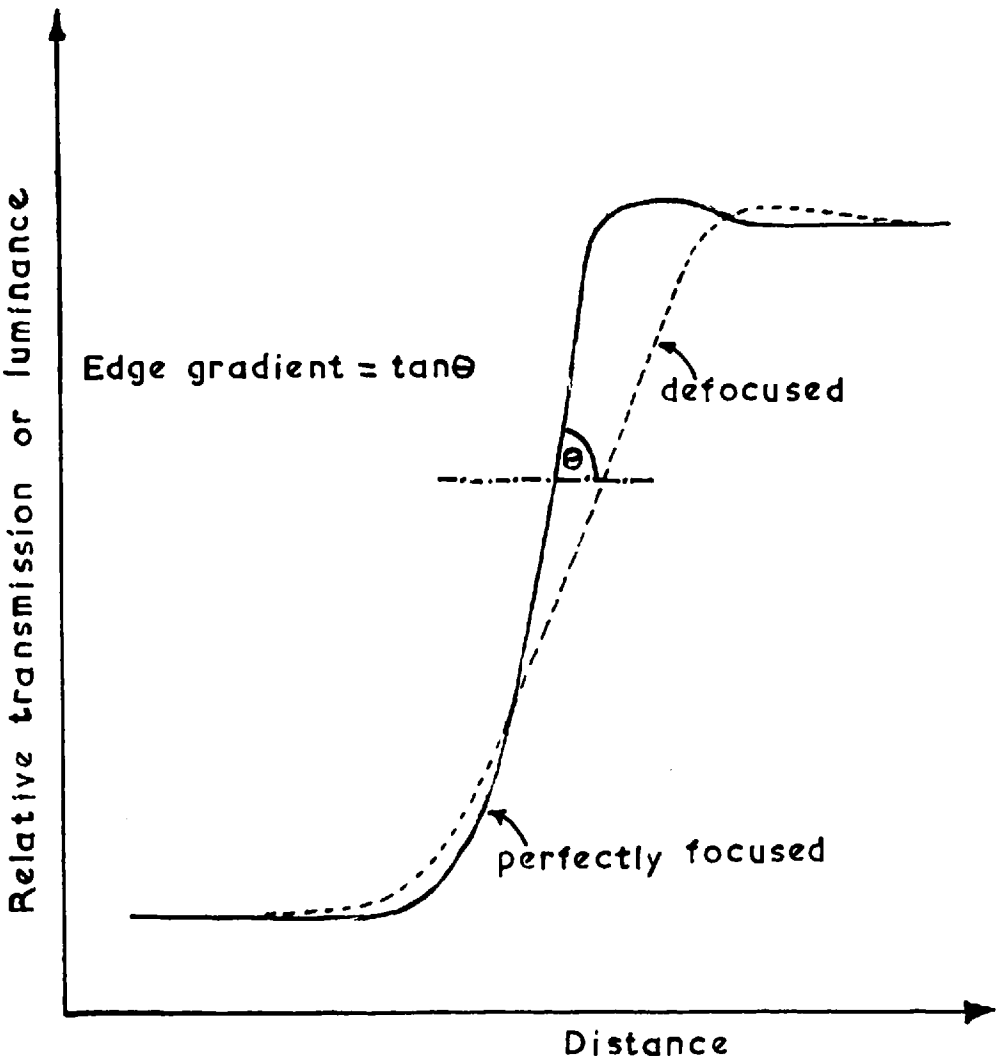


Fig. 5.04 Edge gradient as a measure of image quality

working rule for a tolerance on edge-gradient when simple defocusing is being considered.

The visual depth of focus.

It was decided to investigate the magnitude of the visual depth of focus defined by the range of focal settings through which the visual edge appeared equally sharp and to see if the positions of the bands remained constant within this range.

For measurements of the axial displacements of the objective a millimetre micrometer was bolted onto the microscope stage (fig. 5.05) so that the micrometer stem could locate with a flat $\frac{1}{4}$ inch thick steel plate which was fixed to the microscope barrel with four screws. Measurements made with the micrometer agreed to within 1μ, with the calibrations provided by the manufacturers on the fine focus knob.

With the eye relaxed the author focused with the eye-piece onto the tip of the tungsten wire, as in the survey described in Chapter IV. By slowly racking the objective up and down whilst observing the edge image and the tip of the wire simultaneously it became apparent when the visual edge was sharpest. The range of values on the fine focus knob for which the visual edge appeared sharpest were noted

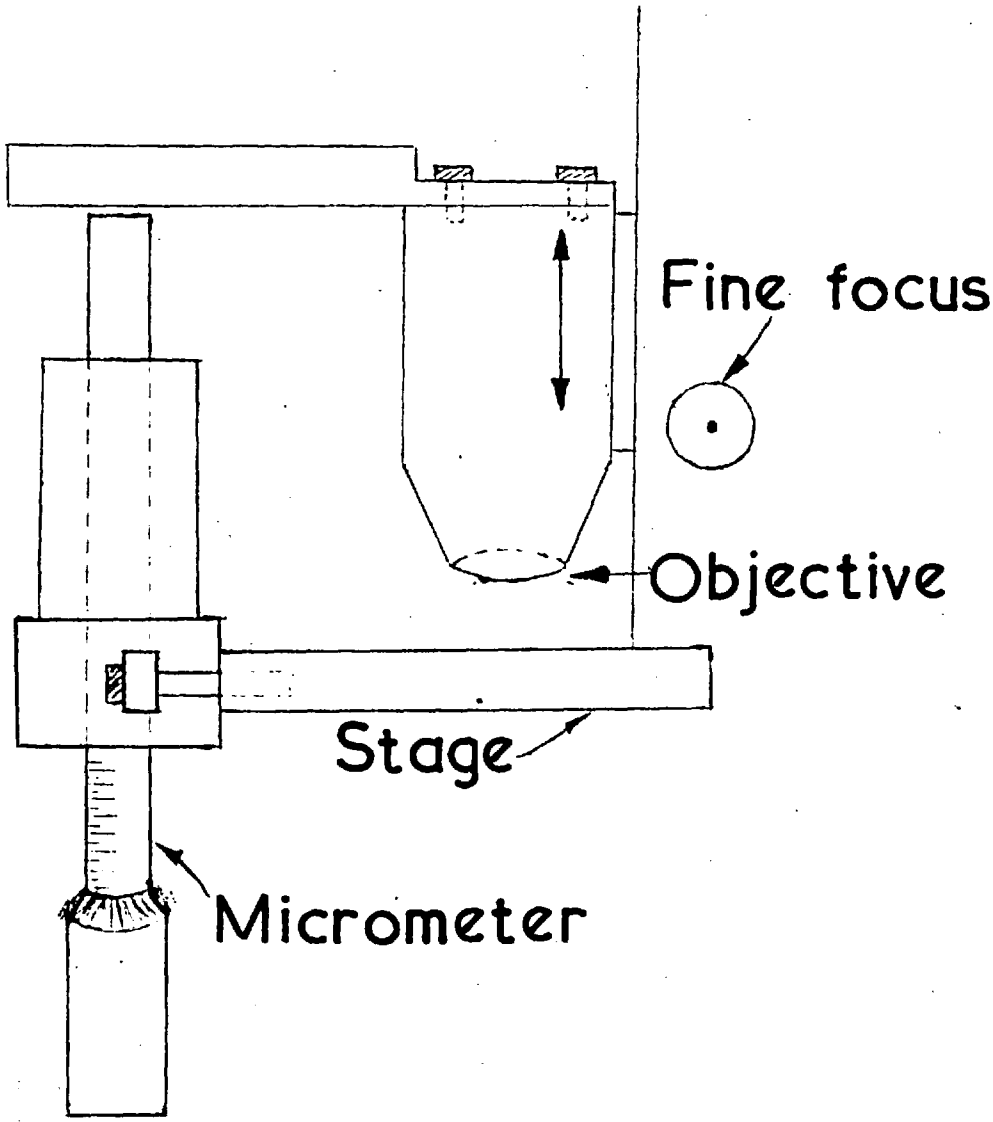


Fig. 5.05

(care being paid to avoid errors due to back-lash). Ten settings were performed to arrive at a mean value of the depth of focus. The experiment was repeated for eight different values of S between 0.25 and 5.08. The retinal illumination was kept constant at 1500 trolands. Fig. 5.06 shows the resulting depth of focus curve; discs denote mean values and the vertical lines indicate extreme readings.

Fig. 5.06 provides some interesting features. Depth of focus decreases monotonically as S decreases (i.e. as the coherence of the light increases) and the depth of focus tends towards a constant value at the extreme ends of the curve where the conditions of coherent and incoherent illumination are approached. In Chapter VI the physical images for a coherently and then an incoherently illuminated edge are discussed in detail. Fig. 6.03 shows the effect of a slight defocus ($\pm$ 7μ for the 0.12 N.A. objective) on the image of a coherently illuminated edge. For the amount of defocus considered the edge gradient has decreased to 85% of its value at the geometrical focus. Fig. 6.06 shows the effect of an equal amount of defocus on the edge gradient (line image) for the case of incoherent illumination and it can be seen that the edge gradient has only dropped to 97% of the in-focus value. The relatively insensitive change in edge gradient with respect to defocus

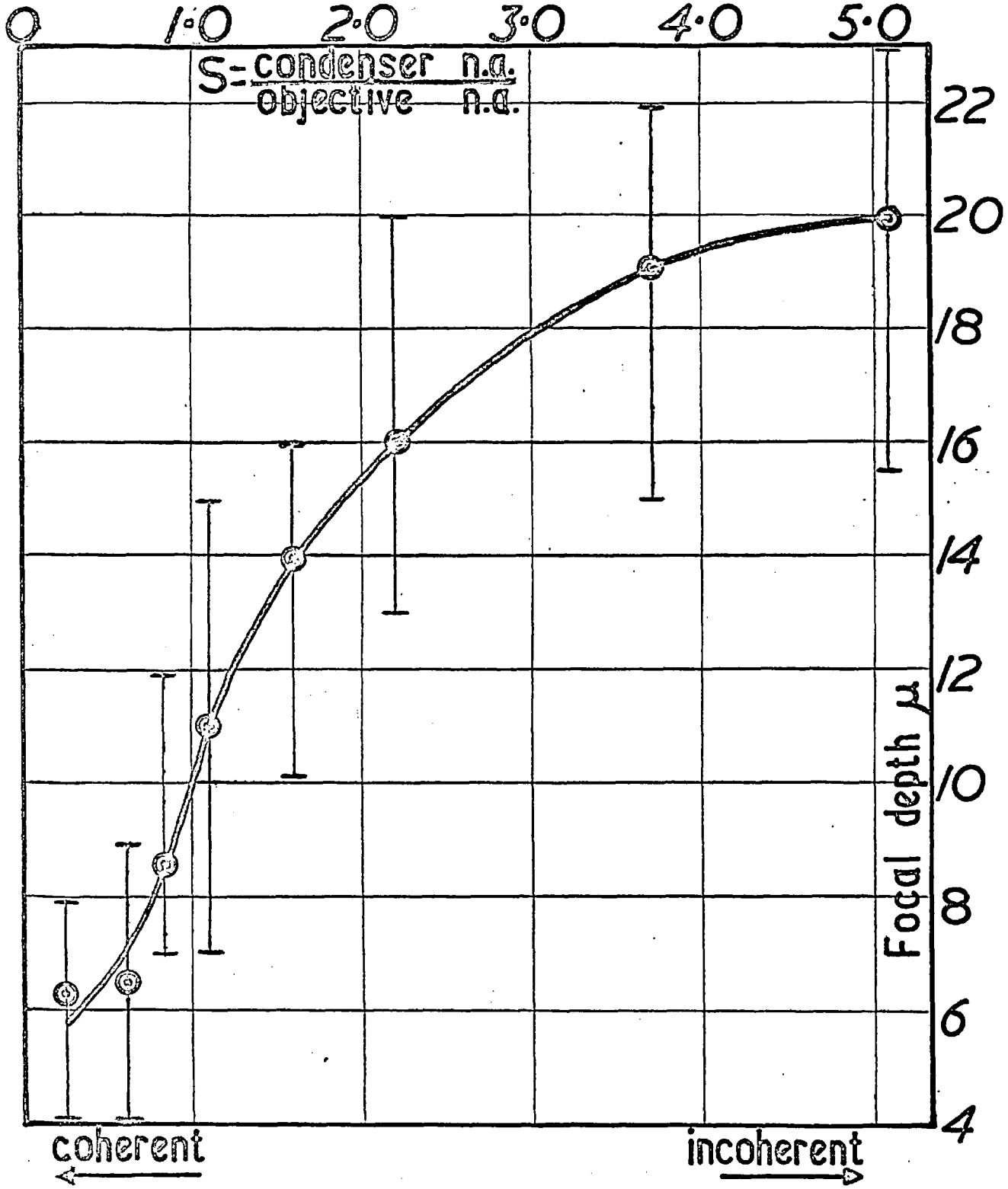


Fig. 5.06. Variation of focal depth with S. Objective n.a. = 0·12
$\lambda = 0{\cdot}53\mu$

for incoherent illumination probably accounts for the increased focal depth compared with the coherent case. Moreover the physical distributions of luminance for low S values result in much more noticeable Mach bands than for cases of higher S and this too must affect the visual tolerance on defocusing. It will be noted that for S = 0.25 the depth of focus is only 6μ which is one sixth the value of the Rayleigh tolerance while that for S = 5.08, 20μ, is still 17μ inside Rayleigh's limit. Experiments with the photo-electric microscope showed that when it was focused at the 50% transmission point the defocus tolerance was 10μ when S = 0.25 and 40μ when S = 5.08.

As an extension of Strehl's approach Marechal (1956) has used scalar diffraction theory to investigate the tolerances on defocusing line and opaque point images for the incoherent and coherent cases. He used a reduction of 20% in the central image intensity as a criterion of tolerance. His calculations also showed that the focal depth was smaller when coherent illumination was employed. When a bright line is illuminated coherently Marechal considers 0.24λ to be the maximum acceptable value for MP in fig. 5.02 while for the incoherent case this value increases to 0.29λ.

Displacements of the Mach bands for small amounts of defocus.

Three values of S were chosen, 0.60, 1.0 and 5.08, at which the author measured Mach bands as a function of defocusing. The range of positions of the focus knob for which the visual edge appeared sharpest was noted; the mean value was chosen as the "best" focus and the band positions were measured at the extreme ends of the in-focus range. Results for the three S values are shown in fig. 5.07. The band positions for the mean focus are drawn between the positions obtained at the two extremes of the depth of focus; the uppermost and lowermost measurements of each block of three indicate above and below the mean focus respectively. It is apparent from fig. 5.07 that for small amounts of defocus, restricted within the visual depth of field, the number of bands seen remain the same and that their positions generally move towards the bright field. An analysis of variance was applied to each boundary to detect if these shifts were significant or not. For "F" ratios lying below the 5% probability level of significance the null hypothesis of equal means can be confidently rejected and where this occurs "D" has been indicated on fig. 5.07 inferring the shift in boundary due to the small amount of defocus was significant. From fig. 5.07 it can be seen that small errors of focus can

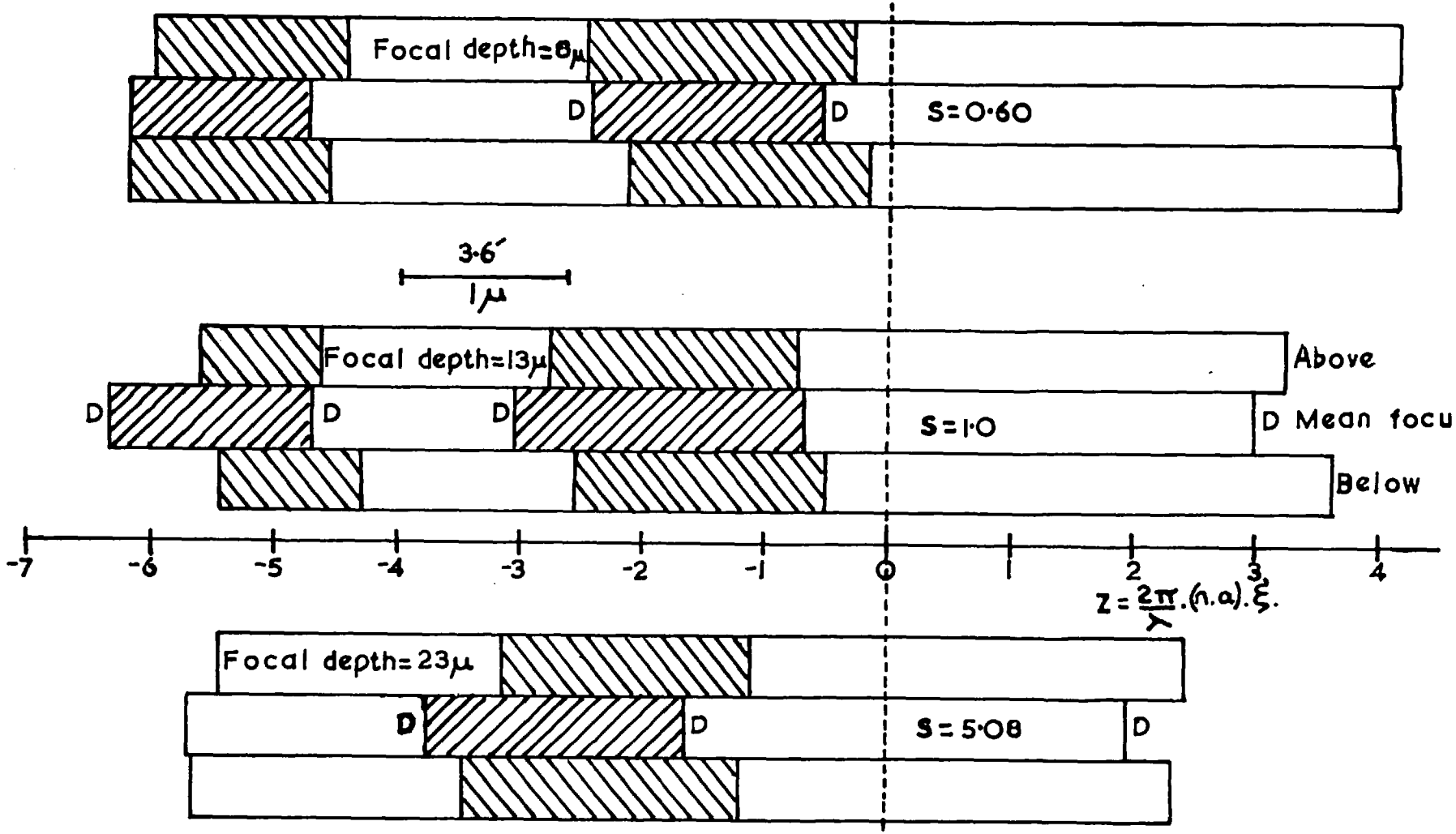


Fig. 5.07. The influence of small amounts of defocus on the Mach bands
Observer: S.H.R. 0·12 n.a. objective, × 20 eyepiece $\lambda = 0{\cdot}53\mu$

lead to band displacements of $\frac{1}{2}$ z unit which is the same order of difference which occurs between various observers' measurements of band boundaries (although in some cases observers' measurements differ by several z units for the faint bands).

The influence of different observers' focal settings.

In order to investigate to what extent small errors of defocus contribute to the wide differences shown in figs. 4.03, 3 pairs of observers whose measurements differed widely in the original survey were chosen; a focal setting was chosen for which both observers agreed that the visual edge was in focus. Then observers made alternate scans across the Mach band boundaries. Each observer performed a scan in five minutes and as the observers made ten scans alternately the effects of focal drifts in the apparatus were reduced to a minimum.

Figs. 5.08a,b show results obtained for A.E.S. and S.H.R. for S = 2.2 and S = 0.60 respectively. For the case of S = 2.2 these two observers showed significant differences (at the 5% level) between their measurements of all four boundaries when they focused independently. When the same focus was employed no significant difference in the position of the visual edge, as well as the position

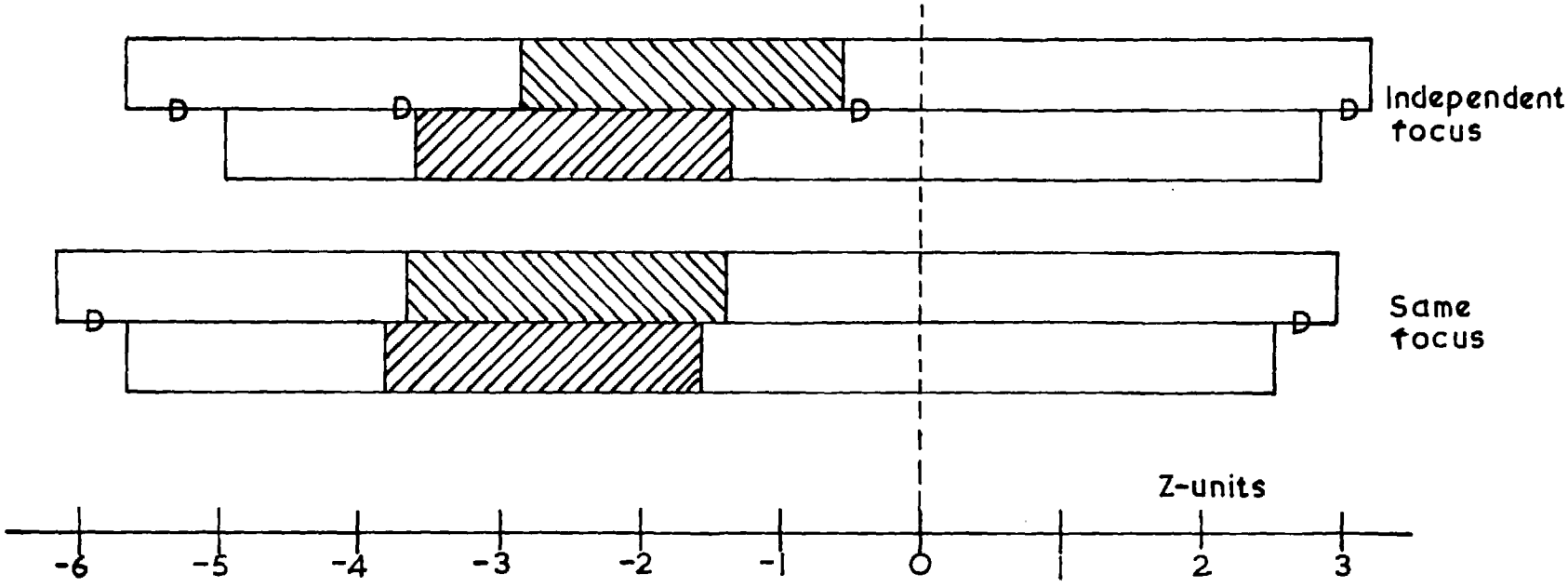


Fig. 5.08a. Observers A.E.S. and S.H.R. S=2·2

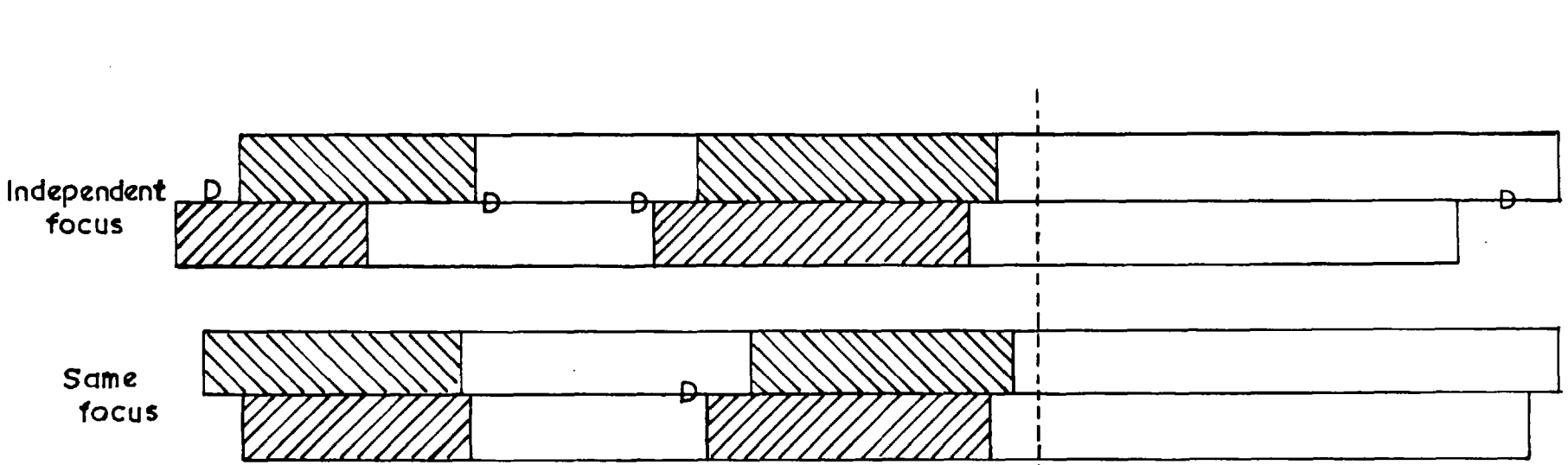


Fig. 5.08b. Observers A.E.S. and S.H.R. S=0·60

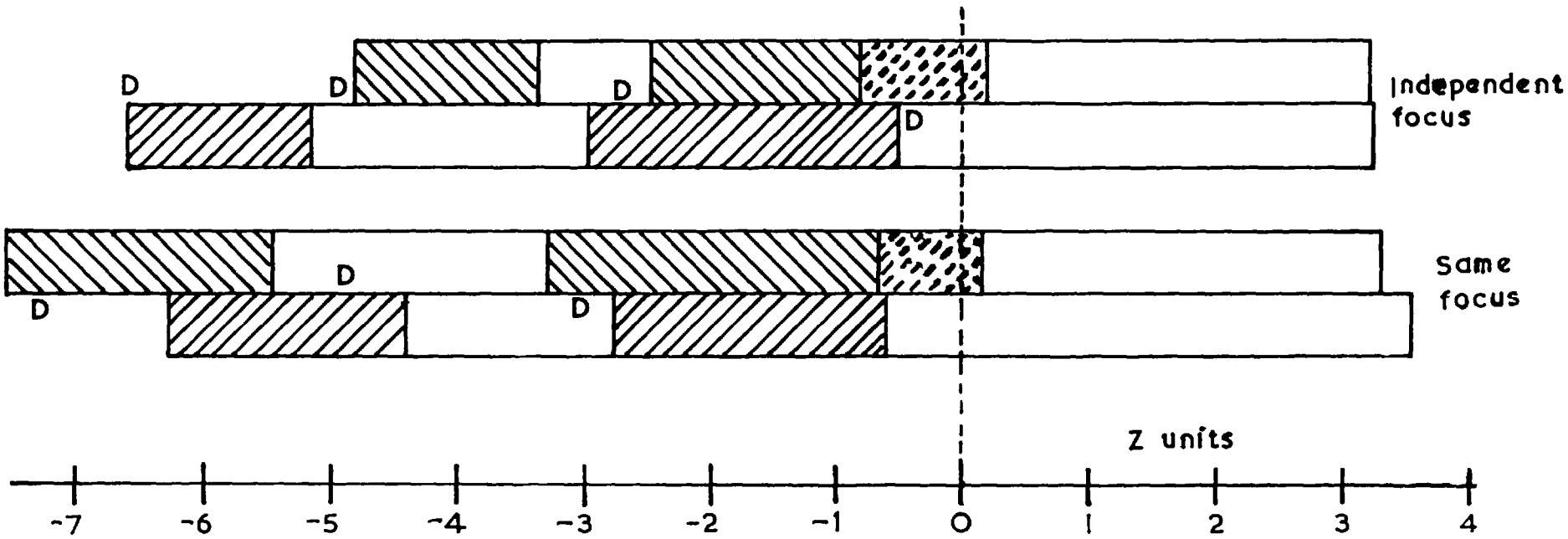


Fig 5.09 Observers E.H. and S.H.R. S=0·60

of one other border, was recorded, although the other two boundaries still showed significant differences. When S = 0.60 four boundaries exhibited significant personal differences when the focal settings were made independently in the survey but for an identical focus only one boundary showed a difference.

The case of E.H. and S.H.R. (fig. 5.09), when S = 0.60, was specially interesting. Not only did the Mach band positions differ quite considerably for these observers but E.H. saw a region of inflection between the first bright band and the edge band plus an extra dark band in the dark field. Within the visual tolerance limit, mentioned above, E.H. still saw these additional features. For identical focal settings the agreement between E.H. and S.H.R. was generally better with the position of the visual edge showing no significant difference whereas for an independent focal setting a significant difference had existed. Nevertheless three pairs of boundaries still showed differences.

The results of C.B. and S.H.R. (fig. 5.10) are somewhat puzzling as the amount of agreement was, in fact, worse when identical focal settings were employed. The most plausible explanation would be that the personal differences between these observers were partly compensated

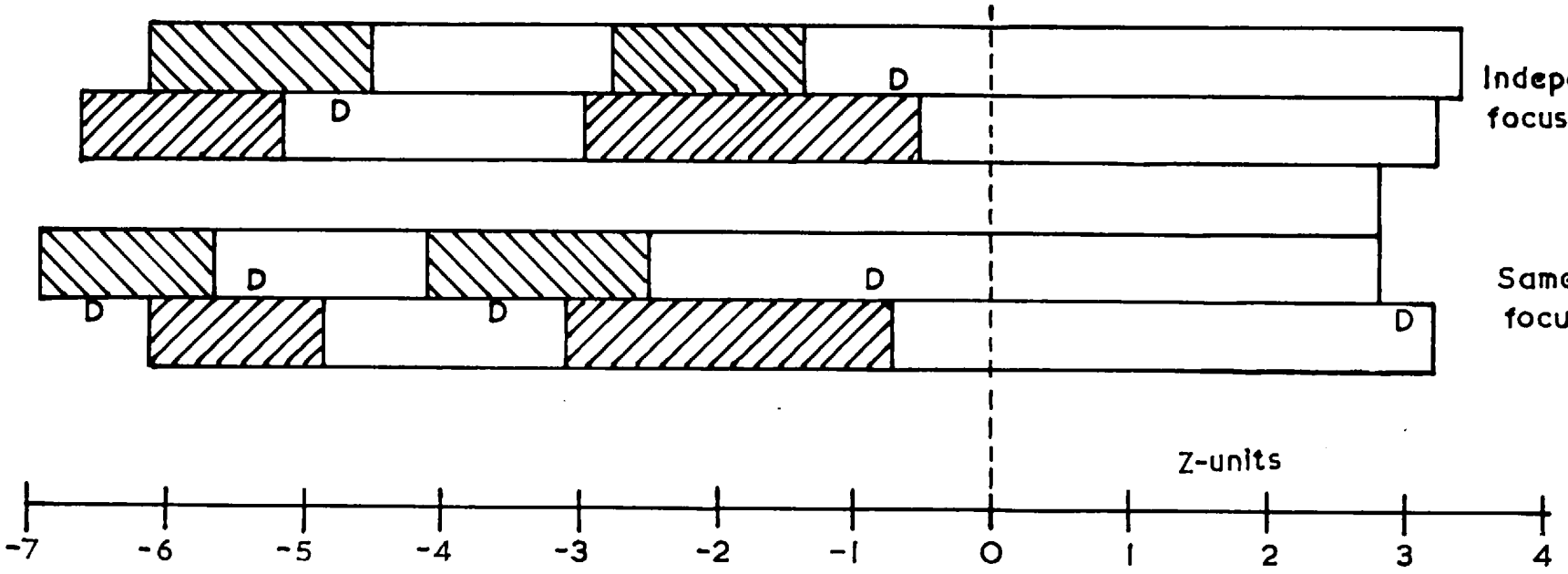


Fig 5.10. Observers C.B. and S.H.R. S=0·60

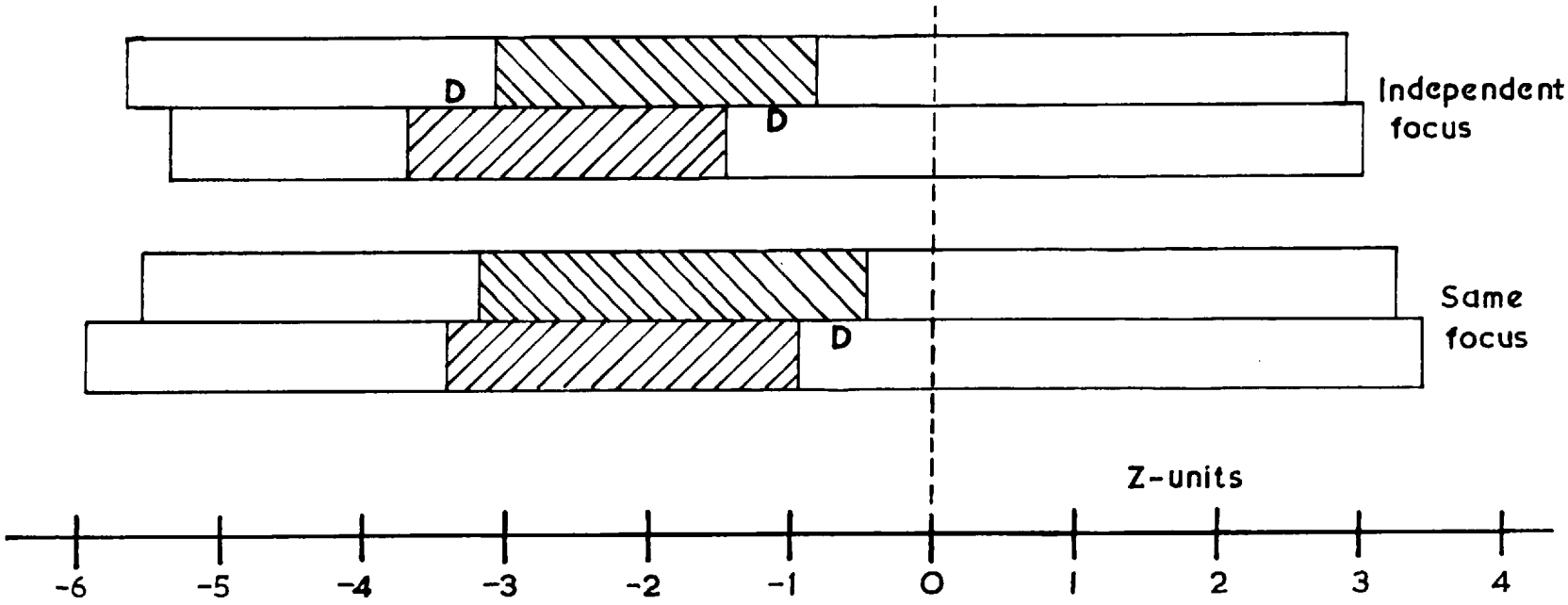


Fig. 5.11. Observers R.H. and P.C. S = 0·60

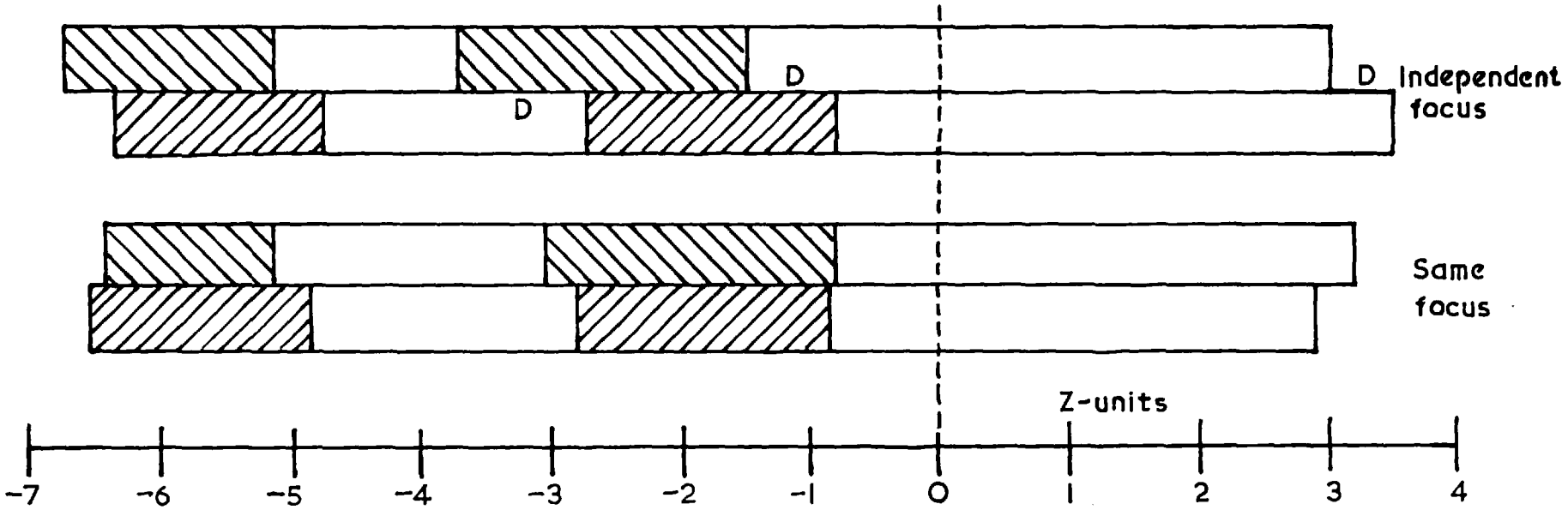


Fig. 5.12. Observers G.O. and P.C. S=0·60

for by having two slightly different physical images when the settings were made independently.

Of the few original observers (from the original survey) available at the time of these investigations no more had exhibited personal differences large enough to warrant their performing experiments of the type just described. Consequently three new observers were chosen: R.H., P.C., and G.O. For S = 0.60 significant differences were detected between R.H. and P.C. and also between G.O. and P.C.

For R.H. and P.C. fig. 5.11 shows that when focal settings were made independently two pairs of boundaries showed significant differences while when the same focus was employed only the visual edge showed a difference.

In the case of G.O. and P.C. (fig. 5.12) no significant differences were obtained when the same focus was employed while for independent focusing three borders showed individual differences.

That small focusing errors generally result in differences between observers' measurements of Mach band positions is probably best shown in fig. 5.13 where the "F" ratio is used as a measure of agreement between pairs of borders. The "F" ratio obtained for the same focus is plotted against the corresponding "F" ratio for the

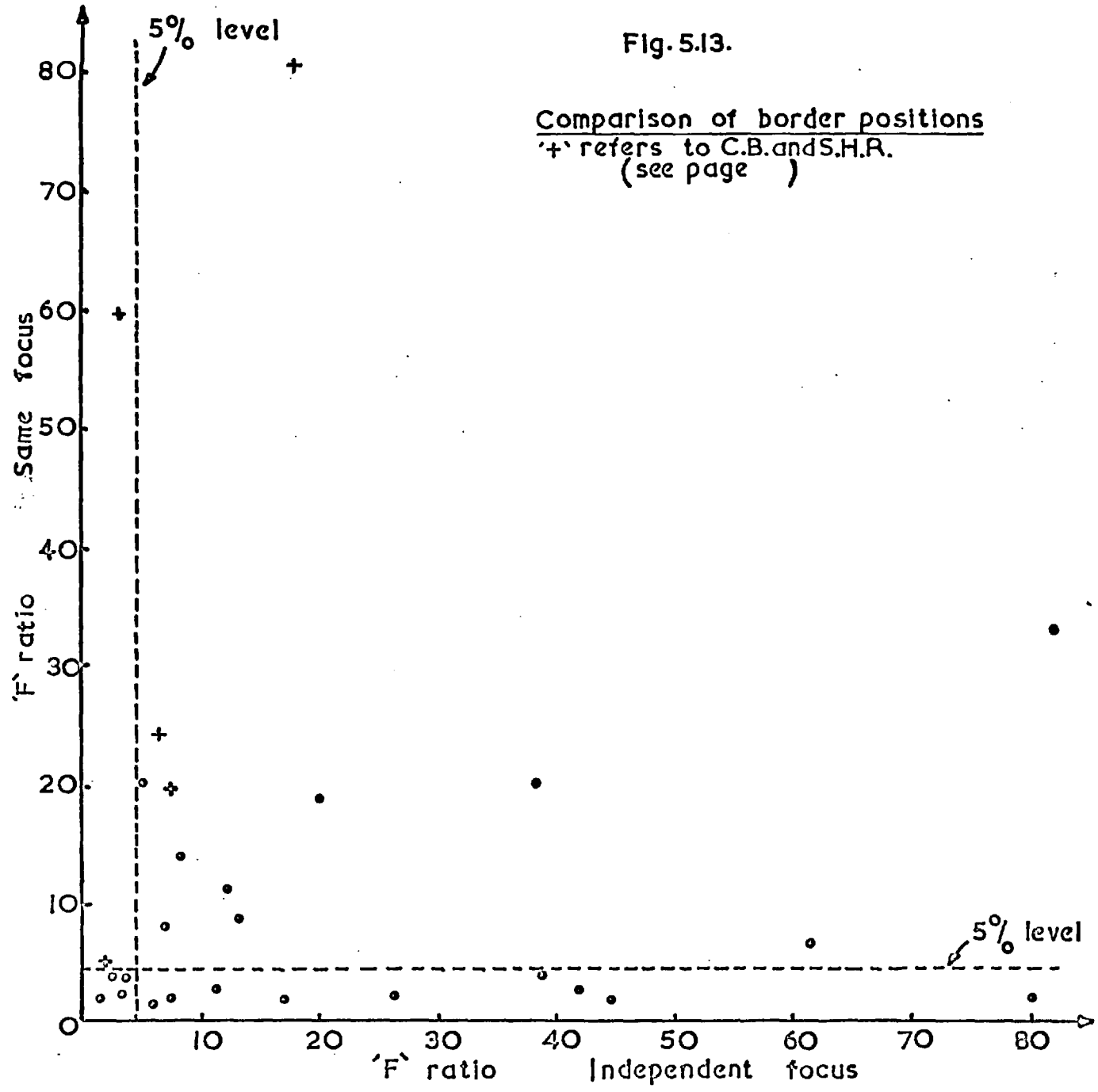


Fig. 5.13.

Comparison of border positions
'+' refers to C.B. and S.H.R.
(see page)

independent focus. When identical focal settints were employed thirteen pairs of borders did not differ significantly at the 5% probability level but when the foci were found independently only six pairs of borders did not differ significantly at this level of significance.

The relative luminances of the Mach bands.

Using the photometric arrangement and techniques described in Chapter IV the author measured the relative luminances of the Mach bands for S = 2.2 and S = 0.60 at the "best" focus and at the two extremes of the depth of focus. While the luminance matches were being made the eye was kept in focus on the tip of a 0.5μ tungsten wire fixed in the centre of the field of view so as to avoid errors of accommodation. For each band the luminance did not change significantly with respect to the focal settings. However if the bands were viewed with the edge defocused beyond the visual depth of field (defined by maximum edge sharpness) the borders between bands became less distinct while the bright bands became less bright and the dark bands not so dark. Herein lies an interesting point concerning the concept of depth of focus. Fig. 5.14 shows a typical subjective impression of the image of an edge seen in microscopy. Curve "A" is for a focal setting

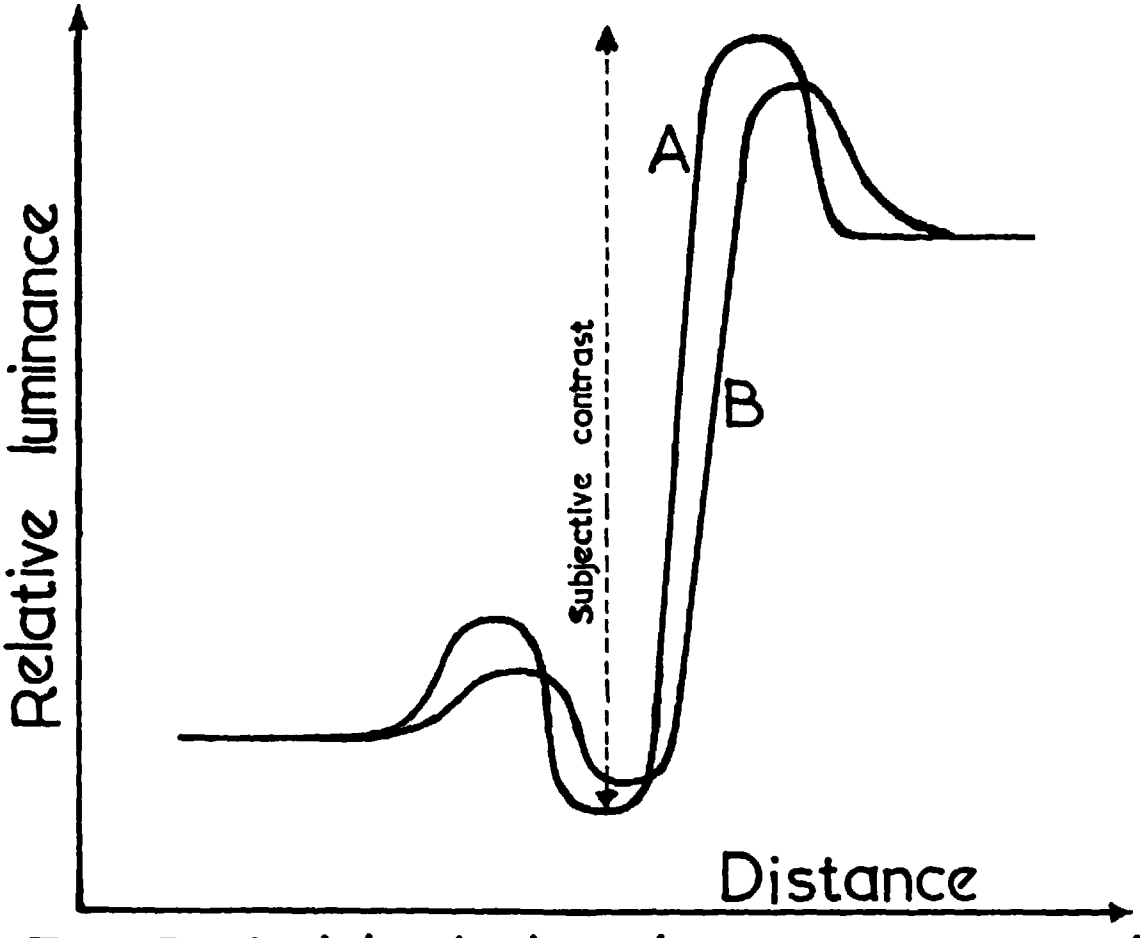


Fig. 5.14 Mach bands seen at an edge.
A: inside depth of focus
B: outside depth of focus

within the visual depth of focus and curve "B" is the impression obtained when the edge is out of focus. We may define the contrast seen at the visual edge as the luminance of the first bright band minus the luminance of the edge band. It follows that provided the sharpness of the edge remains constant so does the contrast seen at the edge.

Chapter VI

Some diffraction calculations for defocused edges

Introduction

The work described in the previous chapter indicates that very slight amounts of defocus, within the Rayleigh tolerance, are enough to change the positions of the Mach bands. It is therefore of interest to see how the second derivative of luminance with respect to distance changes for such small perturbations in the diffraction image. Do the stationary positions of this curve change by the amounts required to produce the Mach band displacements and to effect some of the personal differences, assuming that the second derivative postulate is true? Calculations for coherently and incoherently illuminated edges are described below; scalar diffraction theory is employed as the optical system used was of low numerical aperture (0.12 in the object space and 0.01 in the image space). The more complicated case of partially coherent illumination will not be treated.

General formulae.

Let a ray (fig. 6.01) from an axial point O of the

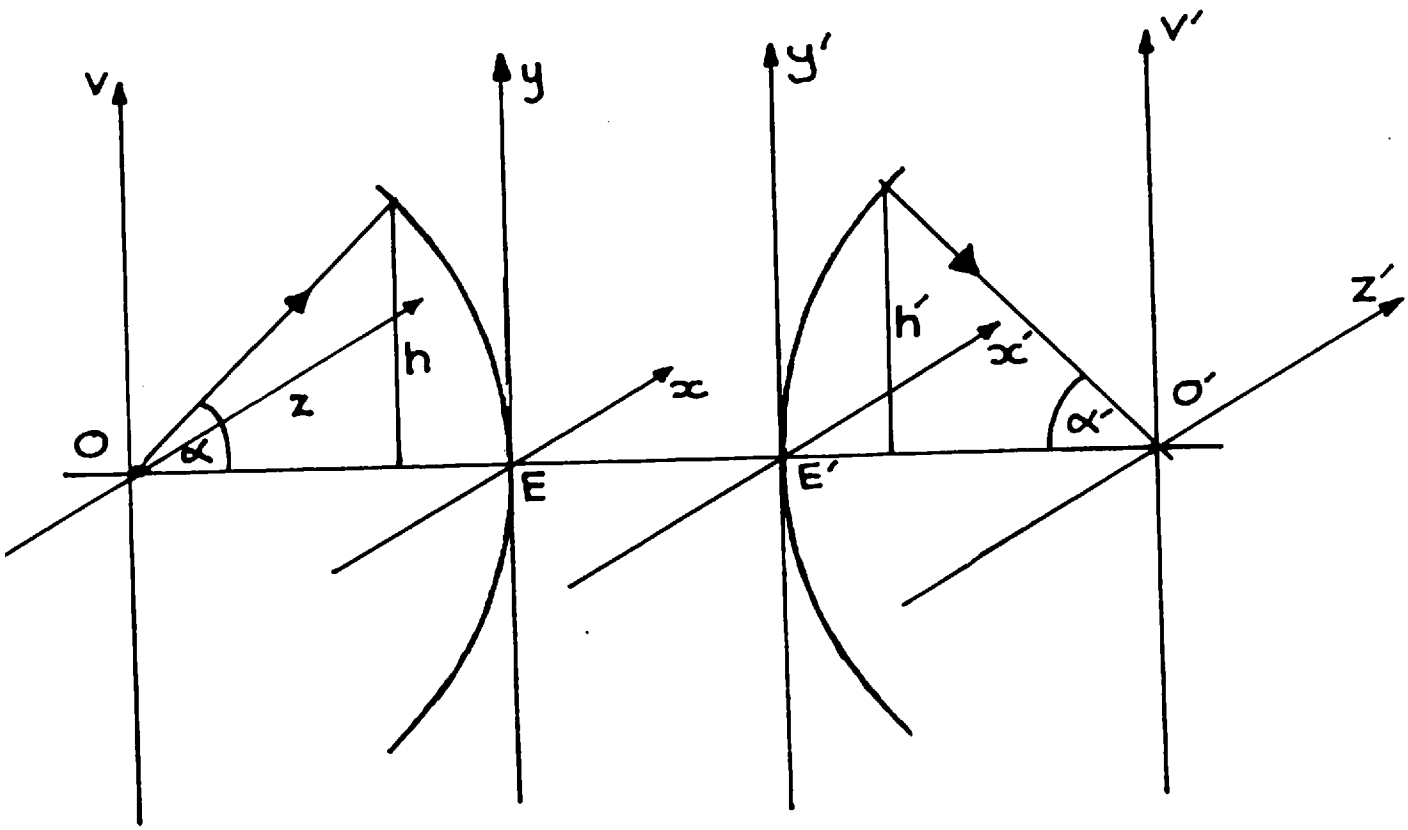


Fig. 6.01

object plane of an optical system be inclined at an angle α to the optical axis and let it intersect a reference sphere in the object space at a height h. The reference sphere has its centre at O and is of such a radius that it passes through E the axial point of the entrance pupil. This ray emerges from the system and proceeds to the axial image point O' making an angle α' with the optical axis and meeting the reference sphere in the image space at a height h'. If any other ray has rectangular co-ordinates (a,b), (a',b') at the object and image reference spheres respectively, the fractional co-ordinates $x = \frac{a}{h} = \frac{a'}{h'}$ $y = \frac{b}{h} = \frac{b'}{h'}$ denote the point of the pupil traversed by the ray. In a system with a circular aperture it is convenient to choose the ray defined by h' to pass through a point at the edge of the entrance pupil so that $x^2 + y^2 = 1$ denotes the limiting aperture. Points in the object plane are then denoted by the rectangular co-ordinates

$$z = \frac{2\pi}{\lambda} n \sin\alpha \, \xi , \quad v = \frac{2\pi}{\lambda} n \sin\alpha \, \eta$$

where n is the refractive index and (ξ, η) the geometrical co-ordinate distances of the point. Similar expressions, with appropriate primes, define rectangular co-ordinates for the image plane.

Let that wavefront, associated with a disturbance at

O, which lies in the object reference sphere have unit amplitude and zero phase. The part of the wavefront that lies outside the circle $x^2 + y^2 = 1$ is not transmitted by the optical system; moreover for each point within this circle there will be, in general, some loss of light and aberrational effects. The pupil function f(x,y) takes account of both these factors by specifying the disturbance on the reference sphere in the image space. The complex amplitude F(z',v') in the image of a point source, situated at (0,0) in the object plane is then given by the Fourier transform:

$$F(z',v') = \int_{-\infty}^{\infty}\int f(x,y) \exp i \quad (z'x+v'y)dxdy \qquad *$$

(See appendix B)

Infinite limits may be employed since f(x,y) is zero outside the region $x^2 + y^2 = 1$.

Coherently illuminated extended object.

Consider an object distribution of amplitude A(z,v) which gives rise to an image distribution of amplitude A'(z',v'). A'(z',v') is given by summing the amplitudes in the images of all the points in the object:

---

* Here z and v are multiplied by a factor of 2π compared with their values in appendix B.

$$A'(z',v') = \iint A(z,v).F(z'-z,v'-v)dzdv$$

where the limits of integration are taken over the object. This integral assumes that the system is isoplanatic and linear with respect to summation of amplitudes. The condition of isoplanatism requires that the diffraction image of a point source situated at the point (z,v) of the object is given by,

$$F(z'-z,v'-v).$$

The intensity in the image is given by,

$$I'(z',v') = \left|A'(z',v')\right|^2$$

Coherently illuminated half-plane (straight edge)

The complex distribution of amplitude in the edge object may be expressed as,

$$A(z) = 1 \quad \text{for } z \geq 0$$

$$A(z) = 0 \quad \text{for } z < 0.$$

The edge is assumed to cut the optical axis as shown in fig. 6.02. Since this object is a one dimensional distribution of amplitude we may write the distribution of amplitude in the image as,

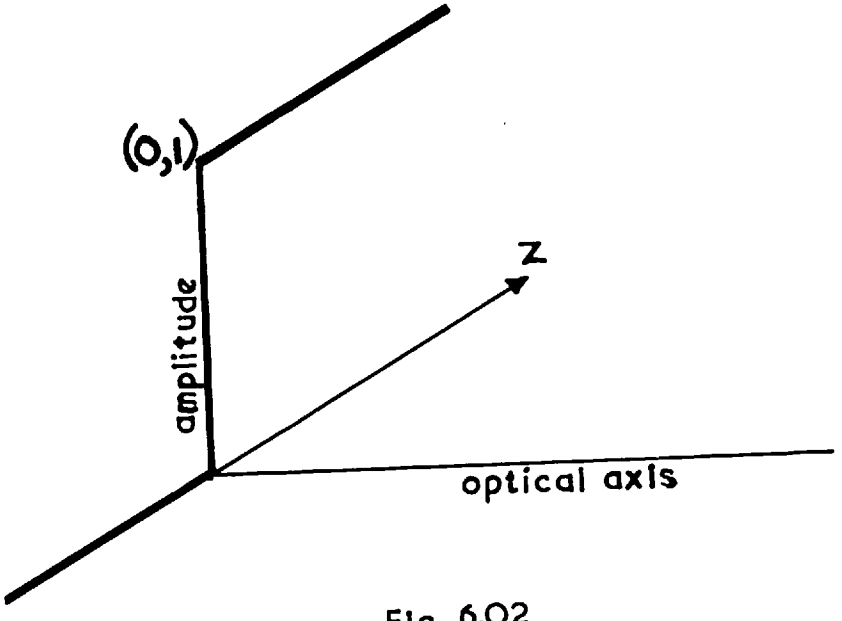


Fig. 6.02

$$A'(z') = \int A(z)\, F(z'-z)\, dz.$$

It can be shown that,

$$a'(x) = a(x) \cdot f(x) + \qquad (1)$$

where a'(x), a(x) and f(x) are the inverse Fourier transforms of A'(z'), A(z) and F(z) respectively:

$$a(x) = \int_{-\infty}^{\infty} A(z) e^{-izx}\, dz$$

$$f(x) = \int_{-\infty}^{\infty} F(z) e^{-izx}\, dz$$

$$a'(x) = \int_{-\infty}^{\infty} A'(z') e^{-iz'x}\, dz'$$

(Titchmarsh, 1937)

The image of a point source F(z,v) is the Fourier transform of the pupil function f(x,y) and by the Fourier transform inversion theorem (Titchmarsh, 1937) we can say that f(x,y) is equal to the inverse Fourier transform of F(z,v). We let,

$$f(x,y) = T(x,y) e^{i\phi(x,y)}$$

where $T(x,y)$ gives the variation of transmission over the pupil and $\phi(x,y)$ expresses the aberration of the wavefront relative to a circular reference sphere centred at the Gaussian image point (Appendix a). For systems of moderate aperture we may assume that $T(x,y)$ does not vary over the pupil so that its value can be put equal to unity. For simple defocusing the aberration function $\phi(x,y)$ takes the form $p(x^2+y^2)$ where the parameter p is related to the geometrical displacement δ of the image plane by,

$$p = \frac{\pi}{\lambda} (N.A.)^2 \delta \quad \text{where (N.A.) equals}$$

the numerical aperture of the system in the image space (Appendix a).

Thus we can write,

$$f(x,y) = e^{ip(x^2+y^2)} \text{ and } f(x) = e^{ipx^2}.$$

Also we have, $a(x) = \frac{1}{2}\left\{\delta(x) - \frac{i}{\pi x}\right\}$

where $\delta(x)$ is a Dirac delta function (Bracewell, 1965).

Hence, $$a'(x) = \frac{1}{2}\left[\delta(x) - \frac{i}{\pi(x)}\right]e^{ipx^2}.$$

From (1) this expression must be equal to the inverse Fourier transform of $A'(z')$ so that, by the Fourier transform inversion theorem,

$$A'(z') = \int_{-\infty}^{\infty} \tfrac{1}{2}\,[\delta(x) - \tfrac{i}{\pi x}]e^{ipx^2}.e^{izx}\,dx.$$

The limits of integration are only formally from $-\infty$ to $+\infty$ and since we integrate over the pupil $x^2+y^2 = 1$, we may write,

$$A'(z') = \int_{-1}^{1} \tfrac{1}{2}\,[\delta(x) - \tfrac{i}{\pi x}]e^{ipx^2}.e^{izx}\,dx.$$

Therefore,

$$A'(z') = \int_{-1}^{1} \tfrac{1}{2}\,\delta(x)e^{ipx^2}.e^{izx}.dx - \int_{-1}^{1} \frac{i}{2\pi x}\,.e^{ipx^2}.e^{izx}\,dx.$$

Now the so called "sifting" property of the delta function (Bracewell, 1965) may be expressed thus,

$$\int_{-\infty}^{\infty} \delta(x)\,f(x)\,dx = f(o)$$

so that $$\int_{-1}^{1} \tfrac{1}{2}\,\delta(x)e^{ipx^2}.e^{izx}.dx = \tfrac{1}{2}\,.$$

Omitting primes we are left with,

$$A(z) = \tfrac{1}{2} + \frac{1}{\pi}\,.\int_{o}^{1} e^{ipx^2}\,.\,\frac{\sin zx}{x}\,.\,dx \qquad (2)$$

This integral does not have a closed analytic solution but if p is small we may expand e^{ipx^2} in series form and employ the first few terms in the expansion since the exponential series is a convergent one. Then,

$$A(z) = \frac{1}{2} + \frac{1}{\pi}\int_0^1 (1+ipx^2 - \frac{p^2x^4}{2} - \frac{ip^3x^6}{6} + \frac{p^4x^8}{24} \quad \frac{ip^5x^{10}}{120} - \frac{p^6x^{12}}{720})$$

$$\times \frac{\sin zx}{x} \cdot dx$$

so that, $A(z) = \frac{1}{2} + \frac{1}{\pi}\,Si(z)$

$$+ \frac{1}{\pi}\int_0^1 (ipx \sin zx - \frac{p^2x^3}{2}\sin zx - \frac{ip^3x^5}{6}\sin zx + \frac{p^4x^7}{24}\sin zx$$

$$+ \frac{ip^5x^9}{120}\sin zx - \frac{p^6x^{11}}{720}\sin zx)dx$$

where Si(z) is the well tabulated sine integral (Abramowitz and Stegun, 1964). Integrating the separate terms by parts we obtain the complex integral,

$$R(z) + i\,\mathcal{I}(z)$$

where

$$R(z) = \frac{1}{2} + \frac{1}{\pi}\,\mathrm{Si}(z) - \frac{p^2}{2\pi}\left(-\frac{\cos z}{z} + 3\frac{\sin z}{z^2} + 6\frac{\cos z}{z^3} - 6\frac{\sin z}{z^4}\right)$$

$$+ \frac{p^4}{24\pi}\left(-\frac{\cos z}{z} + 7\frac{\sin z}{z^2} + 42\frac{\cos z}{z^3} - 210\frac{\sin z}{z^4} - 840\frac{\cos z}{z^5}\right.$$

$$\left. + 2520\frac{\sin z}{z^6} + 5040\frac{\cos z}{z^7} - 5040\frac{\sin z}{z^8}\right)$$

$$- \frac{p^6}{720\pi}\left(-\frac{\cos z}{z} + 11\frac{\sin z}{z^2} + 110\frac{\cos z}{z^3} - 990\frac{\sin z}{z^4}\right.$$

$$- 7920\frac{\cos z}{z^5} + 55440\frac{\sin z}{z^6} - 332640\frac{\cos z}{z^7} - 1663200\frac{\sin z}{z^8}$$

$$- 6652800\frac{\cos z}{z^9} + 19958400\frac{\sin z}{z^{10}} + 39916800\frac{\cos z}{z^{11}}$$

$$\left. - 39916800\frac{\sin z}{z^{12}}\right)$$

and $$\mathcal{G}(z) = \frac{p}{\pi}\left(-\frac{\cos z}{z} + \frac{\sin z}{z^2}\right)$$

$$- \frac{p^2}{6\pi}\left(-\frac{\cos z}{z} + 5\frac{\sin z}{z^2} + 20\frac{\cos z}{z^3} - 60\frac{\sin z}{z^4} - 120\frac{\cos z}{z^5}\right.$$

$$\left. + 120\frac{\sin z}{z^6}\right)$$

$$+ \frac{p^5}{120\pi}\left(-\frac{\cos z}{z} + 9\frac{\sin z}{z^2} + 72\frac{\cos z}{z^3} - 504\frac{\sin z}{z^4} + 3024\frac{\cos z}{z^5}\right.$$

$$+ 15120\frac{\sin z}{z^6} + 60480\frac{\cos z}{z^7} - 181440\frac{\sin z}{z^8} - 362880\frac{\cos z}{z^9}$$

$$\left. + 362880\frac{\sin z}{z^{10}}\right)$$

With p = 0 the expression for A(z) reduces to the more familiar one for the perfectly focused coherently illuminated edge.

$$A(z) = \frac{1}{2} + \frac{1}{\pi} \mathrm{Si}(z).$$

The intensity distribution I(z) is given by,

$$I(z) = R(z)^2 + \mathcal{G}(z)^2 \qquad (3)$$

and for the number of terms considered above our expression is only valid for $z > 1$ for the value of p considered below. At points nearer the geometrical edge (z = 0) the series does not converge quickly and we should have to consider terms with higher powers of p. However the integral,

$$\int_0^1 e^{ipx^2} \cdot \frac{\sin zx}{x} \cdot dx$$

is always zero when z = 0 and thus from equations (2) and (3) the intensity at the geometrical edge remains constant at 0.25.

Fig. 6.03 shows the perfectly focused distribution of intensity and its value when p = 0.60 (The value of p in fig. 5.04 for S = 0.60 was somewhat less than this, $\pm$ 0.30). It should be noted that the same value is obtained if we defocus above or below the Gaussian focus as only even

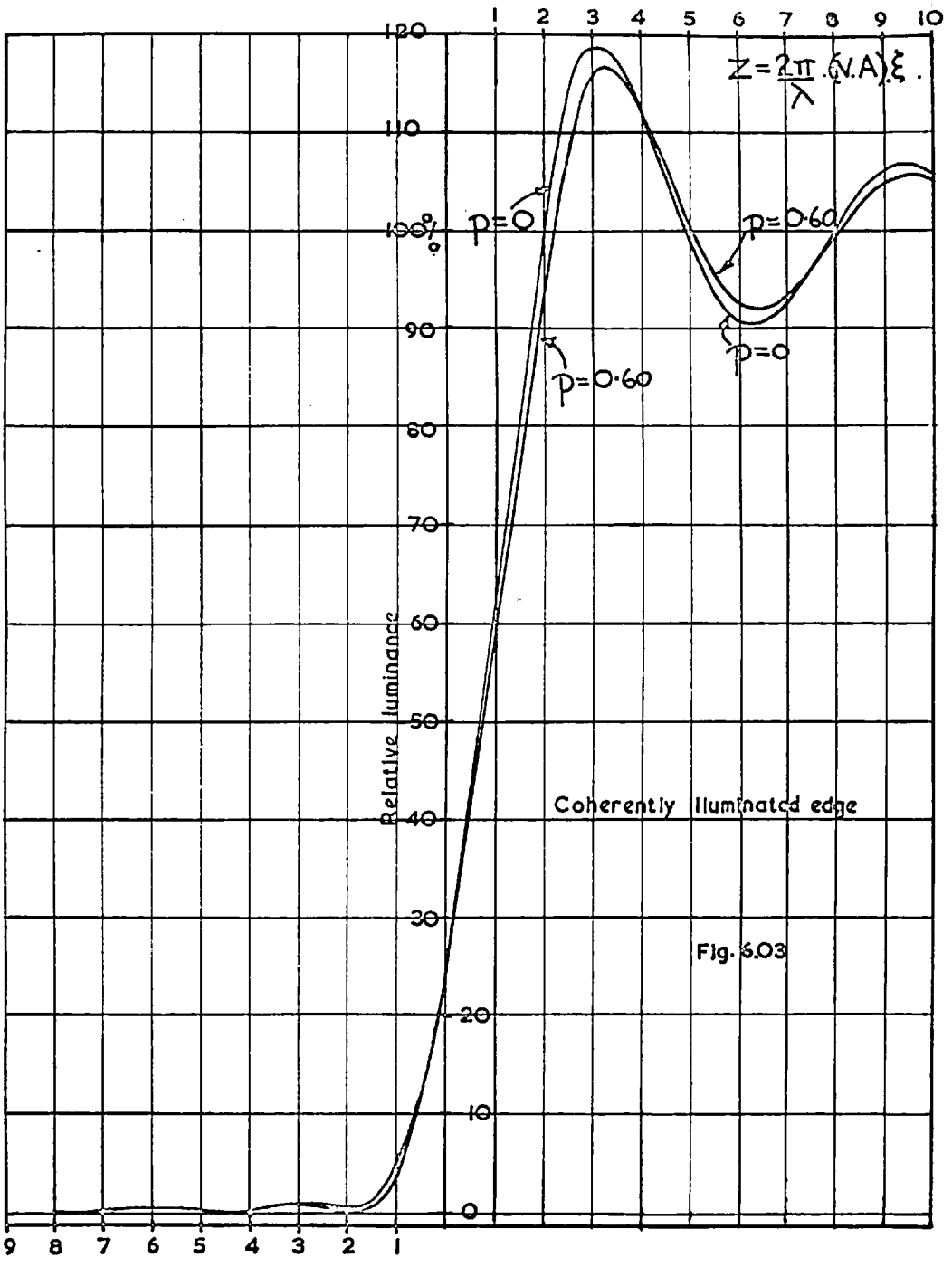
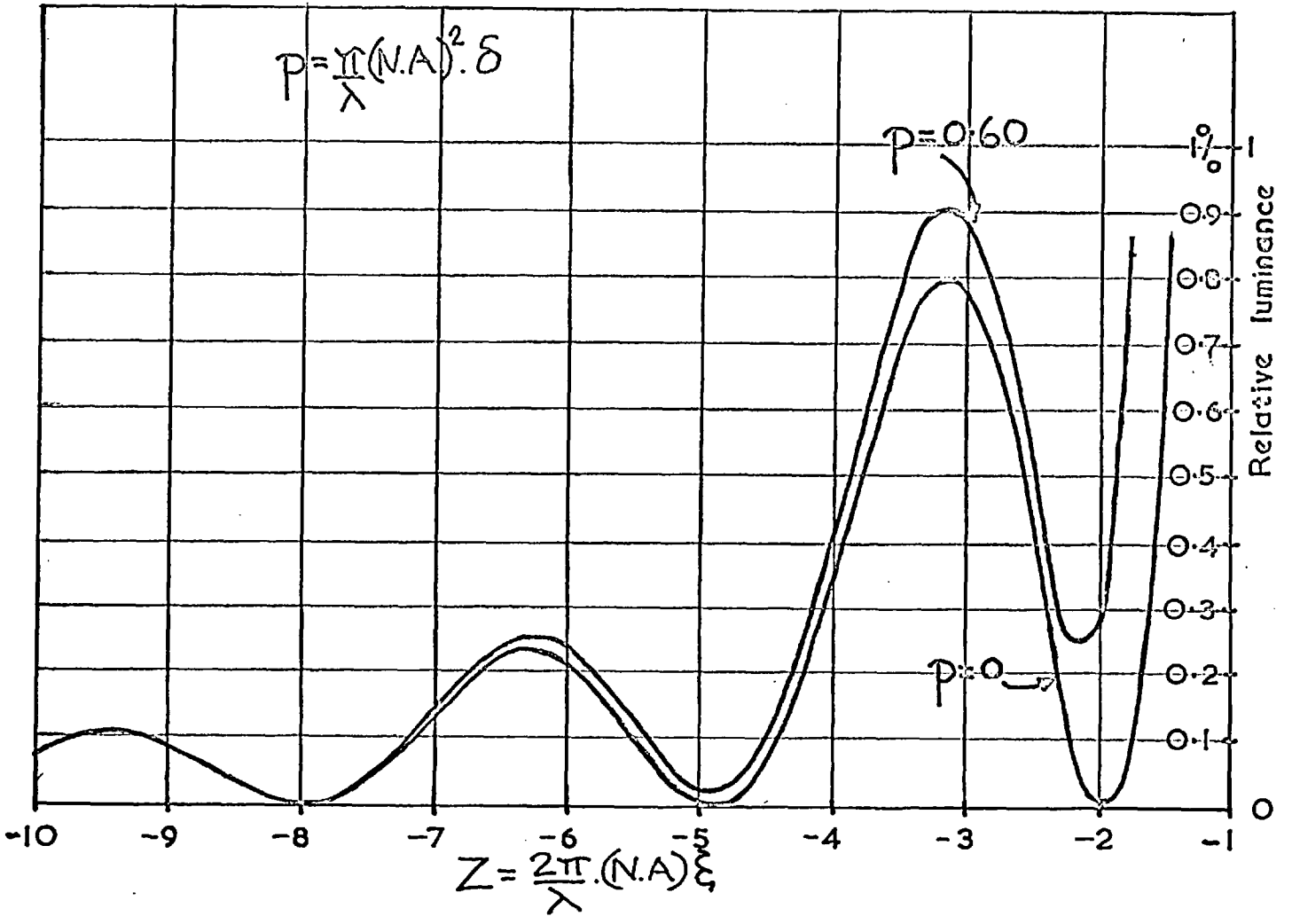

Z = 2π/λ (N.A) ξ .
p=0
p=0·60
p=0·60
p=0
Relative luminance
Coherently illuminated edge
120
110
100%
90
80
70
60
50
40
30
20
10
0
1 2 3 4 5 6 7 8 9 10
9 8 7 6 5 4 3 2 1

Fig. 6.03

Fig 6.04. Coherently illuminated edge image



powers of p are present in the expression for I(z). Fig. 6.04 shows the corresponding curves on a magnified scale for $z < -1$. For the small amount of focus considered it can be seen that the contrast of the fringe structure on the bright side of the image has been reduced while the level of luminance has increased slightly on the dark side of the image. Also, for $z > 0$ the position of the first maximum and minimum have shifted by about a quarter of a z unit into the bright field while the first maximum on the dark side of the field was moved by a similar amount into the dark field. These perturbations have been accompanied by a decrease in the edge gradient.

Having obtained an analytic expression for I(z) we are now in a position to calculate its second derivative. We have,

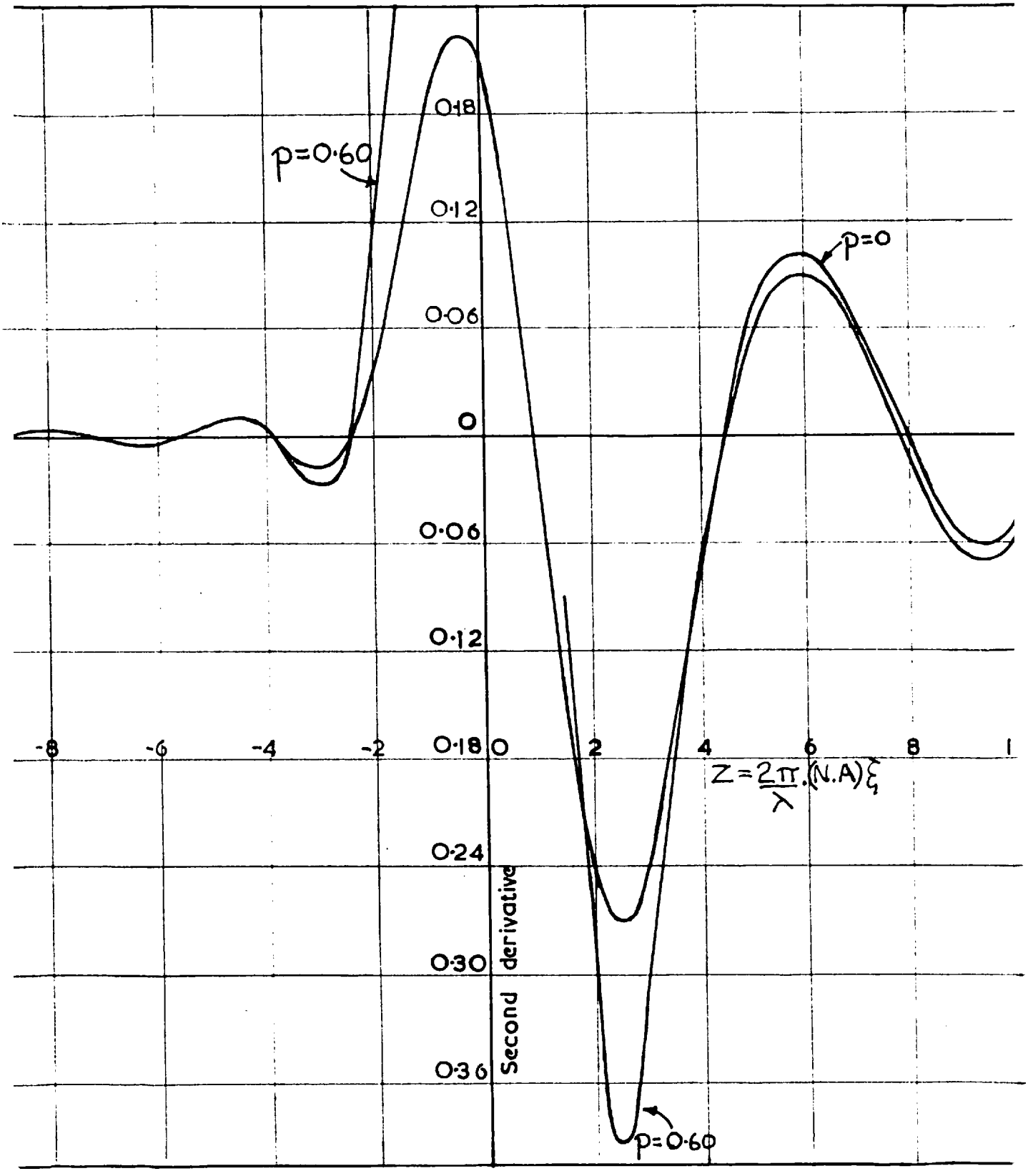
$$I(z) = R(z)^2 + \mathcal{G}(z)^2.$$

Hence,

$$\frac{d^2I}{dz^2} = 2\left\{\left(\frac{dR}{dz}\right)^2 + R\,\frac{d^2R}{dz^2} + \left(\frac{d\mathcal{G}}{dz}\right)^2 + \mathcal{G}\frac{d^2\mathcal{G}}{dz^2}\right\}$$

$\frac{d^2I}{dz^2}$ is plotted in fig. 6.05. If terms in p of higher order than the sixth are to be neglected the expression for $\frac{d^2I}{dz^2}$ is only valid for $z > 1.5$, for similar reasons quoted above for the calculation of I(z). The positions of the stationary values of this curve have not changed for the

.05 Second derivative of the edge image (coherent illumination)



value of p considered although its value at the stationary points has changed by as much as 50% in some cases.

The significance of the small perturbations obtained in the diffraction image for small amounts of defocus will be discussed after the question of incoherent illumination has been considered.

Incoherently illuminated half-plane (straight edge).

The flux distribution in the image of a defocused incoherently illuminated edge was firstly investigated by Welford (Weinstein, 1954). His approach, apart from some changes in nomenclature, will be initially considered here.

Let (ξ, η) be rectangular co-ordinates in the object plane. The intensity distribution in the object may be expressed thus:

$$I = 1 \qquad \text{for } \eta \leq 0$$
$$I = 0 \qquad \text{for } \eta > 0$$

Let (ξ', η') be rectangular co-ordinates in the image plane. Let $A(\xi', \eta')$ be the intensity distribution in the image plane due to a luminous point at the origin in the object plane. The intensity distribution (alternatively we may use the terms flux distribution or luminance distribution) in the image is obtained by integrating the effect of such point sources over the half plane defined by $\eta \leq 0$. We

shall assume that the optical system is isoplanatic and that it adds intensities linearly. Therefore the intensity at any point η_1' in the image plane is given by,

$$I(\eta_1') = \int_{\eta_1}^{\infty} \left\{ \int_{-\infty}^{\infty} A(\xi', \eta') d\xi \right\} d\eta \quad (4)$$

Take rectangular fractional co-ordinates (x,y) in the exit pupil. Let $\phi(x,y)$ be the aberration of the wavefront which is emitted at the origin of the object space. The aberration is taken with respect to a reference sphere centered on the origin of the image space so that ϕ is $\frac{2\pi}{\lambda}$ times the optical path between this sphere and the wavefront (see appendix A). Let $F(\xi', \eta')$ be the complex amplitude in the image produced by this wavefront.

Duffieux and Lansraux (1945) showed that,

$$\int_{-\infty}^{\infty} \left| F(\xi', 0) \right|^2 d\xi' = \int \left| \int \exp i\phi(x,y) dy \right| dx \quad (5)$$

neglecting a factor depending on the scales in the two co-ordinate systems. The integrals on the right-hand side are taken over ranges defined by the extent of the pupil. Alternatively they may be taken between infinite limits if the integrand is defined to be zero outside the pupil. $\left|F(\xi', 0)\right|^2$ is equal to $A(\xi', 0)$ so that from equation (5)

$\int_{-\infty}^{\infty} |F(\xi',0)|^2 d\xi'$ must equal the negative of the gradient of the intensity distribution in the edge image at $\eta' = 0$ or, neglecting a constant scaling factor, the intensity at the middle of the image of an incoherently illuminated line.

Now let the integrand with respect to y on the right-hand side of equation (5) be replaced by exp $i[\phi(x,y) + zy]$ where z is a variable parameter. The integral then represents the central gradient in the image when the aberration is $\phi(x,y) + zy$ instead of simply $\phi(x,y)$ but these two aberration functions are essentially the same, the former being taken with respect to a reference sphere of which the centre is displaced laterally a distance $\eta' = \frac{\lambda}{2\pi} \cdot \frac{z}{(N.A.)}$ (see appendix A)*. Thus the new integral represents the gradient in the edge image at the point η' or the intensity $L(\eta')$ of the image of a line which is coincident with the ξ axis in the object space.

Hence,

$$-\frac{dI(\eta')}{d\eta} = \int \left| \int \exp i\left(\phi(x,y) + \frac{\lambda}{2\pi} \cdot \frac{z}{(N.A.)}\, dy\right)\right|^2 dx$$

$$= L(z).$$

For simple defocusing we have $\phi(x,y) = p.(x^2+y^2)$ (see appendix A). If the exit pupil is circular and of unit radius the integral may be written,

* Here we take $z = \frac{2\pi}{\lambda} \cdot (N.A.) \cdot \eta'$

$$L(p,z) = \int_{-1}^{1} \left| \int_{a}^{a} \exp i\left\{ p(x^2+y^2) + zy \right\} dy \right|^2 dx$$

where $a = +(1-x^2)^{\frac{1}{2}}$.

The factor $\exp ipx^2$ in the integrand may be ignored since it vanishes on taking the modulus so that,

$$L(p,z) = \int_{-1}^{1} \left| \int_{-a}^{a} e^{i(py^2+zy)} dy \right|^2 dx.$$

Using Weinstein's expression for $L(p,z)$ we shall obtain an analytic solution for this integral. On differentiating $L(p,z)$ with respect to z we shall obtain the second derivative of the luminance distribution in the edge image.

For small values of p we may expand $\exp(ipy^2)$ in series form and employ the first few terms in the expansion,

$$\exp(ipy^2) = 1 + ipy^2 - \frac{p^2y^4}{2!} \ldots\ldots$$

Consider the integral,

$$\int_{-a}^{a} (1 + ipy^2 - \frac{p^2y^4}{2}) e^{izy} \, dy.$$

Integrating by parts we obtain for this integral,

$$\int_{-a}^{a} \left[-\frac{ie^{izy}}{z}\left(1 + ipy^2 - \frac{p^2y^4}{2} - \frac{2py}{z} + \frac{2p^2y^3}{iz} - \frac{2ip}{z^2} + \frac{6p^2y^2}{z^2} - \frac{12p^2y}{iz^3} - \frac{12p^2}{z^4}\right)\right]$$

Omitting terms of p^4 and higher order terms we obtain for the square of the modulus of this integral,

$$L(p,z) = 4\frac{\sin^2 za}{z^2} + p^2\left[32a^2\frac{\sin^2 za}{z^4} - 80\frac{\sin^2 za}{z^6} + 64a\frac{\sin za\cos za}{z^5} + 16a^2\frac{\cos^2 za}{z^4}\right] \qquad (6)$$

We now want to integrate this expression with respect to x from -1 to +1 to obtain the line image, L(p,z). Consider the terms separately, leaving out coefficients:

$$\int_{-1}^{1} \sin^2 za\, dx = \int_{-\frac{\pi}{2}}^{\frac{\pi}{2}} \sin^2(z\cos\theta)\cos\theta\, d\theta$$

$$= 2z\int_{0}^{\frac{\pi}{2}} \sin(2z\cos\theta)\sin^2\theta\, d\theta$$

Now $$H_1(2z) = \frac{4z}{\pi}\int_{0}^{\frac{\pi}{2}} \sin(2z\cos\theta)\sin^2\theta\, d\theta$$

where $H_1(2z)$ is a Struve function of the first order (Watson 1944) (see appendix C). Thus,

$$\int_{-1}^{1} \sin^2 za \, dx = \frac{\pi}{2} H_1(2z).$$

We have, $$\int_{-1}^{1} a^2 \sin^2 za \, dx = \int_{-\frac{\pi}{2}}^{\frac{\pi}{2}} \sin^2(z \cos\theta)\cos^3\theta \, d\theta.$$

Integrating the right hand integral by parts we obtain,

$$3 \int_{-1}^{1} a^2 \sin^2 za \, dx = z \int_{-\frac{\pi}{2}}^{\frac{\pi}{2}} \sin(2z \cos\theta)(\sin^2\theta - \sin^4\theta)d\theta + 2 \int_{-\frac{\pi}{2}}^{\frac{\pi}{2}} \sin^2(z \cos\theta)\cos\theta \, . \, d\theta.$$

The first term is expressible in terms of H_1 and H_2 (a second order Struve function) and the second in terms of H_1 as above, so that finally we arrive at,

$$\int_{-1}^{1} a^2 \sin^2 za \, dx = \frac{\pi}{2} H_1(2x) - \frac{\pi}{4} \frac{H_2(2z)}{z}$$

Consider now $\int_{-1}^{1} a \sin za \cos za \, dx$ which is equivalent to $\int_{-\frac{\pi}{2}}^{\frac{\pi}{2}} \frac{1}{2} \sin(2z \cos\theta)\cos^2\theta \, d\theta$ and this integral becomes,

$$\int_0^{\frac{\pi}{2}} \sin(2z\cos\theta)d\theta - \int_0^{\frac{\pi}{2}} \sin(2z\cos\theta)\sin^2\theta\, d\theta$$

which may be expressed in terms of H_o (zero order Struve function) and H_1 so that we are left with

$$\int_{-1}^{1} a \sin za \cos za\, dx = \frac{\pi}{2} H_o(2z) - \frac{\pi}{4} \frac{H_1(2z)}{z} .$$

Finally take the integral $\int_{-1}^{1} a^2 \cos^2(za)\, dx$

which we may express as, $\int_{-\frac{\pi}{2}}^{\frac{\pi}{2}} \cos^2(z\cos\theta)\cos^3\theta\, d\theta.$

This integral can be written as,

$$\int_{-\frac{\pi}{2}}^{\frac{\pi}{2}} \cos^3\theta\, d\theta - \int_{-\frac{\pi}{2}}^{\frac{\pi}{2}} \sin^2(z\cos\theta)\cos^3\theta\, d\theta.$$

The first integral equals $1\frac{1}{3}$ while the second reduces to $-\frac{\pi}{2} H_1(2z) + \frac{\pi}{4} \frac{H_2(2z)}{z}$.

Thus,

$$\int_{-1}^{1} a^2 \cos^2(za)dx = 1\tfrac{1}{3} - \frac{\pi}{2} H_1(2z) + \frac{\pi}{4} \frac{H_2(2z)}{z} .$$

On substituting for these integrals into equation (6) we obtain for the image of an incoherently illuminated line,

$$L(p,z) = \frac{2\pi}{z^2} H_1(2z) + \frac{16p^2}{z^4} \left[\pi H_1(2z) - \frac{\pi}{2} \frac{H_2(2z)}{z} \right.$$

$$- \frac{5}{z^2} \cdot \frac{\pi}{2} \cdot H_1(2z) + \frac{2\pi}{z} \cdot H_0(2z) - \frac{\pi}{z^2} H_1(2z)$$

$$\left. + \frac{4}{3} - \frac{\pi}{2} H_1(2z) + \frac{\pi}{4} \frac{H_2(2z)}{z} \right]$$

which reduces to,

$$L(p,z) = \frac{2\pi}{z^2} \cdot H_1(2z) + \frac{16p^2\pi}{z^4} \left[\frac{1}{2} \cdot H_1(2z) - \frac{7}{2} \frac{H_1(2z)}{z^2} \right.$$

$$\left. - \frac{1}{4} \frac{H_2(2z)}{z} + 2 \frac{H_0(2z)}{z} + \frac{4}{3\pi} \right]$$

Now H_0 and H_1 are well tabulated functions (Watson 1944) but no tables of higher order Struve functions seem to exist so that we require the recurrence relation,

$$H_2(2z) = \frac{H_1(2z)}{z} + \frac{4z}{3\pi} - H_0(2z)$$

which is proved in appendix C. Finally we obtain,

$$L(p,z) = \frac{2\pi}{z^2} H_1(2z) + p^2 \frac{16\pi}{z^4} \left[\frac{9}{4z} H_0(2z) + \left(\frac{1}{2} - \frac{15}{4z^2}\right) H_1(2z) + \frac{1}{\pi} \right]$$

The first term is the expression for the flux distribution in the image of a perfectly focused line and was derived by the German astronomer Struve (1882) while the second term represents a small defocus. The next term contains a factor p^4 which, provided $p < 1$ and $z > 0.1$ is less than $\frac{1}{100}$ the value of the term containing p^2. $L(p,z)$ is plotted in fig. 6.06 for $p = 0$ and for $p = 0.60$. The value at $z = 0$ has been calculated by Steel (1952) and his value has been used to complete the curve for $p = 0.60$. For the small amount of defocus considered it can be seen that the intensity in the central maximum has been reduced by 2.8% and that the intensity on either side of the maximum has increased slightly.

Having obtained the first derivative $L(p,z)$ of the edge image luminance distribution we shall now differentiate this to obtain the second derivative $L'(p,z)$.

We have,

$$L'(p,z) = \frac{2\pi}{z^2}\left\{ H_1'(2z) - \frac{2H_1(2z)}{z} \right\}$$

$$+ \frac{16p^2\pi}{z^2}\left\{ \frac{9}{4}\left[\frac{H_o'(2z)}{z} - \frac{5H_o(2z)}{z^2} \right] + \frac{1}{2}\left[H_1'(2z) - \frac{4H_1(2z)}{z} \right] \right.$$

$$\left. - \frac{15}{4}\left[\frac{H_1'(2z)}{z^2} - \frac{6H_1(2z)}{z^3} \right] - \frac{4}{\pi z} \right\}$$

In appendix C we show that,

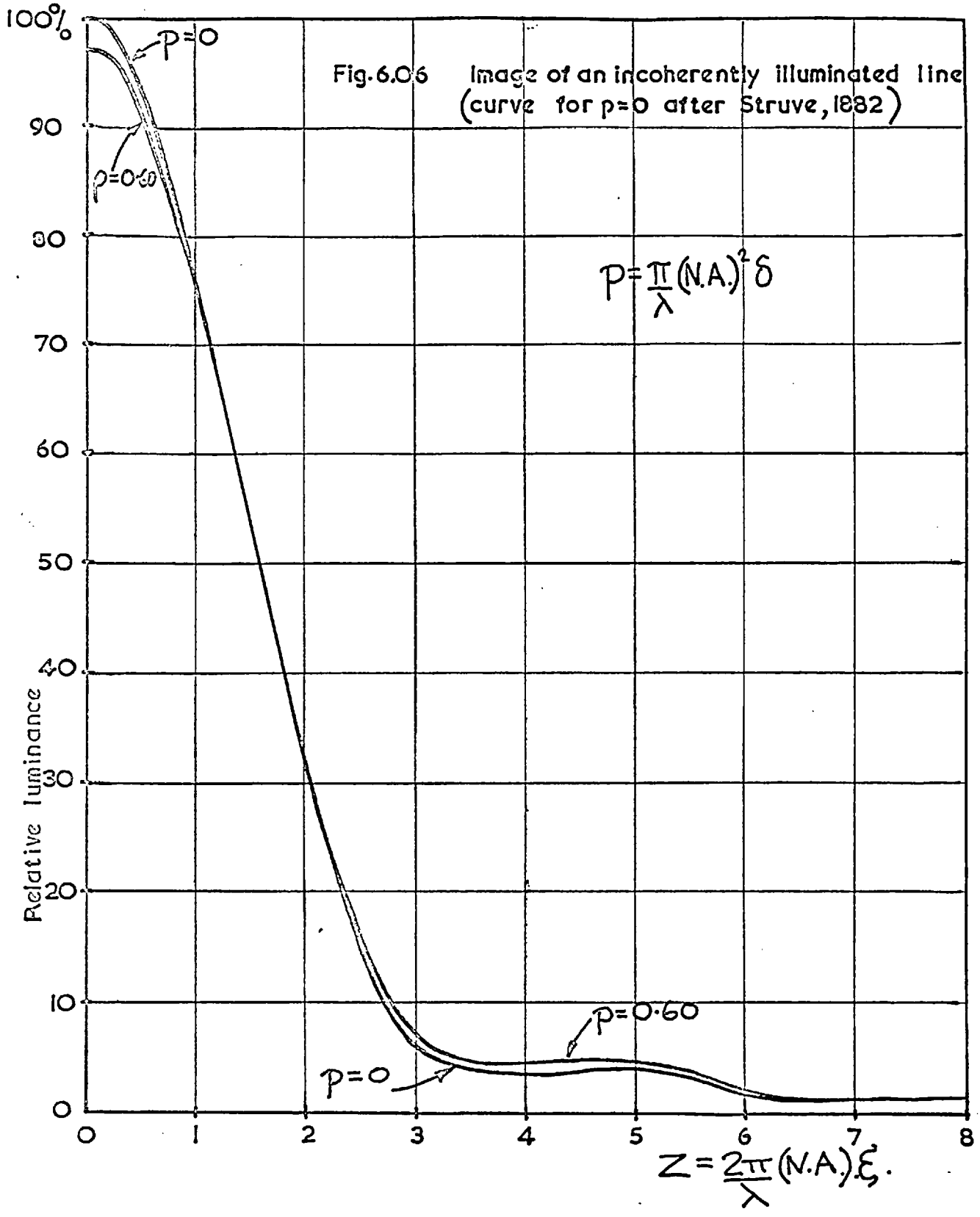


Fig. 6.06 Image of an incoherently illuminated line (curve for p=0 after Struve, 1882)

$$H_1'(2z) = 2H_o(2z) - \frac{H_1(2z)}{z}$$

and,

$$H_o'(2z) = -2H_1(2z) + \frac{4}{\pi} .$$

Substituting these formulae for H_1' and H_o' into the equation for L' we obtain,

$$L'(p,z) = \frac{2\pi}{z^2}\left\{ 2H_o(2z) - \frac{3H_1(2z)}{z} \right\}$$

$$+ p^2 \frac{16\pi}{z^4}\left\{ H_o(2z)\left[1 - \frac{75}{4z^2}\right] + H_1(2z)\left[-\frac{7}{z} + \frac{105}{4z^3}\right] + \frac{5}{\pi z} \right\}$$

Using the values of H_o and H_1 given by Watson (1944), $L'(p,z)$ is plotted in fig. 6.07. The curve for $p = 0$ is that used in fig. 4.14. It can be seen that when $p = 0.60$ the stationary values of the curve have not moved appreciably relative to the perfectly focused curve although the magnitude of the second derivative at these points has changed by as much as 10% in some cases. The curves are anti-symmetric about the axis $z = 0$ so that only values for $z \geq 0$ are shown.

Fig. 6.08 gives Weinstein's computations for the flux density in the edge image for $p = 1.0$ and $p = 0$. For this amount of defocus there has been a slight decrease in the edge gradient.

Fig. 6.07. Second derivative of the edge image in incoherent illumination

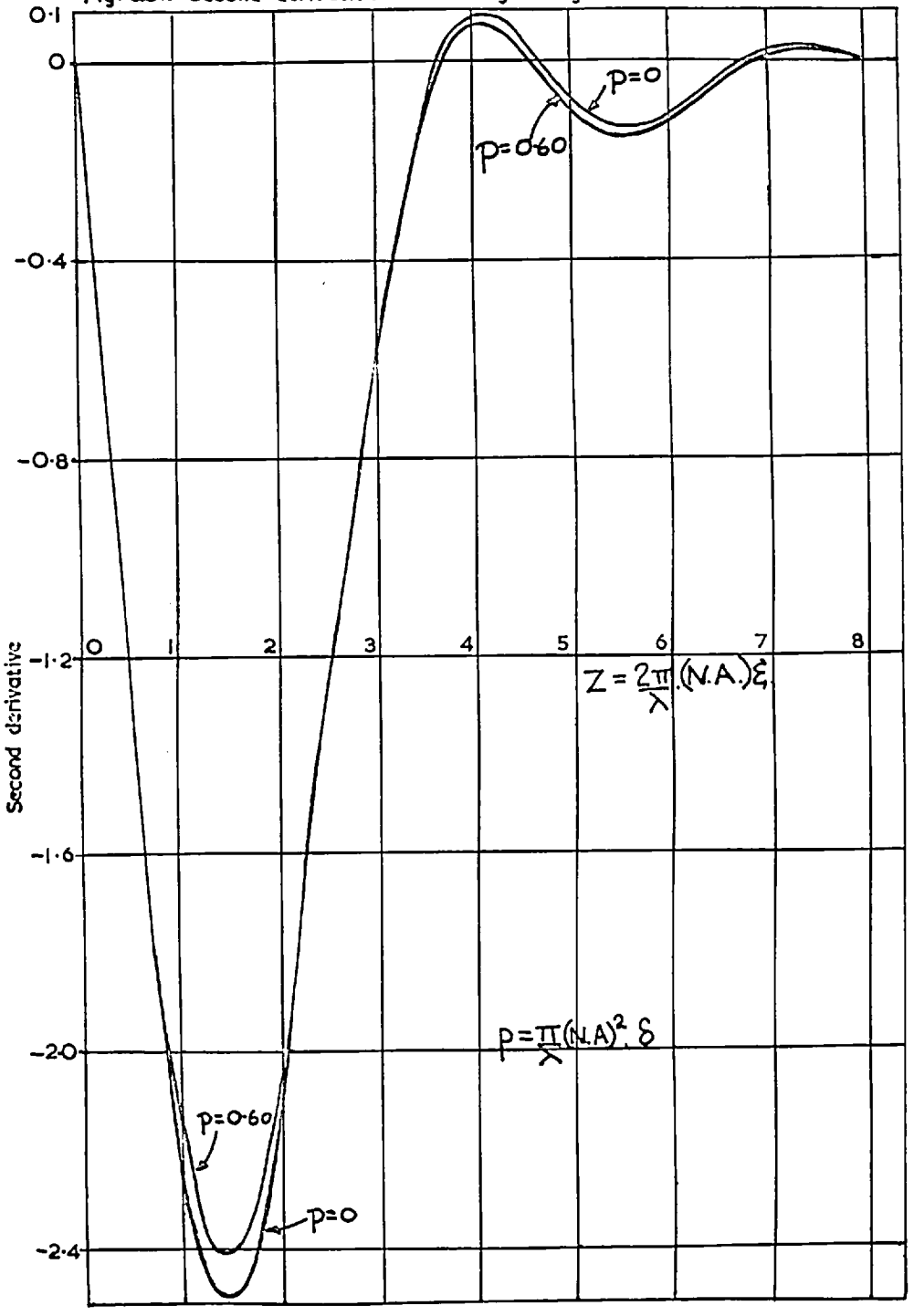


Image of an incoherently illuminated edge (after Weinstein)

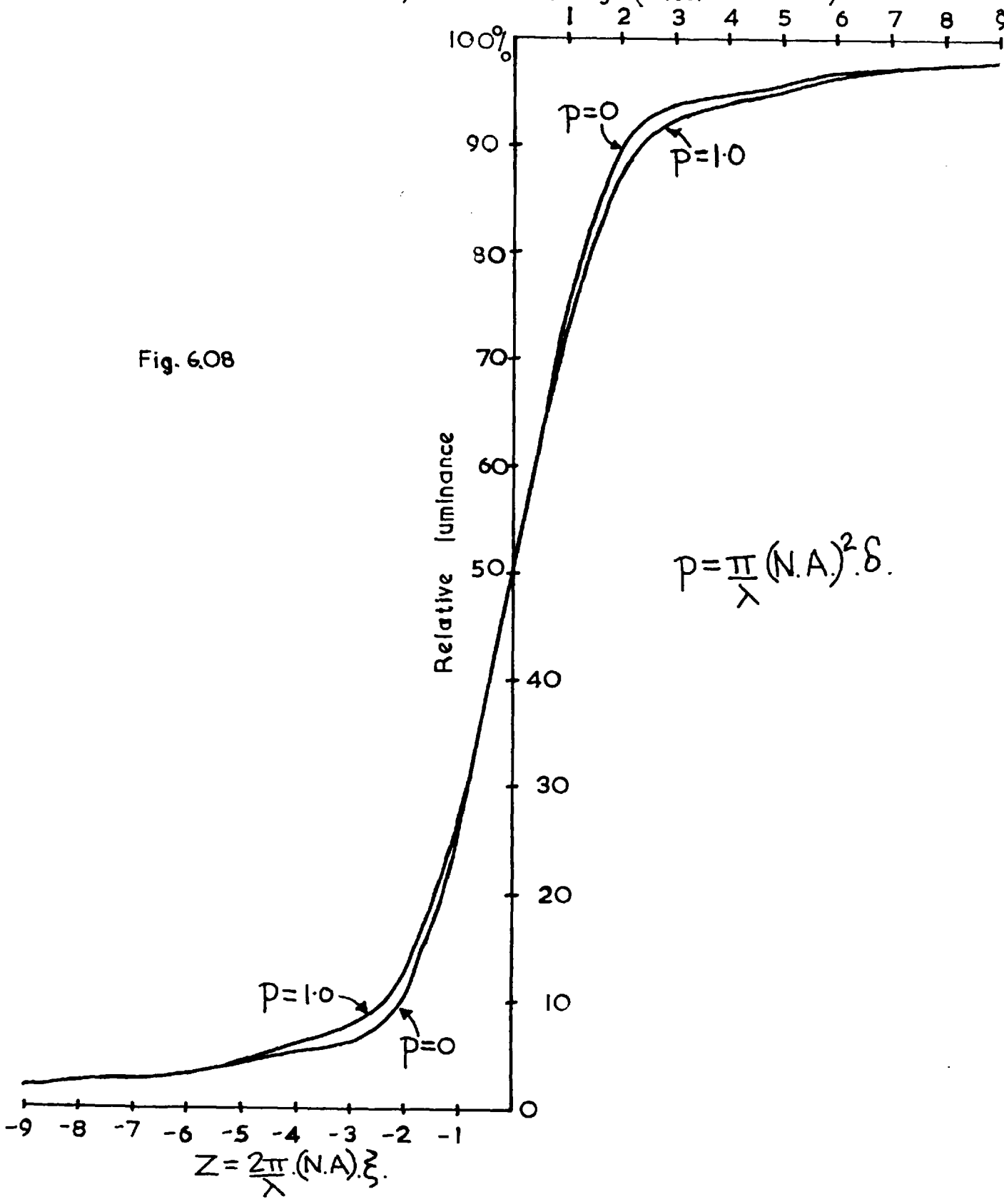


Fig. 6.08

From the relation,

$$\delta = \frac{\lambda}{\pi(N.A.)^2} \cdot p \qquad \text{(appendix A)}$$

we have for the object space that the longitudinal shift in focus, δ, = 7.0μ when p = 0.60 and δ = 11.7μ when p = 1.0; these values would be doubled if we considered the total depth of focus above and below the best focus.

Discussion.

Small amounts of defocus, within the visual depth of focus, are sufficient to produce Mach band displacements of the type shown in fig. 5.04 and sometimes result in personal differences between observer's measurements. For the cases of coherent and incoherent illumination such focusing errors are not sufficient to move the points where the second derivative has stationary values by amounts which are comparable to the observed band displacements. Now it is not possible to obtain completely coherent illumination with the apparatus described above but the conditions of incoherent illumination are very nearly reached at S = 5.08 where measurements of band displacements were made (fig. 5.07). It is plausible to assume that for the intermediate range of partially coherent illumination the positions where the second derivative

has stationary values do not change by any appreciable amount either.

The reasons for the shift in band positions must lie on some other features of the perturbations which have been shown to occur in the physical distributions of luminance (figs. 6.03, 6.08). One such feature is probably the slope of the graded zone between the bright and dark fields. Fiorentini and Radici (1958), who were experimenting with the simpler macroscopic Mach effect, found that for some observers the position of the bright band shifted into the bright field as the slope was decreased although no such inference could be made for the dark band. It has been shown that for small amounts of defocus the edge gradient decreases and also the band positions move into the bright field.

Chapter VII

The effect of a) retinal location and b) binocular vision on the Mach bands

a) Retinal location

Introduction

The French astronomer Arago (1858) noticed that faint stars were made more visible to an observer if the observer did not look directly at them. Le Grand (1957) points out that as the scotopic phase of dark adaptation progresses the fovea loses its predominance and the observer fixates extrafoveally without being conscious of it. According to Simon (1904) this point of fixation may be in any direction with respect to the fovea but it is, on average, 20 minutes of arc from the edge of the fovea after 10 minutes in darkness and 1 degree at the end of one hour. In Chapter IV it has been noted that observers found that direct fixation (i.e. foveal fixation) on a given Mach band decreased its visibility. Also most observers noted that a bright band appeared most distinct when they fixated about 20 minutes of arc away from the band; there was no noticeable change in this position after the observer

had viewed the field for periods of up to an hour. No clues to the origin of these phenomena are provided by the known distribution of rods and cones in the retina. Fig. 7.01 shows the distribution of rods and cones along a horizontal median of the retina (Osterberg, 1935; Wertheim, 1894). The cone density decreases monotonically on either side of the central fovea while the rods show a maximum density at about 10 degrees from the fovea centralis.

Although the retinal illumination produced by the bright clear field during the survey, described in Chapter IV, was sufficiently high (1500 trolands) to produce photopic (cone) vision the discernment of the faint bright and dark bands might have depended to some extent on the response of the rods. According to Polyak (1941) the first rods do not occur within 250μ from the point of foveal fixation. If foveal vision is used strictly to denote that which takes place within the area which is free from rods and contains about 35,000 cones vision is foveal over an apparent angular diameter of about $1^{o}40'$ since in the standard eye 1 minute occupies 4.85μ on the retina. Osterberg (1935) found rods 130μ from the fovea centralis and Rochon-Duvigneaud (1943) gives the maximum radius of the rod free area as only 75μ which is equivalent to an angular diameter of only 30 minutes of arc.

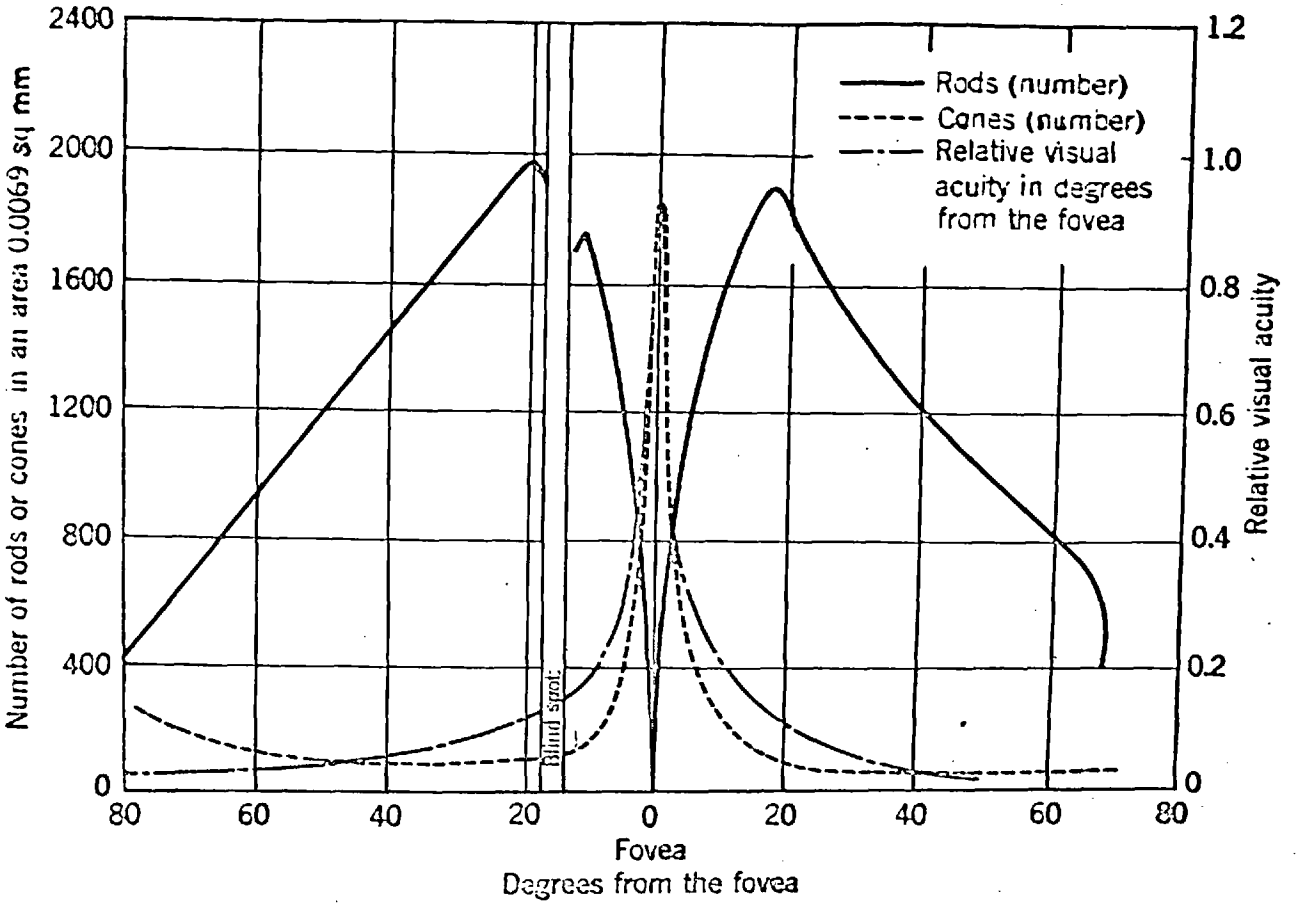


Fig. 7.01 Distribution of rods and cones along a horizontal meridian. Parallel vertical lines represent the blind spot. Visual acuity for a high luminance as a function of retinal location is included for comparison. (From Woodson, 1954; data from Osterberg, 1935, and Wertheim, 1894.)

Fig. 7.01 provides no information about the relative distribution of receptive fields over the retina (a receptive field is a group of receptors over which the responses to illumination are integrated to yield one signal to the brain). No work has so far been published on this subject but it is of great importance here as it is presumably inhibitory processes between neighbouring receptive fields which give rise to the Mach effect.

Apparatus and techniques used to investigate the perception of the Mach bands outside the fovea.

For extra-foveal vision it would have been highly probable that an observer could have mistaken diffraction fringes for Mach bands. It was therefore important to obtain an image free from diffraction bands. An image which contained no diffraction bands was obtained by incoherently illuminating a thin, high contrast straight edge with light of wavelength $\lambda = 0.53 \pm 0.05\mu$, an objective of N.A. = 0.12 was employed and the resulting image was viewed through a X20 eyepiece. In order to obtain good fixation the observer was made to bite a dental impression which was firmly bolted to the microscope stage. The position of the dental impression could be adjusted so that the exit pupil of the microscope was centrally disposed with respect to the observer's eye pupil.

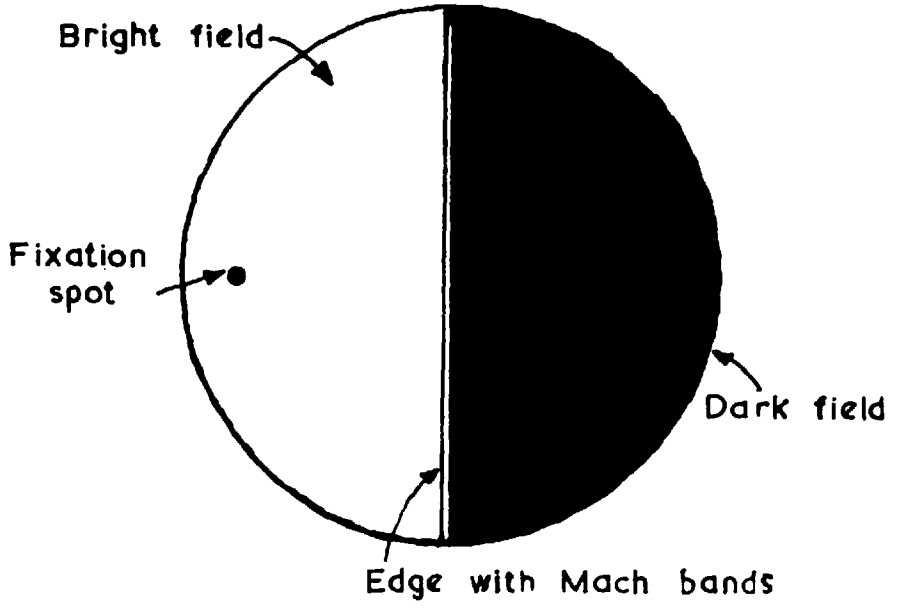


Fig. 7.02. Observation of Mach bands extrafoveally

After viewing the field for five minutes the observer was asked to fixate onto a black spot in the bright field, about 20 degrees from the edge (fig. 7.02). The fixation spot was provided by arranging the tip of a 0.5μ tungsten wire to be in the focal plane of the eyepiece, while the remainder of the wire was out of focus and consequently hardly noticed. The wire was fixed to a Beck filar eyepiece mount (with the graticule removed) so that the observer could move the fixation spot across the field of view by turning a drum graduated in millimetres.

The fixation spot was placed initially in the bright field. Then the observer followed the fixation spot until the Mach bands were seen with the spot stationary (invariably the bands could be seen while the fixation spot was moving before they could be seen with the eye fixated on the spot when it was stationary. At this point all three observers could perceive three Mach bands: the first bright band, the edge band and the second bright band. There was no position for which a particular band appeared before the others although the second bright band was the most distinct. The drum reading was noted and then the observer moved the fixation spot so that it coincided with the visual edge and this position was recorded. Next the observer slowly followed the fixation spot until the bands disappeared

simultaneously (the drum reading being noted). The final measurement was the most difficult as the observer had to view the field with the spot stationary at about fifteen minutes of arc intervals to ascertain if the bands had disappeared but on subsequent scans the number of such intervals was reduced because the observer knew roughly where the bands disappeared. The first scan served merely to acquaint the observer with the required techniques and these results were subsequently rejected. Six scans were performed over a period of about thirty minutes.

Following the fixation spot in the other direction (dark field to bright field) produced an unwanted contrast effect in which one bright and one dark band, each subtending about one degree, were seen. Consequently measurements of the type described in the previous paragraph were not possible when the fixation spot was moved from the dark field into the bright field.

If the fixation spot and the primary edge image are separated by a distance d in the focal plane of the eyepiece then the angular displacement θ of the edge image on the retina with respect to the fovea centralis is given by,

$$\theta = \frac{d}{f_e} \qquad \text{(fig. 7.03)}$$

where f_e is the focal length of the eyepiece. The small small angle approximation is valid since $\theta < 6^{\circ}$.

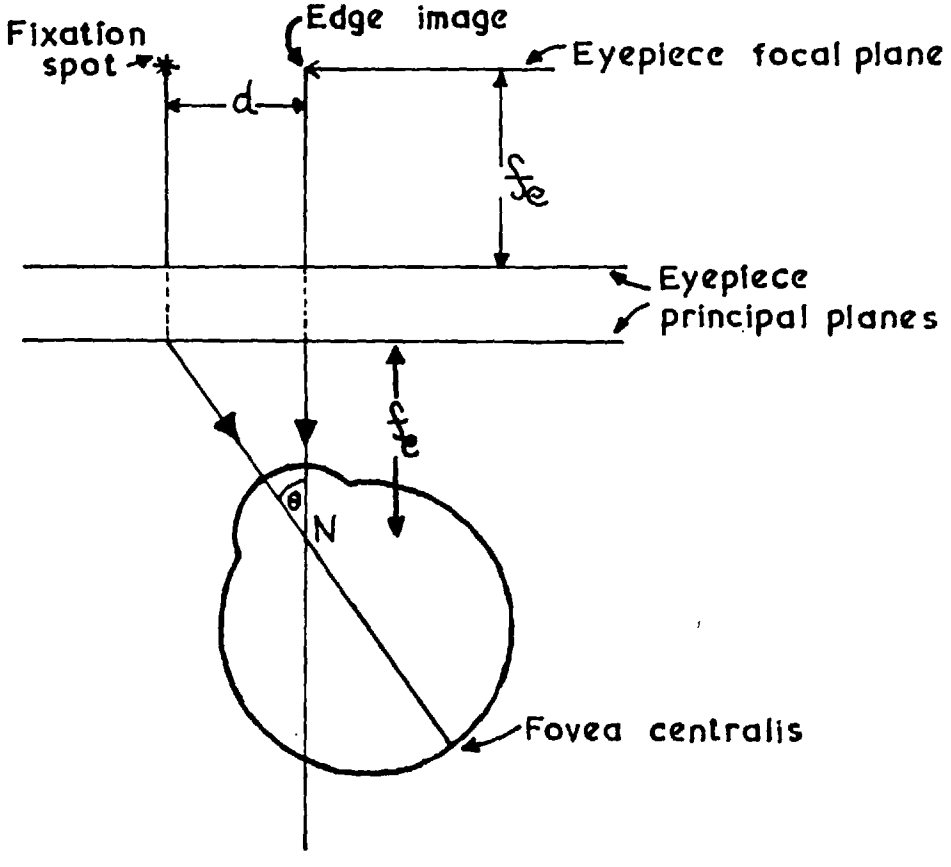


Fig. 7.03 Extrafoveal observation of Mach bands

Fig. 7.04 shows the maximum angular displacements (along a horizontal median) from the central point of fixation (fovea centralis) at which the Mach bands were seen. All three observers A.E.S., G.O., and S.H.R., could see the Mach bands well outside the fovea. The observers verified that the bands appeared most distinct about 20 minutes of arc from the central point of fixation; this position could not be accurately located however and the figure quoted should be considered only as a rough estimate. At the maximum value of θ the bands disappeared fairly abruptly and the six scans for each observer showed a spread from the mean of not more than $\pm$ 10%.

It is plausible that the Mach bands disappeared at the positions shown in fig. 7.04 because at such distances from the fovea the receptive fields have become comparably large with respect to the physical edge image on the retina (about 40 minutes of arc, figs. 4.07, 8, or approximately 180μ). Subsidiary experiments could be performed in which magnified edge images would be viewed extra-foveally. Then we should expect the Mach bands to disappear at larger values of θ. Beyond the positions shown in fig. 7.04, up to about 20 degrees eccentric from the fovea centralis, the Mach bands could be made to reappear if the observer's eye were not stationary (as described above). This can be explained

Maximum angular displacements, along a horizontal median, from the fovea centralis at which the Mach bands were seen.

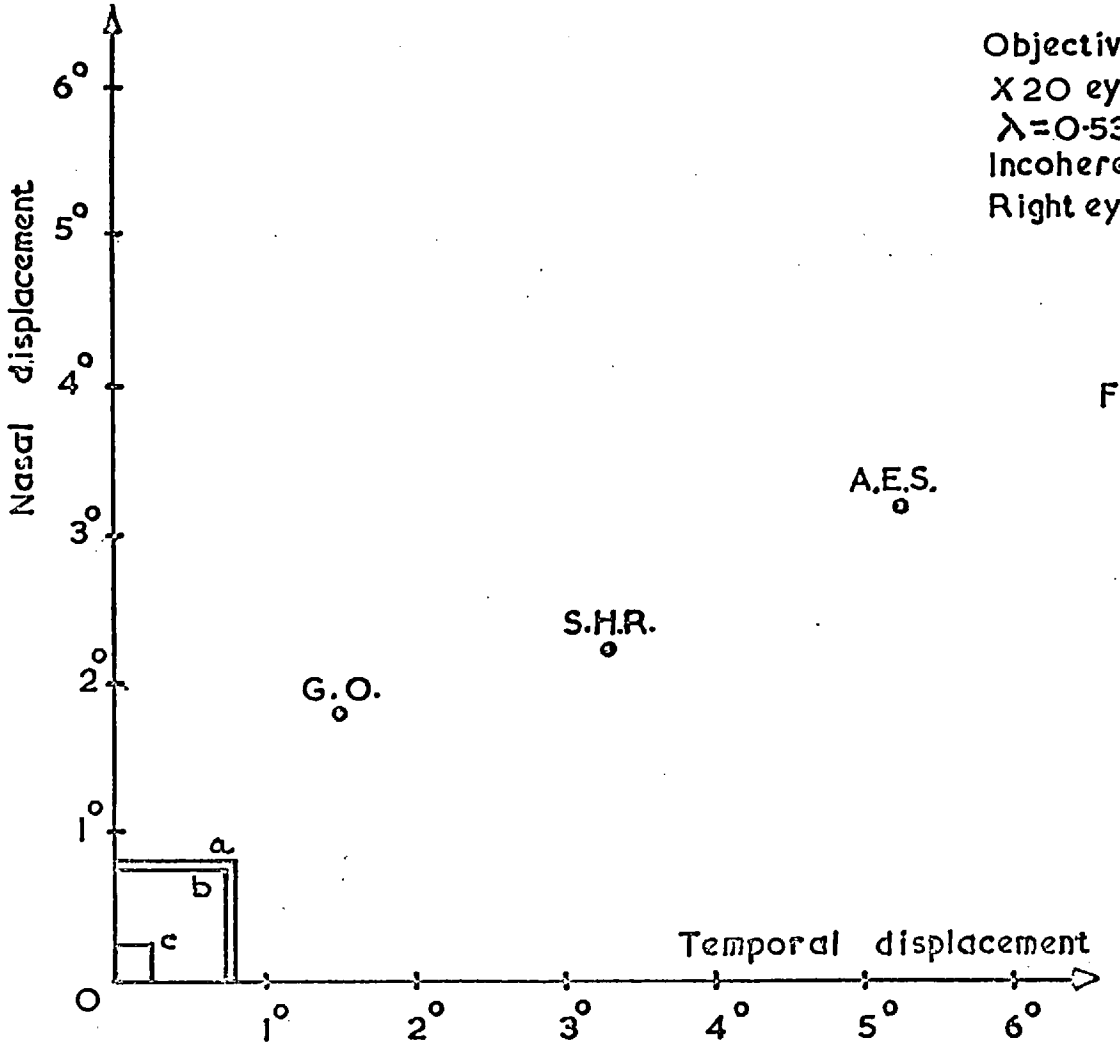


Fig. 7.04

Squares 'a' 'b' and 'c' show the extent of the fovea quoted by Polyak (1941), Osterberg (1935) and Rochon-Duvigneaud (1943) respectively.

if we assume that the edge image was able to fall successively on neighbouring fields quickly enough to evoke the necessary lateral inhibitions between the receptive fields which give rise to the Mach effect. We have not considered the effect of the small involuntary eye movements which an eye performs when it fixates onto a target (Ditchburn 1956) but there can be little doubt that they aid the perception of the Mach bands as the receptive fields become larger when θ increases.

b) Binocular vision

Introduction.

We shall now consider binocular vision which may be defined as the use of two eyes in such a co-ordinated manner as to produce a single mental impression of an external object. The use of microscopes with binocular eyepieces is widespread and apart from the advantage of stereoscopy which is obtained with some of the low power types (e.g. the Greenough model) binocular microscopes afford much more comfort to the observer by permitting the natural use of both eyes. No detailed work has been reported concerning Mach effects which arise in binocular vision so that this subject seemed worthy of some preliminary investigations.

Apparatus and techniques.

A Beck binocular attachment employing a Jentsch prism system was used (fig. 7.05). Light from the objective entered the first prism and was split into two beams by the semi-reflecting surface ab and then travelled via two prisms into two matched Huygens eyepieces (X10). The separation of the two beams thus produced, could be varied to allow for different observers' interocular distances. The left-hand eyepiece could be focused independently. This binocular system was used in conjunction with the existing photo-electric microscope described above. A positive relay lens, consisting of two 50 cm. focal-length plano-convex lenses with their curved surfaces in contact (so as to reduce spherical aberration) was situated 2 cm in front of the surface cb. This lens combination imaged the primary microscope image at I' in the focal planes F_1, F_2 of the eyepieces. While this would have been unnecessary if only simple observations were to have been made the presence of the relay lens was needed when the binocular attachment was used in conjunction with the photometer prism, as described below. As a result of light losses by reflection and absorption at the various prism surfaces it was difficult to obtain sufficiently bright images with the 0.12 N.A. objective so that a

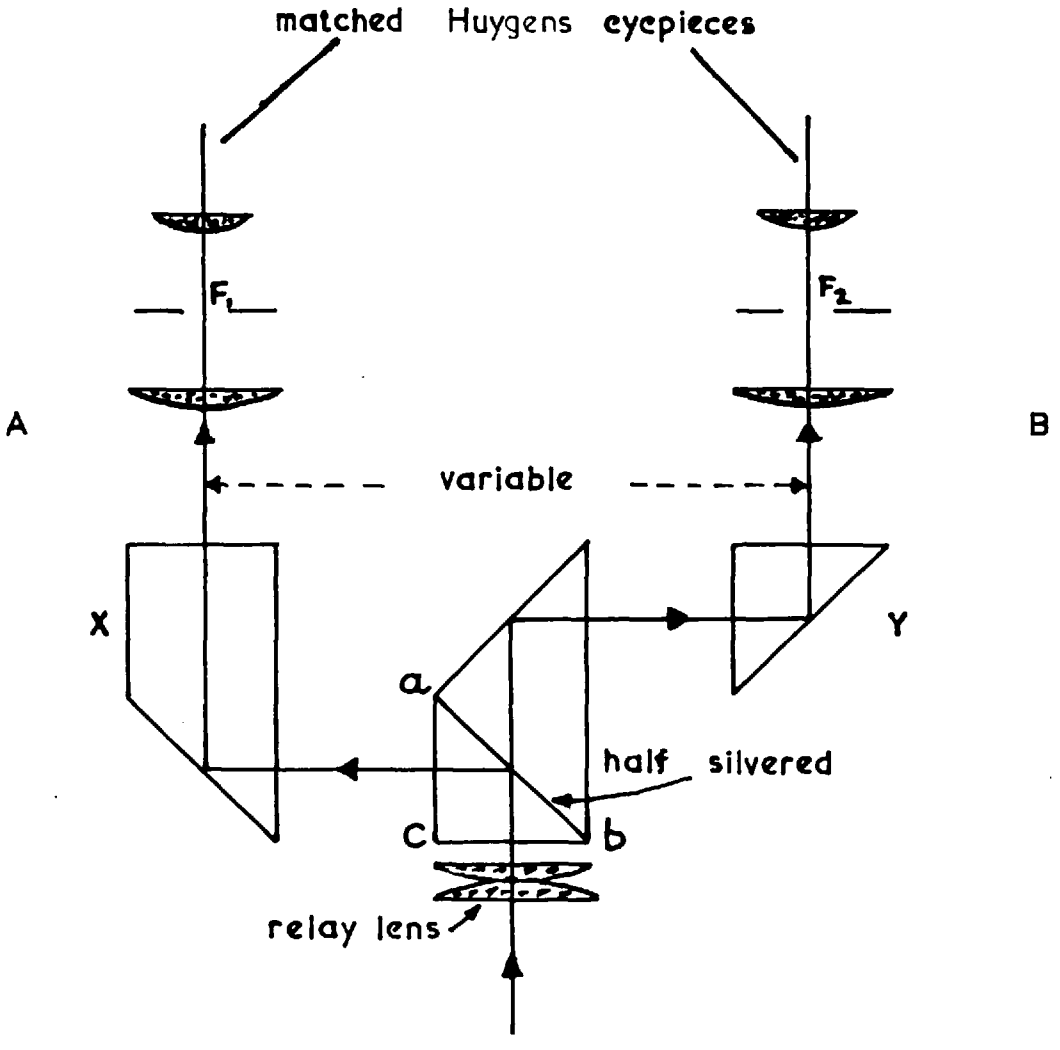


Fig. 7.05 Beck binocular attachment

0.65 N.A. Beck objective, giving a magnification of 74 times, was employed to achieve a reasonably high level of retinal illumination (1500 trolands) with light of wavelength $0.53 \pm 0.5\mu$.

The test object was a thin, high contrast straight edge with a reference aperture similar to that described in Chapter III. An S value of 0.75 was chosen as it gave a reasonably high level of retinal illumination and produced three well defined Mach bands.

The tip of a 0.5μ tungsten wire was held centrally at the focal plane of one of the eyepieces to facilitate measurements of the Mach band boundaries; this eyepiece could be inserted into either of the binocular tubes so that either the left or right eye could be used for such measurements.

The illumination of each exit pupil was verified to be equal with the aid of an S.E.I. photometer. Also by measuring the Mach bands with the right eye it was found that the imaging properties of the two prism paths did not differ significantly.

With the condenser properly centered so that it filled the objective evenly with light the observer covered the left-hand eyepiece, which had independent focusing, and viewing with the right eye adjusted the coarse and fine

focus knobs until the edge was sharply in focus. Then the cover was transferred to the right-hand eyepiece and the left-hand image was brought into focus by using the independent eye-piece focusing alone. Next, with the cover removed and viewing with both eyes the observer adjusted the interocular distance until a perfectly clear field of view was obtained with both eyes observing at the same time. This last adjustment resulted in a slight defocus so that the focusing procedure had to be repeated. All these adjustments were made with relaxed accommodation so that the final images were seen at infinity.

For luminance matches the photometer prism (used previously for the survey described in Chapter IV) could be interposed between the relay lens and the objective so that an image of the comparison slit with the edge image was focused at F_1, F_2. Thus there was a field of view similar to that shown in fig. 3.02 in each ocular. When luminance matches were performed the 0.5μ tungsten wire was removed.

Using the same techniques as described in Chapter IV, each of the observers determined the position of the Mach bands relative to the reference aperture; ten scans were performed with the left eye, right eye and finally with both eyes. These measurements were followed by corresponding measurements on the relative luminances of the

bands, six matches being performed for each band. Results are plotted in the form of luminance profiles (on logarithmic scale) in figs. 7.06a,b,c,d and e. Distances are measured relative to the geometrical edge which was determined by scanning with the 0.12 N.A. objective using incoherent illumination.

The results provide no evidence to suggest that one eye was dominant in its role of interpretation of the image when binocular vision was employed. No significant difference (at the 5% probability level) could be detected between the three separate visual edges (i.e. for the right eye 'R', left eye 'L' and both eyes 'B') for each of the observers S.H.R., M.J.M., J.M.R., P.R.H., and S.B.N. There was no significant difference between any of the border positions recorded by P.R.H., while M.J.M., S.H.R., and J.M.R. could detect no significant difference in the three mean positions (R, L and B) for the border between the first bright band and the clear field.

From the results of M.J.M., S.H.R., J.M.R., and P.R.H. there seems to be a tendency for the bright bands to be seen less brightly when the image was viewed binocularly compared with the monocular case.

The results of S.B.N. provide some unusual features. This observer complained of discomfort during the experiments

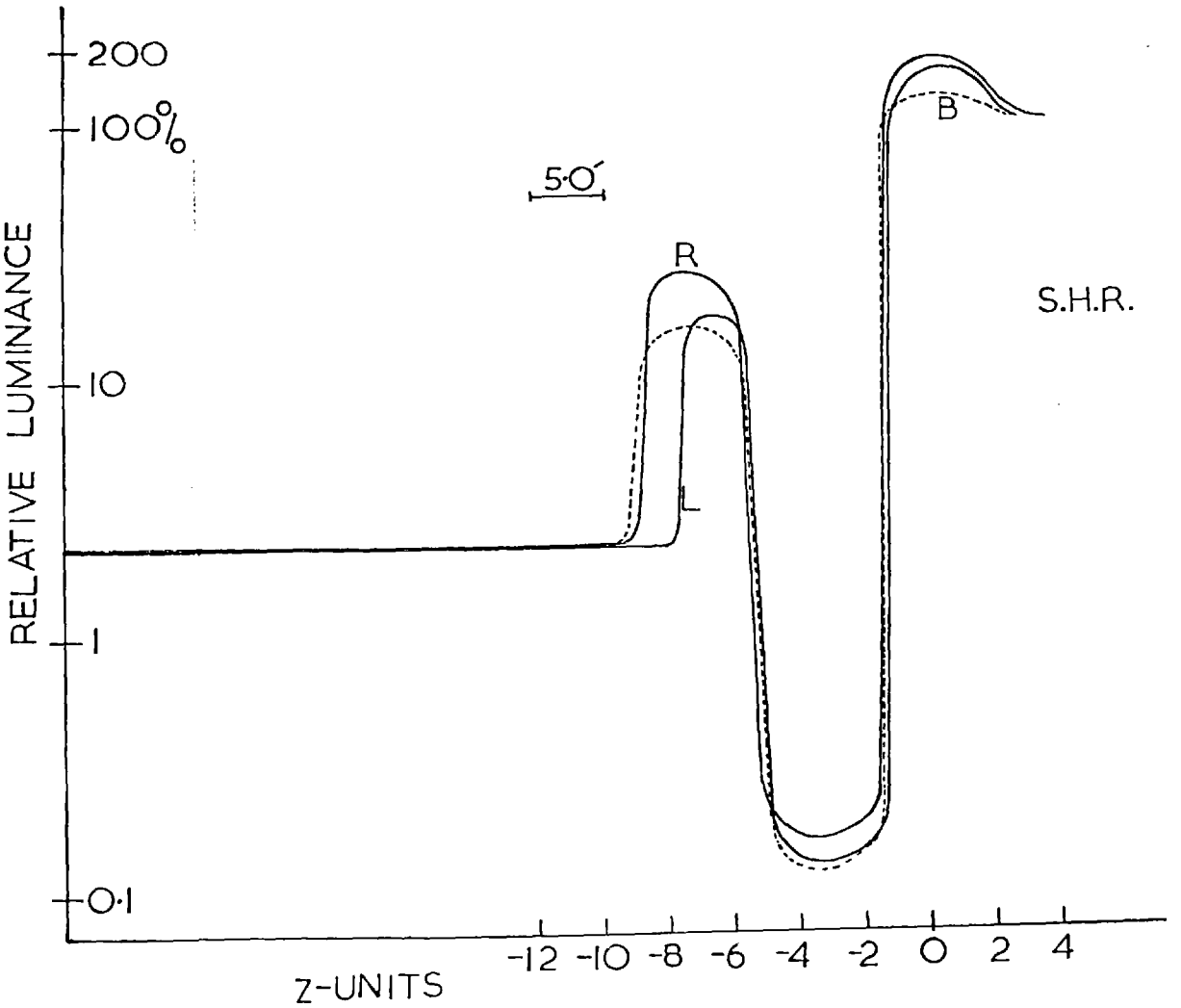


Fig. 7.06a. Mach bands seen at an opaque edge with the left, right and both eyes. Observer S.H.R.

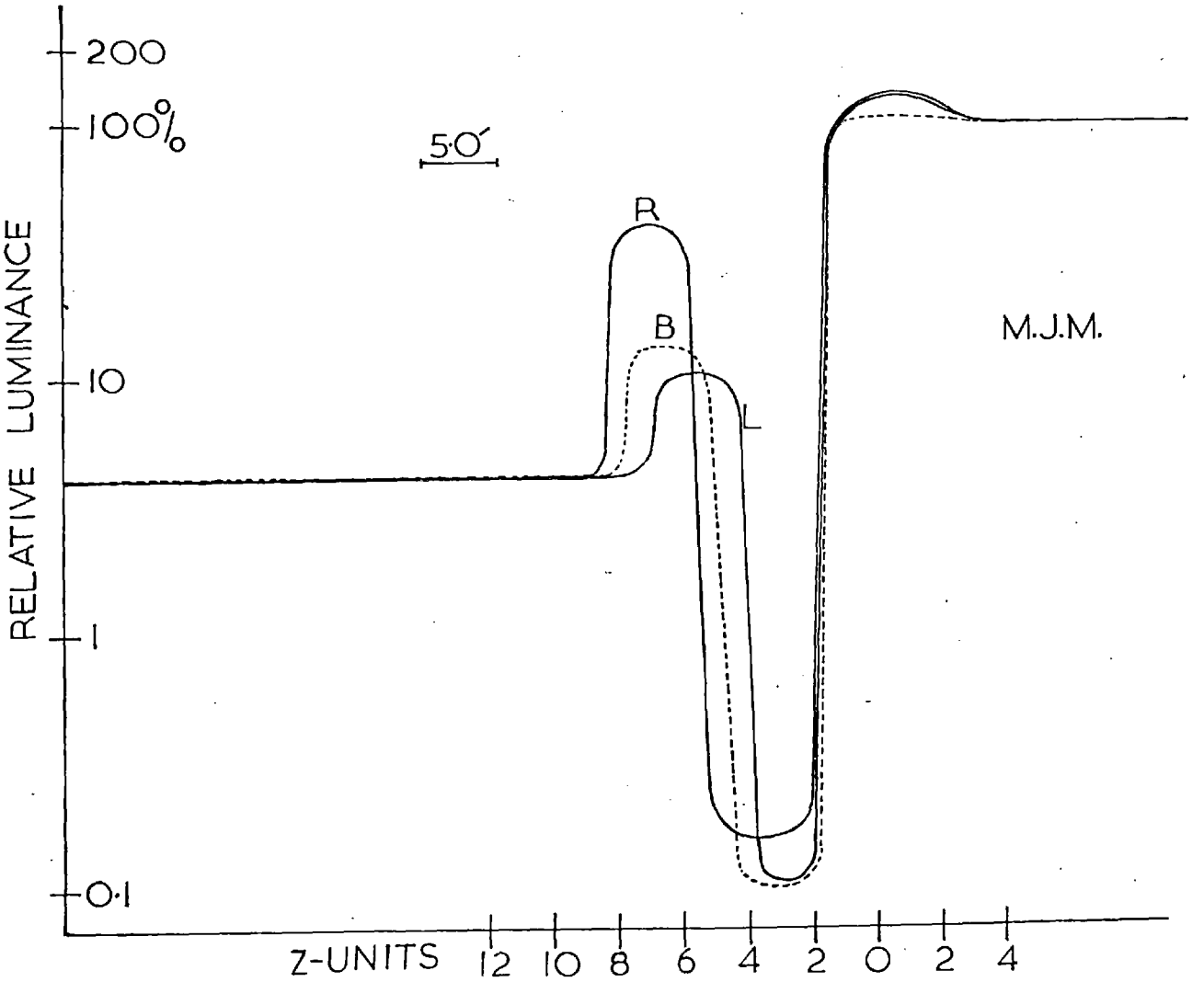


Fig. 7.06b. Mach bands seen at an opaque edge with the left, right and both eyes. Observer M.J.M.

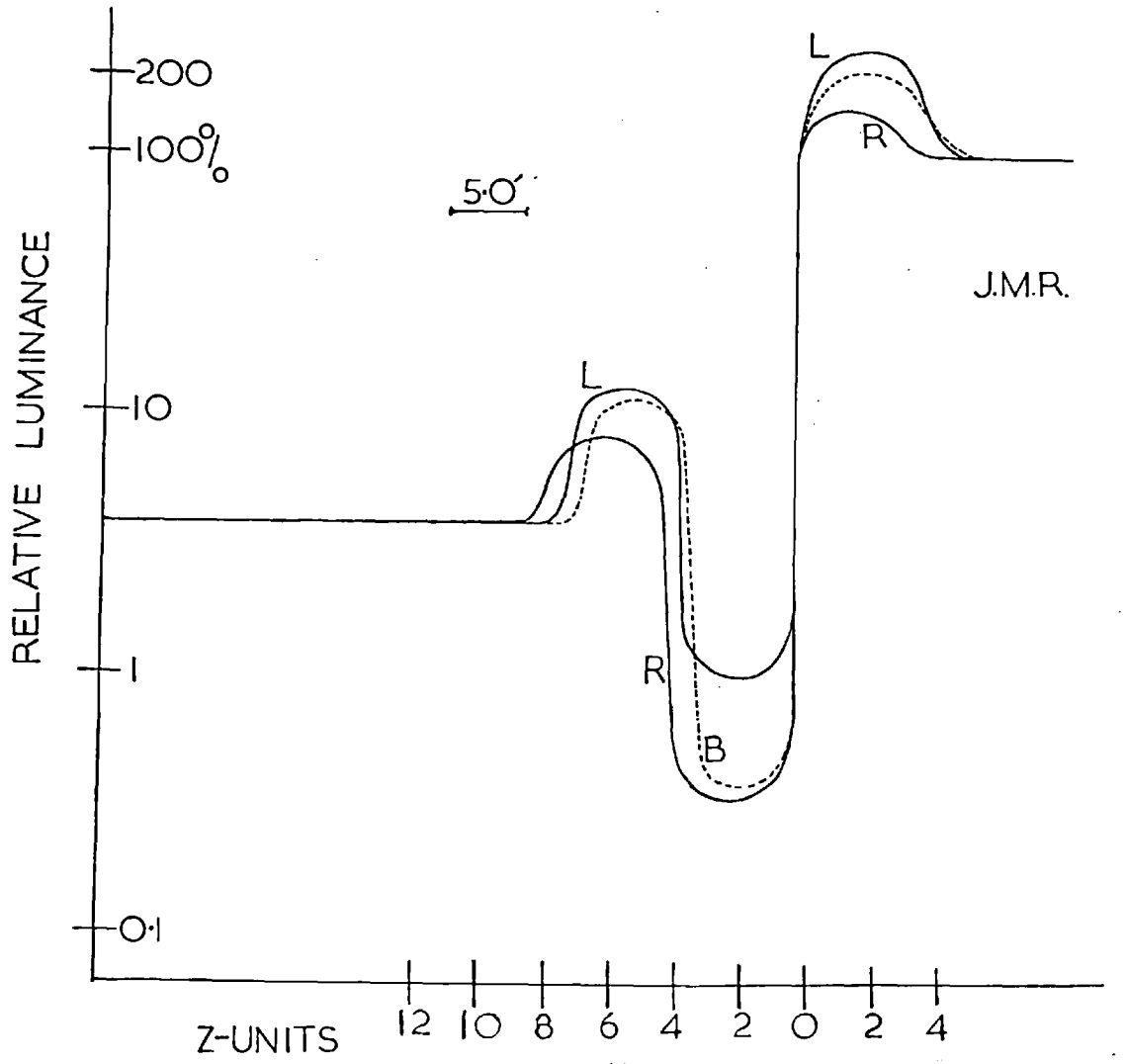


Fig. 7.06c. Mach bands seen at an opaque edge with the left, right and both eyes. Observer J.M.R.

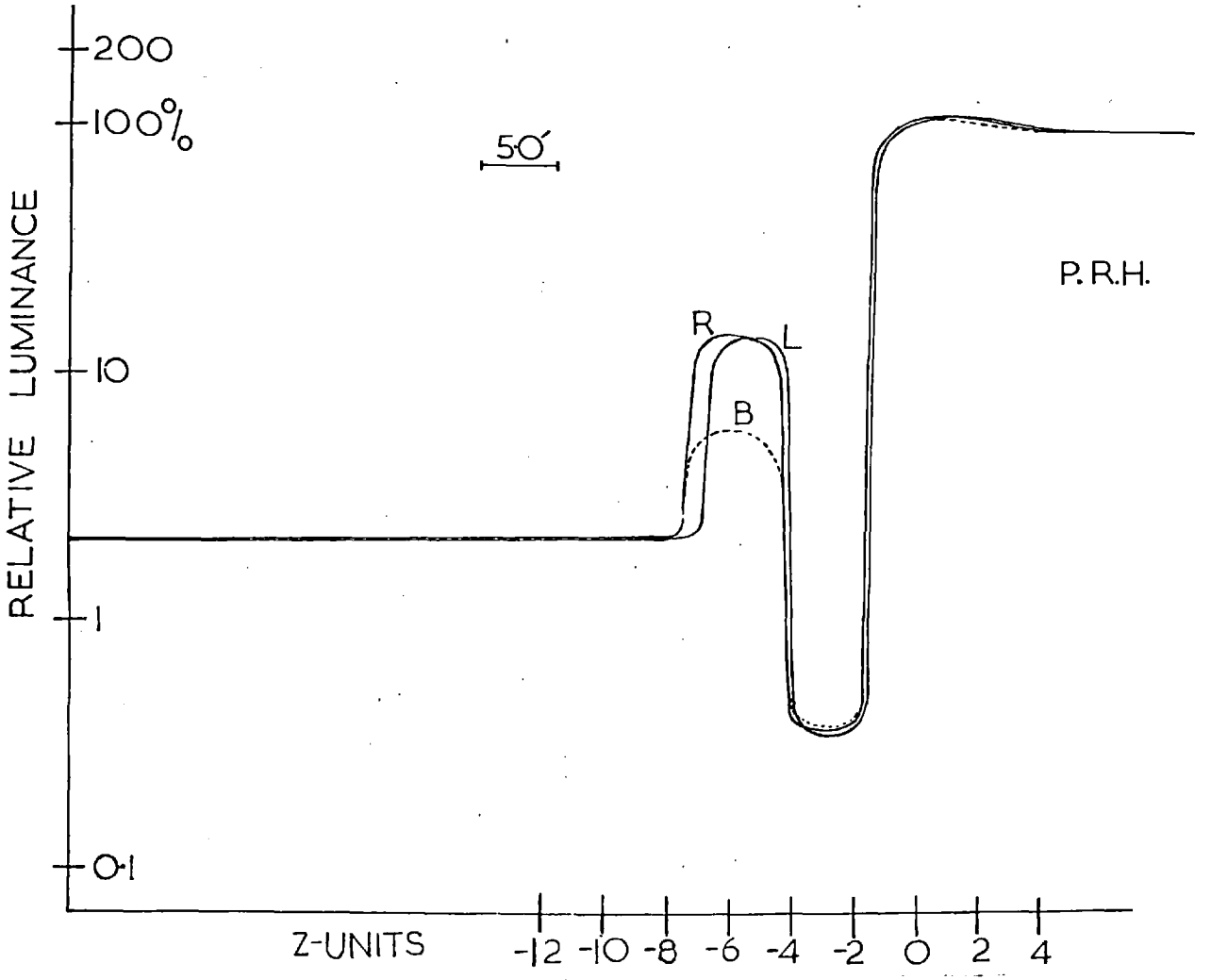


Fig. 7.06d. Mach bands seen at an opaque edge with the left, right and both eyes. Observer P.R.H.

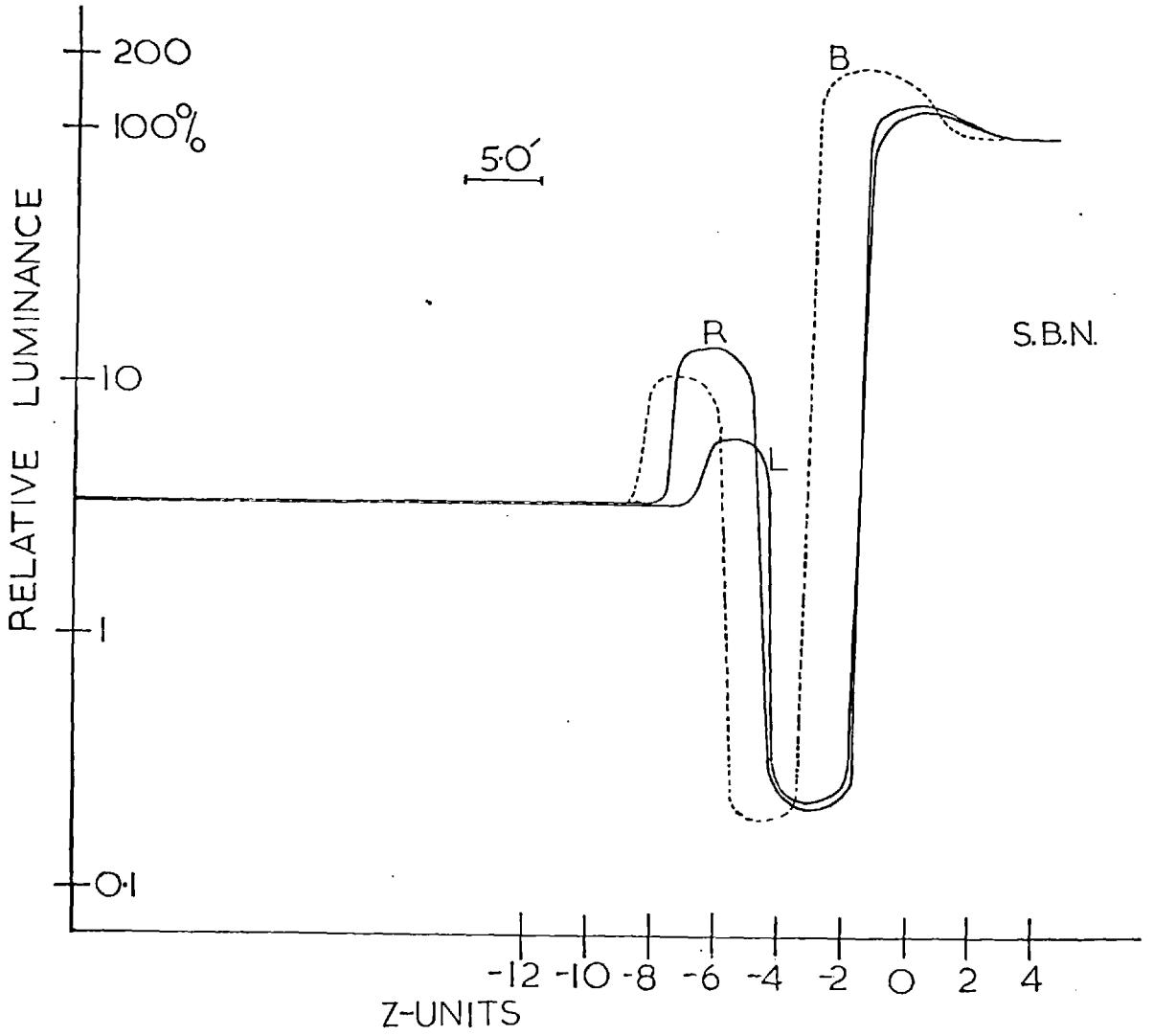


Fig. 7.06e. Mach bands seen at an opaque edge with the left, right and both eyes. Observer S.B.N.

as the binocular attachment did not permit a sufficiently small interocular distance. The minimum interocular distance provided by the attachment was 55 mm. and S.B.N.'s value was somewhat less than this. There can be little doubt that this accounted for the disagreement between his binocular and monocular measurements.

We may conclude that, with a well adjusted binocular attachment, the perception of the Mach bands does not depend, to any large extent, on whether an observer uses his left eye, right eye or both eyes, but naturally the use of a binocular attachment is to be preferred when prolonged observation is needed.

Chapter VIII

Summary of conclusions and discussion

The Mach effect is seen to be a very complicated visual phenomenon which depends on a number of factors. The work described in this thesis has exposed the wide personal differences that exist between different observers' interpretations of the Mach effect in microscopy where it assumes a multiple band structure. The spatial scale of the bands is similar to that of diffraction fringes present in the physical image although the position and brightnesses of the Mach bands do not correspond with the physical fringes and even when no diffraction fringes are present (as with incoherent illumination) an observer will still see Mach bands at the image of an edge. Sometimes, as in cytology, it is easy to mistake the Mach bands for actual detail present in the object (e.g. dark membranes around a cell).

While the various mathematical models (described in Chapter I), which relate to the macroscopic effect, succeed in predicting the gross features of the Mach effect their quantitative efficacy in predicting actual positions, widths and relative luminances is not good. Furthermore the possibility of a quantitatively useful mathematical model

for use in microscopy, where the Mach effect is more complex and the personal variations are more diverse, seems remote. The second derivative postulate seems, at best, only a rough approximation for predicting the band positions.

Under the carefully controlled conditions used for the survey on twenty observers a variation between individuals of about one z unit was obtained for the determination of the visual edge. This fact is of importance in the visual sizing of particles. Moreover in routine microscopy the level of illumination is not so carefully controlled so that we should expect even larger errors to occur here.

The microscopic Mach effect has been shown to be very sensitive to slight perturbations caused in the physical image produced by small amounts of defocusing. The edge gradient of the physical image changes faster, for a given amount of defocus, when coherent illumination of the object is employed as compared with the use of incoherent illumination. This probably accounts for the visual depth of focus being smaller when coherent illumination is employed. However, as the condenser aperture is stopped down, so achieving greater spatial coherence, the physical images become more complex with attendant diffraction fringes and individual differences are more manifest.

The visibility of the Mach bands approaches a maximum

about 20 minutes of arc from the fovea centralis and the perception of the bands is not confined to the fovea. Slight movements in the retinal image increase the visibility of the Mach bands.

Experiments with a binocular eyepiece show that the microscopic Mach effect does not depend, to any great extent, on whether an observer uses his left eye, right eye or both eyes to view the image.

The Mach effect is sometimes considered to be a mechanism whereby image quality is improved by the sharpening of edge gradients occurring in the retinal image. The concept of image improvement is a naïve one as this would infer that the neural processes which give rise to the Mach effect actually increase the information content of the signals sent from the retina to the brain but, in fact, the Mach bands are a troublesome source of artifacts in the image and the visual edge, although sharpened, is often displaced relative to the physical edge. It seems plausible that the Mach effect may be a retinal mechanism which emphasises luminance contour borders so that the higher centres of detection, located in the brain, can discern such features more easily.

There is much research that needs to be done before the full extent of the influence of the Mach effect on

microscopic imagery is fully appreciated. Hubel and Weisel (1959, 62) have shown that many of the cells in the visual cortex of the cat respond only to lines with a certain orientation. Each cell has a particular angle to which it is most responsive. A number of studies have shown that thin lines and gratings can be perceived more readily when they are aligned in the vertical or horizontal orientation as compared with an oblique orientation (Taylor, 1963; Campbell et al, 1966). It would therefore seem worthwhile to investigate the appearance of the Mach bands for different azimuthal orientations of the retinal image.

The influence of the Mach effect on the images of lines, discs and apertures of different contrasts and at different retinal locations should be studied while the role of the Mach effect in phase contrast and interference microscopy, where the physical images are particularly complex, ought to be investigated.

Appendix A

Wave aberrations

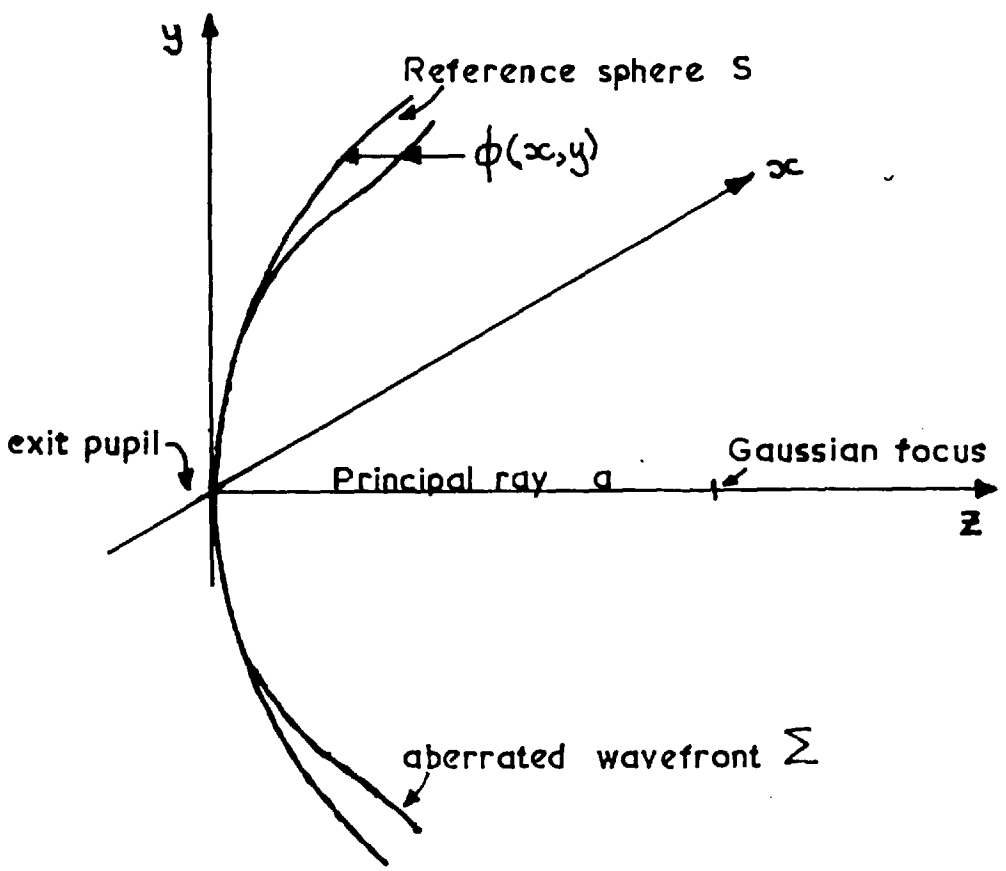
The discussion of wave aberrations follows that given by Welford (1962).

In fig. A.1 let 'a' be the principal ray of a pencil and let Σ be the wavefront of this pencil at the exit pupil. Take 'a' as the z axis of a rectangular co-ordinate system with the x and y axes being in the exit pupil plane (x and y are the relative co-ordinates defined in Chapter VI). Then the equation of Σ may be written as $z = f(x,y)$. We choose a reference sphere S with its centre at the Gaussian focus of the pencil; the exit pupil plane is tangential to S. Let the equation of S be $z_o = f_o(x,y)$ and let n be the refractive index of the medium. Then the wavefront aberration

$$W(x,y) = n(z-z_o) = n\left\{f(x,y) - f_o(x,y)\right\}.$$

If there were no aberration Σ would coincide with S and the light disturbances from all points of Σ would arrive at O in exactly the same phase. Thus $W(x,y)$ is a measure of the variation in phase of the disturbances of different points in Σ relative to S. In radians this phase difference is expressed as $\frac{2\pi}{\lambda} W(x,y) = \phi(x,y)$.

Fig. A.I.


y
Reference sphere S
$\phi(x,y)$
x
exit pupil
Principal ray a
Gaussian focus
z
aberrated wavefront Σ

Longitudinal displacement of focus. (fig. A.2)

Let a ray cut the exit pupil reference sphere in (X,Y) where X,Y are geometrical rectangular co-ordinates. This ray and the principal ray 'a' intersect at the Gaussian focus O_1. Let the reference sphere be of radius R and centered at O_2. The equation of the reference sphere is,

$$Z = \frac{X^2+Y^2}{2R} .$$

Now the equation of the wavefront with aberration $W(X,Y) = a_1(X^2+Y^2)$ must be,

$$Z_o = (\frac{1}{2R} + a_1)(X^2 + Y^2)$$

which represents a spherical surface centered on a point $-2a_1R^2$ nearer to the exit pupil than the centre of the reference sphere so that,

$$W(X,Y) = na_1(X^2+Y^2)$$

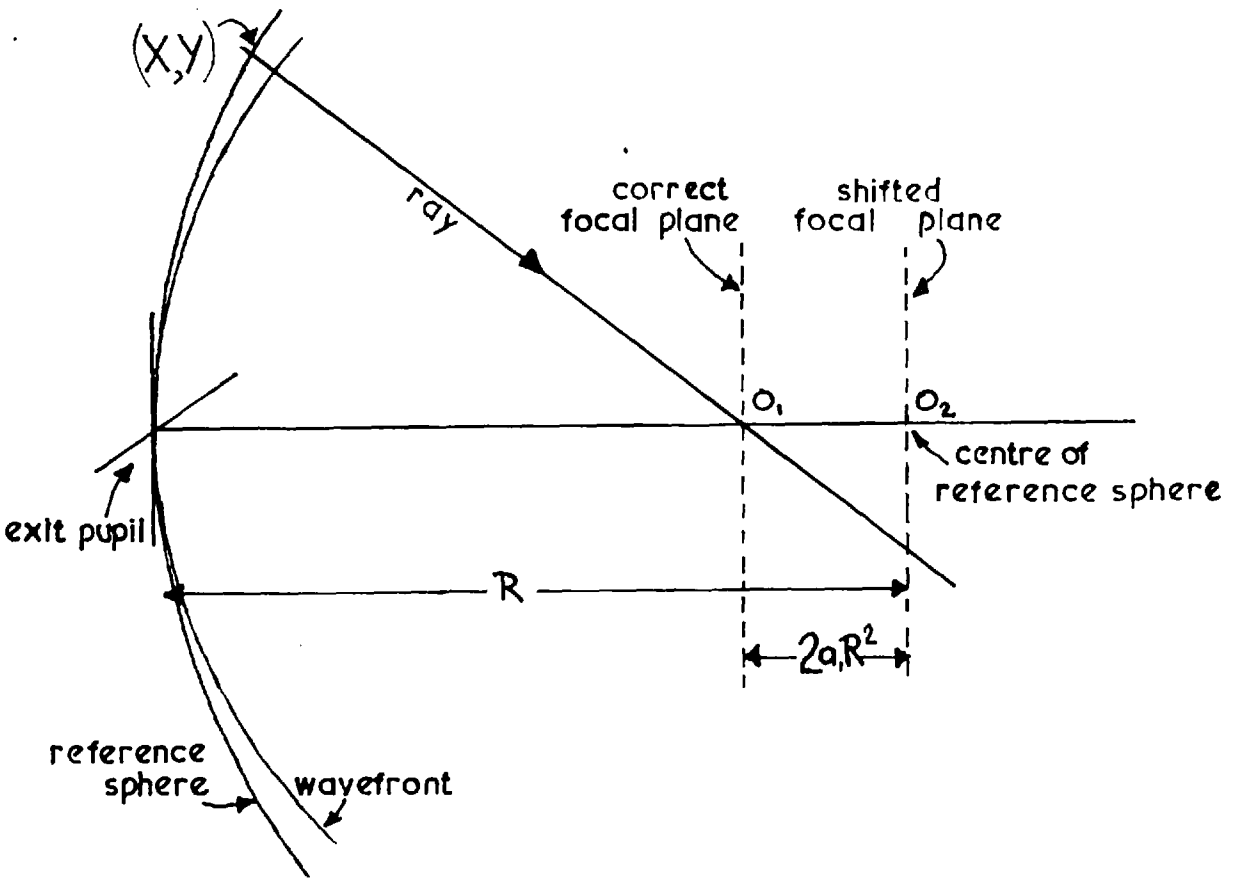
$$\therefore \quad \phi(X,Y) = \frac{2\pi}{\lambda} na_1(X^2+Y^2).$$

We have $O_2O_1 = 2a_1R^2 = \delta$.

Therefore $\phi(X,Y) = \frac{n\pi}{\lambda} \cdot \frac{(X^2+Y^2)}{R^2} \cdot \delta$

Let h be the height at which the marginal ray cuts the exit

Fig A.2.


(X,Y)
ray
correct
focal plane
shifted
focal plane
O_1
O_2
centre of
reference sphere
exit pupil
R
$2a_1R^2$
reference
sphere
wavefront

pupil sphere, then in terms of the relative co-ordinates $x = \frac{X}{h}$, $y = \frac{Y}{h}$ we have,

$$\phi(x,y) = \frac{n\pi}{\lambda} \left(\frac{h}{R}\right)^2 (x^2+y^2).\delta.$$

For systems of moderate aperture we may write $\frac{h}{R} = u$ where u is the angle which the marginal ray makes with the axis so that,

$$\phi(x,y) = \frac{n\pi}{\lambda} \cdot u^2(x^2+y^2)\delta$$

or $$\phi = p(x^2+y^2)$$

where $$p = \frac{\pi}{\lambda} \cdot u^2 \cdot \delta.$$

Transverse displacement of focus.

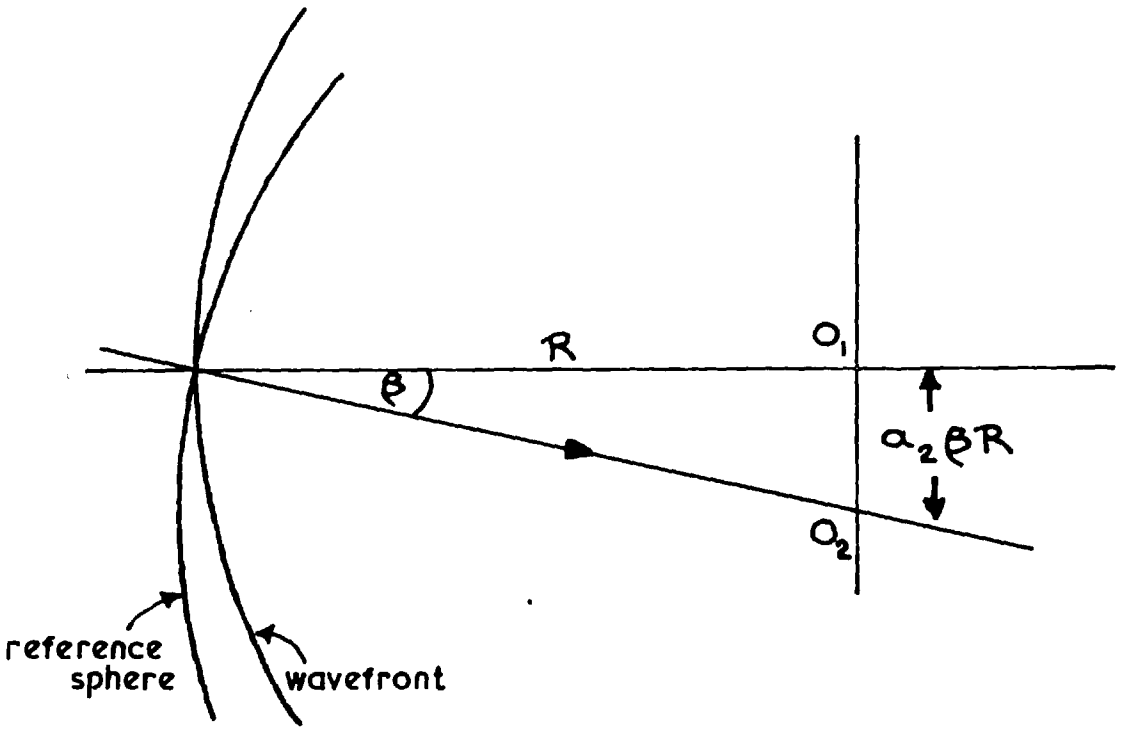
In this case we tilt the reference sphere so that its radius makes an angle β with the axis. Let the centre of the reference sphere O_2 be displaced a distance η from the centre of the wavefront with its focus at O_1 (fig. A.3). If β is small we may write $\eta = a_2\beta R$ where R is the radius of the wavefront.

The equation of the reference sphere is $z = \frac{1}{2R}(X^2+Y^2) + a_2\beta Y$ and the aberration associated with it equals $na_2\beta Y$.

Thus $$\phi(y) = \frac{2\pi}{\lambda} na_2\beta hy$$

$$= \frac{2\pi}{\lambda} na_2\beta R \cdot \frac{h}{R} y.$$

Fig. A.3.



But $a_2\beta R = \eta$ and $\frac{h}{R} = u$ so we may write

$$\phi(y) = zy$$

where $z = \frac{2\pi}{\lambda} \cdot nu \cdot \eta$ and (nu) is the numerical aperture of the system.

Appendix B

Calculation of the image of a luminous point (Point Spread Function)

The mathematical proofs contained here follow those given by Born and Wolf (1959) and also Francon and Marechal (1960).

Diffraction phenomena can be calculated in a simple manner on the basis of the Huygens-Fresnel principle. Consider a wavefront Σ (fig. B.1) which is, by definition, a surface over which the phase of all the light disturbances is constant. It is assumed that each point of Σ behaves as a secondary source which emits a diverging spherical wavelet. At some point P the amplitude of the light disturbance is found by summing all the contributions due to the wavelets emitted by every point on the wavefront . Consider an element of area dA of the wavefront and let the complex amplitude of the disturbance here be U_o. Then the complex amplitude dU of the light disturbance due to this secondary source at some point P distance R from dA is given by,

$$dU = U_o \frac{e^{-ikR}}{R} \cdot dA$$

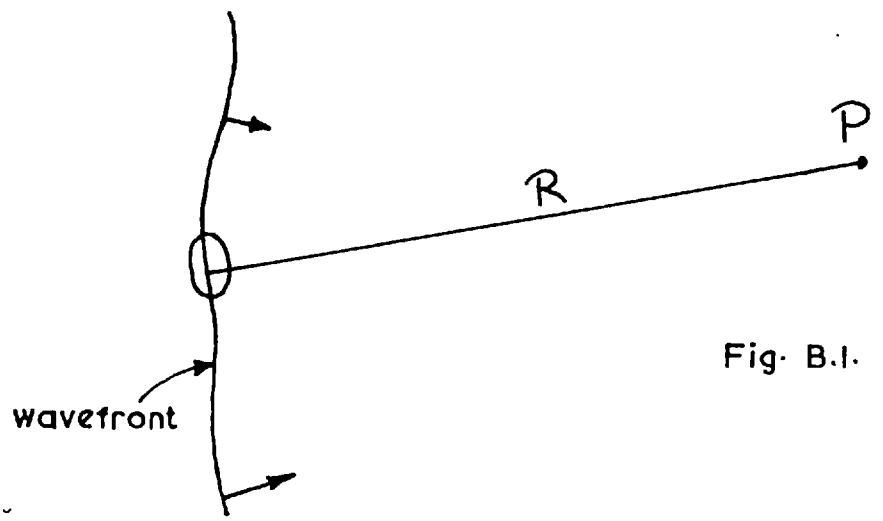


Fig. B.1.

where $k = \frac{2\pi}{\lambda}$ (λ being the wavelength of the light). Thus the net disturbance Up at P due to all elements of Σ is given by,

$$U_p = K \iint_{\Sigma} U_o \, e^{-ikR} \, dA \qquad (1)$$

We now consider a wavefront emitted by a point source which has passed through an optical system; the Gaussian (geometrical) image of this point is at O (fig. B.2) at the origin of the co-ordinates (ξ, η) in the image plane. We take rectangular co-ordinates (X,Y) in the exit pupil plane and let the wave aberration of the wavefront at the exit pupil be W(X,Y). W is measured relative to a circular reference sphere centered at O. The (X,Y) plane is tangential to the reference sphere at the axial point E. We shall firstly consider this distribution of amplitude over a focal sphere centered at E. The image plane (ξ, η) is tangential to the focal sphere at O. Consider a point $P(\xi, \eta, \zeta)$ on the focal sphere and an element of the wavefront dA at B(X,Y). If we produce PB to meet the reference sphere at P_o the wave aberration W is defined by the optical path length $[P_oB]$. We should multiply this value of W by sec θ to obtain the form of W adopted in appendix A for the wave aberration but for most optical

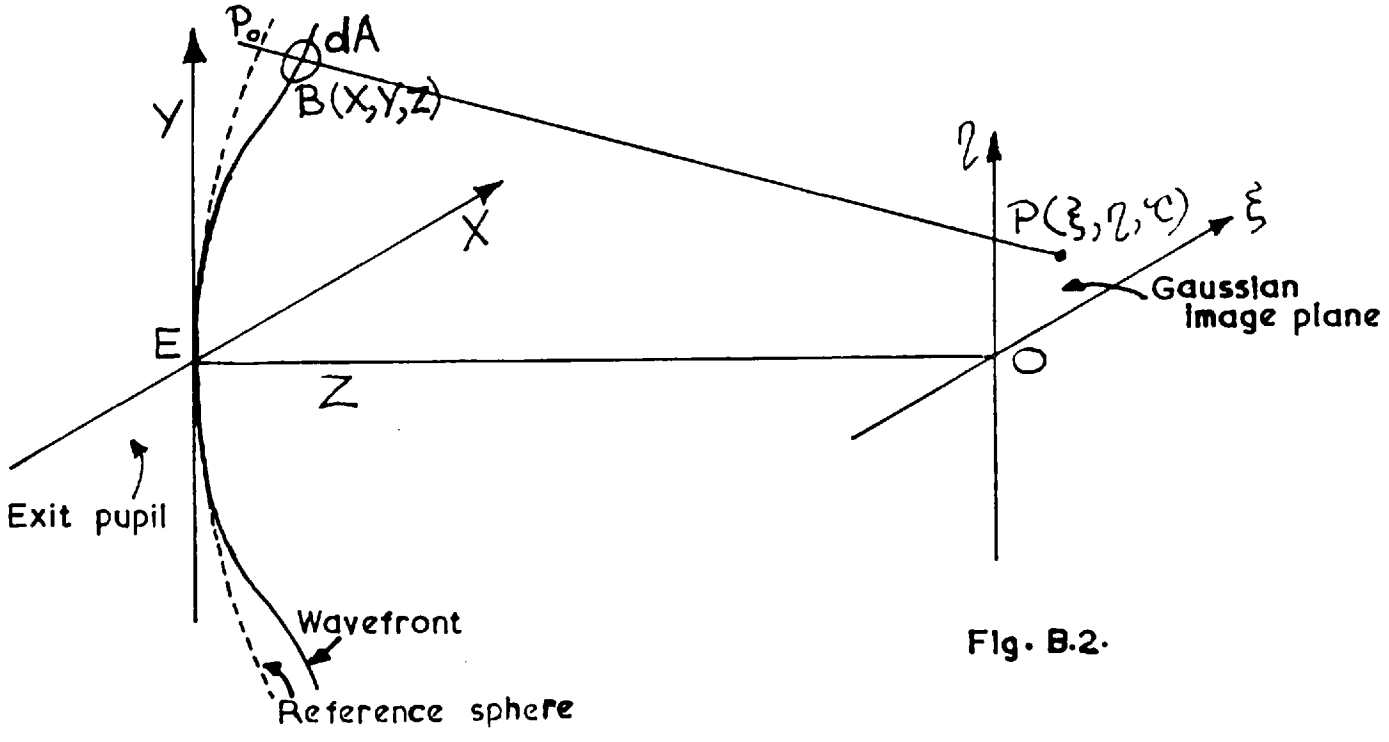

P_{oi}
dA
B(X,Y,Z)
Y
X
E
Z
Exit pupil
Wavefront
Reference sphere
η
P(ξ,η,ζ)
ξ
Gaussian
Image plane
O

Fig. B.2.

systems of moderate aperture we may assume sec θ to be unity over the aperture.

The phase of the disturbance at P_o = the phase at $E + kW(X,Y)$. Let the amplitude variation over the wavefront be described by the function $\alpha(X,Y)$. For a uniform converging spherical wave the complex amplitude at a distance R_o from its focus O is given by

$$U_o = \frac{e^{ikR_o}}{R_o}$$

and for a non-uniform aberrated wave we have

$$U_o = \alpha(X,Y)e^{i[kR_o+kW(X,Y)]}$$

We write $\alpha(X,Y)e^{ikW(X,Y)} = f(X,Y)$ which is known as the pupil function. Then from (1) the complex amplitude U_p of the disturbance due to all the wavelets emitted from the aberrated wavefront is given by (apart from a constant term)

$$U_p = \iint f(X,Y) \frac{e^{ik(R_o-R)}}{R_o R} \, dA$$

where R is the variable which expresses the distance R from each element dA from P. The integration is taken over the exit pupil.

Now for most practical purposes P is no more than 50 wavelengths from the point O and R_o is usually of the order

of 10 cm or more so that we may write $RR_o = R_o^2$. Also $dA = \frac{dxdy}{\cos\theta}$ and for systems of moderate aperture we can put $\cos\theta = 1$. Thus, apart from a constant factor we may say,

$$U_p = \iint f(X,Y)e^{ik(R_o-R)}\,dx\,dy \qquad (2)$$

where the integration is taken over the exit pupil.

From fig. B.3 we find the relations,

$$P_oP^2 = R^2 = (X-\xi)^2 + (Y-\eta)^2 + (Z-\zeta)^2 \qquad (3)$$

and

$$(P_oO)^2 = R_o^2 = X^2 + Y^2 + (Z-R_o)^2 \qquad (4)$$

(4) is merely the equation of a variable point (X,Y,Z) on a sphere of radius R_o whose centre is at the point $(0,0,R_o)$. Subtracting (4) from (3),

$$R_o^2 - R^2 = 2X\xi - \xi^2 + 2Y\eta - \eta^2 + 2Z\zeta - \zeta^2 - 2ZR_o + R_o^2$$

and knowing that $R_o^2 = \xi^2 + \eta^2 + \zeta^2$ we obtain,

$$R_o - R = \frac{2(X\xi + Y\eta) - 2Z(R_o-\zeta)}{R_o+R}$$

Also $$\frac{1}{R_o+R} = \frac{1}{2R_o-(R_o-R)} = \frac{1}{2R_o(1-\frac{R_o-R}{2R_o})}$$

Now $$R_o-R = \frac{X\xi + Y\eta}{R_o} - \frac{Z(R_o-\zeta)}{R_o}\,.$$

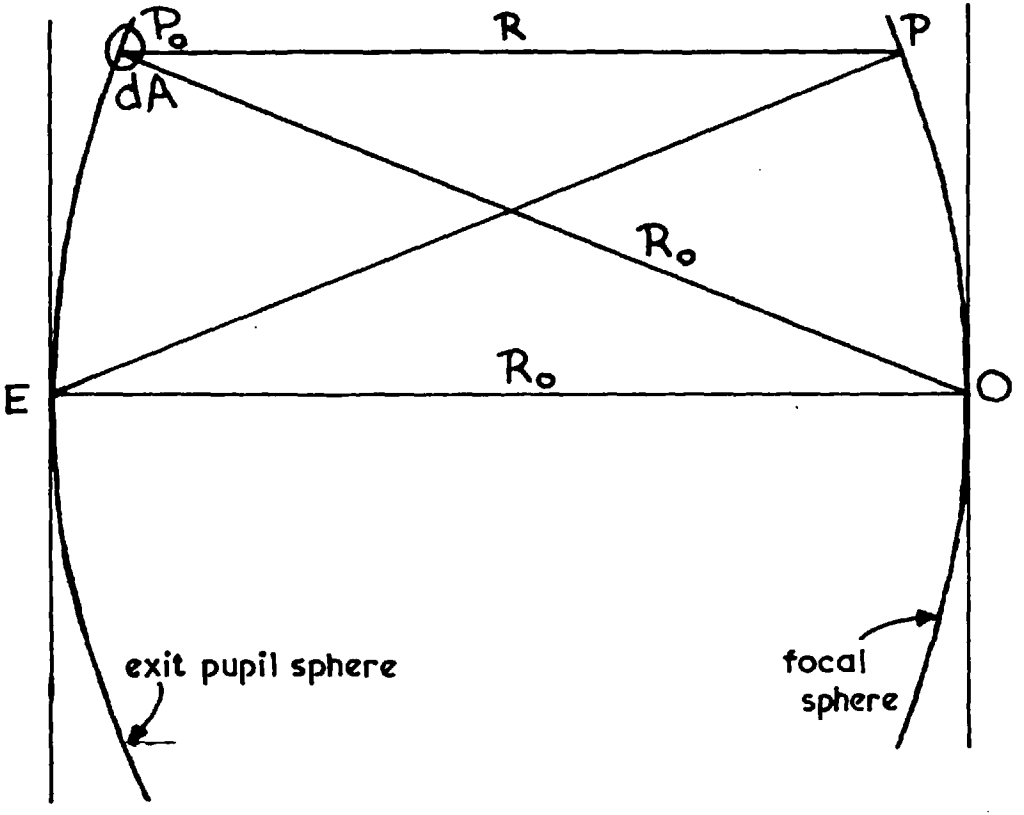


Fig. B.3.

The last term is for all practical purposes negligibly small compared to the first so that,

$$R_o - R = \frac{X\xi + Y\eta}{R_o}$$

We now employ relative co-ordinates for the exit pupil (Ch. V).

$$x = \frac{X}{h} \; ; \quad y = \frac{Y}{h}$$

and over the focal sphere we employ reduced co-ordinates,

$$z = \frac{n \sin \alpha}{\lambda} \cdot \xi \quad ; \quad v = \frac{n \sin \alpha}{\lambda} \cdot \eta$$

For systems of moderate aperture we may write $\sin \alpha = \frac{h}{R_o}$ and we arrive at the relation,

$$k(R_o - R) = 2\pi(zx + vy)$$

Writing U_p as $F(z,v)$ we find from (2) that,

$$F(z,v) = \iint f(x,y) e^{i2\pi(zx+vy)} \, dxdy$$

This integral may be taken over infinite limits if $f(x,y)$ is defined to be zero outside the pupil $x^2 + y^2 = 1$. Therefore,

$$F(z,v) = \int_{-\infty}^{\infty}\int_{-\infty}^{\infty} f(x,y) e^{i2\pi(zx+vy)} \, dxdy$$

which states that the point spread function $F(z,v)$ is the Fourier transform of the pupil function $f(x,y)$. From the inverse Fourier transform relationship (Titchmarsh, 1937) we may write,

$$f(x,y) = \int_{-\infty}^{\infty}\int F(z,v)e^{-i2\pi(zx+vy)}\,dxdv$$

The expression for $F(z,v)$ describes the distribution of amplitude over the focal sphere but for all practical purposes where the point (z,v) is no more than 50 wavelengths from 0, we may assume that the relationship is valid to a high degree of accuracy for the Gaussian image plane as well.

Appendix C

Some relations concerning Struve functions

We may define a Struve function of the ν^{th} order as,

$$H_\nu(z) = \frac{2(\frac{1}{2}z)^\nu}{\Gamma(\nu+\frac{1}{2})\Gamma(\frac{1}{2})} \int_0^{\frac{\pi}{2}} \sin(z\cos\theta)\sin^{2\nu}\theta\, d\theta$$

(Watson 1944)

where $$\Gamma(n+\tfrac{1}{2}) = \frac{1.3.5 \ldots\ldots (2n-1).\Gamma(\frac{1}{2})}{2^n}$$

and $$\Gamma(\tfrac{1}{2}) = \pi^{\frac{1}{2}}$$

Hence we obtain,

$$H_0(2z) = \frac{2}{\pi} \int_0^{\frac{\pi}{2}} \sin(2z\cos\theta)d\theta$$

$$H_1(2z) = \frac{4z}{\pi} \int_0^{\frac{\pi}{2}} \sin(2z\cos\theta)\sin^2\theta\, d\theta$$

$$H_2(2z) = \frac{8z^2}{3\pi} \int_0^{\frac{\pi}{2}} \sin(2z\cos\theta)\sin^4\theta\, d\theta$$

$$H_3(2z) = \frac{16z^3}{15\pi} \int_0^{\frac{\pi}{2}} \sin(2z\cos\theta)\sin^6\theta \, d\theta.$$

It can be shown that

$$H_{\nu-1}(z) + H_{\nu+1}(z) = \frac{2\nu}{z} H_\nu(z) + \frac{\frac{1}{2}(z)^\nu}{\Gamma(\nu+\frac{3}{2})\Gamma(\frac{1}{2})}$$

(Watson 1944)

from which we can obtain the relation,

$$H_2(2z) = \frac{H_1(2z)}{z} + \frac{4z}{3\pi} - H_0(2z)$$

$H_1'(2z)$ and $H_0'(2z)$

It can be proved that (Watson 1944)

$$H_{\nu-1}(z) - H_{\nu+1}(z) = 2H'_\nu(z) - \frac{(\frac{1}{2}z)^\nu}{\Gamma(\nu+\frac{3}{2})\Gamma(\frac{1}{2})} \qquad (1)$$

where the dashed symbol infers the first derivative with respect to z

also,

$$H_{\nu-1}(z) + H_{\nu+1}(z) = \frac{2\nu}{z} H_\nu(z) + \frac{(\frac{1}{2}z)^\nu}{\Gamma(\nu+\frac{3}{2})\Gamma(\frac{1}{2})} \qquad (2)$$

Adding the equations (1) and (2) we obtain,

$$H'_{\nu}(z) = H_{\nu-1}(z) - \frac{\nu}{z} H_{\nu}(z)$$

If we put $\nu = 1$ and replace z by 2z we obtain,

$$\underline{H_1'(2z) = 2H_o(2z) - \frac{H_1(2z)}{z}}$$

Subtracting (2) from (1) we obtain,

$$H_{\nu}'(z) = \frac{\nu}{z} H_{\nu}(z) - H_{\nu+1}(z) + \frac{(\frac{1}{2} z)^{\nu}}{\Gamma(\nu + \frac{3}{2})\Gamma(\frac{1}{2})}$$

If we put $\nu = 0$ and replace z by 2z we obtain,

$$\underline{H_o'(2z) = - 2H_1(2z) + \frac{4}{\pi}}$$

References

ABRAMOWITZ, M. and STEGUN, I.A. (1964) "Handbook of Mathematical Functions" National Bureau of Standards.

AIRY, G.B. (1835) Camb. Phil. Trans. 6, 379.

ARAGO (1858). Oeuvres completes 10, 255.

BEITEL, R.J. (1936). J. Gen. Psychol. 14, 31.

BEKESY, G. von. (1960). J. Opt. Soc. Am. 50, 1060.

BITTINI, M. et al (1960). Atti. Fond. Ronchi. 15, 62.

BORN, M. and WOLF, E. (1959). Principles of Optics. Pergamon.

BRACEWELL, R. (1965). The Fourier Transform and its Applications. McGraw Hill.

BRYNGDAHL, O. (1964). Kybernetik 2, 71.

BRYNGDAHL, O. (1966). Optica Acta 13, 55.

CAMPBELL, F.W. and GUBISCH, R. (1967). J. Physiol., to be published.

CAMPBELL, F.W. et al (1966). J. Physiol. 187, 427.

CHARMAN, W.N. (1961). Ph.D. thesis. The Visual Sizing of non-periodic Objects by Microscopy. University of London.

CHARMAN, W.N. and WATRASIEWICZ, B.M. (1964). J. Opt. Soc. Am. 54, 791.

CHEATHAM, (1952). J. of Exp. Psychol. 43, 369.

CHEVREUL, M.E. (1890). The Principles of Harmony and Contrast of Colours. George Bell and Sons, trans. by C. Martel.

DAVIES, O. (1947). Statistical Methods in Research and Production, I.C.I. publication.

DITCHBURN, R.W. (1956). Research, 9, 466.

DITCHBURN, R.W. and GINSBORG, B.L. (1962). Nature, 170, 36.

DUFFIEUX, P.M. and LANSRAUX, G. (1945). Rev. opt. 24, 76.

DUFFIEUX, P.M. (1946). L'integrale de Fourier et ses applications a l'optique. Rennes, Societe anonyme Oberthur.

ERCOLES, A.M. and FIORENTINI, A. (1959). Atti. Fond. Giorgio Ronchi, XIV, 235.

FIORENTINI, A.((1956). Prob. Contemp. Optics.

FIORENTINI, A. and ERCOLES, A.M. (1957). Optica Acta 4, 150.

FIORENTINI, A. and RADICI, T. (1957). Atti. Fond. Giorgio Ronchi XII, 453.

FIORENTINI, A. and RADICI, T. (1958). Atti. Fond. Georgio Ronchi, XIII, 145.

FRANCON, M. and MARECHAL, A. (1960). "Diffraction Structure des Images", Paris. Editions de la Revue d'Optique Theorique et Instrumental.

FRY, G.A. (1948). Am. J. Optom. and Arch. Am. Acad. Optom, 25, 162.

GRAHAM (1965) et al, "Vision and Visual Perception". John Wiley and Sons.

GRANIT, R. (1933), J. Physiol 77, 207.

GRANIT, R. (1946), J. Physiol, 105, 45.

GREEN, P.H. (1958), Factors in Visual Acuity. Aeromedical Div. U.S. Air Force Office of Sc. Research, AF 18 (600) Project 9777 Univ. of Chicago.

HARTLINE, H.K. and GRAHAM, L. (1932), J. Cellular and Comp. Physiol 1, 277.

HARTLINE, H.K. and RATLIFF, F. (1954). Science 120, 781.

HARTWIG, E. (1958). Optik, 15, 414.

HOPKINS, H.H. (1955). Proc. Roy. Soc. 231, 91.

HOPKINS, H.H. (1962). Proc. Phys. Soc. 79, 889.

HUBEL, D.H. and WIESEL, T.N. (1959). J. Physiol 148, 574.

HUBEL, D.H. and WIESEL, T.N. (1962). J. Physiol, 160, 106.

HURVICH, L.M. and JAMESON, D. (1964). Outlines of a Theory of the Light Sense by E. Hering. Trans. Harvard Univ. Press, Camb. Mass.

LEELAWONGS, R. (1964). M.Sc. Thesis "The Mach Effect in Microscopy and in Vision of Macroscopic Objects." University of London.

LEGRAND, Y. (1957). Light, Colour and Vision, New York, John Wiley and Sons Inc.

LOWRY, E.M. and De PALMA, J.J. (1961). J. Opt. Soc. Am. 51, 740.

LUDVIGH, E. (1953). Perception of Contour (Parts I and II). Project report of U.S. Naval School of Aviation Medicine, Naval Air Station, Pensacolo, Florida.

MACH, E. (1965). Sitz. der math. nat. Classe der Kaiser Akad. der Wiss. Wien. 52/2, 303.

MACH, E. (1866a). Sitz. der math. nat. Classe der Kaiser Akad. der Wiss. Wien. 54/2, 131.

MACH, E. (1866b). Sitz. der math. nat. Classe der Kaiser Akad. der Wiss. Wien. 54/2, 393.

MACH, E. (1868a). Sitz. der math. nat. Classe der Kaiser Akad. der Wiss. Wien. 57/2, 11.

MACH, E. (1906). Sitz. der math. nat. Classe der Kaiser Akad. der Wiss. Wien. 115, 633.

MACH, E. (1868). Vierteljahresschrift für Psych. in ihren Beziehungen zur Morph. u. Path des Central-Nervensyst. 2, 38.

MARECHAL, A. (1956). Encyclopedia of Physics, ed. S. Flugge. Vol. XXIV. Berlin Springer-Verlag, 163.

MARIMONT, R.B. (1963). J. Opt. Soc. Am. 53, 400.

MAZOW, B.O. (1960). Vision of the Ageing Patient, ed. Hirsch and Wick. Chilton, New York.

MENZEL, E. (1959). Naturwiss. 46, 316.

MENZEL, E. (1965).et al. Optik 23, 169.

McCOLLOUGH, C. (1955). J. Exp. Psychol 49, 141.

OSTERBERG (1935). Acta Opthalm. 13, 103.

PEDLER, C. (1965). Colour Vision, CIBA Foundation 52.

POLYAK, S.L. (1941). The Retina. Chicago University Press.

RATLIFF, F. et al (1958). Ann. New York Acad. Sc. 74, 210.

RATLIFF, F. (1965). Mach Bands. Holden Day.

RAYLEIGH, LORD (1879). Camb. Phil. Soc. 3, 373.

ROCHON-DUVIGNEAUD, A. (1943). Les yeux et la vision des vertebres. Paris, Masson.

RONCHI, L. et al (1963). Optik 20, 132.

RUDDOCK, K.H. (1964). Ph.D. Thesis. The Effect of Age upon Colour Matching and Colour Discrimination. University of London.

SAID, F.S. and WEALE, R.A. (1959). Gerontologia p. 213.

SIMON (1904). Zts. Psych. Phys. Sinnes. 36, 186.

SLATER, P.N. (1960). Optics in Metrology. Pergamon Press, New York 269.

SPENCER, C.J.D. and WELFORD, W.T. (1961). J. of Sc. Inst. 38, 328.

STEEL, W.H. (1952). Rev. Opt. 31, 334.

STENSTRÖM, S. (1946). Ocular Anatomy ed. J.D. Spooner. London, Hatton Press, 1957.

STREHL, K. (1902). Z. Instrumkde. 22, 213.

STRUVE, H. (1882). Wied. Ann. 17, 1008.

TAYLOR, M.M. (1963). J. Opt. Soc. Am. 53, 763.

TAYLOR, W.K. (1956). Information Theory, ed. by C. Cherry. New York, Academic Press.

TITCHMARSH, E.C. (1937). Theory of Fourier integrals. Oxford Univ. Press.

WADSWORTH, F.L.O. (1894). Astrophys. J. 2, 264.

WATRASIEWICZ, B.M. (1963). Optica Acta 10, 209.

WATRASIEWICZ, B.M. (1964). Ph.D. thesis. The Visual Mach Effect in microscopy. Univ. of London.

WATRASIEWICZ, B.M. (1965a). Optica Acta 12, 167.

WATRASIEWICZ, B.M. (1965b). Optica Acta 12, 391.

WATSON, G.N. (1944). A Treatise of the Theory of Bessel Functions. Camb. Univ. Press.

WILLMER, E.N. (1961). J. Theoret. Biol. 2, 141.

WEINSTEIN, W. (1954). (now W.T. WELFORD). J. Opt. Soc. Am. 44, 610.

WELFORD, W.T. (1960). J. Opt. Soc. Am. 50, 21.

WELFORD, W.T. (1962). Geometrical Optics. North Holland Publishing Co.

WERTHEIM (1894). Ocular Anatomy, ed. J.D. Spooner. London, Hatton Press, 1957.

WRIGHT, W.D. (1946). The Measurement of Colour. Hilger and Watts.

Acknowledgements

My sincere thanks are due to Dr. W. T. Welford for his kind encouragement and astute criticism throughout the course of my research and during the preparation of this thesis.

I should also like to thank the observers who performed the measurements so willingly.

Finally I am indebted to the Medical Research Council for a maintenance grant.

Reprinted from The Microscope & Crystal Front, *Vol. 15, No. 6, pp. 216-229, September-October, 1966, Microscope Publications Ltd., P.O. Box 84, 57/58 North Street, Brighton, Sussex.*

The role of the Mach Effect in critical microscopical investigations*

S. H. ROWE

Physics Department,
Imperial College of Science and Technology,
London, S.W.7

THE observation of a particulate system under a microscope provides the most fundamental method of size classification and particle shape analysis. In recent years the visual effects which occur at the borders of the images of such particles have received considerable attention[1], especially with regard to the length measurement of objects which have dimensions approaching the resolution limit of the microscope. As a result of diffraction effects, and to a lesser degree the effects of aberrations and scattering, the edges of the primary image of a particle or aperture display an intensity variation which depends on the form of the object and the optical parameters of the microscope. When viewed through an eyepiece, the subjective impression of the boundary of the image is markedly different from the physical intensity distribution as measured by a photo-electric microscope. In general the subjective luminance gradient at the boundary of an opaque object or clear aperture is steeper than the physical distribution of intensity and a physically smooth distribution (similar to that obtained when using incoherent illumination for example) will display subjective diffraction-like Mach bands[2].

The images of discs and apertures always appear to be ringed by these subjective bands which are often erroneously attributed solely to diffraction effects. In general at least three bands are seen and they subtend a total angle of about half a degree at the observer's eye. The Mach bands become clearly visible when critical measurements are made at the borders of the images (see Fig. 1) of bright or dark regions. The human mechanisms which produce the Mach bands are still under considerable discussion although it is now thought that the Mach effect is produced by the interactions between the electrical messages received and transmitted by the mosaic of receptors in the human retina.

Watrasiewicz[3] has found that the position, width and intensity of the Mach bands depend on eyepiece power, luminance

* Presented at Micro-65

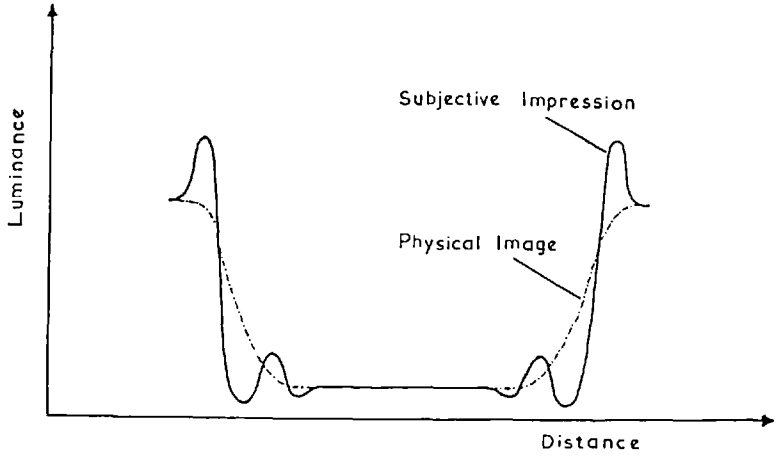


Fig. 1. Mach bands obtained when viewing an opaque particle.

of the image, the wavelength of the light employed and the contrast of the object relative to its background; while from work done by Leelawongs[1] on a macroscopic scale it seems highly likely that the diameter of the exit pupil of the microscope affects the position and widths of the Mach bands too. The following account describes a survey performed with twenty observers to investigate the personal variation of number, position and width and intensity of the Mach bands observed under constant physical conditions.

Experimental procedure

The object used for the experiment was a thin, high contrast straight edge between transparent and opaque fields. It was imaged in light of wavelength $\lambda = 0{\cdot}53 \pm 0{\cdot}05\ \mu$ by a well corrected objective of N.A. 0·12 which produced a magnification of 13×. On viewing the primary image with a ×20 eyepiece an observer saw a series of Mach bands parallel to the edge; the total width subtended by the bands at the eye was about 35 minutes of arc and individual bands subtended, on average, five minutes of arc.

Positions and widths of the bands were measured with the aid of a micrometer block system previously employed by Charman[2]. The edge image was moved past the tip of a wire (0·5 μ diameter) held in the primary focal plane of the eyepiece. Settings were made successively across the edge image at the borders of the various bright and dark bands by scanning the eye down the length of bands whilst the observer slowly moved the image until the border of a band appeared to be in line with

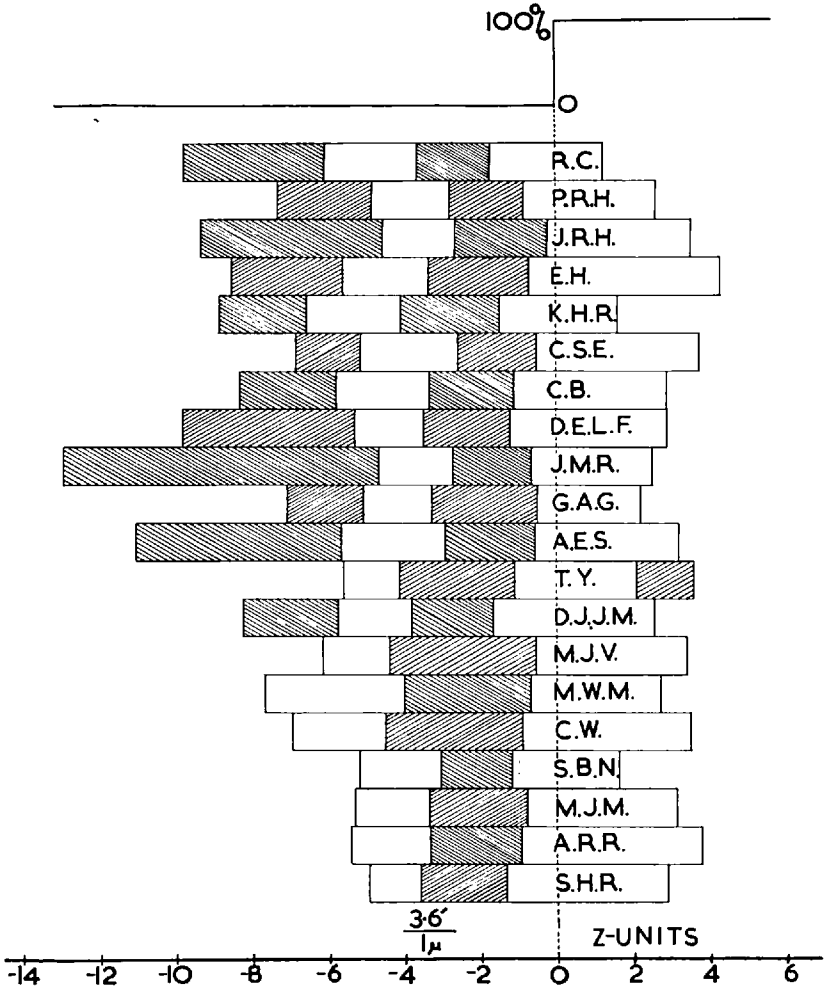


Fig. 2. Mach bands seen at an opaque edge S = 2·2. Distances are measured relative to the geometrical edge.

the tip of the wire. The readings were all measured relative to a 1·2 μ circular hole situated 16 μ from the edge. Ten successive scans across the image were made to determine mean positions of the bands. Each observer performed the experiment with two different values of S ($S = \frac{\text{condenser N.A.}}{\text{objective N.A.}}$); firstly with

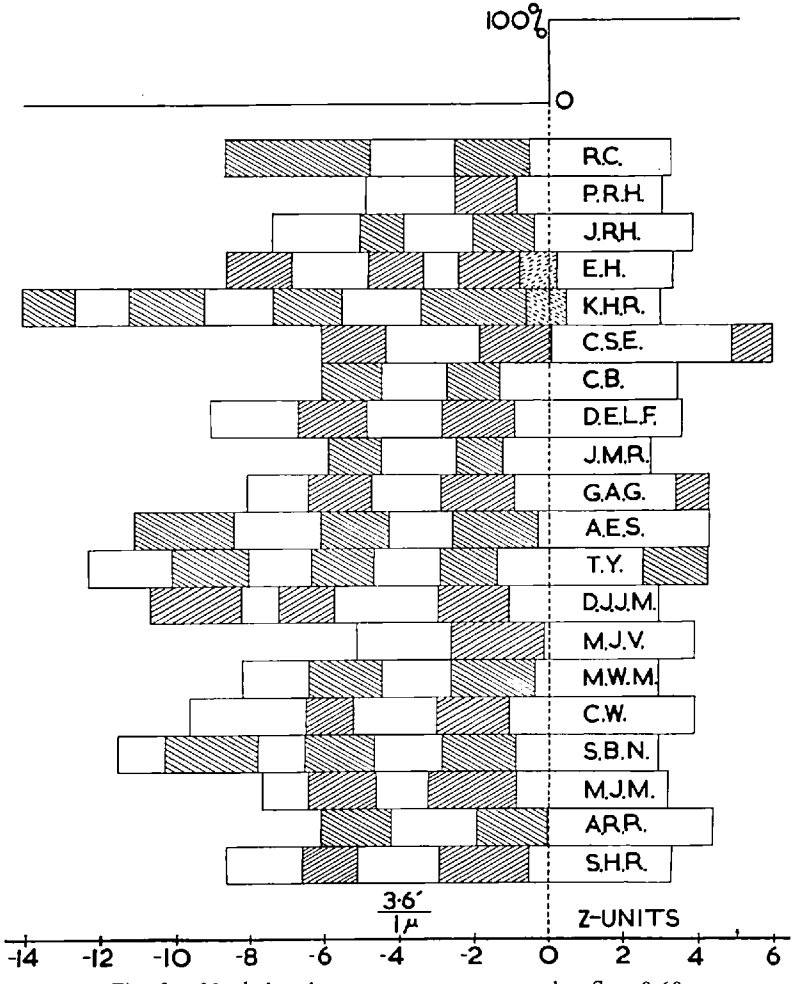


Fig. 3. Mach bands seen at an opaque edge S = 0·60.

S = 2·2 corresponding to nearly incoherent illumination and secondly with S = ·60 corresponding to nearly coherent illumination. The results for twenty observers are shown in Figs. 2 and 3*.

* Distances are expressed in Z units. $Z=\frac{2\pi}{\lambda} \times (\text{N.A.}) \times \mu$ where λ equals the wavelength of the light employed, μ equals the distance in the object space and (N.A.) is the numerical aperture of the objective.

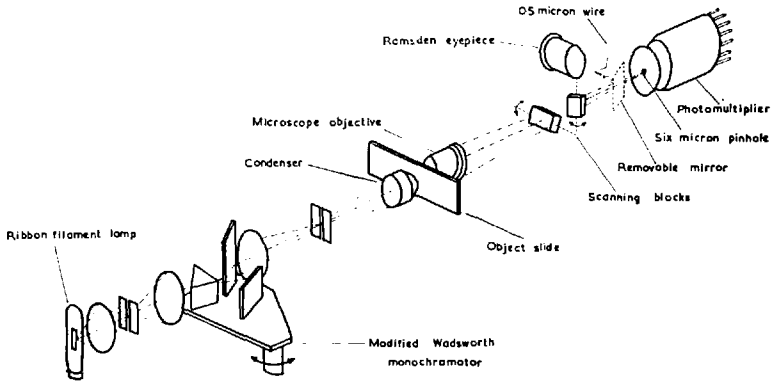


Fig. 4. Schematic representation of the apparatus used to measure the physical and subjective images.

The true position of the geometrical edge relative to the aperture was determined by scanning across the edge with a photo-electric microscope and noting the point where the intensity had dropped to 50% of the clear field intensity. This was measured to an accuracy of $\pm 0{\cdot}10\ \mu$.

A diagram of the apparatus, which is similar to that used by Charman and Watrasiewicz[6] is shown in Fig. 4.

The relative luminance variation of the subjective image was

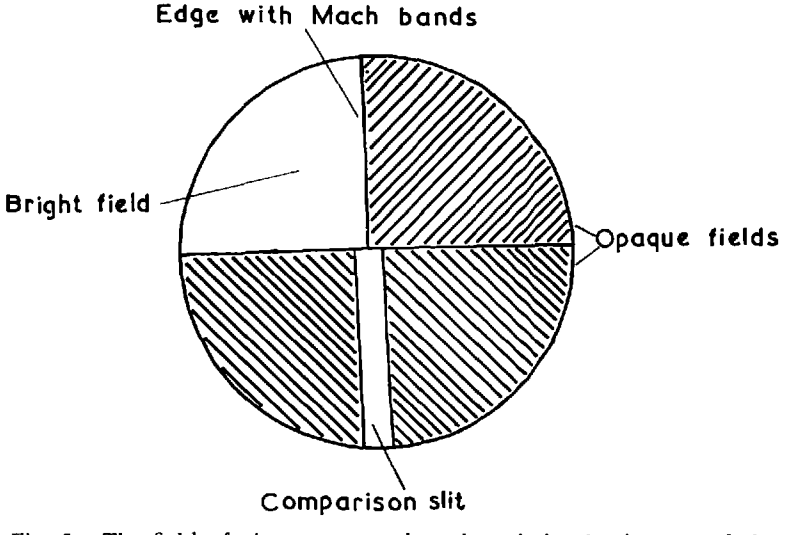


Fig. 5. The field of view as seen when the relative luminances of the Mach bands were measured.

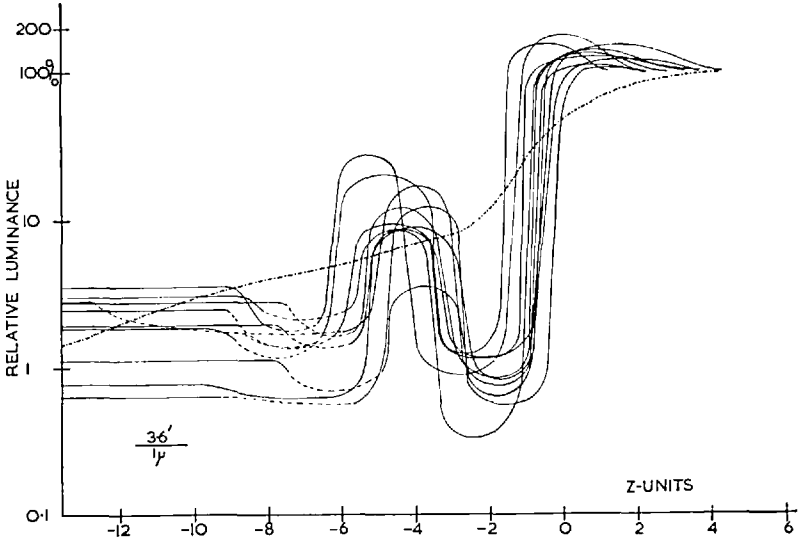


Fig. 6. Luminances profiles as seen by the observers R.C., P.R.H., J.R.H., E.H., K.H.R., C.S.E., C.B., D.E.L.F., J.M.R., and G.A.G. S = 2·2.

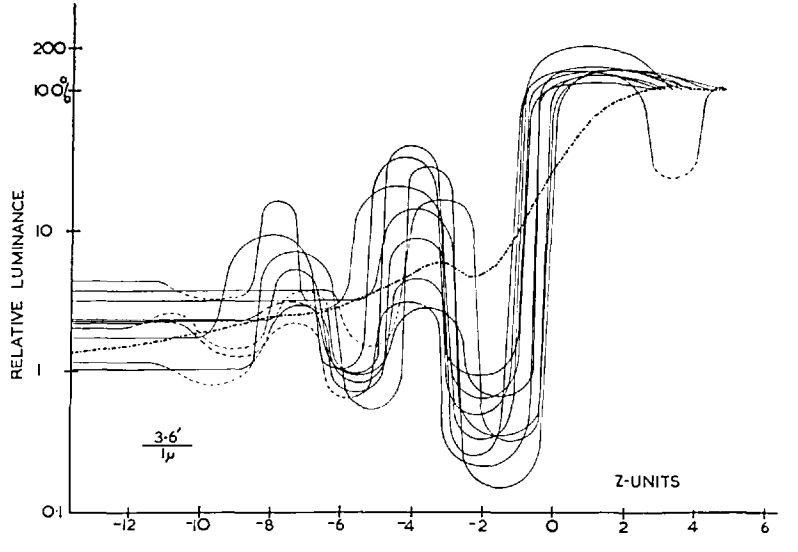


Fig. 7. Luminance profiles as seen by the observers A.E.S., T.Y., D.J.J.M., M.J.V., M.W.M., C.W., S.B.N., M.J.M., A.R.R. and S.H.R., S=~~2·2~~ 0·60

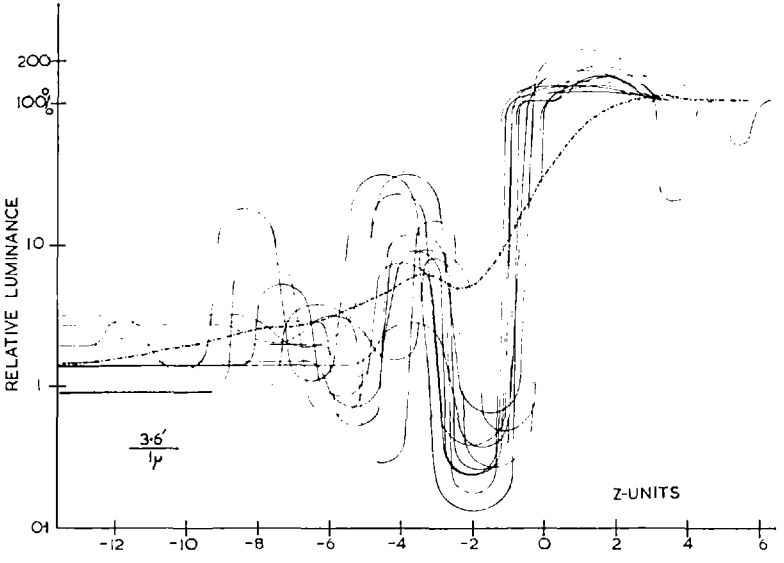


Fig. 8. Luminance profiles as seen by the observers represented in Fig. 6. S = 0·60.

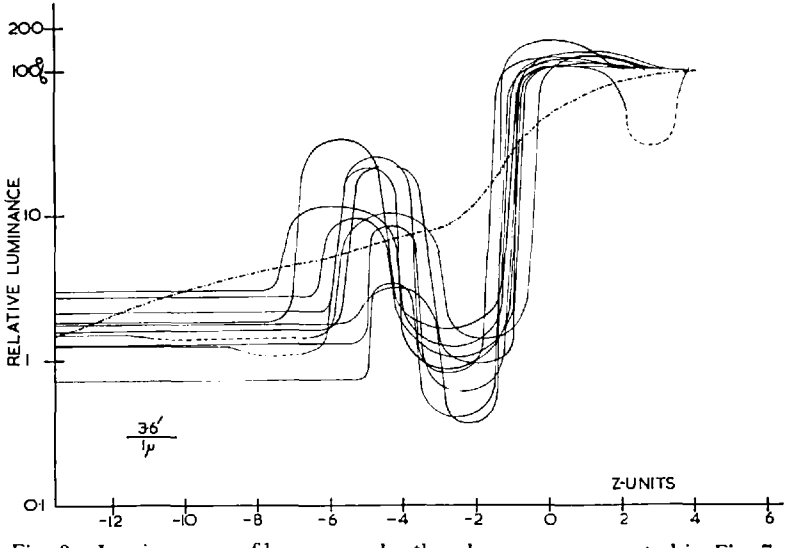


Fig. 9. Luminance profiles as seen by the observers represented in Fig. 7. S = 0·60.

measured using a visual microphotometer previously used by Watrasiewicz[3]. The image of a bright slit, illuminated with light of wavelength $=\cdot 53\ \mu$ in a dark surround and the image of the edge appeared in the upper and lower halves of the field of view respectively, the length the slit was made parallel to the edge (see Fig. 5). The width of the slit was made as narrow as possible but not so narrow that the Mach bands at the edges of the slit could interfere with the main area of the slit which was used for matching purposes. At the eye the slit subtended about 2°. A circular neutral density wedge giving an overall attenuation of 1000:1 was used to vary the luminance of the slit. Since the angular subtenses of the Mach bands were so small it was only possible to make a brightness match with the central portion of each band. After an observer had viewed the field for five minutes it was found that consistent matches could be made, although for the bright bands an accuracy better than $\pm 10\%$ of the luminance could not be obtained for most observers. The brightness of the dark bands could only be measured to an accuracy of $\pm 30\%$. During the survey the diameter of the exit pupil of the eyepiece (0·23 mm.) was very much smaller than that of the natural pupil of the eye (about 3 mm.) and since the observations were made on axis with monochromatic light, the distribution of retinal illumination might be expected to correspond (apart from the effect of scatter in the ocular media) with the distribution of luminance in the primary microscope image. Throughout the experiments the retinal illumination was kept constant at 1500 trolands* ($\pm 20\%$). Results are plotted on a logarithmic scale in Figs. 6, 7, 8 and 9 and they are normalised so that the clear field luminance was 100%. The measured physical distribution of intensity due to Charman[5] is also shown. In some cases an observer could measure the position of a particular faint band but, when the photometer prism was added to the eyepiece (to facilitate the appearance of the comparison slit image in the field of view of the eyepiece) the band could no longer be discerned, owing to the presence of scattered light. Such bands are indicated by dotted lines in the luminance profiles showed in Figs. 6, 7, 8 and 9.

The general appearance of the edge reported by observers was as follows:

1. The continuously bright field (clear field)
2. A bright band of greater luminance than the clear field (referred to below as 'the first bright band')
3. A dark band (referred to below as 'the edge band')

---

* 1 troland corresponds to a luminance of 1 candela/m^2 seen through a pupil of 1 mm^2 area.

4. A bright band (referred to below as ' the edge band ')
5. A series of less distinct bright and dark bands
6. The continuously dark field.

While the general appearance of the Mach patterns is substantially the same, Figs. 2 and 3 show that there are some striking differences between observers with regard to the number of bands seen. For $S = 2{\cdot}2$ observers S.H.R., A.R.R., M.J.M., S.B.N., C.W., M.W.M. and M.J.V. saw three bands while the other thirteen observers clearly saw four bands. One of the latter group of observers T.Y., saw a dark band on the bright side of the edge while for $S = {\cdot}60$ observers C.S.E. and G.A.G. saw this band also.

In the case of $S = 0{\cdot}60$ K.H.R. and E.H. saw hitherto unreported inflection points in the image; between the first bright band and the edge band a region of luminance equal in magnitude to the clear field was seen. The variation in the number of bands observed for $S=0{\cdot}60$ was greater than when $S=2{\cdot}2$. For example K.H.R. and T.Y. saw nine and eight bands respectively while P.R.H. and M.J.V. could only see three bands.

Figs. 6, 7, 8 and 9 show that variations between observers were very pronounced. It is difficult to pick out any general trends from Figs. 6, 7, 8 and 9 and attempts to correlate positions or widths of bands have not been successful. However Fig. 10 shows a scatter diagram in which the relative luminance for the first bright band for $S = 0{\cdot}60$ is plotted against its relative luminance for $S = 2{\cdot}2$. Fig. 11 shows a similar diagram for the second bright band. It is apparent from these diagrams that certain observers see a given Mach band more brightly than others. However, an observer who sees a particular band (e.g. the first bright band) more brightly than average does not necessarily see another band more brightly than average.

On each scatter diagram two regression lines[7] (1) and (2) are drawn. Let us denote readings taken for $S={\cdot}6$ by y, and those for $S=2{\cdot}2$ by x. The equation of (1) is $Y=\bar{y}+b(x-\bar{x})$ where

$$b=\frac{\Sigma(x-\bar{x})\times(y-\bar{y})}{\Sigma(x-\bar{x})^2};$$

this gives us the best estimate of y when x is known by minimising the sum of the squares of the vertical deviations from the line (1). The best estimate of x when y is known is obtained from the equation of (2)

$$X=\bar{x}+b'\ (y-\bar{y}) \text{ where } b'=\frac{\Sigma(x-\bar{x})\times(y-\bar{y})}{\Sigma(y-\bar{y})^2};$$

this minimises the sum of the squares of the horizontal deviations from

the line (2). If the variables x and y were perfectly linearly correlated (1) and (2) would be the same. A measure of the degree of correlation is the correlation coefficient[7], r, given by,

$$r = \frac{\Sigma(x-\bar{x})\times(y-\bar{y})}{\sqrt{\Sigma(x-\bar{x})^2\Sigma(y-\bar{y})^2}}$$

which would be unity for a perfectly linearly correlated sample.

The correlation coefficients for the first and second bright bands and also for the dark edge band were calculated. To assess the significance of the correlation coefficient recourse is made to statistical tables[7] which give the probability, P, that a given correlation coefficient could be obtained from the same number of samples drawn at random from an uncorrelated population. For the first bright band $r = 0{\cdot}79$ and $P = 0{\cdot}001$. For the second bright band $r = 0{\cdot}62$ and $P = 0{\cdot}001$. For the edge band $r = 0{\cdot}28$. This showed clearly that a definite correlation existed in the case of the first and second bright bands but no such correlation could be inferred for the edge band.

From the Figs. 2 and 3 in which the band positions are plotted we can see that there are differences in the positions of the boundaries between bands as measured by different observers. Now each plotted position was the mean of ten readings and clearly we require some statistical evidence to determine if the differences between observers could have been solely due to random measuring errors or if fundamental personal differences existed between observers. The method which can deal adequately with these problems is the Analysis of Variance[7].

Analysis of Variance

Consider the measurements made on one boundary. Let r = number of observers, m = number of observations made by each observer, then n = rm = total number of observations. Let x_{it} denote the t^{th} observation made by the i^{th} observer. Then let $x_i = \frac{1}{m}\sum_{t=1}^{m} x_{it}$ = the mean value for the i^{th} observer,

$$\text{let } \bar{x} = \frac{1}{r}\sum_{i=1}^{r} x_i = \frac{1}{n}\sum_{it} x_{it} = \text{grand mean}$$

The sum of the squared deviations of all n = rm observations from the grand mean $\bar{x}$, can be written as m times the sum of squared deviations of the r observer means from the grand mean plus the sum of squared deviations of individual observations from their respective observer means.

$$\sum_{i=1}^{r}\sum_{t=1} (x_{it}-\bar{x})^2 = m\sum_{i=1}^{r} (x_i-\bar{x})^2 + \sum_{i=1}^{r}\sum_{t=1}^{m} (x_{it}-x_i)^2$$

We make the null hypothesis that the means of the populations of observations x_{it} for the r observers are all equal (i.e. there are no personal differences between observers apart from random sampling errors). If the null hypothesis is true we have three unbiased estimates of the common variances of the r populations obtained by dividing the sums of squares in the equation above b ytheir respective degrees of freedom. The estimates are:—

$$S_1^2 = \frac{1}{n-1} \sum_i \sum_t (x_{it} - \bar{x})^2$$

$$S_2^2 = \frac{m}{r-1} \sum_i (x_i - \bar{x})^2$$

$$S_3^2 = \frac{1}{n-r} \sum_i \sum_t (x_{it} - x_i)^2$$

If the null hypothesis of equal means is true the last two quantities should be equal (except for sampling error). We divide S_2^2 by S_3^2 to form the F ratio:—

$$F = \frac{S_2^2}{S_3^2}$$

We reject the null hypothesis at the significance level of probability, P, if F exceeds the critical value of F given in statistical tables[7] of the F distribution. With the value of F must be associated the number of degrees of freedom involved which for S_2^2 is $(r-1)$ and for S_3^2 is $(n-r)$. (A probability $P=10\%$ means that the observed value of F would occur about once every ten trials if the null hypothesis were true. A low probability indictes that the null hypothesis is false).

An Analysis of Variance was firstly carried out on the results for twenty observers with regard to the position of the visual edge, which is the point at which an observer sees the most rapid change in luminance from the dark edge band to the first bright band. The F ratios obtained for $S = 0{\cdot}6$ and $S = 2{\cdot}2$ were 3·92 and 8·11 respectively. Both these ratios lie below the 1% probability level of significance so that the null hypothesis could be confidently rejected. Having thus established that personal differences were present it was decided to divide the twenty observers into groups of observers whose means did not differ significantly. Three such groups of five were isolated:—

C.S.E., A.E.S., M.J.V., M.W.M., A.R.R.,
C.B., D.E.L.F., T.Y., C.W., S.B.N.,
P.R.H., E.H., J.M.R., G.A.G., M.J.M.

In each of these groups, for both $S = 0{\cdot}60$ and $S = 2{\cdot}2$, the F ratio was above the 10% significance level of probability so

that there was no evidence to suggest that the null hypothesis was false. However, when an analysis of variance was performed on any of the above groups with regard to the position of other Mach band boundaries significant variations between individual observers' means within the groups were shown.

The results obtained for brightness matching show that if an observer sees a particular Mach band more brightly than the average value obtained for all observers when viewing a given physical light distribution (i.e. for $S = 2{\cdot}2$) it will be highly probable that he sees the same band more brightly than average when the physical distribution is changed (i.e. for $S = 0{\cdot}60$). Similarly there are observers who see a particular Mach band less brightly than average in both cases. From these results it would seem worthwhile to perform experiments using more S values to confirm the trend suggested by the results for the two S values quoted above.

We have seen above how three special groups of observers emerged; within each group no significant difference in the position of the visual edge could be detected. The remaining five observers could not be specified into any such group although it is plausible that if the number of observers were increased further special groups would become evident.

Experiments were performed with five of the above observers in which a binocular eyepiece attachment was employed. The result of these experiments show that the Mach pattern as seen by a given observer does not depend, to any great extent, on whether he uses his left eye, right eye or both eyes to view the image.

Attempts to explain Mach effects have involved ideas involving retinal inhibitions[8], and F. W. Campbell has suggested (private communication) that the central region of the fovea is an inhibition-free area. Campbell's theory is supported by the fact that most of the observers reported that a bright band appeared most distinct when they fixated about 20′ from the band. In further experiments with three observers it was found that the Mach effect can occur outside the fovea and in some cases the Mach bands could be seen 10° from the optic axis of the eye.

From the foregoing results, it is evident that wide variations exist between observers in their interpretation of the visual microscope image. Clearly great uncertainty arises in the form of an object whose image is the same order of dimensions as the observed Mach effects and information gained from such observations must be severely limited. In fact the Mach effect is another sources of artifacts in the optical image, like optical aberrations and diffraction and also the curious edge effects in phase contrast. Current investigations suggest that some of the

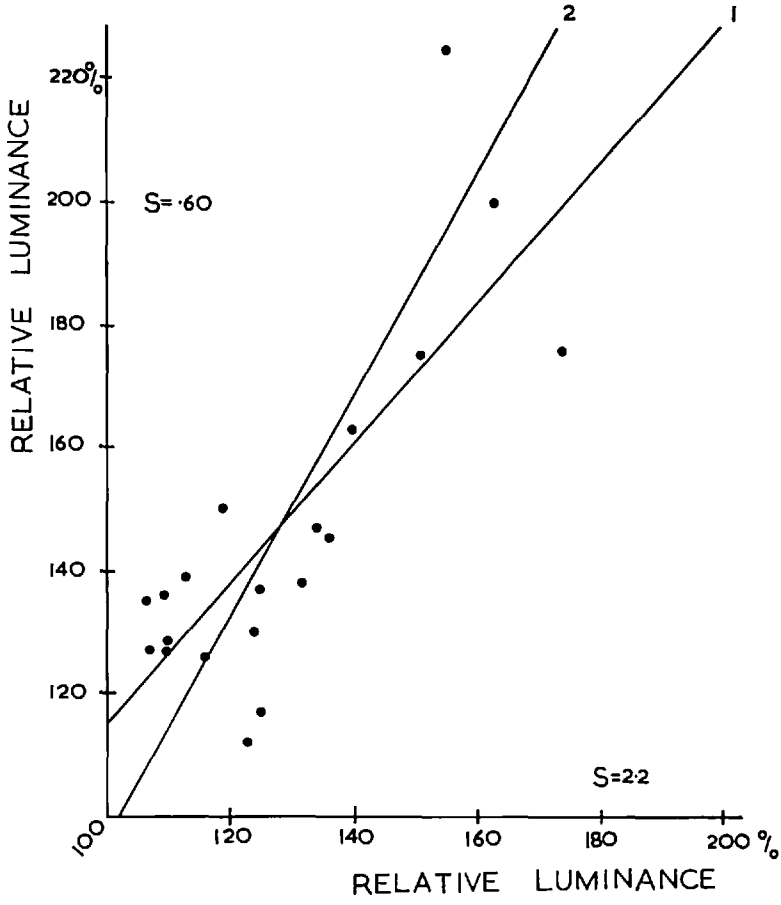


Fig. 10. Scatter diagram. The relative luminance for the first bright band for S = 0·60 is plotted against its relative luminance for S = 2·2.

personal differences referred to above can be ascribed to minute focussing errors made by observers although even when these are allowed for there seems little hope of defining some kind of 'standard observer' for Mach effects and any theory must allow considerable room for a 'personal equation'.

Acknowledgements

My sincere thanks are due to Dr. W. T. Welford for his guidance and encouragement throughout the course of this work. I am also very grateful to the observers who offered their help so willingly.

Acknowledgement is made to the Medical Research Council of Great Britain for a maintenance grant.

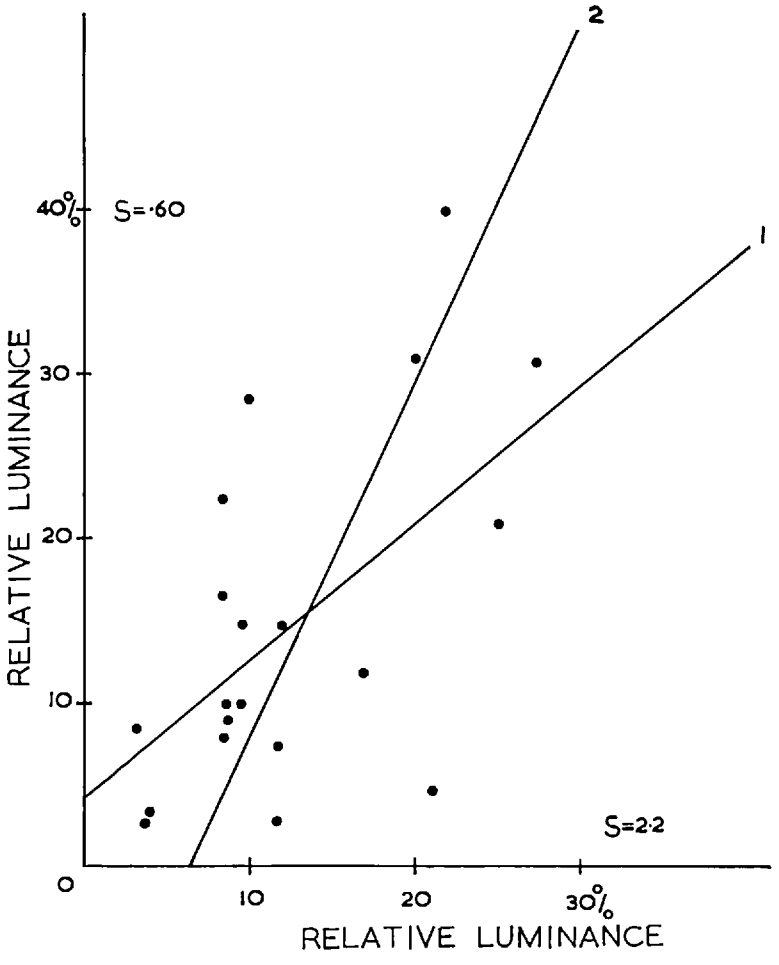


Fig. 11. Scatter diagram. The relative luminance for the second bright band for S = 0·60 is plotted against its relative luminance for S = 2·2.

REFERENCES

1 WATRASIEWICZ, B. M. (1963). *Optica Acta*, **10**, 209.
2 MACH, E. S. B. (1865). *Wien Akad Wiss*, **52**, 2, 303.
3 WATRASIEWICZ, B. M. (1964). Ph.D. Thesis, University of London.
4 LEELAWONGS, R. (1964). M.Sc. Thesis, University of London.
5 CHARMAN, W. N. (1963). *J. Opt. Soc. Am.*, **53**, 410.
6 CHARMAN, W. N. and WATRASIEWICZ, B. M. (1964). *J. Opt. Soc. Am.*, **54**, 791.
7 DAVIES, O. 'Statistical Methods in Research and Production'.
8 RATLIFFE, F., HARTLINE, H. K. and MILLER, W. H. (1963). *J. Opt. Soc. Am.*, **53**, 110.

Printed by Thanet Printing Works, Church Hill, Ramsgate, Kent.